"The expression and functional role of Tenascin-R during axon regeneration in the adult goldfish, *Carassius auratus*"

by

Ruth McBride

Thesis presented for the Degree of DOCTOR OF PHILOSOPHY

in the Department of Human Biology in the

Faculty of Health Sciences

UNIVERSITY OF CAPE TOWN

October 2006

"So many of our dreams at first seem impossible, then they seem improbable, and then when we summon the will, they soon become inevitable."

Christopher Reeve

25/9/1952 – 10/10/2004

Dedication

As fellow thesis-writers the world over will attest, a dissertation is not the result of the individual efforts of the author but also that of their family and friends. I would therefore like to dedicate my work to those whom I love and cherish:

To my mom and dad, Margie and Ian, who have both worked very hard to give me everything I ever needed and wanted – thank you for supporting my ongoing studies both financially and emotionally. I hope that you will now feel assured that I've received a "good education".

To my sister Sarah, who has also opted for the extended learning programme – thank you for making me feel as though what I was doing was big and important.

And to my husband Ross, who is probably more relieved than anyone else that this thesis is complete and that the "working world" will soon become a reality for me – thank you for believing in me and for your constant encouragement towards our official title, that of Dr and Mr McBride!

True friends are hard to find and so I'd also like to take this opportunity to thank Louise and Fiona, who from distances afar have remained ever thoughtful and faithful throughout this journey.

Above all though, I give thanks and praise to God, through Jesus Christ, who makes all things possible.

Acknowledgements

First and foremost, I would like to thank my supervisor and mentor Dr Dirk M. Lang for his unfailing enthusiasm, guidance and moral support. Dirk, you are not only a great mind but a great person and I will always consider you one of my greatest friends.

Thanks also to Professor Sue H. Kidson, in whose department this work was carried out, and who gave me encouragement and advice, as well as numerous oppertunities to expand my interests and skills.

I would like to thank the members of the Cell Biology Division for their friendship and support, and for lifting the inevitable cloud of boredom that often occurs in the basic sciences, with fun and laughter.

I would also like to express my appreciation to the Department of Human Biology's technical staff that has helped me sort out problems ranging from faulty incubators to crinkling sections. They are Bruce Dando, Barbara Möhr, Toni Wiggins, Sharon Marshall and Melaney Peterson. I am also indebted to the departmental assistants, Charles Pelston and Ray Fortuin, who were always willing to heed my requests, no matter how big or how small.

A special thanks also to Professor Gerhard Van der Horst, at the University of the Western Cape, for his assistance with statistical analysis of the data, and to Benjamin Hart for his invaluable formatting assistance.

Finally, I would like to acknowledge the funding agencies that sponsored the project as well as my own personal and travel expenses:

To the Deutsche Forschungsgemeinschaft, Medical Research Council of South Africa and the University of Cape Town Research Council for grants to Dr Dirk M. Lang,

To the University of Cape Town Postgraduate Office for their consistent funding over the course of my doctorate,

To the International Brain Research Foundation, the Society for Neuroscientists in Africa and the Southern African Neuroscience Society for funding to attend two local conferences, an international conference and two week-long African neuroscience schools, and

To the Stella and Paul Loevenstein Charitable and Educational Trust for funding to attend an international conference.

Declaration

I, **Ruth McBride**, hereby declare that this Ph.D. thesis is my own, unaided work, unless specifically acknowledged otherwise in the text, and that no part of it has been submitted for a degree to any other university.

I empower the University of Cape Town to reproduce for the purpose of research either the whole or any portion of the contents in any manner whatsoever.

Signed by candidate

October 2006

Table of Contents

Acknowledgements i
Declaration ii
Table of Contents iii
List of figures vi
List of abbreviations viii
Abstract x
Chapter 1: Introduction and Aims 1
1.1 Historical review of axon regeneration and tenascin-R in the mammalian central nervous system 1
1.2 The structure of TN-R 5
1.3 The expression pattern of TN-R 5
1.4 Known functions of TN-R 6
1.5 Known interaction partners of TN-R 9
1.5.1 Immunoglobulin superfamily interaction partners 9
1.5.2 ECM interaction partners 10
1.6 *In vitro* substrate properties of mammalian TN-R 12
1.6.1 Effect on neural cell adhesion and neurite outgrowth 12
1.6.2 Effect on glial cell adhesion and migration 13
1.7 The goldfish retinotectal system as a model for CNS repair 14
1.8 The mammalian olfactory system as a model of CNS repair 16
Chapter 2: Methodology 19
2.1 Animals 19
2.2 Goldfish optic nerve crush 19
2.3 Goldfish CNS tissue preparation 19
2.4 Antibodies and test proteins 20
2.5 Immunoperoxidase 20
2.6 Immunohistochemistry and immunocytochemistry 21
2.7 Cell cultures 22
2.8 Culturing of PC12 cells on sections of unlesioned and regenerating goldfish optic nerve 23
2.9 Microexplants of goldfish retina grown on homogenous, mixed and patterned substrates of TN-R 23

2.10 OP13 cell adhesion assay **24**

2.11 Neonate rat DRG cell adhesion assay **24**

2.12 Neonate rat Schwann cell cell adhesion assay **25**

Chapter 3: Results 26

3.1 Antibodies to tenascin-R react specifically with tenascin-R in the CNS of adult goldfish and stain purified tenascin-R protein peptides **26**

3.2 TN-R expression in the adult goldfish brain is predominantly localized in myelinated regions **27**

3.3 TN-R is expressed is in the unlesioned and regenerating adult goldfish retinotectal system **27**

3.3.1 TN-R expression in the retina 29

3.3.2 Expression of TN-R ligands and ECM interaction partners in the retina 30

3.3.3 TN-R expression in the optic nerve 37

3.3.4 Expression of TN-R ligands and ECM interaction partners in the optic nerve 45

3.3.5 Expression of TN-R and its interaction partners in the optic tectum 49

3.4 Regenerating goldfish optic nerve sections which express TN-R are permissive for the outgrowth of mammalian CNS neurites **53**

3.5 Homogenous fish TN-R is an inhibitory substrate for goldfish RGCs *in vitro* **55**

3.6 The OP13 cell line is a heterogeneous population of cells which express glial cell markers and receptors to TN-R and Nogo-A **59**

3.7 Mammalian TN-R is anti-adhesive for a novel OEG cell line **63**

Chapter 4: Discussion 72

4.1 The expression pattern of fish TN-R in the adult goldfish brain mimics that seen in the adult mammalian brain **72**

4.2 The expression pattern of fish TN-R in several locations along the optic pathway does not indicate an inhibitory role in the growth of new or regenerating retinal ganglion cell axons **73**

4.2.1 The expression of TN-R, its ligands and its interaction partners in the retina 73

4.2.2 The expression of TN-R, its ligands and its interaction partners in the optic nerve 81

4.2.3 The expression of TN-R, its ligands and its interaction partners in the optic tectum 87

4.3 The substrate properties of goldfish CNS tissue are altered during the process of regenerating **90**

4.4 Fish TN-R may not inhibit goldfish RGCs axon growth *in vivo*.....93

4.5 The OP13 cell line may represent a potentially novel OEG cell line 97

4.6 Mammalian TN-R is anti-adhesive for glial cells that may be transplanted at the site of SCI injury 99

4.7 Nogo-P4 is adhesive for glial cells that may be transplanted at the site of SCI injury.....102

4.8 A possible physiological role for Nogo-A during myelination in the PNS 104

Chapter 5: Conclusion.....106

Appendix I: Cell culture media and other solutions 110

Appendix II: Protocols and procedures.....115

Appendix III: Raw data corresponding to OP13 cell adhesion assay and statistical analysis .....

.....118

References.....126

List of figures

Figure 1. Gross anatomy of the adult goldfish brain, dorsal view. 28

Figure 2. Overview of the expression pattern of TN-R in the adult goldfish brain. 28

Figure 3. The expression pattern of TN-R in the retina before an optic nerve crush. 30

Figure 4. The expression pattern of TN-R and E587 in the retina after an optic nerve crush. 32

Figure 5. The expression pattern of TN-R and F3 in the retina before and after an optic nerve crush. 33

Figure 6. The expression pattern of TN-R and CSPGs in the retina before and after an optic nerve crush. 34

Figure 7. The expression pattern of TN-R and laminin in the retina before and after an optic nerve crush. 35

Figure 8. The expression pattern of TN-R and fibronectin in the retina before and after an optic nerve crush. 36

Figure 9. Characterization of the unlesioned adult goldfish optic nerve. 38

Figure 10. The expression pattern of TN-R and TAG-1 in the unlesioned nerve. 39

Figure 11. Characterization of the lesioned optic nerve 1 week after an optic nerve crush. ...40

Figure 12. Characterization of the lesioned optic nerve 3 weeks after an optic nerve crush...41

Figure 13. Characterization of the lesioned optic nerve 6 weeks after an optic nerve crush...42

Figure 14. Expression of TN-R in the unlesioned and regenerating optic nerve. 43

Figure 15. Reoccupation of the lesion site by TN-R–expressing but not MBP-expressing oligodendrocytes 3 weeks after an optic nerve crush. 44

Figure 16. Expression of TN-R at the optic chiasm during optic nerve regeneration. 45

Figure 17. Expression of F3 and TN-R in the unlesioned and regenerating optic nerve..... 46

Figure 18. Expression of laminin and TN-R in the unlesioned and regenerating optic nerve.48

Figure 19. Expression of fibronectin and TN-R in the unlesioned and regenerating optic nerve..... 49

Figure 20. Characterization of the adult goldfish optic tectum before and after an optic nerve crush, rostral view. 51

Figure 21. Expression of TN-R and MBP in the optic tectum before and after an optic nerve crush, rostral view. 52

Figure 22. Expression of fibronectin and laminin in the optic tectum before and after an optic nerve crush. 53

Figure 23. PC12 cells avoid growing on a section of unlesioned goldfish optic nerve but grow freely on a section of regenerating goldfish optic nerve. 55

Figure 24. Neurite outgrowth from goldfish RGC microexplants is inhibited on homogenous substrates of both fish and mammalian TN-R. 58

Figure 25. Goldfish retinal ganglion cell neurite outgrowth is restricted by a sharp substrate border of mouse TN-R but not fish TN-R. 59

Figure 26. Phase contrast images of the OP13 cells depict a morphologically heterogenous population of cells. 61

Figure 27. OP13 cells express glial cell markers and the receptors to TN-R and Nogo-A. 62

Figure 28. TN-R is an anti-adhesive substrate for OP13 cells in a short-term cell adhesion assay. 64

Figure 29. Nogo-P4 is an adhesive substrate for OP13 cells in a short-term cell adhesion assay. 67

Figure 30. Quantitative analysis of the short-term OP13 cell adhesion assay showed that TN-R was anti-adhesive for the adhesion of OP13 cells and that Nogo was an adhesive substrate. 68

Figure 31. OP13 cells avoid a sharp border substrate of mouse TN-R 69

Figure 32. Nogo-P4 is an adhesive substrate for Schwann cells in a short-term cell adhesion stripe assay. 71

List of abbreviations

CAM cell adhesion molecule

CNS central nervous system

CS chondroitin sulphate

CSPG chondroitin sulphate proteoglycan

DRG dorsal root ganglia

ECM extracellular matrix

EGF epidermal growth factor

FN III fibronectin type III

GAG glycosaminoglycan

GPI glycosyl-phosphatidylinositol

Ig immunoglobulin

IgSF immunoglobulin superfamily

INL inner nuclear layer

IPL inner plexiform layer

MAG myelin-associated glycoprotein

NCAM neural cell adhesion molecule

OEG olfactory ensheathing glia

OFL optic fiber layer

OMgp oligodendrocyte myelin glycoprotein

ONL outer nuclear layer

OPL outer plexiform layer

PNS peripheral nervous system

RGC retinal ganglion cell

SAC stratum album centrale

SCI spinal cord injuries

SO stratum opticum

TN-R tenascin-R

VL vagal lobe

Abstract

Tenascin-R (TN-R) is an extracellular matrix (ECM) glycoprotein believed to contribute towards the failure of axon regeneration in the central nervous system (CNS) of adult mammals. Using the goldfish model of CNS repair and new antibodies against fish TN-R, it was shown that TN-R exhibits an unexpected spatiotemporal expression along the goldfish retinotectal pathway during the time course of retinal ganglion cell (RGC) axon regeneration in that there is no significant downregulation of TN-R immunoreactivity in the optic nerve. The persistent colocalized expression of this putative axon growth-inhibiting protein together with growth-supportive laminin in locations and at timepoints related to the growth of newly added and regenerating RGC axons, as well as the growth-supportive substrate properties of goldfish optic nerve expressing TN-R, suggested that fish TN-R may not be functionally similar to its mammalian homologue. *In vitro* RGC outgrowth assays on homogenous substrates of purified fish TN-R however indicated that, like mammalian TN-R, fish TN-R as a sole substrate is inhibitory for neurite outgrowth. When a substrate of TN-R was mixed with laminin, the extent of neurite outgrowth was comparable to that seen on a substrate of laminin alone. The overlapping expression pattern of TN-R and laminin along the retinotectal pathway that was demonstrated *in vivo* by immunohistochemistry may therefore provide an explanation for why goldfish RGC axons are able to regenerate through the injured optic nerve in the presence of high levels of TN-R expression. To further explore the role TN-R in a regenerating part of the nervous system, the mouse olfactory system was used as a model of CNS repair. *In vitro* cell adhesion assays showed that mammalian TN-R is anti-adhesive for a novel olfactory ensheating glial (OEG) cell line, a cell type that holds promise for transplant-mediated repair of the CNS. This finding suggested that, in addition to its inhibitory influence on axon growth both during development and after CNS injury, mammalian TN-R may also impede the migration of implanted glial cells. Moreover, the anti-adhesive effects of mammalian TN-R were even more potent than that of Nogo-P4, a peptide constituting the potent myelin-associated axon outgrowth inhibitor Nogo-A. Further cell adhesion assays using Schwann cells indicated that these cells preferentially adhere to a mixed substrate of the Nogo-A peptide and laminin, suggesting a potential interaction of these proteins and a role in Schwann cell development and myelination in the peripheral nervous system. In summary, despite the finding that purified fish and mammalian TN-R have inhibitory effects on neurite outgrowth, these proteins may subserve different functions depending on the repertoire and

expression patterns of their interaction partners, such as laminin. Mammalian TN-R does not only inhibit the growth of axons, but also the migration of OEG, thus being a potentially limiting factor for the integration of such cells implanted into the CNS in order to promote repair.

Chapter 1: Introduction and Aims

1.1 Historical review of axon regeneration and tenascin-R in the mammalian central nervous system

The search for a cure for paralysis is one of the biggest challenges facing modern medicine today. Traumatic injury that damages the axons running in the spinal cord leads to a devastating loss of sensory and motor function, as seen in spinal cord injury (SCI) patients. Unlike in the peripheral nervous system (PNS), where injured neurons regenerate extensively, the central nervous system (CNS) is capable of only limited repair. The failure of adult mammalian CNS axons to fully regenerate following a physical insult is attributed to a complicated interplay between the intrinsic properties of the neuron and the extrinsic glial cell and extracellular matrix (ECM) environment in the CNS.

The optic nerve of higher vertebrates has long been used as a reliable experimental system in which to investigate the failure of mature CNS neurons to regenerate after axotomy (review by Chierzi and Fawcett, 2001). In the rodent visual system, retinal ganglion cells (RGCs) in the neural retina transduce light stimuli into electrical signals that are carried along their axons, which course through the optic nerve and terminate at specific targets in the superior colliculus. A lesion applied to the optic nerve triggers apoptosis of the RGCs (Rabacchi et al., 1994) and leads to substantial neuronal losses. In fact, almost 95% of the RGCs die after an optic nerve lesion (Villegas-Perez et al., 1988). This is followed by degeneration of the RGC axons, via a molecularly distinct self-destruct programme within the axon itself (review by Raff et al., 2002), and subsequent permanent blindness. In light of this poor neuronal survival rate and the failure of axons to regrow, early pioneers believed that adult CNS neurons intrinsically lacked the ability to regenerate. In his famous book Degeneration and Regeneration of the Nervous System, the Spanish neuroanatomist Santiago Ramon y Cajal stated that "It is to be presumed that the optic nerve will react to traumatic violence not like a peripheral nerve but like the spinal cord, that is by small and frustrated regenerative efforts" (Cajal, 1928, in review by Bahr and Bonhoeffer, 1994). The inherent growth potential of axotomized adult CNS neurons is indeed poor (Chen et al., 1995; Chong et al., 1996; Goldberg et al., 2002), and this programmed loss of regenerative ability correlates with an increase in neuronal age (review by Fawcett, 1992).

As far back as the beginning of the last century, Tello (1911) demonstrated however that, if provided with a growth-supportive substrate to grow along, regeneration of adult CNS axons

was possible. By grafting a peripheral nerve, which is able to regenerate, into the adult rabbit brain, regrowth of CNS axons across the lesion site was observed (in review by Bandtlow and Schwab, 2000). There is strong evidence to suggest that the growth-promoting effect of transplanted peripheral nerves is dependent on the presence of the Schwann cells surrounding the nerve. These PNS glia secrete a variety of neurotrophic factors, ECM molecules, and cell adhesion molecules (CAMs) that stimulate axonal growth (reviews by Martini, 1994; Fu and Gordon, 1997). The ability of Schwann cells to stimulate the regeneration of axotomized axons, by modulating inhibitory pathways (Ahmed et al., 2006), in the adult mammalian optic nerve is now well established (David and Aguayo, 1981; Villegas-Perez et al., 1988) Despite the regrowth of axons along transplanted peripheral nerve grafts, the majority of the axons failed to exit the graft. There was convincing data to suggest that the RGCs died because of neurotrophic deprivation (review by Goldberg and Barres, 2000). An attempt to save axotomized neurons by delivery of neurotrophic factors elicited, however, only weak, transient responses (review by Goldberg and Barres, 2000). The failure of the majority of the axons to exit the graft, even when neurotrophic factors were concurrently administered, was thought to be due to an inhibitory microenvironment surrounding the graft. The extrinsic non-neuronal environment and its responses to injury are now therefore presently considered to be the main cause of regenerative failure in the adult mammalian CNS.

The cells that surround the neurons in the mammalian CNS, collectively known as glial cells, were first described in 1846 by Rudolf Virchow (Virchow, 1846, in review by Baumann and Pham-Dinh, 2001). Virchow called these cells "nervenkitt" or "nerve glue" in line with the notion that they were the connective tissue of the brain (review by Baumann and Pham-Dinh, 2001). It was not until the 1920s that Santiago Ramon y Cajal and Rio Hortega recognized all of the major glial classes, namely the macroglia, which consist of astrocytes and oligodendrocytes, and the microglia (review by Sivron and Schwartz, 1995). After having been regarded as mere supportive elements for so long, glia are now emerging as key mediators in many dynamic processes within the nervous system, both during normal physiological functioning and in disease. Glial cells in the CNS optic nerve interact with closely apposing axons; not only during nervous system development but also following injury, and the properties of glial cells in lesioned nerves contribute quite substantially to the success or failure of axon regeneration in the CNS (review by Jessen, 2004).

Astrocytes constitute the most abundant cell type in mammalian CNS (review by Giaume and McCarthy, 1996). They respond to a CNS injury by forming the so-called glial scar, a matrix of connective tissue that forms in the damaged region (review by Fawcett and Asher, 1999)

and by depositing a number of ECM molecules in and around the glial scar. In particular, the chondroitin sulfate proteoglycans (CSPGs) become upregulated and exert an inhibitory influence on the axons trying to cross the lesion site (reviews by Bolvolenta and Fernaud-Espinosa, 2000, Shearer and Fawcett, 2001).

The presence of axon growth inhibitors in the myelin of mammalian oligodendrocytes was first suggested in the late 1980s. *In vitro* studies conducted by Carbonetto and his colleagues (1987) showed that the adult CNS was a poorly adhesive substrate for axon growth, especially on myelinated areas. Their results indicated that there must be an inhibitory component or components present in the myelin sheath of oligodendrocytes that was causing the inhibitory effect. In addition, *in vitro* experiments showed that oligodendrocytes and CNS myelin exerted inhibitory effects on the adhesion and outgrowth of neurons and fibroblasts (Schwab and Caroni, 1988a). Biochemical analysis revealed that the inhibitory activity of rat myelin resided in two protein fractions of 35 kDa and 250 kDa (Caroni and Schwab, 1988a), and these proteins were called neurite growth inhibitors NI-35 and N-250, respectively. The monoclonal antibody IN-1 was raised against NI-35/250 and was able to neutralize its inhibitory effects (Caroni and Schwab, 1988b; Buffo et al., 2000). Analysis of NI-35/250 led to the identification and purification of the bovine homologue bNI220 (Spillmann et al., 1998). The gene coding for bNI-220, called *nogo*, gives rise to three splice variants, with *nogo-A* being the main varient expressed in oligodendrocytes (Chen et al., 2000; GrandPré et al., 2000; Prinjha et al., 2000). In addition to Nogo-A, other myelin-associated inhibitors are also present, namely myelin-associated glycoprotein (MAG) (McKerracher et al., 1994; Mukhopadhyay et al., 1994) and oligodendrocyte myelin glycoprotein (OMgp) (Wang et al., 2002a; Kottis et al., 2002). It has been shown that Nogo-A, MAG and OMgp all bind to a common surface receptor, the Nogo-66 receptor (NgR) (Fournier et al., 2001; Domeniconi et al., 2002; Liu et al., 2002; Wang et al., 2002b). The elimination of these myelin-associated inhibitors, their receptors or downstream signaling cascades alone is, however, insufficient to induce axon regeneration. The search for other inhibitors has therefore also extended beyond the surface of the myelin sheath and into the surrounding ECM.

The ECM, secreted by the resident cells, is a complex network of proteins and carbohydrates which fills the space between cells. The ECM has three major protein components: (i) proteins and polysaccharides in the form of glycoproteins (mostly protein) and proteoglycans (mostly carbohydrate), (ii) insoluble collagen fibers, and (iii) soluble multiadhesive matrix molecules, such as laminin and fibronectin, which bind cell surface adhesion receptors. Most matrix components common in other tissues, including collagens, laminin, and fibronectin,

are less abundant in the adult mammalian brain parenchyma. This led to the early assumption that an ECM was not present in the CNS. The ECM of the CNS, however, has a unique composition. The striking feature of this matrix is the prominence of lecticans, a diverse group of CSPGs, hyaluronic acid, and multimeric glycoproteins, such as the tenascins. The ECM plays a pivotal role during development: it represents a major contributor of molecular signals, either diffusible or membrane-bound, that may guide neural and glial progenitors along migratory pathways to their final positions (review by Sanes, 1989). The ECM also plays a role following injury: there is an increase in the deposition of ECM molecules in and around the glial scar which is formed by reactive astrocytes and invading oligodendrocyte precursors at the site of injury. In addition to the CSPGs, the tenascins are also highly expressed in this area (Laywell et al., 1992) and are thought to inhibit axon regeneration.

The tenascin family of ECM glycoproteins comprises at present of five members. In chronological order of their identification they are tenascin-C, -R, -X, -Y and -W (review by Pesheva and Probstmeier, 2000a). Tenascin-C and tenascin-R are the most structurally related members of this family and were initially collectively called *J1*, which appeared in four molecular forms, namely, 160, 180, 200 and 220 kDa (Kruse et al., 1985; Faissner et al., 1988). The higher molecular weight forms, J1-200 and J1-220, were later shown to be independent molecular pairs from the lower molecular weight forms, J1-160 and J1-180 (Faissner et al., 1988). J1-200 and J1-220 were then found to be closely related to or identical to tenascin, originally called myotendinous antigen, as it was selectively distributed around budding epithelia in developing tendons, myotendinous junctions, teeth, and mammary glands. Myotendinous antigen was later named "tenascin" (TN), the combination of two Latin verbs "tenere" (meaning to hold) and "nasci" (meaning to be born), which provides the roots of the English words "tendon" and "nascent", describing its location and developmental expression pattern (Chiquet and Fambrough, 1984). Elsewhere, Grumet and colleagues (1985) described an ECM glycoprotein in chick, which they named *cytotactin* (C), that had molecular components and a differential expression pattern similar to those of J1, and hence the term tenascin-C. Pesheva et al. (1993) later renamed the J1-160 and J1-180 glycoproteins *janusin* after the Roman god *Janus* who had two faces. This was an apt naming as janusin diplayed two quite contrasting characteristics: depending on (i) the cell type and its differentiation state, (ii) the time of interaction, and (iii) the matrix composition, janusin either promoted or inhibited neurite outgrowth, and was either adhesive or anti-adhesive to cells (Pesheva et al., 1993). A few years later Rathjen and co-workers (1991) described an ECM protein in the chick nervous system with a molecular weight and expression pattern similar to that of the mouse J1-160/180 and named it *restrictin,* after which it was finally

designated a new simplified nomenclature, *tenascin-restrictin* (TN-R), the name by which it is now referred to (review by Pesheva and Probstmeier, 2000a).

There is substantial *in vivo* and *in vitro* evidence to suggest that TN-R is an axon growth-inhibiting protein. Its persistent presence in mammalian models of CNS injury may result from the inefficient clearance of myelin debris (Lazarov-Spiegler et al., 1998), or its release from CNS myelin membranes into the ECM by myelin membrane metalloproteases, which become upregulated in almost all types of CNS injury (review by Pesheva and Probstmeier, 2000a).

1.2 The structure of TN-R

The predicted amino acid sequences of chicken and rat TN-R reveal a similarity of more than 80% and that of human TN-R shows a homology to chick and rat of 75% and 93%, respectively (review by Pesheva and Probstmeier, 2000a). The protein comprises of a set of structural motifs: a cyeteine rich N-terminal region, required for oligomerization, followed by 4.5 epidermal growth factor (EGF)-like domains, 8 fibronectin type III (FN III)-like repeats, and a C-terminal globular region homologous to the fibrinogen calcium ion (Ca^{2+}) binding sequence. These protein modules are lined up like beads on a string and give rise to long and extended molecular complexes which contain numerous potential sites for *N*- and *O*-glycosylation (review by Pesheva and Probstmeier, 2000a).

TN-R glycoproteins are expressed in the CNS of different vertebrate species as two major isoforms with apparent molecular weights of 160 kDa and 180 kDa (Pesheva et al., 1993). These isoforms are generated by alternative splicing of the sixth FN III-like homologous repeat, although the actual difference between TN-R 160 and TN-R 180 at a protein level is still a matter of consideration (Fuss et al., 1993). The single arms of the two isoforms are linked together via disulfide bridges to build dimers (TN-R 160) and trimers (TN-R 180) (Pesheva et al., 1989).

1.3 The expression pattern of TN-R

TN-R is predominately expressed in the CNS by cells of the O-2A lineage, namely, oligodendrocytes and type-2 astrocytes, during the period of active myelination, whereafter both mRNA and protein levels are downregulated to lower levels in adulthood (Pesheva et al., 1989; Bartsch et al., 1993; Fuss et al., 1993). In the PNS, TN-R is transiently expressed

by Schwann cells at early developmental stages, whereafter protein levels are also downregulated to lower levels in adulthood (Probstmeier et al., 2001).

TN-R expression is not limited to glial cells. It is also found in perineuronal nets and the surrounding neuropil of small subpopulations of neurons (review by Celio and Blumcke, 1994; Saghatelyan et al., 2001; Kappler et al., 2002). Perineuronal nets are aggregations of certain ECM components around specific subpopulations of neurons (review by Celio et al., 1998). These include motor neurons in the brain and spinal cord (Rathjen et al., 1991; Angelov et al., 1998), inhibitory interneurons in the cerebellum, hippocampus and olfactory bulb (Fuss et al., 1993; Wintergerst et al., 1996), as well as in the retina (Rathjen et al., 1991). The expression of TN-R in these perineuronal nets becomes visible between the third and fourth postnatal week, and unlike glial-associated TN-R, is not downregulated in adulthood (Fuss et al., 1993; Wintergerst et al., 1996).

The expression of TN-R in the CNS under pathological conditions has been investigated in a number of CNS models of disease or trauma. These included in multiple schlerosis (Gutowski et al., 1999), after transection of the postcommisural fornix in the adult rat (Probsteimer et al., 2000b), after a lesion of the ventral funiculus in the adult rat (Deckner et al., 2000; Lindholm et al., 2001), after an optic nerve lesion in an adult mouse (Becker et al., 2000a), after dorsal rhizotomy in the adult rat (Zhang et al., 2001), and after epileptic seizures in adult rats (Brenneke et al., 2004). The upregulation of TN-R in multiple schlerosis plaques, in the glial scar at the site of SCI, and in the hippocampal neuropil after seizures, coincides with neuronal losses and regenerative failure, suggesting a putative role for TN-R in the pathology of CNS injury and disease.

1.4 Known functions of TN-R

TN-R has been implicated in a variety of both neural-matrix and glial-matrix interactions. These include neural cell adhesion and migration, axon growth inhibition/guidance, oligodendrocyte migration and myelination, localization and immobilization of ion channels, neuronal protection, and the assembly of perineuronal nets.

Saghateylyan and colleagues have recently identified a role for TN-R in neuronal migration (Saghatelyan et al., 2004). In the adult mammalian brain, neuroblasts arising in the forebrain migrate tangentially along the rostral migratory stream and then radially into the core of the olfactory bulb, where they mature into local interneurons (review by Alvarez-Buylla and García-Verdugo, 2002). It has now been shown that TN-R plays a key role in directing

neuroblasts to their respective destinations in the olfactory bulb by initiating the detachment of the neuroblasts from their migrating chains (Saghatelyan et al., 2004). In addition, the transplantation of TN-R-expressing cells into non-neurogenic regions in the brain re-routes migrating neuroblasts towards these regions, offering a promising therapeutic use for TN-R in the transplantation of stem cells in the future (Saghatelyan et al., 2004).

TN-R may function in axon growth inhibition/guidance during development. It has been hypothesized that functional interactions between sodium channel β2 subunits, which are homologous to the TN-R neuronal receptor F3 (Isom et al., 1995), and TN-R may be important for neuronal defasiculation or growth cone guidance during CNS development (Xiao et al., 1998, 1999). Homophilic binding of β2 subunits leads to cell aggregation in Drosophila and this suggests that through binding to β2 subunits or other CAMs on adjacent axons, β2 subunits may contribute to axon fasiculation (Isom et al., 1995). The corollary of that is that the binding of β2 subunits to other molecules, such as TN-R, instead of β2 subunits on adjacent axons, may lead to defasiculation (Xiao et al., 1999). There is *in vitro* evidence to support this idea. Fibroblasts that have been transfected with β2 subunits are repelled on TN-R- or TN-R domain-containing substrates (Xiao et al., 1999). It is possible that growth cone repulsion, and thus axon guidance, is facilitated through the interaction of TN-R with sodium channel β2 subunits present at the growth cones (Xiao et al., 1999). Further proof that the binding of TN-R to axons via F3 leads to axon defasciculation was provided by Pesheva and colleagues (1989, 1991, 1993), who showed that the repulsion of CNS neurites on a substrate of TN-R is mediated by F3.

TN-R plays a role in the molecular control of oligodendrocyte migration and myelination. During development of the mammalian CNS, O4/sulfatid+ oligodendrocyte progenitors proliferate in the ventral regions of the spinal cord and ventricular zones of the forebrain, and then migrate into the presumptive white matter where they differentiate into mature oligodendrocytes which express myelin-specific lipids and proteins (review by Miller, 1996). The observation that in the absence of other cell types *in vitro*, O4+ progenitor cells are fully committed to terminal differentiation (Gard and Pfeiffer, 1989), and that these cells differentiate asynchronously in different CNS regions (Schwab and Schnell, 1989), indicated that the mechanism promoting the timed differentiation of these progenitors was intrinsic to these cells and regulated by local environmental signals (Pesheva et al., 1997). The expression of TN-R by oligodendrocytes and in myelin coincides with the process of myelination, whereafter both mRNA and protein levels are downregulated to lower levels in adulthood (Fuss et al., 1993; Pesheva et al., 1993). This timed expression alluded to the

possibility that TN-R was one of these local signals. Indeed, Pesheva et al. (1997) have subsequently reported that TN-R induces the upregulation of TN-R and myelin protein expression, suggesting an autocrine TN-R-mediated mechanism of oligodendrocyte differentiation.

TN-R plays a role in neural ion channel localization, immobilization, and function. The rat brain voltage-gated sodium channels mediate the influx of sodium ions (Na^+) that are responsible for the initiation of the action potential, and therefore electrical signalling, in neurons. These channels are localized in high densities at the axon hillock (Catterall, 1981; Wollner and Catterall, 1986), where action potentials are triggered, and at nodes of Ranvier (Ritchie and Rogart, 1977), where saltatory conduction of the action potential occurs in myelinated axons. *In vitro* binding assays have shown that the β2 subunit of purified sodium channels binds to the FN III-like repeats 1-2 and 6-8 of TN-R (Srinivasan et al., 1998; Xioa et al., 1999). Considering that TN-R is expressed on the cell surface of oligodendrocyte processes, and these processes myelinate axons, beginning at the axon hillock and then between the nodes of Ranvier, TN-R is well positioned to localize and immobilize the sodium channels in the axonal surface membrane, and may therefore represent a critical communication link between the axon and the oligodendrocyte at these locations (Srinivasan et al., 1998; Xiao et al., 1999).

TN-R plays a role in neuroprotection. TN-R is expressed in perineuronal nets surrounding certain neural cell bodies in the CNS (Celio and Blumcke, 1994). Net-associated neurons in the rat hippocampus are able to survive a toxic insult and are not removed by activated microglia (Schüppel et al., 2002), thus making them less susceptible to neurodegeneration. TN-R is a component of perineuronal nets and is either downregulated or proteolytically removed by activated microglia in a model of facial nerve axotomy, thus making the neurons vulnerable to neurodegeneration (Angelov et al., 1998). The neuroprotective effect of TN-R has been localized to its EGF-like repeats, which inhibit the adhesion and migration of microglia (Liao et al., 2005).

And finally, the functions of TN-R *in vivo* have been alluded to through a number of knock-out studies. Mice deficient in TN-R expression show a reduced axonal conduction velocity in the optic nerve (Weber et al., 1999), which likely relates to the role TN-R plays in sodium channel localization and immobilization. The staining of perineuronal nets in TN-R-knock-out mice is punctate and the labeling along dendrites is also markedly reduced or absent (Weber et al., 1999; Haunso et al., 2000). There is also no staining for the CSPGs neurocan and phosphacan in cortical perineuronal nets, suggesting that TN-R is essential for attracting

or retaining these CSPGs in cortical perineuronal nets, and therefore involved in the assembly and structure of perineuronal nets (Haunso et al., 2000). Extrasynaptic transmission between neurons, and between neurons and glia, is mediated by the diffusion of neuroactive substances in the extracellular space. TN-R-deficient mice show significant changes in the diffusion properties of neuroactive substances or water, thereby also suggesting an important role for TN-R in extracellular space diffusion, and therefore extrasynaptic transmission (review by Sykova, 2004).

1.5 Known interaction partners of TN-R

1.5.1 Immunoglobulin superfamily interaction partners

The immunoglobulin superfamily (IgSF) of CAMs acts in concert with other CAMs and ECM proteins, for example TN-R, to regulate important biological processes such as migration, axonal growth, and axonal guidance during development of the nervous system. TN-R binds to the IgSF member neurofascin (Völkmer et al., 1998) but its best characterized neuronal receptor is F3 (Rathjen et al., 1991).

F3, the mouse homologue (Gennarini et al., 1989) of chick contactin/F11 (Brümmendorf et al., 1989), is a glycosyl-phosphatidylinositol (GPI)-anchored glycoprotein of the IgSF of CAMs that is expressed on the cell surface of neurons (Rathjen et al., 1987; Gennarini et al., 1989; Zisch et al., 1992). F3 has a molecular weight of 135 kDa and is structurally similar to the mouse L1 antigen that is implicated in cell-to-cell adhesion during the formation and organization of axon bundles (Rathjen and Schachner, 1984; Rathjen et al., 1987). F3 is thought to play a major role in regulation of axonal growth, fasciculation, and formation of axon trajectories (Rathjen et al., 1987). Indeed, mice lacking F3 gene expression display major malformations in axon guidance and fasciculation, and only survive a few weeks after birth (Berglund et al., 1999). In addition, *in vitro* application of antibodies against F3 interferes with fasciculation of embryonic chick retinal ganglion cells (Rathjen et al., 1987), indicating the importance of this molecule for neuronal development.

The immunoglobulin (Ig)-like domains (review by Brümmendorf and Rathjen, 1993; Pesheva et al., 1993) and FN III-like domains (Nörenberg et al., 1995) of TN-R bind to the Ig-like domains of F3 (Rathjen et al., 1991), and the interaction between these domains may not only be relevant for neuron-glia interactions but also constitute a general mechanism to regulate cell-to-cell and cell-to-matrix interactions. The interaction between TN-R and F3 enhances

F3-mediated neurite extension, suggesting a modulatory activity of TN-R on F3 (Nörenberg et al., 1995).

1.5.2 ECM interaction partners

The ECM is a complex network of macromolecules including glycoproteins and proteoglycans. These molecules have been shown to play a pivotal role in tissue morphogenesis; and in the developing nervous system, adhesive interactions between cells with each other and with the ECM plays a key role in neuronal pattern formation (review by Faissner and Steindler, 1995). Similarly to many other ECM molecules with a multidomain structure, TN-R is involved in both hereterophilic and homophilic interactions via its core protein and glycosaminoglycan (GAG) glycoconjugates.

1.5.2.1 Interactions with ECM glycoproteins

1.5.2.1.1 Heterophilic interactions with laminin

The laminins are a family of large glycoproteins (Timpl, 1979), some of which are associated with the basement membrane of cells while others not (Koch et al., 1999). The potent axon growth and guidance capacities of laminin, and the critical role it plays in PNS regeneration, has been well documented (reviews by Martini, 1994, McKerracher et al., 1996, Fu and Gordon, 1997, Grimpe and Silver, 2002). The effect of TN-R on laminin-mediated axon outgrowth is dependent upon the cell type involved. The outgrowth of embryonic and adult RGC axons from mouse retinal explants is significantly reduced on homogenous substrates of TN-R, and when presented with a sharp substrate border of TN-R, RGC axons do not cross into TN-R-containing territory, even in the presence of laminin, suggesting that the inhibitory activity of TN-R is able to override the positive effects of laminin (Becker et al., 2000a). In comparison, dorsal root ganglia (DRG) growth cones are able to grow faster on a substrate of TN-R mixed with laminin than on laminin alone (Taylor et al., 1993).

1.5.2.1.2 Heterophilic interactions with fibronectin

TN-R interacts with fibronectin by binding to heparin-binding and integrin-binding fragments on the fibronectin molecule, leading to an inhibition of fibronectin-mediated cell adhesion and neurite outgrowth (Pesheva et al., 1994). The inhibitory effect of TN-R binding to the heparin-binding fibronectin fragment is largely due to the presence of chondroitin sulphate (CS) GAG chains on its backbone, which are likely to compete with adhering cells for the binding of cell surface heparan sulfate proteoglycans or CSPGs on the fibronectin molecule (Probstmeier et al., 2000a, b).

1.5.2.1.3 Heterophilic interactions with TN-C

TN-R interacts with a structurally and functionally related glycoprotein of the same tenascin family, namely TN-C, via CS GAGs (Probstmeier et al., 2000a). This has been show *in vitro* where (i) chondroitinase-treated TN-R, which denudes the core protein of CS, shows reduced binding to immobilized TN-C, and (ii) soluble GAGs partially interefer with binding (Probstmeier et al., 2000a). Using a sandwich-binding assay, Zacharias et al. (1999) have also demonstrated the ability of TN-R and TN-C to form larger molecular complexes and link F3 polypeptides by forming a molecular bridge but the molecular nature of the interaction remains unknown. When offered as a mixed substrate *in vitro*, TN-C does not interfere with TN-R-dependent neurite outgrowth (Probstmeier et al., 1999). The presence of these two anti-adhesive ECM molecules at sites of regeneration is therefore likely to enrich the repertoire of axon growth-inhibitory molecular cues (review by Pesheva and Probstmeier, 2000a).

1.5.2.1.4 Heterphilic interactions with MAG

Oligodendrocyte-expressed MAG has been shown to act as a functional TN-R receptor (Yang et al., 1999). The MAG binding sites on TN-R have been identified as the fibrinogen domain and the EGF-like repeats, and *in vitro*, TN-R neutralizes the neurite growth-inhibitory effects of MAG on hippocampal and cerebellar neurons (Yang et al., 1999).

1.5.2.1.5 Homophilic TN-R-TN-R interactions

The two TN-R isoforms interact in a homophilic manner by a divalent cation-dependent mechanism. Both the 160 kDa and 180 kDa isoforms are capable of binding divalent ions, such as Ca^{2+} (predominantly the 180 kDa isoform), Zn^{2+}, Cu^{2+} and Co^{2+} (Pesheva et al., 1991). As a consequence of these interactions, the molecules undergo self-aggregation, resulting in the formation of specialized matrix architecture, as has been shown for other ECM glycoproteins (review by Pesheva and Probstmeier, 2000a). The self-assembly of TN-R molecules into larger polymers, in particular, is proposed to be involved in the construction of the unique matrix architecture of perineuronal nets and at the nodes of Ranvier where the protein is accumulated (review by Pesheva and Probstmeier, 2000a).

1.5.2.2 Interactions with ECM proteoglycans

Proteoglycans have a much higher ratio of polysaccharide to protein than glycoproteins and collagens, and are an important structural component in the ECM of all tissues, including the CNS (review by Wu et al., 2005). Proteoglycans are composed of core proteins covalently

linked to GAG chains that include a large group of CSPGs. A subgroup of CSPGs, the lecticans, which include aggregan, versican, neurocan and brevican, bind to TN-R via their C-type lectin domains contained within the C-terminal of the core protein (Aspberg et al., 1995; Hagihara et al., 1999).

Evidence of a physiological role for the interaction between TN-R and CSPGs is suggested by their coimmunoprecipitation in rat brain extracts (Xiao et al., 1997; Milev et al., 1998; Hagihara et al., 1999; Asher et al., 2002) and their overlapping expression pattern in the CNS (Aspberg et al., 1995; Hagihara et al., 1999; Asher et al., 2002). The similar distribution pattern and function of TN-R and these CSPGs may indicate that TN-R interferes with CSPG action and vice versa (review by Wu et al., 2005). On the other hand, the interaction between these molecules may also be functionally complementary, as they both contribute towards the macromolecular organization of perineuronal nets, protecting the microenvironment of those neurons (review by Wu et al., 2005). The importance of the interaction between TN-R and CSPGs in perineuronal nets is underscored by the observation that the distribution and shape of these structures in TN-R-deficient mice is clearly different from that in wild-type animals (Weber et al., 1999; Brückner et al., 2000; Haunso et al., 2000).

The interaction between TN-R and CSPGs is also relevant under pathological conditions. Both TN-R and versican are upregulated by oligodendrocytes after CNS injury (Probstmeier et al., 2000b; Asher et al., 2002) and may exist as a complex, thus contributing to the inhibitory ECM environment of the lesion site (Asher et al., 2002).

1.6 *In vitro* substrate properties of mammalian TN-R

The multiple functions of TN-R are reflected by its contradictory action as a promoter and inhibitor of neurite outgrowth, and as an adhesive and anti-adhesive molecule. These *in vitro* properties are dependent on the interactive cell type, the repertoire of cellular receptors and/or signalling cascades, the matrix composition, or spatial distribution and posttranslational modifications of the glycoprotein (Morganti et al., 1990; review by Pesheva and Probstmeier, 2000a).

1.6.1 Effect on neural cell adhesion and neurite outgrowth

In mammals, TN-R has been shown to be a repulsive substrate for CNS neurons (Pesheva et al., 1989, 1991) and also inhibits neurite outgrowth from an adhesive substrate onto a TN-R-containing area when it is offered as a substrate border (Pesheva et al., 1991, 1993; Taylor et al., 1993). This inhibition is mediated by the TN-R receptor F3 (Pesheva et al., 1993). The F3

binding site on TN-R has been mapped to the FN III-like repeats 2-3 of TN-R (Nörenberg et al., 1995). Despite acting as a repellent for neurites both *in vitro* as well as *in vivo*, TN-R enhances neurite outgrowth of hippocampal and cerebellar neurons (Yang et al., 1999) and induces actin-rich microprocesses and branches along chick tectal neurite shafts via F3 (Zacharias et al., 2002).

An important observation concerning the homophilic interactions of TN-R is that divalent cation-induced molecular aggregation affects the substrate properties of TN-R in relation to neuronal cell adhesion and neurite outgrowth. Preincubation of TN-R-160 and TN-R-180 with divalent cations such as Ca^{2+} or Zn^{2+}, prior to their coating as substrates, leads to a neutralization of their neurite outgrowth-inhibitory properties (Pesheva et al., 1991). The self-aggregation of TN-R is, therefore, likely to affect their cell binding domain(s) resulting in a reduced affinity for or accessibility to F3 or other, yet unidentified neuronal receptors involved in repellent response mechanisms (Pesheva et al., 1991). The ionic composition of the ECM may therefore be another determinant of TN-R function in neural cell adhesion and neurite outgrowth.

1.6.2 Effect on glial cell adhesion and migration

TN-R has a differential effect on the adhesion of glial cells: it is an adhesive substrate for oligodendrocytes, supports the attachment of astrocytes and is anti-adhesive for microglia.

Substrate-bound TN-R supports the adhesion and process formation of O4/sulfatide+ oligodendrocytes independently of the CNS region or age from which they were derived (Pesheva et al., 1997). A substrate of TN-R promotes the clustering of cell bodies and the projection of long and less branched processes. At the molecular level this interaction is mediated by protein binding to membrane surface sulfatides, as suggested by the selective interference of O4 antibodies and sulfatides with cell adhesion to TN-R (Pesheva et al., 1997). TN-R has been shown to support the attachment but not the stable adhesion and spreading of astrocytes (Pesheva et al., 1989). The mechanism whereby this interaction is mediated differs from that described for neurons or oligodendrocytes as astrocytes do not express the TN-R receptor F3 or sulfatides (Pesheva et al., 1989).

It is surprising that TN-R is a permissive substrate for oligodendrocytes but not for astrocytes as these two cell types are physiological partners. In a mixture with laminin, however, TN-R supports the adhesion of more astrocytes compared to TN-R alone (Pesheva et al., 1989). This combination of ECM molecules reflects the *in vivo* situation more closely, indicating that the adhesion of astrocytes to TN-R is more favourable that what the *in vitro* evidence

suggests. TN-R is an anti-adhesive substrate for microglia (Angelov et al., 1998). This inhibitory effect is even more potent than for astrocytes as combining TN-R with laminin does not improve the adherence of microglia to TN-R substrates (Angelov et al., 1998). The downregulation of TN-R in perineuronal nets surrounding the cell bodies of facial nerves after a peripheral nerve injury seems to make these neurons accessible to the stable adhesion of activated microglia, which has cytotoxic effects (Angelov et al., 1998). This mechanism has been suggested to account for the loss of motor neuron protection and subsequent neurodegeneration (Angelov et al., 1998).

1.7 The goldfish retinotectal system as a model for CNS repair

It is well established that fish possess the ability for CNS regeneration throughout their adult life. Among the teleostean fishes, the goldfish has been commonly used as a model for CNS repair due to their affordability, availability and relatively simple CNS anatomy that is easy to dissect. In the goldfish visual system, the optic nerve is able to regenerate after an optic nerve crush has been performed and restore normal function (Attardi and Sperry, 1963; Jacobson and Gaze, 1965). In addition, spinal cord lesions in adult goldfish have also demonstrated the ability of goldfish CNS axons to regenerate (Bernstein and Gelderd, 1970). The regrowth of CNS axons in the spinal cord is, however, age dependent (Bernstein, 1964) and selective, as not all descending supraspinal projections are able to regenerate (Sharma et al., 1993).

The goldfish retinotectal system (consisting of the retina, optic nerve, optic tract and optic tectum) exhibits two impressive features, namely neurogenesis and axon regeneration. The retina grows throughout the lifetime of the fish from a peripheral germinal zone where new RGCs are continuously added (Meyer, 1978). Axons of these newly generated RGCs make complex pathway choices on their way to their targets in the optic tectum (Easter and Stuermer, 1984). In addition, these axons are able to preferentially regrow along their specified optic pathway after being severed or crushed (Attardi and Sperry, 1963; Jacobson and Gaze, 1965). After a lesion to the optic nerve of an adult goldfish, the RGCs show no evidence of axotomy-induced apoptosis (Meyer et al., 1985) and, despite a few axons commiting path finding errors, the vast majority of regenerating axons are capable of correct path finding and thus of restoring vision. This may be possible through the persistent expression of guidance molecules in adult fish. Indeed, some guidance molecules are expressed in an instructive pattern in the developing as well as in the adult lesioned and unlesioned optic pathway of teleost fish (ephrins: Becker et al., 2000b; netrin: Petrausch et

al., 2000a; Rodger et al., 2000; CSPGs: Becker and Becker, 2002). The neuron intrinsic properties of goldfish RGCs are believed to explain why they are able to survive the programmed cell death that axotomy stimulates and regenerate their axons: they are known to upregulate their mRNA production and re-express several growth-associated proteins concurrent with axonal regrowth (Benowitz et al., 1981; Benowitz and Lewis, 1983). The ability of these nerves to regenerate was previously correlated with the ability of sections of goldfish optic nerve to support the neuronal attachment and axonal growth of neuroblastoma cells or embryonic neurons (Carbonetto et al., 1987). This suggested that the substrate properties of the fish CNS were growth-promoting, and therefore that the extrinsic CNS microenvironment, namely the glial cells and ECM, created a favourable milieu in which the regeneration of the goldfish RGC axons was promoted.

As is the case in mammals, the major glial cell types in the fish CNS are astrocytes, oligodendrocytes (Wolburg, 1981; Maggs and Scholes, 1990; Bastmeyer et al., 1993) and microglia (Dowding et al., 1991). Fish optic nerve astrocyte processes partition the optic nerve and are arranged in a special manner in order to give the fish optic nerve the high mechanical strength it needs during strong eye movements (Easter et al., 1981), and oligodendrocytes myelinate the majority of axons (Murray, 1982). The response of fish CNS glial cells to nerve injury has been most intensively studied in the visual pathway. When the optic nerve of the fish is cut, the non-permissive glial scar, which negatively affects the regrowth of lesioned CNS axons in mammals, does not form (Hirsch et al., 1995). After an optic nerve crush, goldfish astrocytes disappear from the lesion site and are only detectable again after at least 16 days post-injury (review by Bernhardt, 1999). Microglia are abundant in the crushed fish optic nerve, where they increased in number to a maximum at 2-3 weeks after the crush, and decreases after 3 months post-crush (Battisti et al., 1995; Velasco et al., 1995). The rapid microglial removal of myelin debris could perhaps remove the putative axon growth inhibitors, suggesting that microglia could contribute to the regenerative capacity of fish CNS. Granular macrophages, unique to goldfish, also increases in number near the crush site within hours of the lesion, where they remain elevated during the time axons are elongating (Battisti et al., 1995).

Oligodendrocytes in the fish optic nerve respond to injury much like the PNS Schwann cells (review by Stuermer et al., 1992) in that they dedifferentiate from cells which express myelin molecules to axon growth-promoting glial cells which ultimately remyelinate the regenerated axons (Wolburg et al., 1981; Stuermer and Easter, 1984). Goldfish oligodendrocytes secrete trophic molecules (Schwalb et al., 1995, 1996), which stimulate axon outgrowth and also

produce the CAM E587 antigen *in vivo* in a spatiotemporal correlation with retinal axon regeneration (Ankerhold et al., 1998). When isolated from normal or lesioned optic nerves, goldfish oligodendrocytes in culture also synthesise CAMs (Bastmeyer et al., 1994).

Fish oligodendrocytes were originally thought to be supportive of axonal growth as axons from goldfish and rat retinal explants grew extremely well on immature oligodendrocytes isolated from normal or lesioned goldfish optic nerves (Bastmeyer et al., 1991, 1993). This led researchers to believe that fish CNS myelin and oligodendrocytes were devoid of neurite growth inhibitors (Bastmeyer et al., 1991; Wanner et al., 1995). Considering that even rat immature oligodendrocytes are not inhibitory to axonal growth (Schwab and Caroni, 1988a), it is not surprising that immature fish oligodendrocytes support axonal growth and there is now sufficient evidence to prove that they are indeed inhibitory substrates: (i) myelin isolated from fish optic nerve or spinal cord is only barely permissive to the growth of adult fish axons (Bastmeyer et al., 1991), (ii) application of IN-1 monoclonal antibodies, which were originally directed against rat myelin inhibitors (Caroni and Schwab, 1988b), neutralize the growth inhibition of fish myelin (Sivron et al., 1994), demonstrating not only that fish myelin contains growth inhibitors, but also that these inhibitors are similar or identical to those of rat CNS myelin, and (iii) sections of fish optic nerve are inhibitory to growth of adult mammalian retinal axons (Sivron et al., 1994). These observations led to the conclusion that mature fish oligodendrocytes *in vivo* are probably inhibitory to axonal regeneration (review by Sivron and Schwartz, 1995).

The results of Sivron et al. (1994) were however subsequently refuted when it was shown that inadequate controls were used to determine the presence of axon outgrowth inhibitors (Wanner et al., 1995) and it has since been demonstrated that at least one oligodendrocyte-associated axon growth-inhibiting protein, namely TN-R, is expressed in the fish CNS (Becker et al. 2004; Pesheva et al., 2006). This has raised the question of whether this protein is differentially expressed along the goldfish retinotectal system during the time course of RGC axon regeneration, and if so, the functional role it plays in goldfish RGC axon regeneration.

1.8 The mammalian olfactory system as a model of CNS repair

The mammalian olfactory system develops from the olfactory placode and comprises of the olfactory epithelium (PNS tissue) and the olfactory bulb (CNS tissue) (Marin-Padilla and Amieva, 1989). Olfactory receptor neurons arise in the olfactory epithelium and extend their axons to the olfactory bulb. The olfactory system is an unusual tissue in that it, like the fish

visual system, can support neurogenesis throughout life (Graziadei and Monti- Graziadei, 1979). Moreover, this neurogenic capacity and the permissivity of the olfactory bulb to axonal growth, persist after transection of the olfactory nerve (Graziadei and Monti-Graziadei, 1980; Doucette et al., 1983). Under normal conditions, olfactory receptor neurons have a life span of 4-8 weeks, depending on the species (Carr and Farbman, 1992). After this period, they are replaced by new neurons originating from basal stem cells in the olfactory epithelium. During normal cell turn over or after injury, new olfactory receptor neurons generated from these stem cells in the PNS extend axons through the cribiform plate and re-enter the olfactory bulb in the CNS, re-synapsing with second order neurons in the glomerular layers (review in Schwob, 2002). This is one of the rare situations in which peripheral axons are able to enter the adult CNS environment and form synapses, and it is thought that this unusual ability may be due in part to the specialized properties of olfactory ensheathing glia (OEG) (Raisman, 1985; review by Doucette, 1990; Doucette, 1991), which provide ensheathment *in vivo* for the unmyelinated olfactory axons within both the PNS and CNS portions of the olfactory nerve (Doucette, 1984, 1993; Raisman, 1985). This has led OEG to become a compelling candidate for transplant-mediated CNS repair after various types of injuries, including rhizotomy of spinal dorsal roots (Ramòn-Cueto and Nieto-Sampedro, 1994; Navarro et al., 1999), lesions of spinal cord axons (Li et al., 1997; Ramòn-Cueto et al., 2000; Keyvan-Fouladi et al., 2003; Moreno-Flores et al., 2006), and RGC lesions in the optic nerve (Li et al., 2003).

OEG have become very popular because of their ability to promote long distance growth *in vitro* and *in vivo* of regenerating axons (Ramòn-Cueto and Nieto-Sampedro, 1994; Smale et al., 1996; Li et al., 1997; Perez-Bouza et al., 1998; Ramòn-Cueto et al., 1998, 2000; Leaver et al., 2006), and to remyelinate spinal cord axons (Franklin et al., 1996; Imaizumi et al., 1998; Barnett et al., 2000). The use of OEG in transplant-mediated CNS repair has many advantages over other cell types (review by Barnett and Riddell, 2004). Human OEG can be directly isolated from biopsies of the olfactory mucosa and grown in large numbers to enable autologous transplants to be performed (Feron et al., 1998), OEG are less likely to induce hypertrophy of CNS astrocytes and CSPG expression than Schwann cells in adult CNS white matter (Lakatos et al., 2000, 2003), and regenerating fibres are able to grow beyond the OEG graft and into the host spinal cord on the opposite side of the lesion (Li et al., 1998; Ramòn-Cueto et al., 1998, 2000).

Despite the promise that OEG hold, there is a lack of unequivocal evidence that OEG are directly associated with axon regeneration and remyelination, and so the mechanisms

whereby their transplantation brings about functional improvements therefore remains unclear. Further *in vitro* characterization of OEG, in particular, their migratory potential, is required before their clinical use can be furthered. The ability of OEG to migrate after transplantion is important for both SCI and neurodegenerative diseases, such as multiple sclerosis, where numerous sites of demyelination persist. As the olfactory system conserves many of its developmental plastic properties, it is reasonable to assume that OEG retain their ability to migrate with new and regenerating axons in either the olfactory system or any other system that requires a growth-promoting conduit for axons to regenerate along. The initial studies that characterized OEG behaviour after transplantation relied on prelabeling that resulted in extensive false positive signals (Ruitenberg et al., 2002), yielding an overestimation of the migratory capacity of OEG *in vivo*. More recently, improved labeling techniques have however demonstrated that OEG remain quite localized to the implantation site (Ruitenberg et al., 2002; Li et al., 2003; Boyd et al., 2004). As the mammalian injury site is known to contain axon growth-inhibiting proteins, the migratory potential of these cells may be limited by the presence of such proteins, for example, TN-R.

A group at the Department of Molecular Cell Biology at the University of Cape Town has established a set of cell lines derived from the embryonic mouse olfactory epithelium (Illing et al., 2002). Polymerase chain reaction results have shown that clone OP13 expresses $p75^{NGFR}$ (Illing et al., 2002), a known marker of OEG (Ramòn-Cueto and Nieto-Sampedro, 1992).

Against this background, it appeared attractive to analyze the expression and functional role of TN-R in the context of different model systems of axon regeneration, such as the fish visual system and the mammalian olfactory system.

The specific objectives of this study were therefore:

1. To map the expression pattern of fish TN-R and its interaction partners in the adult goldfish retinotectal system after optic nerve injury and to evaluate the permissivity of fish optic nerve tissue for axon growth.
2. To compare the influence of fish and mammalian TN-R on fish and mammalian CNS neurite outgrowth.
3. To characterize a novel cell line as a model system for studies of OEG migration.
4. To analyze the role of TN-R in the migration of OEG and Schwann cells.

Chapter 2: Methodology

2.1 Animals

Adult goldfish, *Carassius auratus*, were obtained from a local pet shop. The fish were housed in aerated tanks at room temperature and fed dried fish food *ad libitum*. Neonate Wistar rats were obtained from the University of Cape Town Animal Unit. All animal experiments were conducted according to guidelines set out by the Animal Ethics Committee of the University of Cape Town (Ethical approval numbers: 099-4/2000 and 01/13).

2.2 Goldfish optic nerve crush

For lesions to the optic nerve, individual adult goldfish were deeply anaesthetized by immersion in ethyl 3-aminobenzoate methanesulfonate salt (MS222; 0.05%; Sigma, Germany) for 5 minutes (min). The right eye was gently lifted from its socket and the exposed optic nerve was crushed halfway between the eyeball and the optic chiasm under visual control using watchmaker's forceps. A translucent stripe across the otherwise opaque optic nerve at the site where the forceps had been applied indicated a successful crush of the nerve. After surgery, gills were flushed with tank water by gently pulling the fish through the water. The fish resumed breathing within a few minutes and began normal feeding shortly thereafter. After designated time points (1, 3, and 6 weeks) the fish were terminally anaesthetized in MS222 (0.1%) and dissected.

2.3 Goldfish CNS tissue preparation

The eyeball, optic nerves connected at optic chiasm, and optic tectum were dissected out, photographed with a Wild Heerbrugg Stereo Dissection microscope (Switzerland), and then embedded in tissue freezing medium (Leica, Germany). The blocks of tissue were quick-frozen in liquid nitrogen and stored at -80°C until use. The frozen tissue samples were cut into 10 µm sections on a cryostat (Leica) and placed onto aptese-coated glass slides for immunohistochemistry and immunoperoxidase. Sections of goldfish optic nerve which had been dissected out 3 weeks after the optic nerve crush sections were also placed onto poly-L-lysine (PLL)-coated coverslips for tissue culture. The uninjured left optic nerve served as an internal control. For culturing retinal ganglion cells (RGCs) from goldfish, a conditioning optic nerve crush was performed approximately 2 weeks before each experiment in order to

stimulate RGC outgrowth (Landreth and Agranoff, 1976). (n = a minimum of 3 animals was used for each time point)

2.4 Antibodies and test proteins

The rabbit polyclonal antibody TN-R against rat brain-derived tenascin-R (Angelov et al., 1998) and monoclonal antibodies tn-R1 (Pesheva et al., 1989) and tn-R6 (Pesheva et al., 2006) against a mixture of chick and human brain-derived tenascin-R, have been previously characterized. The following polyclonal antibodies were also used: rabbit sera against F3 (24III and 41.6) (kind gift from Professor G. Gennarini, Bari, Italy), rabbit anti-laminin (Serotec, UK), rabbit anti-fibronectin (Telios Pharmaceuticals Incorporated, USA), rabbit anti-epsilon 587 (generated by Dr D.M. Lang, South Africa, unpublished), rabbit anti-TAG-1 (supernatant) specific to purified recombinant TAG-1 protein (Lang et al., 2001), rabbit anti-Nogo-A (Alpha Diagnostics, USA), and rabbit anti-Nogo-66-receptor (NgR, Alpha Diagnostics). The following monoclonal antibodies were also used: mouse anti-O4 (supernatant) specific to sulfatides (kind gift from Dr P. Pesheva, Bonn, Germany), mouse anti-CS-56 (Sigma) to chondroitin-4 sulfate and chondroitin-6 sulfate (Avur and Geiger, 1984), anti-epsilon 587 (E587) to epsilon (generated by Dr D.M. Lang, South Africa, unpublished), rat anti-myelin basic protein (MBP, kind gift from Dr C. Livingston, Munich, Germany), and mouse anti-Thy-1 (Biotrend, Germany). In addition, the fluorescent stain 4', 6-diamidino-2-phenylindole (DAPI), was used to visualize cell nuclei (Sigma).

The following test proteins and fragments were used: laminin from EHS sarcoma (1mg/ml, Sigma), fish (carp) tenascin-R (TN-R, sample F7, 80 µg/ml), mouse TN-R (an equal mixture of sample m.JN, 596 Ag, and 621 Ag; 70, 20 and 70 µg/ml respectively), human TN-R (H-FOM, 80 µg/ml), and a rat nogo inhibitory peptide (Nogo-P4, 20 µl/ml, Alpha Diagnostic,). The immunoaffinity purified tenascin-R proteins were a kind gift from Dr P. Pesheva, Bonn, Germany. Bovine serum albumin (BSA, 1 mg/100ml, fatty acid-free, Roche Diagnostics) and poly-L-lysine (PLL, 100 µg/ml, Sigma) were also used.

2.5 Immunoperoxidase

Immunoperoxidase staining was performed using a VECTASTAIN Elite ABC Kit (Vector Laboratories, USA). Air-dried frozen sections of the goldfish CNS (optic nerve, brain and rostral spinal cord) on objective slides were fixed in cold methanol (MeOH, AnalaR®, SA) at

-20°C for 5 min before staining. The slides were washed 3 x 5 min in phosphate buffered saline (PBS, pH 7, 4), incubated in 0.3 % hydrogen peroxide (H_2O_2, Associated Chemical Enterprizes (PTY) Ltd, SA) in MeOH for 30 min at room temperature (RT) to quench the endogenous peroxidise in the tissue, and washed again for 4 x 10 minutes in PBS. The sections were then blocked with 1% BSA in PBS for 1 hr at RT and incubated with rabbit anti-TN-R diluted 1:1000 in blocking solution overnight at 4°C in a humidified chamber. The following day the sections were washed for 3 x 5 min in PBS, incubated with goat anti-rabbit biotinylated secondary antibody diluted 1:1000 in blocking solution for 1 hr at RT in a humidity chamber, where after they were again washed 4 x 10 min in PBS. At the same time as the slides were being washed, the VECTASTAIN Elite ABC reagent was pre-reacted for 30 min at RT. The sections were then incubated with the VECTASTAIN Elite ABC complex for 30 min at RT in a humidified chamber and then briefly washed 2 x 5 min in PBS before being incubated in the peroxidise substrate solution. Once the desired stain intensity had developed, the sections were rinsed in tap water for 10-15 min, airdried and mounted with entellan (Merck, Germany). (n = 1)

2.6 Immunohistochemistry and immunocytochemistry

Cryosections of goldfish CNS tissues were fixed in cold MeOH for 5 min at -20°C, washed 3 x 10 min in PBS with agitation and blocked with 1% BSA for 1 hr at RT. The sections were then incubated with primary antibodies of interest and incubated overnight at 4°C. The sections were then washed with PBS for 3 x 10 min with agitation and incubated with the appropriate Cy3-conjugated (Sigma) or Alexa 488-conjugated secondary antibodies (Molecular Probes, The Netherlands) diluted 1:1000 in PBS containing 1% for 2hrs at RT in the dark. Then sections were again washed 3 x 10 min and incubated with DAPI (0.5 µg/ml in PBS) for 10 min at RT in the dark. The sections were then washed 1 x 10 min and coverslipped in Mowiol (Sigma) containing n-propylgallate (Sigma) as an anti-fading agent. Cultures of pheochromocytoma (PC12) cells (kind gift from Dr M. Schwab, Zürich, Switzerland) grown on sections of regenerating goldfish optic nerve were first incubated with anti-Thy-1 (1:200) for 1 hr at 37°C to stain the PC12 cells, washed in medium for 5 min at RT and then fixed in methanol for 5 min at -20°C, followed by 4% paraformaldehyde (PFA, AnalaR®) in PBS for 5 min at RT. The cultures were then washed with PBS for 3 x 10 min, incubated with anti-TN-R (1:500, 1% BSA in PBS) for 2 hrs at RT, to stain the goldfish optic nerves, followed by secondary antibodies and DAPI as described above. OP13 cultures were

first incubated live with NgR (1:500) for 1 hr at 37°C, washed in medium for 5 min at RT and then fixed in MeOH for 5 min at -20°C, followed by 4% PFA in PBS for 5 min at RT. The cells were then washed with PBS for 3 x 10 min, incubated with anti-F3 sera (1:1000, 1% BSA in PBS) for 2 hrs at RT followed by secondary antibodies and DAPI as previously described. The fluorescent signal was detected on a Zeiss Aviovert 200 fluorescent microscope using the appropriate filters. The DAPI filter was used to detect nuclei, the FITC filter was used to detect the Alexa-488 signal, and the Texas Red filter was used to detect Cy3 signal. The excitation and emission wavelength for the DAPI filter set was 365 nm and 397 nm, respectively. The excitation and emission wavelength for the Texas Red filter set was 546 nm and 590 nm, respectively. The excitation and emission wavelength for the Alexa-488 filter set was 450-490 nm and 515-565 nm, respectively. Digital black and white images were taken with each fluorescent filter and then colorized in one of the three channels (blue, green or red). The three separate colored channels were then overlayed as layers in Adobe® Photoshop® 7.0, and the colocalization of labeled structures could then be ascertained. When capturing images to compare the fluorescent intensity of control sections of goldfish retina, optic nerve or optic tectum with the fluorescent intensity of sections from regenerating tissue, the same exposure times were used. For negative controls, either the primary antibodies were omitted or both the primary and secondary antibodies were omitted.

2.7 Cell cultures

Mixed glial cultures from adult goldfish CNS were prepared by mechanical trituration of the optic nerve, brain and spinal cord and cultured on PLL-coated coverslips for up to 2 weeks at 28°C in a 1:1 mixture of Leibovitz L-15 (L-15, 0.693 g/50 ml, Highveld Biological, SA) and Ham's F12 media (0.563 g/50 ml, Highveld Biological), containing 10% fetal calf serum (FCS, Highveld Biological), 4% methyl cellulose (Sigma), 2 mg/ml $NaHCO_3$ (Saarchem), fungizone (0.25 µg/ml, Sigma) and gentamycin sulphate (50 µg/ml, Sigma). Goldfish RGCs were grown in a 1:1 mixture of L-15 and Ham's F12 media containing 15% FCS, fungizone and gentamycin sulphate. PC12 cells were first grown in proliferation medium containing Dulbecco's modifies Eagle's MEM (DMEM, Highveld Biological), FCS (10%) and penicillin/streptomycin (1:1000, Sigma) at 37°C for 5-7 days. The proliferation medium was then replaced with differentiation medium containing DMEM, FCS (1%), nerve growth factor (NGF, 100 ng/ml, Sigma), forskolin (1 µM, Sigma), insulin-transferrin-selenium-A supplement (1:100, GibcoBRL, USA), and penicillin/streptomycin at 37°C for 2-3 days or

until the cells displayed extensive processes. OP13 cells were first grown in proliferation medium containing DMEM, FCS (10%) and penicillin/streptomycin at 33° C for 5-7 days. The proliferation medium was then replaced with differentiation medium containing DMEM, FCS (1%), NGF, forskolin, insulin-transferrin-selenium-A, and penicillin/streptomycin at 39°C for 2-3 days. The single suspensions of dorsal root ganglia (DRG) were grown in DMEM media containing 1% FCS, NGF, forskolin, insulin-transferrin-selenium-A supplement, and 1% penicillin/streptomycin (DRG medium)at 37°C for 48 hrs. Schwann cells were grown in DMEM containing 10% FCS, and 1% penicillin/streptomycin.

2.8 Culturing of PC12 cells on sections of unlesioned and regenerating goldfish optic nerve

A suspension of differentiated PC12 cells was seeded onto sections of 3 weeks post-injury goldfish optic nerve. The PC12 cells and underlying optic nerve sections were covered with PC12 differentiation medium and an uncoated coverslip was placed on top to sandwich it. The cultures were grown for 2-3 days after which phase contrast photographs were taken on a Zeiss Axiovert 200 fluorescent microscope. Thereafter, the cultures were fixed and stained for immunocytochemistry. (n = 3)

2.9 Microexplants of goldfish retina grown on homogenous, mixed and patterned substrates of TN-R

Goldfish were dark-adapted for 2 hrs and then terminally anaesthetized in 0.1% MS222. The eye on the pre-conditioned side was removed and the retina dissected out. The retina was flat-mounted onto a piece of sterile nitrocellulose membrane (Amersham, Netherlands) and as much of the basal lamina and capillary network overlying the RGC layer as possible was removed. The retina was then cut into 200 x 200 µm squares using a McIlwain tissue chopper (The Mickle Laboratory Engineering Company Ltd, USA). The retinal microexplants were resuspended in RGC medium and plated onto coverslips that had been coated with (i) laminin as a sole substrate (80 µg/ml), (ii) purified fish TN-R as a sole substrate (70 µg/ml), (iii) purified mouse TN-R as a sole substrate (80 µg/ml), (iv) purified human TN-R as a sole substrate (80 µg/ml), (v) laminin and purified fish TN-R, (vi) laminin and purified mouse TN-R, or (vii) laminin and purified human TN-R. To analyze outgrowth on patterned substrates, the retina was cut into long strips with a diameter of 200 µm. The retinal strips

were plated RGC-side down onto coverslips that had been coated with alternating lanes of PLL and purified fish or mouse TN-R. The cultures were grown at 28°C for 2-3 days after which phase contrast photographs were taken on the Zeiss Aviovert 200 microscope. Thereafter, the patterned substrate cultures were fixed and stained for immunohistochemistry. (n = 4)

2.10 OP13 cell adhesion assay

This cell adhesion assay has been previously described (Yang and Hynes, 1996). Once the OP13 cells had differentiated in culture, they were trypsinized (trypsin/EDTA, both Sigma) and seeded onto 9 mm round coverslips that had previously been coated with either (i) laminin alone, (ii) mouse TN-R alone, (iii) laminin and mouse TN-R, (iv) Nogo-P4 alone, or (v) laminin and Nogo-P4. Phase contrast images were taken using the Zeiss Axiovert 200 microscope after 6, 12 and 24 hrs. The number of adherent cells were manually counted and recorded. One-way analysis of variance (ANOVA) and unpaired *t*-tests were performed using the MetCalc ® version 4.16f statistical programme. A P value of less than 0.05 was considered statistically significant. All data are presented as mean ± standard deviations. In order to confront the OP13 cells with a sharp border substrate of TN-R, the OP13s were also plated onto coverslips that that had been coated with alternating lanes of PLL and mouse TN-R. After 24 hrs, the cultures were fixed and stained with anti-$p75^{NTFR}$ to label the OP13 cells and with anti-TN-R to visualize the TN-R stripes. (n = 4)

2.11 Neonate rat DRG cell adhesion assay

Neonate Wistar rat pups (P1) were sacrificed by decapitation in accordance to animal welfare regulations. The spinal cord was dissected out and the DRG removed. In order to obtain a suspension of small DRG tissue explants as well as single cells, the ganglia were chopped on a McIlwain tissue chopper set at 100 µm in both a vertical and horizontal direction. The single suspension of DRG fragments was then seeded onto coverslips that had been coated with either (i) laminin as a sole substrate, (ii) mouse TN-R as a sole substrate, (iii) laminin and mouse TN-R, (iv) Nogo-P4 as a sole substrate, or (v) laminin and Nogo-P4, and grown in DRG medium at 37°C for 48 hrs. Phase contrast images were taken using the Zeiss Axiovert 200 fluorescent microscope after 24 and 48 hrs. (n = 3)

2.12 Neonate rat Schwann cell cell adhesion assay

Neonate Wistar rat pups (P1) were sacrificed by decapitation in accordance to animal welfare regulations. Peripheral nerves were dissected out and chopped on a McIlwain tissue chopper set at 100 µm. The peripheral nerve explants were grown in grown for 2-3 days until Schwann cells had begun extending from the explants in sufficient numbers. The cultures were then trypsinised and seeded onto 22 mm square coverslips that had previously be coated with either (i) laminin alone, (ii) Nogo-P4 alone, or (iii) laminin and Nogo-P4. In order to confront the Schwann cells with a substrate boundary of Nogo-P4, the Schwann cells were also plated onto coverslips coated with alternating lanes of laminin and Nogo-P4. Phase contrast images were taken using the Zeiss Axiovert 200 microscope after 24 hrs. (n = 1)

Chapter 3: Results

3.1 Antibodies to tenascin-R react specifically with tenascin-R in the CNS of adult goldfish and stain purified tenascin-R protein peptides

Tenascin-R (TN-R) was detected in adult goldfish with a polyclonal antibody and two monoclonal antibodies (tn-R1 and tn-R6), raised in rabbit against the full length sequence of affinity purified rat TN-R (Pesheva et al., 2006). Both the polyclonal and monoclonal antibodies have been characterized and tested for specificity in a number of vertebrate species. These include fish (shark, carp, trout, goldfish), amphibians (newt, salamander, frog), reptiles (water snake, lizard, tortoise), birds (chick, pigeon), and mammals (hedgehog, rat, rabbit, cattle, pig, humans) (Pesheva et al., 2006). To confirm that the antibodies were specific for TN-R in adult goldfish and to demonstrate TN-R in the central nervous system (CNS) of the adult goldfish, western blot analysis was previously performed on protein homogenates of whole brains of adult goldfish using both the polyclonal and monoclonal antibodies (Pesheva et al., 2006). Both antibodies were highly specific to the TN-R protein in the goldfish CNS and did not cross react with related tenascin family members, namely tenascin-C, tenascin-X or tenascin-W (Pesheva et al., 2006). All antibodies to TN-R used showed similar staining patterns in immunohistochemistry, which were very similar to those observed in adult mice, chicken, salamander and goldfish (Rathjen et al., 1991; Bartsch et al., 1993; Becker et al., 1999; Becker et al., 2004). Specificity was further confirmed by demonstrating the characteristic accumulation of the molecules at the nodes of Ranvier in the spinal white matter and within perineuronal nets in the spinal gray matter (Pesheva et al., 2006). Antibodies to TN-R also stained purified TN-R protein peptides that were used in this study for stripe assays (Figure 31).

Although the specificity of the F3 sera in the goldfish CNS was not verified by western blot, goldfish, zebrafish and amphibian homologs of F3 with a basic structure and expression pattern similar to those in higher vertebrates have been reported (Nagata et al., 1996; Gimnopoulos et al., 2002; Haenisch et al., 2005). It is therefore reasonable to assume that an antibody against the mammalian antigen will be able to specifically detect the protein in the CNS of goldfish. The typical neuronal surface staining pattern seen in the immunohistochemical results resembled the staining pattern seen in other vertebrate species (Gennarini et al., 1989; Haenisch et al., 2005), indicating that the F3 sera specifically stained

this cell adhesion molecule expressed by the goldfish retinal ganglion cell (RGC) axons.

The specificity of the myelin basic protein (MBP) antibody in the goldfish CNS was confirmed through personal communication with Dr DM Lang. The fibronectin antibody specifically labels goldfish tissue (Hirsch et al., 1995) and the laminin antibody has been shown to be specific in other lower vertebrates (Gordon-Weeks et al., 1992). Moreover, the staining of the connective tissue and well as the blood vessels by the fibronectin and laminin antibodies further indicated their specificity (Gordon-Weeks et al., 1989; Stewart and Pearlman, 1987).

3.2 TN-R expression in the adult goldfish brain is predominantly localized in myelinated regions

The goldfish brain consists of various lobes, most of which are paired (Figure 1). The expression of TN-R in the goldfish CNS was examined in cryosections of goldfish brain using a commercial immunoperoxidase kit. TN-R was associated with myelinated axon tracts in different brain regions (Figure 2). TN-R staining was weak in the predominantly unmyelinated regions of the forebrain, namely the telencephalon but was stronger in myelinated regions of the mid- and hind-brain, namely the optic tectum (OT; where the retinal ganglion cell axons finally terminate), cerebellum (CB), tegmentum (Teg), vagal lobe (VL), olfactory bulb (OB), as well as in the rostral spinal cord. This myelin-associated expression pattern resembles that seen in the mammalian CNS and may therefore suggest that fish TN-R has a similar function to mammalian TN-R; however, similarities in distribution do not necessarily mean similarity in function.

3.3 TN-R is expressed in the unlesioned and regenerating adult goldfish retinotectal system

In order to analyze the expression pattern of TN-R along the retinotectal system in the unlesioned compared to the lesioned adult goldfish optic pathway, a set of TN-R monoclonal or polyclonal antibodies was used in combination with other antibodies to stain frozen sections of the retina, optic nerve, and optic tectum 1, 3 and 6 weeks after an optic nerve crush.

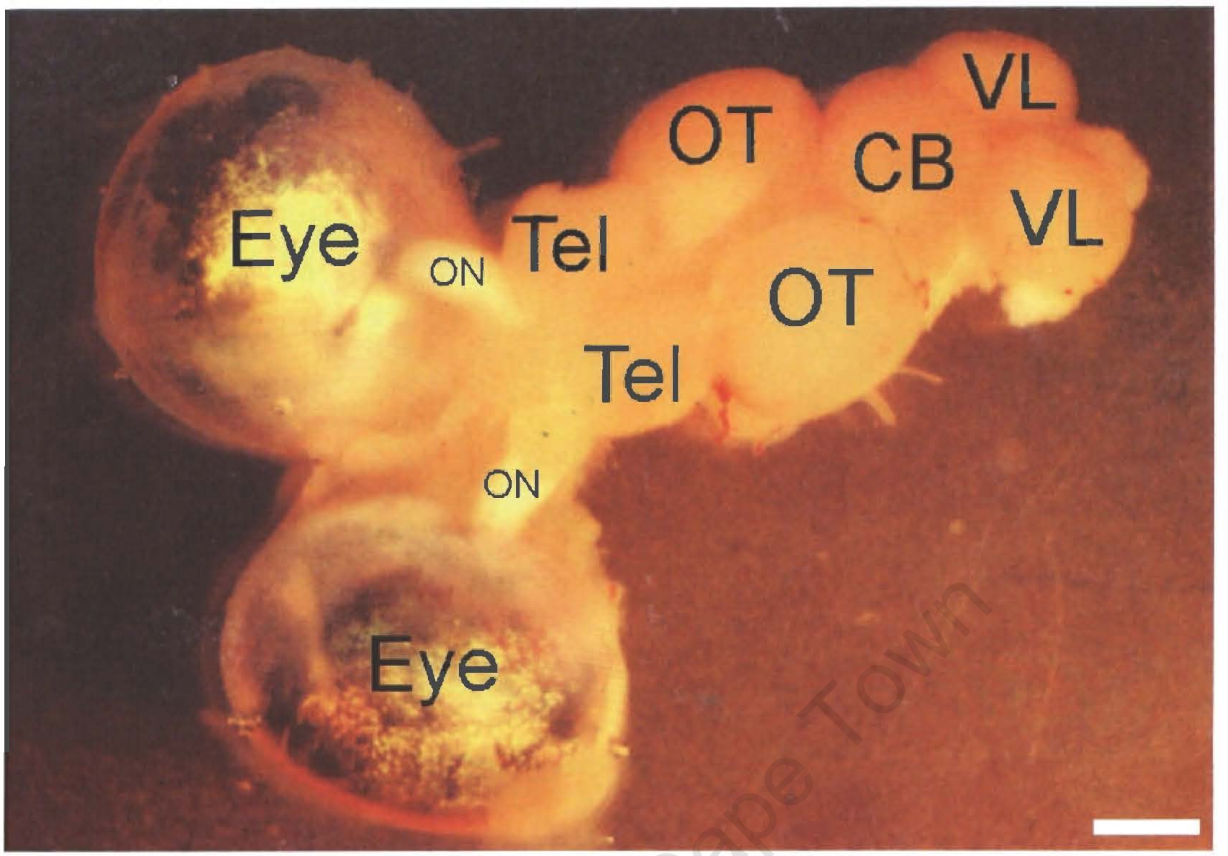

Figure 1. Gross anatomy of the adult goldfish brain, dorsal view. The brain consists of various lobes, most of which are paired. The axons of the retinal ganglion cells exit the retina at the back of the eye ball, run through the optic nerves (ON), which meet at the optic chiasm (not seen), and then form the optic tract (not seen) before terminating in the optic tectum (OT). Telencephalon (Tel), cerebellum (CB), and vagal lobe (VL). Scale bar = 1 mm

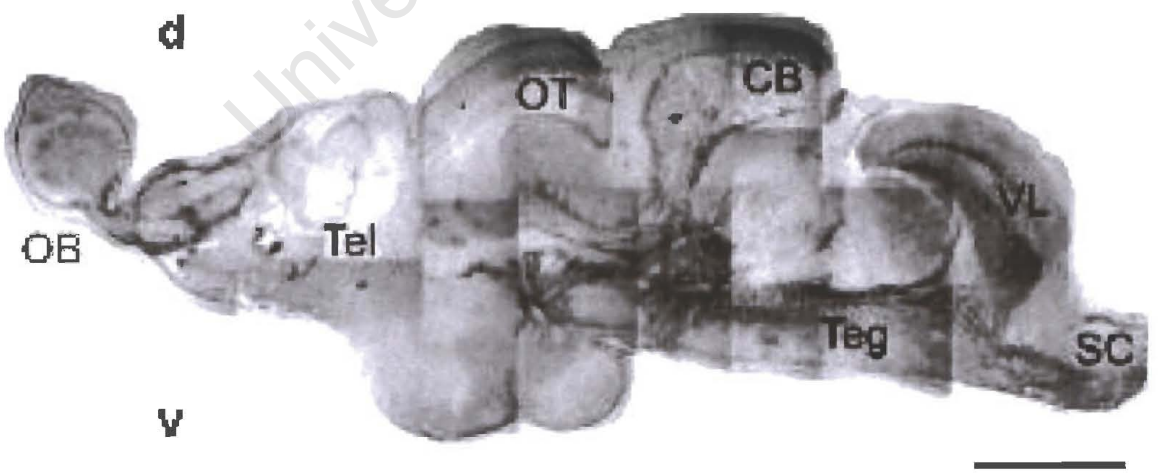

Figure 2. Overview of the expression pattern of TN-R in the adult goldfish brain. In sagital sections of the brain, TN-R immunoperoxidase labeling is associated with myelinated axon tracts in the olfactory bulb (OB), optic tectum (OT), cerebellum (CB), vagal lobe (VL), tegmentum (Teg), and spinal cord (SC). Telencephalon (Tel), dorsal (d) and ventral (v). Scale = 1 mm

3.3.1 TN-R expression in the retina

The retina is a highly organized tissue of the central nervous system (CNS) consisting of three major functional classes of neurons arranged in several layers: the photoreceptor cells, local interneurons (bipolar, horizontal, and amacrine cells), and the retinal ganglion cells (RGCs). The fluorescent stain 4',6-diamidino-2-phenylindole (DAPI) was used to stain the cell bodies of these neurons (Tarnowski et al., 1991). The outermost layer, closest to the pigmented part of the retina, contains the photoreceptor cells, namely the rods and cones. These cells lie in what is known as the outer nuclear layer (ONL; Figure 3a), and synapse with bipolar cells in the inner nuclear layer (INL; Figure 3a). Between these two layers, the photoreceptors, bipolar and horizontal cells make synaptic connections with each other in the outer plexiform layer (OPL; Figure 3a). The bipolar cells in turn synapse with RGCs, the axons of which run in the optic fiber layer (OFL; Figure 3a), and exit the eye in the optic nerve to deliver visual information to the brain. The bipolar, amacrine, and RGCs make synaptic connections with each other in the inner plexiform layer (IPL; Figure 3a).

At each designated time point in the retina on the side of the unlesioned optic nerve, there was intense TN-R immunoreactivity in the fascicles of RGC axons in the OFL (Figure 3b). The OFL was identified by the staining pattern of the rabbit polyclonal anti-epsilon 587 antigen (E587) antibody, which selectively labels new and regenerating RGC axons in the OFL (Vielmetter et al., 1991; Figure 3c, arrow heads). E587-positive fibers were observed growing in both TN-R-positive (Figure 3d, arrow heads) and TN-R-negative (Figure 3d, asterisks) regions in the OFL. TN-R immunoreactivity was also prominent in the OPL (Figure 3b).

In the retina on the side of the optic nerve that had received a crush injury 1 week earlier, TN-R expression remained more or less similar to what was observed in the retina on the side of the unlesioned optic nerve except that the intensity was weaker in some regions of the OFL while stronger throughout the OPL (compare figure 3b to figure 4a). At the same time point, there was an increase in the number of E587-positive fibers in the OFL (compare figure 3c to figure 4b), consistent with earlier observations during RGC axon regeneration (Ankerhold et al., 1998; Ankerhold and Stuermer, 1999). Whereas in the retina on the side of the unlesioned optic nerve only individual E587-positive fibers were seen; here E587-labeled fascicles of fibers were observed (Figure 4b, arrow heads). These new and regenerating axons were seen growing in both TN-R-positive (Figure 4c, arrow heads) and TN-R-negative (Figure 4c, asterisk) regions of the OFL. After 6 weeks, the intensity of TN-R immunoreactivity in the

OFL had still not returned to that seen in the retina on the side of the unlesioned optic nerve (compare figure 3b to figure 4d) but remained strong in the OPL. A further increase in the numbers of E587-positive fibers was seen at 3 (not shown) and 6 weeks (Figure 4e, arrow heads) after the optic nerve crush.

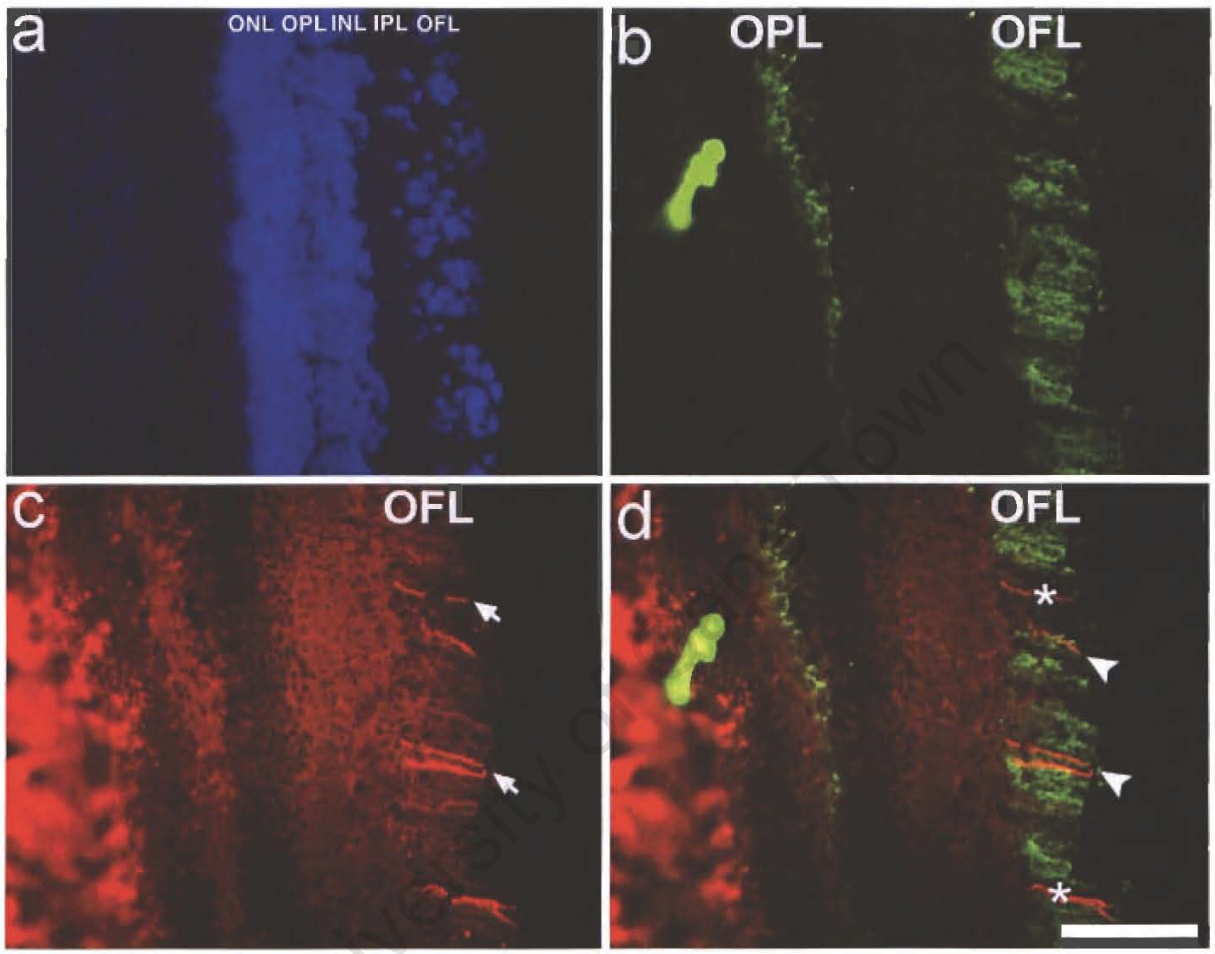

Figure 3. The expression pattern of TN-R in the retina before an optic nerve crush. (a), DAPI staining shows the arrangement of nuclei in the different retinal layers: the outer nuclear layer (ONL), outer plexiform layer (OPL), inner nuclear layer (INL), inner plexiform layer (IPL), and the optic fiber layer (OFL). **(b),** mouse monoclonal anti-TN-R antibodies stain the OFL as well as the OPL. **(c),** rabbit polyclonal anti-E587 antibodies label new retinal ganglion (RGC) axons in the OFL (arrows). **(d),** merged image of (c) and (d) shows E587-positive fibers growing in both TN-R-positive regions (arrow heads) and TN-R-negative (asterisk) of the OFL. Scale bar = 50 μm

3.3.2 Expression of TN-R ligands and ECM interaction partners in the retina

3.3.2.1 TN-R and F3

In the retina on the side of the unlesioned optic nerve, rabbit sera (24III) against the neural cell adhesion molecule F3 labeled a few RGC axons in the OFL (Figure 5b, arrow heads) and

weakly stained the other retinal layers (Figure 5b). These sparse F3-labeled fibers were seen growing in the TN-R-positive OFL (Figure 5c). One week after the optic nerve crush, the F3 (24III) sera labeled both an increased number of individual RGC axons (Figure 5e, arrow heads) and axon fasicles in the OFL (Figure 5e, arrow), as well as other axon profiles belonging to either bipolar, amacrine, and or RGCs in the IPL (Figure 5e, asterisk). F3-labeled fibers were observed growing in both TN-R-positive (Figure 5f, arrow heads) and TN-R-negative (Figure 5f, asterisk) regions of the OFL. Three weeks after the optic nerve crush, the polyclonal rabbit sera (41.6) against F3 labeled numerous RGC axons in the OFL (Figure 5h, arrow heads). These F3-labeled fibers were observed growing in TN-R-positive regions in the OFL, as evidenced by their colocalized yellow staining pattern (Figure 5i, arrow heads). By 6 weeks, only a few axons throughout the retinal layers were labeled by the F3 (41.6) sera (Figure 5k, arrow heads), and again these sparse fibers were seen growing in the TN-R-positive OFL, as evidenced by their colocalized yellow staining pattern (Figure 5l, arrow heads). At this time point, weak TN-R staining of perineuronal nets in the INL was also observed (Figure 5j, asterisk).

3.3.2.2 TN-R and CSPG

In the retina on the side of the unlesioned optic nerve, the mouse monoclonal antibody against chondroitin sulphate proteoglycans (CSPGs) stained the OFL (Figure 6b), where there was a significant colocalization of TN-R and CSPG expression (Figure 6c). Three weeks after the optic nerve crush this substantial degree of colocalization of TN-R and CSPG was still observed in the OFL and, to a lesser extent, in the OPL (Figure 6f). The change in the resulting colour of the superimposed red (CSPG) and green (TN-R) images from yellow before the lesion to orange 3 weeks after the lesion suggests that an increase in CSPG levels or a decrease in TN-R occurs after the optic nerve crush. By 6 weeks, however, both TN-R and CSPG immunoreactivity had decreased to levels weaker than those observed in the unlesioned retina (compare figure 6a to figure 6g and figure 6b to figure 6h, respectively) and only slight colocalization was still be observed in the OPL (Figure 6i).

3.3.2.3 TN-R and laminin

In the retina on the side of the unlesioned optic nerve, the rabbit polyclonal antibody against laminin labeled numerous processes of the OFL (Figure 7b, arrow heads), where there was significant colocalization of TN-R and laminin expression (Figure 7c). These processes could be related to blood vessels (Esser and Lin, 1988; Mandarino et al., 1993) but could also

belong to astocytes, which in mammals are known to express laminin (Leisi et al., 1984), or they could even belong to oligodendrocytes, which in fish are comparable to Schwann cells (Bastmeyer et al., 2004) which secrete laminin (Cornbrooks, 1983). Three weeks after the optic nerve crush, anti-laminin antibodies continued to intensely stain processes in the OFL (Figure 7e, arrow heads). Again, there was significant colocalization of TN-R and laminin staining in the OFL but spatial differences were seen in some areas, especially the outermost OFL, where the change in the resulting colour of the superimposed red (laminin) and green (TN-R) images from yellow before the lesion to orange three weeks after the lesion suggests that an increase in laminin levels or a decrease in TN-R occurs after the optic nerve crush (Figure 7f). No suitable section section from a six weeks postinjury goldfish optic nerve at the lesion site was cut or stained.

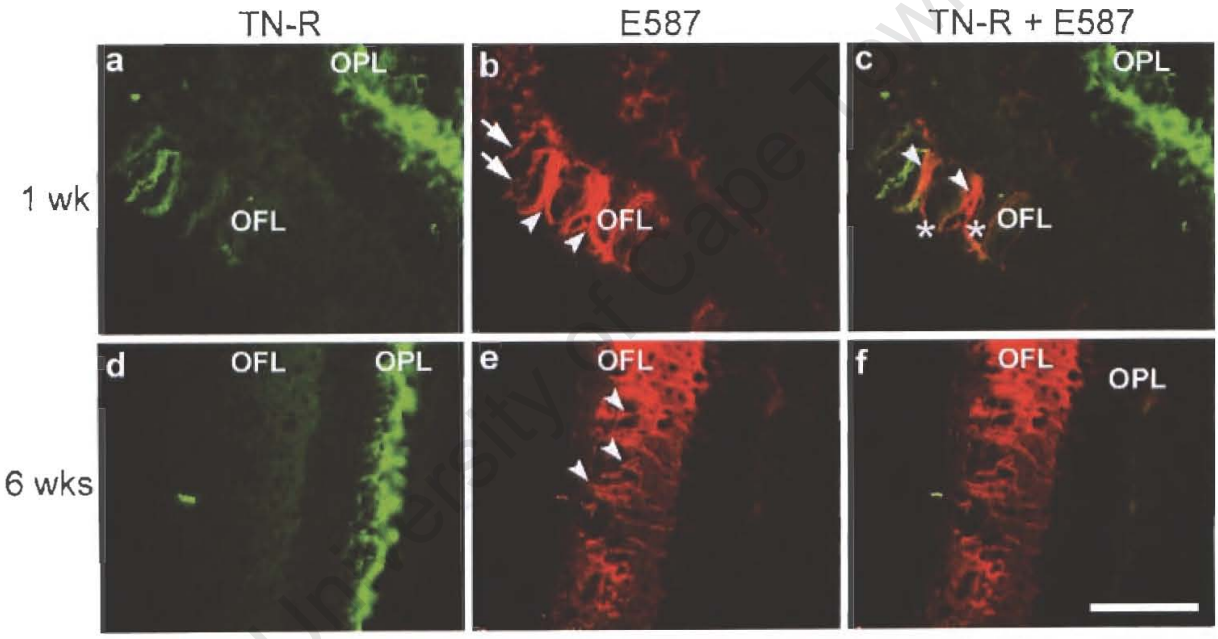

Figure 4. The expression pattern of TN-R and E587 in the retina after an optic nerve crush. **(a),** after 1 week (wk), the staining intensity of TN-R is weaker in some regions of the outer fiber layer (OFL) but remains strong in the outer plexiform layer (OPL). **(b),** after 1 wk, there is an increase in the number of E587-labeled fibers in the OFL. Both individual axons (arrows) and fascicles of axons (arrow heads) can be seen. **(c),** merged image of (a) and (b) shows E587-labeled fibers in both TN-R-positive and TN-R-negative (asterisk) regions (arrow heads) of the OFL. **(d),** after 6 wks, the staining intensity of TN-R in the OFL is weaker than in (a) but remains strong in the OPL. **(e),** after 6 weeks, there is a further increase in the number of E587-labeled fibers in the OFL. **(f),** merged image of (d) and (e) shows increased numbers of E587-labeled fibers growing in the TN-R-weak OFL. Scale bar = 50 μm

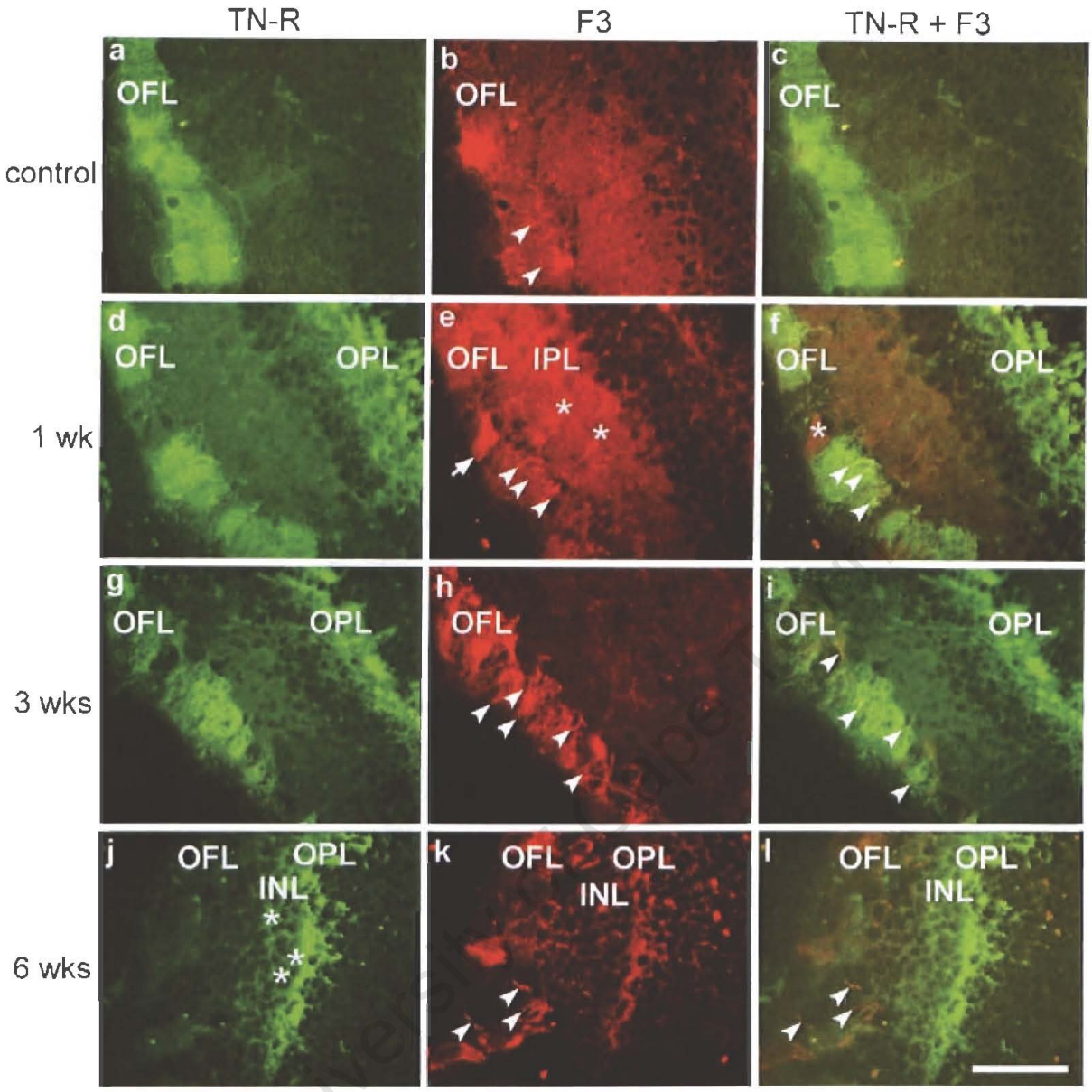

Figure 5. The expression pattern of TN-R and F3 in the retina before and after an optic nerve crush. **(a)**, in the retina on the side of the unlesioned optic nerve (control); mouse monoclonal antibodies against TN-R intensely stain the OFL. **(b)**, in the control retina, rabbit F3 (24III) sera stains isolated RGC fibers (arrow heads) in the OFL. **(c)**, merged image of (a) and (b) shows that these few F3-positive fibers are growing in TN-R-positive regions of the OFL. **(d)**, in the retina on the side of the lesioned optic nerve after 1 week (wk), intense TN-R immunoreactivity is still observed in the OFL as well as in the OPL. **(e)**, after 1 wk there is an increased number of individulal RGC fibers (arrow heads) as well as fascicles of RGCs (arrow) labeled with F3(24III) in the OFL. **(f)**, merged image of (d) and (e) shows these F3-positive fibers growing in both TN-R-positive (arrow heads) and TN-R-negative (asterisk) regions of the OFL. **(g)**, after 3 wks the intensity of TN-R immunoreactivity is decreased in the OFL compared to at 1 wk in (d) but increased in the OPL. **(h)**, in the retina on the side of the lesioned optic nerve after 3 wks, F3 (41.6) sera labels numerous RGC fibers in the OFL (arrow heads). **(i)**, merged image of (g) and (h) shows that these F3-positive fibers are growing in TN-R-positive regions of the OFL, as evidenced by their colocalized yellow staining (arrow heads). **(j)**, in the retina on the side

of the lesioned optic nerve after 6 wks, the intensity of TN-R immunoreactivity in the OFL is further decreased compared to at 3 wks in (g) but remains strong in the OPL. Weak TN-R staining of perineuronal nets (asterisk) in the INL is also observed. **(k),** in the retina on the side of the lesioned optic nerve after 6 wks, only a few fibers throughout the retinal layers were labeled with F3 (41.6) sera. **(l),** these sparse F3-positive fibers were seen growing in the TN-R-positive OFL as evidenced by their colocalized yellow/orange staining (arrow heads). Scale bar = 50 μm

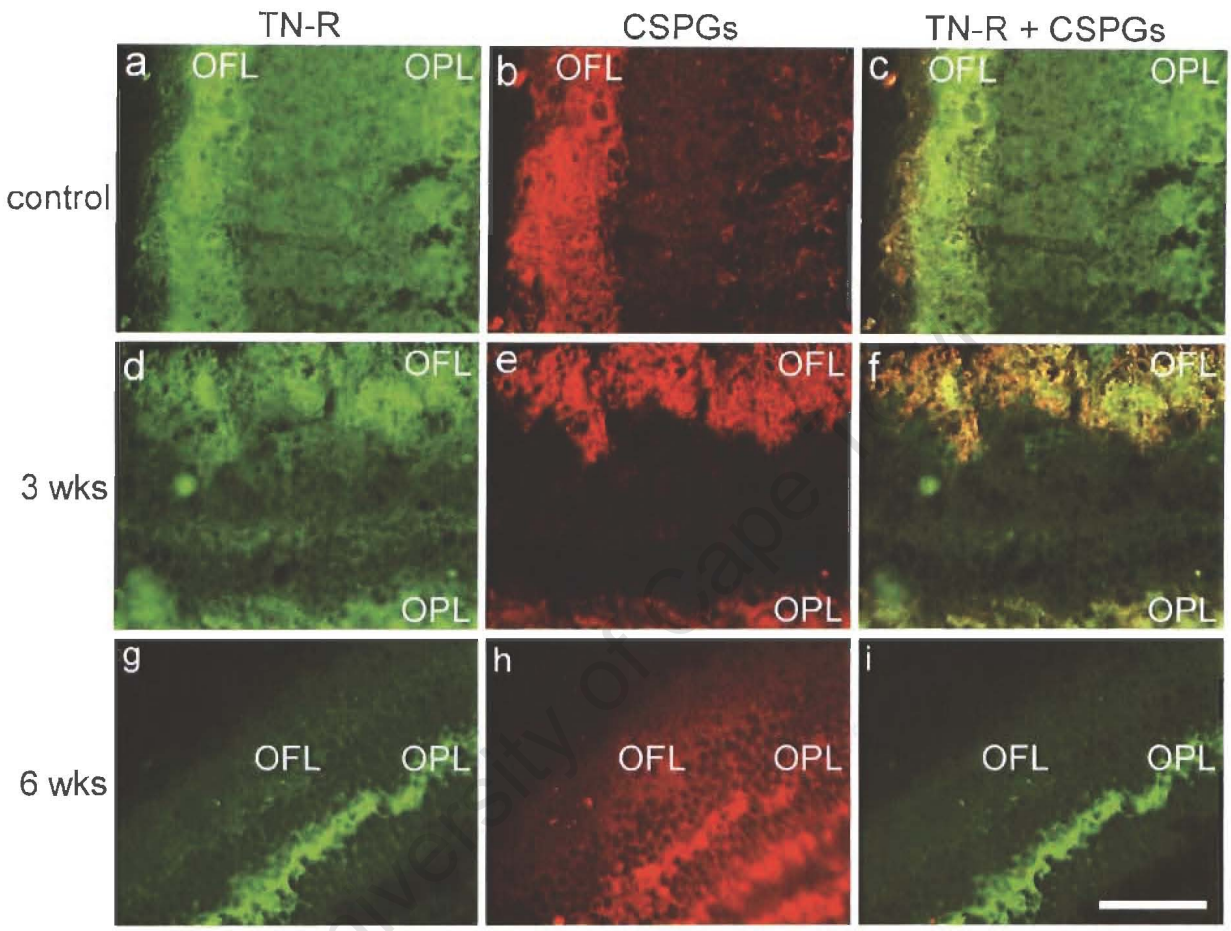

Figure 6. The expression pattern of TN-R and CSPGs in the retina before and after an optic nerve crush. **(a),** in the retina on the side of the unlesioned optic nerve (control), rabbit polyclonal antidodies against TN-R intensely stain the OFL. **(b),** in the control retina, mouse monoclonal antibodies against CSPGs also intensely stain the OFL. **(c),** merged image of (a) and (b) shows that TN-R and CSPG colocalize substantially in the OFL. **(d),** in the retina on the side of the lesioned optic nerve after 3 weeks (wks), TN-R continued to be strongly expressed in the OFL as well as in the OPL. **(e),** after 3 wks, CSPGs also continued to be strongly expressed in the OFL as well as in the OPL. **(f),** merged image of (d) and (e) shows that TN-R and CSPG continue to colocalize in the OFL and in the OPL. **(g),** after 6 wks, the intensity of TN-R immunoreactivity in the OFL was markedly decreased compared to at 1 wk post-injury in (d). **(h),** after 6 wks, the intensity of CSPG immunoreactivity in the OFL was markedly decreased compared to at 1 wk post-injury in (e). **(i),** merged image of (g) and (h) shows that TN-R and CSPG only somewhat colocalize in the OPL. Scale bar = 50 μm

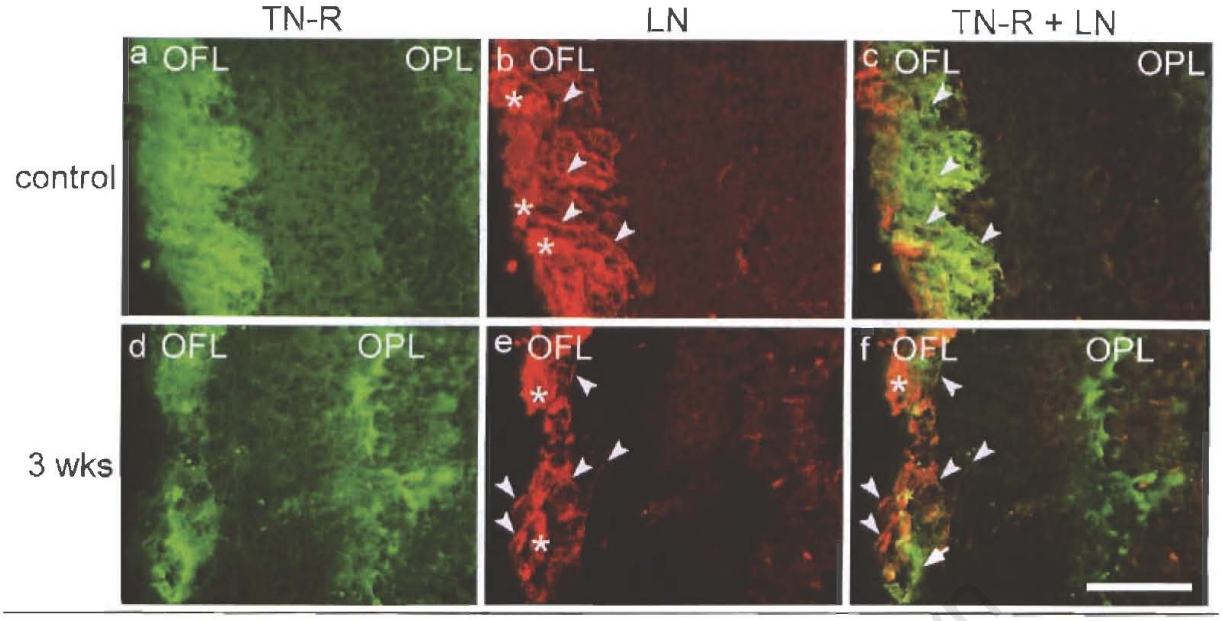

Figure 7. The expression pattern of TN-R and laminin in the retina before and after an optic nerve crush. **(a),** in the retina on the side of the unlesioned optic nerve (control), mouse monoclonal antibodies against TN-R intensely stain the OFL and weakly stain the OPL. **(b),** in the control retina, rabbit polyclonal antibodies against laminin (LN) stain many processes in the OFL (arrow heads). There are also regions of intense LN staining where individual processes are indiscernible (asterisk). **(c),** merged image of (a) and (b) shows that these numerous LN-labeled processes colocalize considerably with TN-R in the OFL (arrow heads), as evidenced by their orange/yellow staining. **(d),** in the retina on the side of the lesioned optic nerve after 3 weeks (wks), the intensity of TN-R immunoreactivity remained intense in the OFL and labeling in the OPL was stronger. **(e),** 3 wks after the optic nerve crush, there was an increase in the number of LN-stained processes in the OFL. (f), merged image of (d) and (e) shows that these LN-stained processes colocalized with TN-R in some regions of the OFL (arrow heads), while in other regions the LN staining predominated (asterisk) or the TN-R staining predominated (arrow). Scale bar = 50 µm

3.3.2.4 TN-R and fibronectin

In the retina on the side of the unlesioned optic nerve, rabbit polyclonal antibodies against fibronectin labeled isolated processes in the OFL (Figure 8b, arrow heads), where there was a significant colocalization of TN-R and fibronectin expression (Figure 8c). One week after the optic nerve crush, there was an increase in the number of fibronectin-stained processes and some of them were seen in the more inner retinal layers (compare the number of arrow heads in figure 8b with figure 8e). These processes may be related to blood vessels but could also belong to astrocytes which, in mammals, are known to express fibronectin (Leisi et al., 1984; Tom et al., 2004) and enter the retina where they are closely associated with blood vessels in the OFL (Jiang et al., 1994; MacLaren, 1996). Again, there was significant colocalization of TN-R and fibronectin staining in the OFL (Figure 8f). The maximum number of fibronectin-

stained processes was seen at 3 weeks (Figure 8h, arrow heads). After 6 weeks, there were still more fibronectin-labeled processes in the OFL compared to in the unlesioned retina (compare the number of arrow heads in figure 8b with figure 8k), and fibronectin-labeled processes were seen within the TN-R-positive OFL (Figure 8l).

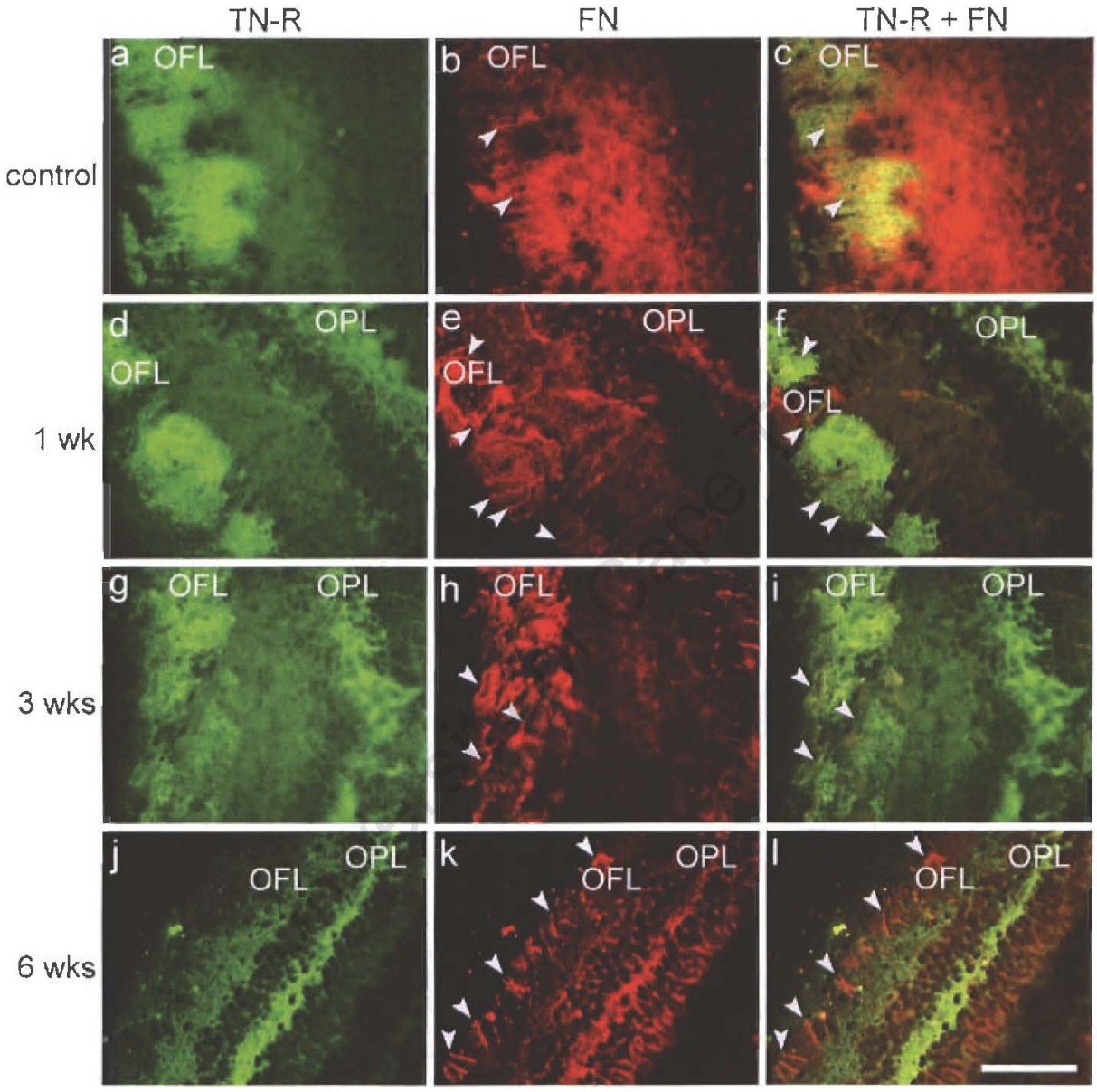

Figure 8. The expression pattern of TN-R and fibronectin in the retina before and after an optic nerve crush. (a), in the retina on the side of the unlesioned optic nerve (control), monoclonal antibodies against TN-R intensely label the OFL. **(b),** in the control retina, polyclonal antibodies against fibronectin (FN) stain a few isolated processes in the OFL (arrow heads). **(c),** merged image of (a) and (b) shows that these few FN-labeled processes colocalize with TN-R in the OFL (arrow heads), as evidenced by their orange/yellow staining. **(d),** in the retina on the side of the lesioned optic nerve after 1 week (wk), the intensity of TN-R immunoreactivity remained strong in the OFL and labeling could also be seen in the OPL. **(e),** 1 wk after the optic nerve crush, there was an increase in the number of FN-labeled processes in the OFL compared to in the control retina in (b).

(f), merged image of (d) and (e) shows that these FN-stained processes colocalize with TN-R in the OFL (arrow heads), as evidenced by their orange/yellow staining. **(g),** 3 wks after the optic nerve crush the intensity of TN-R immunoreactivity in the OFL and OPL still remains intense. **(h),** 3 wks after the optic nerve crush the intensity of FN-immunoreactivity in the OFL was at its highest. A few individual FN-labeled processes could be seen within the FN-positive OFL (arrow heads). **(i),** merged image of (g) and (h) shows that there is still considerable colocalization between TN-R and FN in the OFL and that the individual FN-labeled processes colocalize with TN-R there (arrow heads), as evidenced by their orange/yellow staining. **(j),** 6 wks after the optic nerve crush, the intensity of TN-R immunoreactivity in the OFL is weaker compare to at 1 wk in (d) and 3 wks in (g). **(k),** 6 wks after the optic nerve crush, although the overall intensity of FN staining in the OFL was weaker than at 3 wks in (e), there are still more FN-labeled processes in the OFL (arrow heads) compared to in the control retina in (b). **(l),** a merged image of (j) and (k) shows that these FN-labeled processes lie within the TN-R-positive OFL (arrow heads). Scale bar = 50 µm

3.3.3 TN-R expression in the optic nerve

The optic nerve contains bundles of RGC axons that form fascicles that are bound by the glia limitans and surrounded by a connective tissue sheath. Blood vessels are also contained within the nerve. The only cell bodies found in the optic nerve belong to glial cells, either those of oligodendrocytes, which myelinate the RGC axons, or those of astrocytes, which partition the fascicles and contribute to the glial limitans. Connective tissue cell nuclei are also present as fibroblasts and leptomeningeal cells are located in the outer nerve sheath and between the fascicles.

The unlesioned nerves were easily recognized by their orderly arranged rows of predominantly glial nuclei (Figure 9b), myelin-basic protein (MBP)-positive myelinated axons (Figure 9d), and clusters of E587 stained fibers at the nerve margin (Figure 9f, arrow heads). TN-R staining in the unlesioned optic nerve was weak at low magnification (Figure 14a) but at higher magnification was seen to be ECM-associated and punctate in appearance (Figure 14b). Double-labeling of E587 and TN-R proved unreliable: the TN-R antibodies seemed to bind to the E587 antibodies such that TN-R staining pattern looked very similar to the E587 staining pattern. A combination of TN-R and the TAG-1 antibody, which labels a subpopulation of RGCs, was therefore used to determine whether newly growing axons grew within or avoided TN-R-positive regions of the intact optic nerve. Interestingly, TAG-1-positive RGC axons were seen traversing TN-R-positive regions of the uninjured optic nerve (Figure 10c, arrow heads), suggesting that the growth of these axons during the normal lifetime of the goldfish is not inhibited by the presence of TN-R.

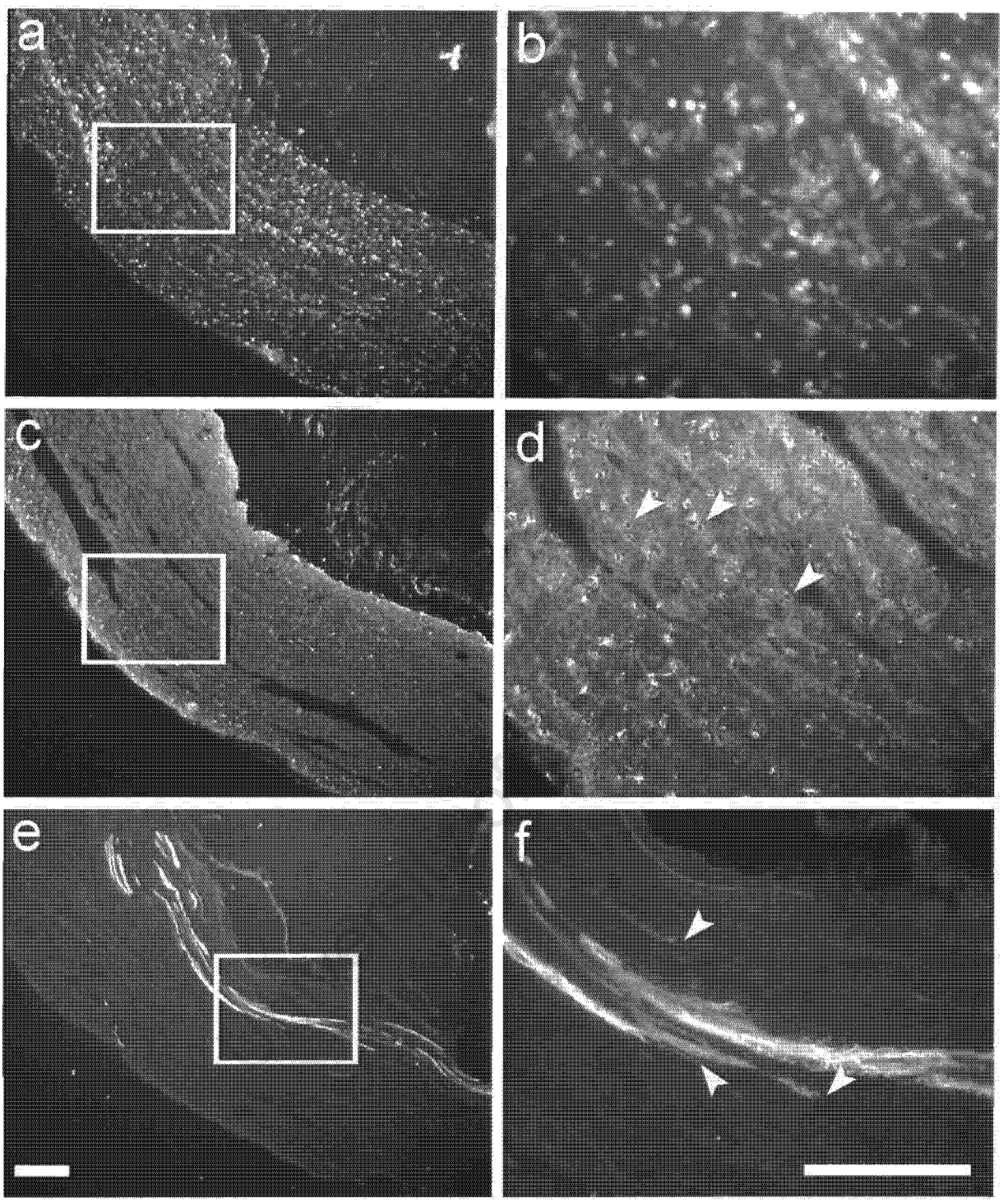

Figure 9. Characterization of the unlesioned adult goldfish optic nerve. **(a),** DAPI stains the orderly arranged rows of nuclei. **(b),** high power magnification of insert in (a) shows typical nuclei staining. **(c),** rat monoclonal anti-MBP antibodies stain the myelin sheaths. **(d),** high power magnification of insert in (c) shows oligodendrocyte cell bodies. Some oligodendocytes have been cut in cross-section and are seen as ring-like structures (arrow heads). **(e),** rabbit polyclonal anti-E587 antibodies stain a small population of newly growing RGC axons along the periphery of the optic nerve. **(f),** high power magnification of insert in (e) shows individual RGC axons (arrow heads). Scale bar in (a), (c), and (e) = 100 μm, Scale bar in (b), (d), and (f) = 50 μm

Figure 10. The expression pattern of TN-R and TAG-1 in the unlesioned nerve. (a), mouse monoclonal TN-R antibodies stain the neural component of the optic nerve. **(b),** rabbit polyclonal anti-TAG-1 antibodies stain the axons of newly growing nasal retinal ganglion cells (RGCs) growing along the optic nerve. **(c),** merged image of (a) and (b) shows TAG-1 labeled axons growing in TN-R-positive regions of the optic nerve. Scale bar = 100 μm

One week after the optic nerve crush had been performed; the regenerating nerve had a very different appearance. There was an increase in the number of nuclei at the lesion site (Figure 11a, arrow heads), probably corresponding to invading fibroblasts and proliferating astrocytes (Hirsch et al., 1995). The nuclei had lost their linear arrangement and some appeared pyknotic. There was also a marked decrease in the intensity of MBP staining, particularly at the lesion site (Figure 11c), indicating that the oligodendrocytes there had died or dedifferentiated (Ankerhold and Stuermer, 1998). The increase in E587 immunoreactivity above the lesion site, on the retina side (Figure 11d), indicated that new and regenerating RGC axons had begun their journey of regrowth back towards the optic tectum. In fact, a few individual RGC axons had already crossed the lesion site (Figure 11e, arrow heads). The oligodendrocytes in the lesion site also downregulated TN-R expression there (Figure 14c, asterisk). Although the TN-R staining intensity was weaker at the lesion site, it was maintained in the part of the optic nerve adjacent to the retina (Figure 14d) and in the part of the optic nerve adjacent to the chiasm (Figure 14e) at levels comparable to and possibly even higher than, the unlesioned nerve (Figure 16b).

After 3 weeks, the majority of the regenerating RGC axons had crossed the lesion site, as indicated by the staining of E587-labeled fibers along the length of the nerve (Figure 12e). At this stage the oligodendrocytes at the lesion site had not yet begun reexpressing MBP (Figure 12d) but had begun reexpressing TN-R both directly above and below the lesion site (Figure 15a and figure 15d), while at the lesion site itself, TN-R staining was still sparse (Figure 14g). In the region of the optic nerve adjacent to the chiasm, there seemed to be a slight decrease in TN-R staining intensity compared to the unlesioned optic nerve but there was by

no means a downregulation of TN-R (Figure 16d). No suitable section from a six weeks postinjury goldfish was cut or stained.

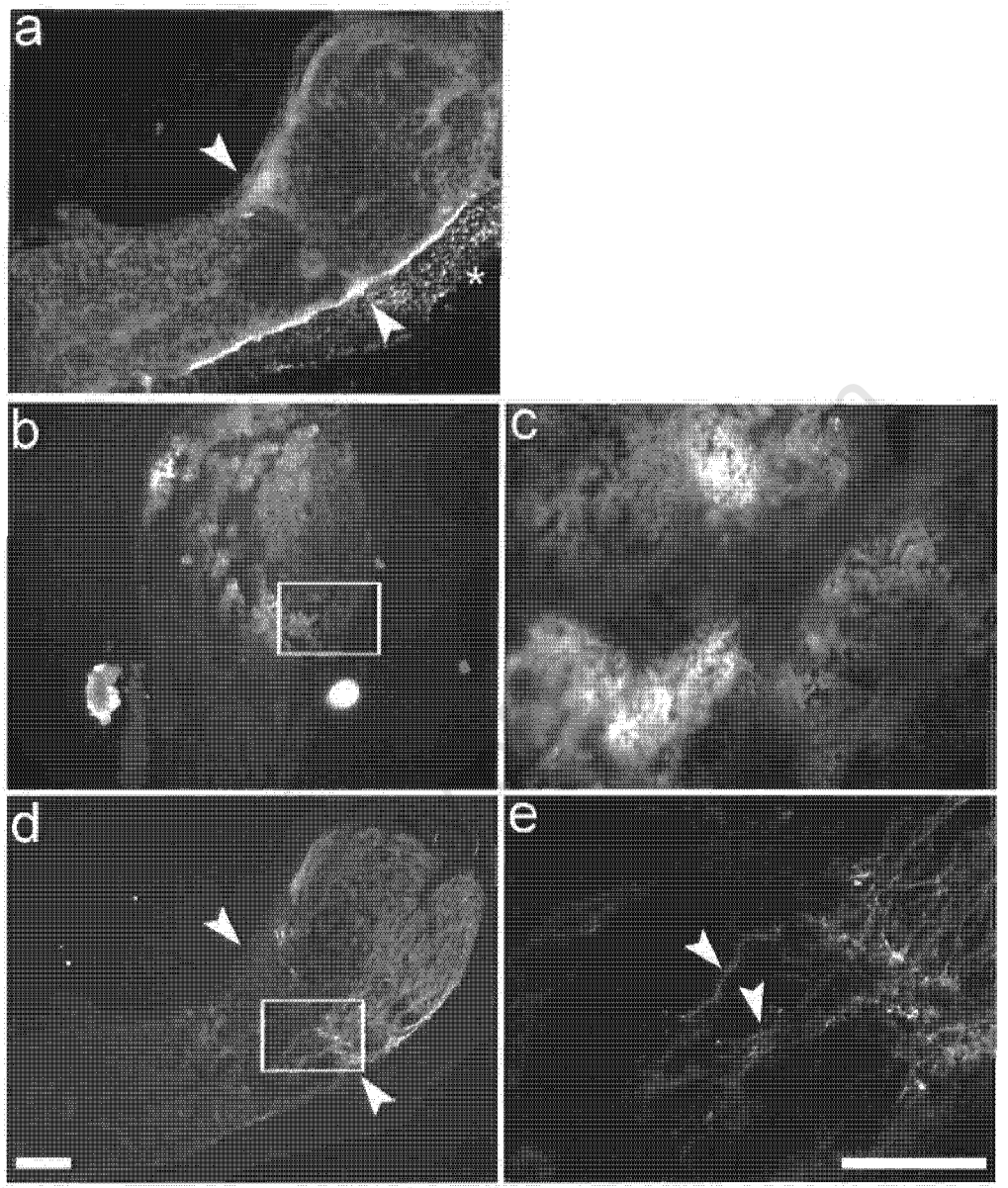

Figure 11. Characterization of the lesioned optic nerve 1 week after an optic nerve crush. **(a),** DAPI stains an increased number of nuclei, especially near the lesion site (between the arrow heads). Connective tissue nuclei in the optic tendon, which is closely associated with the nerve, can be seen (asterisk). **(b),** anti-MBP antibodies weakly stain the injured nerve. **(c),** high power magnification of insert in (b) shows regions of nerve where some oligodendrocytes have dedifferentiated and downregulated MBP expression. **(d),** anti-E587 antibodies intensely label the axons of newly growing and regenerating RGCs as they begin to traverse the lesion site (arrow heads). **(e),** high power magnification of insert in (d) shows individual RGC axons (arrow heads) which have already crossed the lesion site. Scale bar in (a), (b), and (d) = 100 μm, Scale bar in (c), and (e) = 50 μm

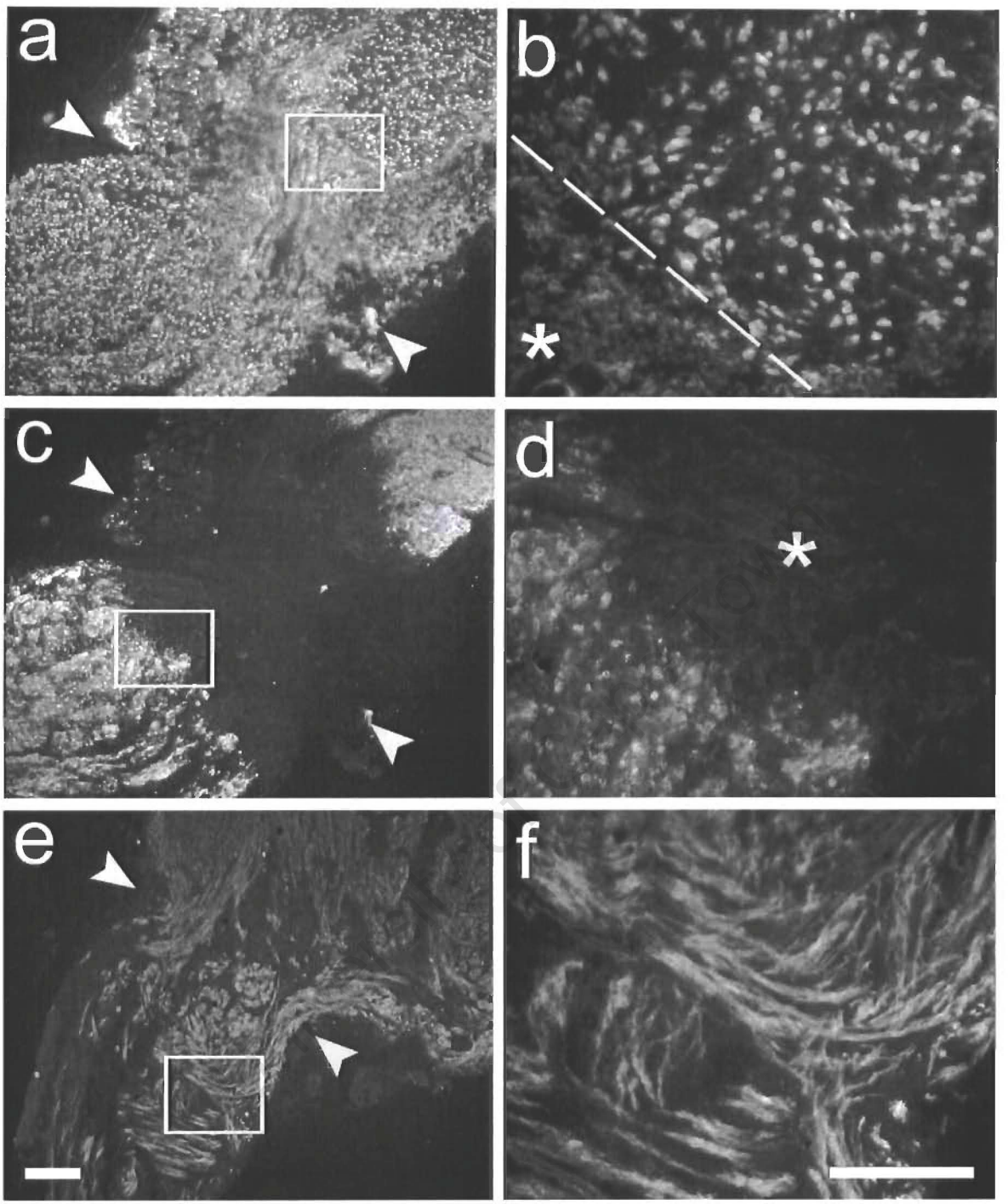

Figure 12. Characterization of the lesioned optic nerve 3 weeks after an optic nerve crush. (a), DAPI stains an even greater number of nuclei, particularly in the lesion site (between the arrow heads). **(b),** high power magnification of insert in (a) shows typical nuclei above of the lesion site (dashed line) along side atypical nuclei in the lesion site (asterisk). **(c),** MBP staining in the lesion site (between the arrow heads) is absent. **(d),** high power magnification of the insert in (c) shows oligodendrocytes below the lesion site, on the optic chiasm side, which continue to express MBP. **(e),** E587-labeled fascicles of regenerating RGC axons extend throughout the length of the nerve. **(f),** high power magnification of insert in (d) shows individual RGC axons which have crossed the lesion site and are approaching the optic chiasm. Scale bar in (a), (c), and (e) = 100 μm, Scale bar in (b), (d), and (f) = 50 μm

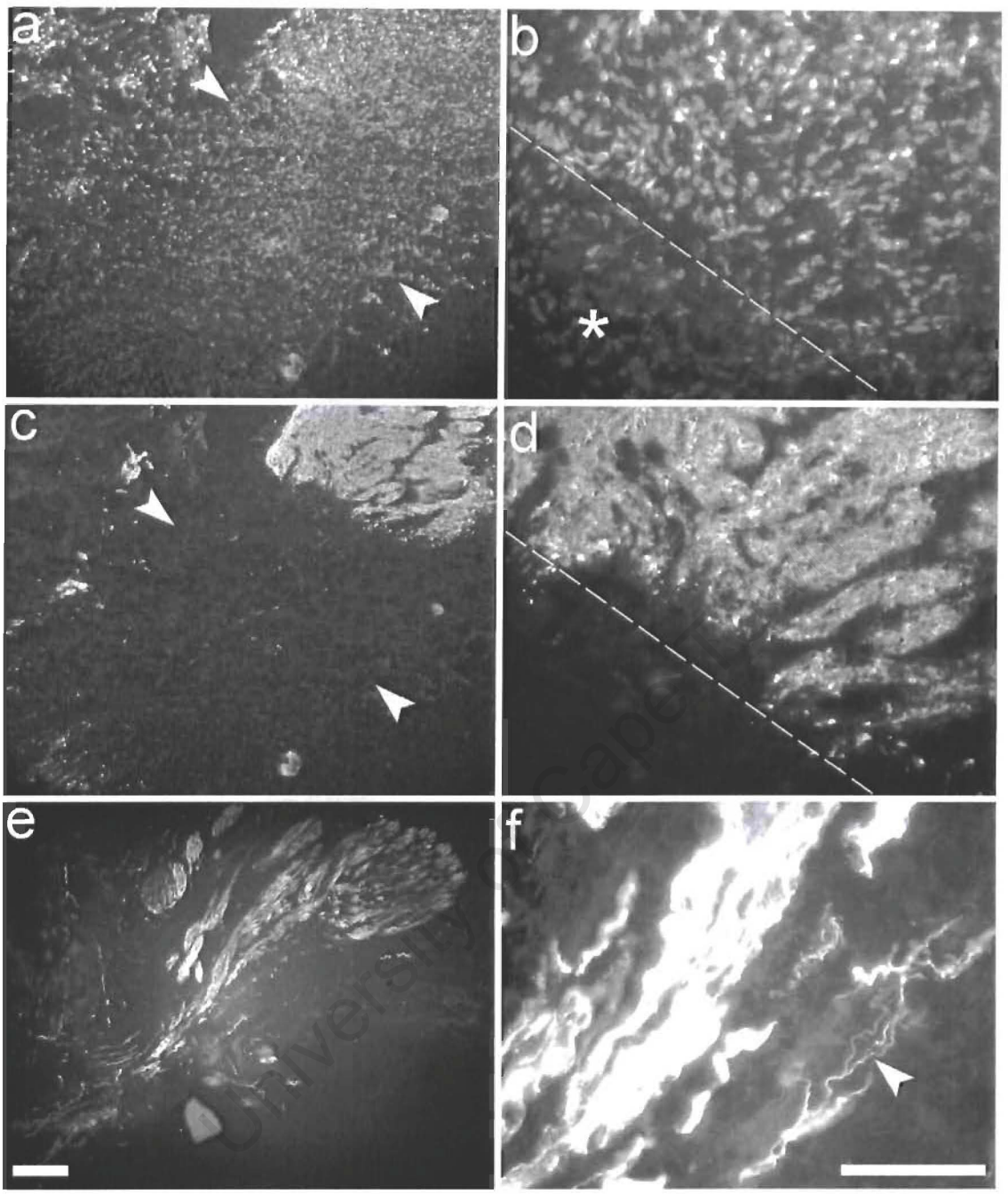

Figure 13. Characterization of the lesioned optic nerve 6 weeks after an optic nerve crush. (a), DAPI staining continues to delineate the lesion site (between the arrow heads) by virtue of the numerous and disorderly arranged nuclei. **(b),** high power magnification of insert in (a) shows typical nuclei above the lesion site (dashed line) along side atypical nuclei in the lesion site (asterisk). **(c),** absence of MBP staining in the lesion site (between arrow heads) is still observed. **(d),** high power magnification of insert in (c) shows oligodendrocytes above the lesion site (dashed line), which continue to express MBP. **(e),** anti-E587 antibodies continue to stain numerous fascicles of regenerating RGC axons throughout the length of the nerve. **(f),** high power magnification of insert in (d) shows both individual RGC axons (arrow head) as well as larger fascicles of axons. Scale bar in (a), (c), and (e) = 100 μm, Scale bar in (b), (d), and (f) = 50 μm

Six weeks post-injury, by which time most of the regenerating RGC axons would have reached the tectum, there was continued upregulation of E587 expression (Figure 13e). The oligodendrocytes located at the lesion site had still not yet differentiated into mature myelinating phenotypes, as evidenced by the persistent absence of MBP staining (Figure 13c). At this point in the time course, TN-R expression at the lesion site was slighty stronger than at 3 weeks post-injury but was still weaker compared to unlesioned optic nerve levels (not shown). At the chiasm-near end of the optic nerve, the intensity of TN-R staining in the 6 weeks post-injury optic nerve was however comparable to that observed in the unlesioned optic nerve (Figure 16f).

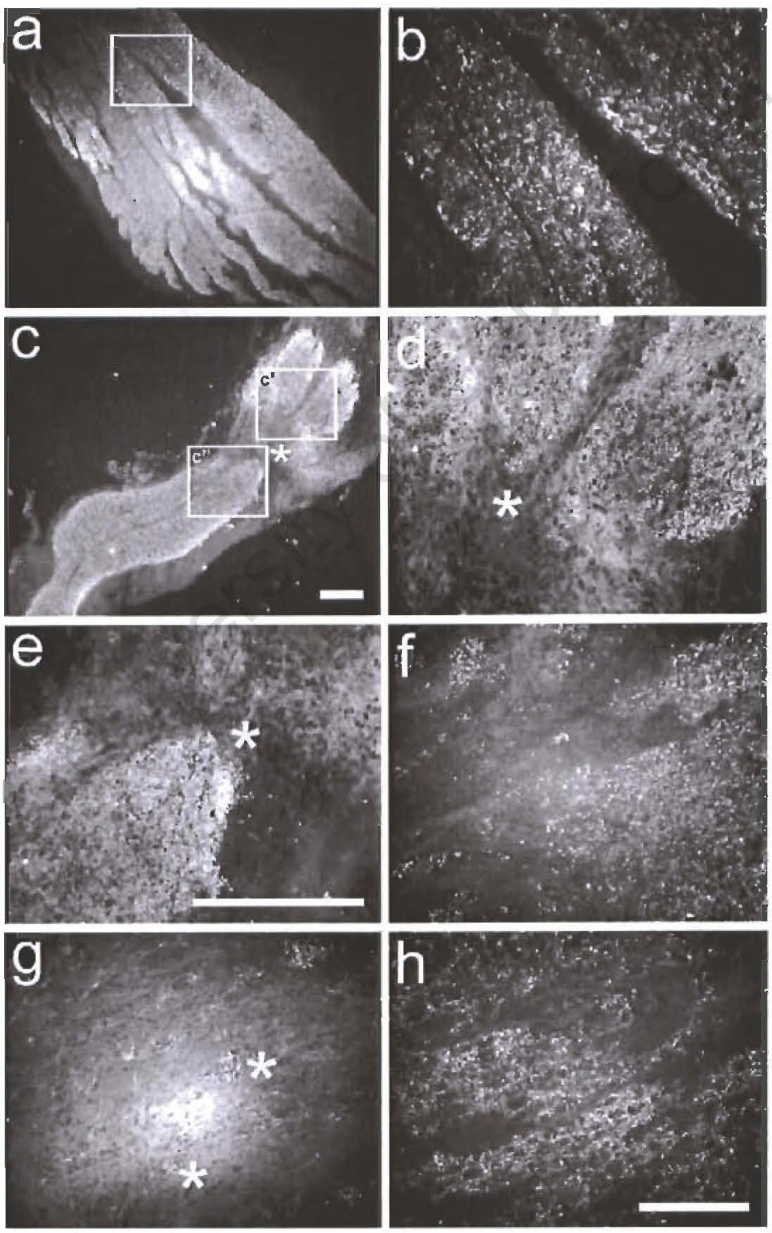

Figure 14. Expression of TN-R in the unlesioned and regenerating optic nerve. (a), anti-TN-R antibodies weakly stain the unlesioned nerve. **(b),** high power magnification of insert in (a) shows punctuate staining of

TN-R within the ECM of the fascicles. **(c),** one week after the optic nerve injury, TN-R staining is markedly decreased at the lesion site (asterisk). **(d),** high power magnification of (c') shows that TN-R continues to be expressed in the lesioned nerve in regions above the lesion site (asterisk), on the retina side. **(e),** high power magnification of (c") shows that TN-R also continues to be expressed in the lesioned nerve in regions below the lesion site (asterisk), on the chiasm side. **(f),** 3 weeks after the optic nerve injury, a high power magnification of the nerve above the lesion site, on the retina side, shows a weaker intensity of TN-R staining compared to at 1 week in (d). **(g),** 3 weeks after the optic nerve injury, a high power magnification of the nerve at the lesion site shows only weak TN-R staining. **(h),** 3 weeks after the optic nerve injury, a high power magnification of the nerve below the lesion site, on the chiasm side, shows a weaker intensity of TN-R staining compared to at 1 week in (e). Scale bar in (a) and (c) = 100 μm, Scale bar in (b), (d), (e) = 100 μm, Scale bar in (f), (g) and (h) = 50 μm

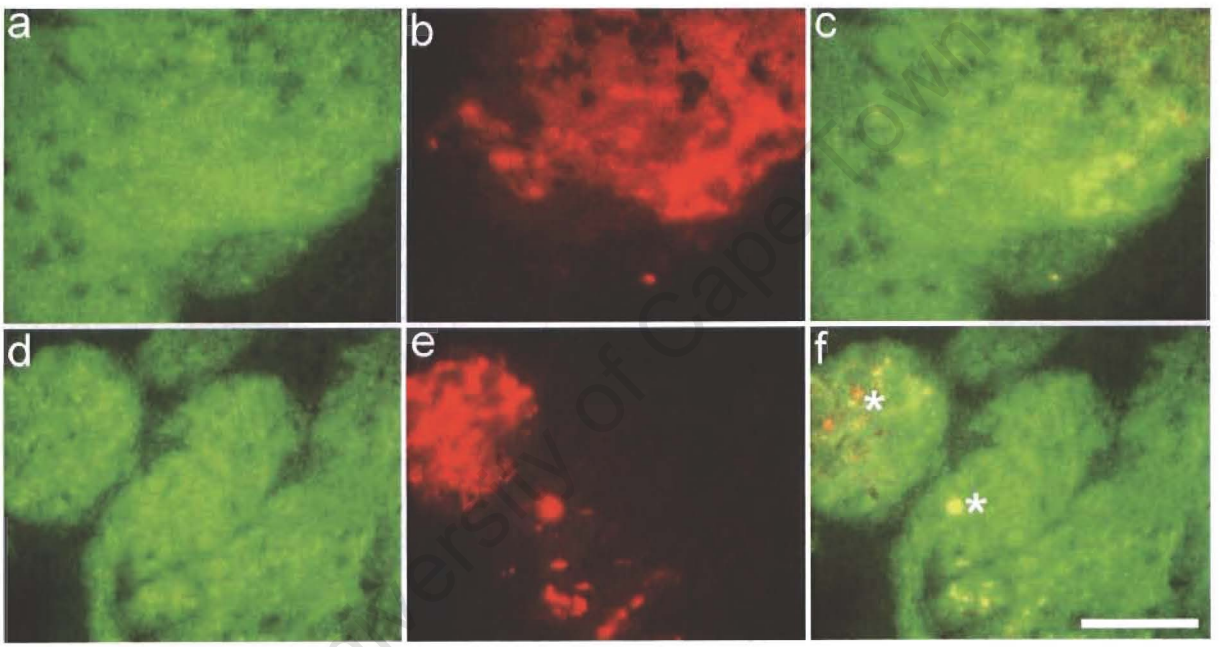

Figure 15. Reoccupation of the lesion site by TN-R–expressing but not MBP-expressing oligodendrocytes 3 weeks after an optic nerve crush. (a), rabbit polyclonal anti-TN-R antibodies stain the optic nerve immediately above the lesion site, on the retina side. **(b),** monoclonal rat anti-MBP antibodies stain a smaller area of the corresponding nerve region in (a). **(c),** merged image of (a) and (b) shows that olidogendrocytes immediately above the lesion site, on the retina side, begin upregulating TN-R expression before MBP expression, as evidenced by the predominantly green staining. **(d),** TN-R staining in the optic nerve immediately below the lesion site, on the chiasm side. **(e),** MBP staining is weak in the the corresponding nerve region in (d). **(f),** merged image of (d) and (e) shows that oligodendrocytes immediately below the lesion site, near the chiasm end, begin upregulating TN-R expression before MBP expression, as evidenced by the predominantly green staining. There were a few spots of colocalized TN-R and MBP staining (asterisk). Scale bar = 50 μm.

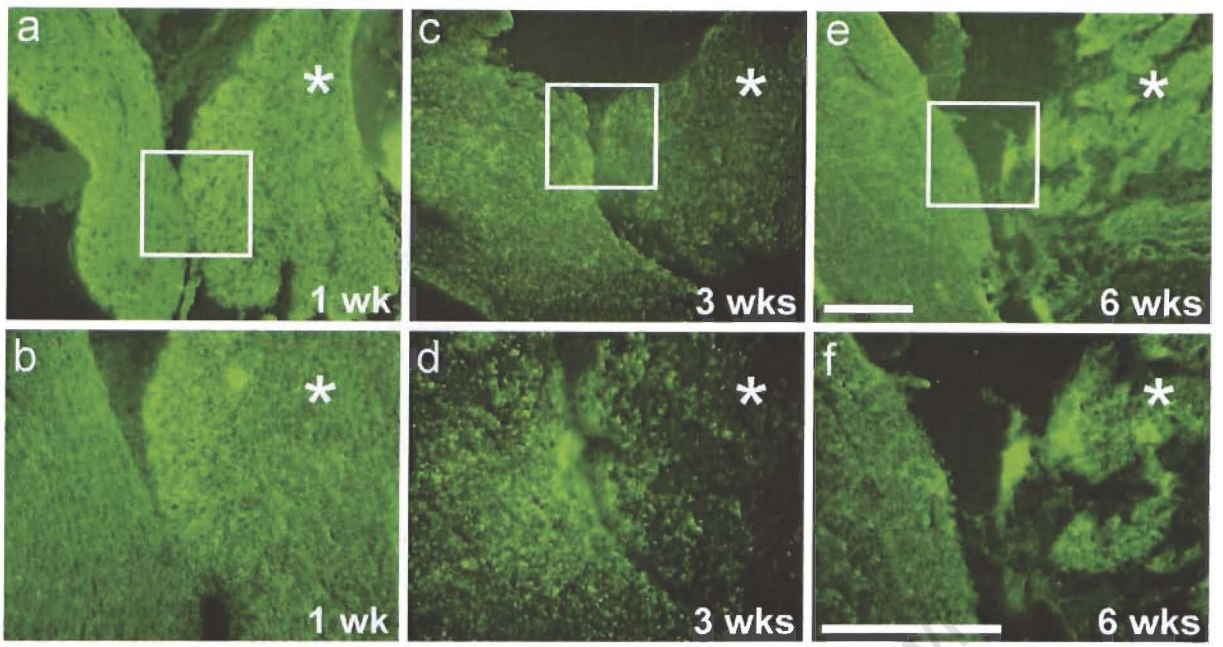

Figure 16. Expression of TN-R at the optic chiasm during optic nerve regeneration. a), 1 week (wk) after the optic nerve crush, intense TN-R staining is seen in the unlesioned and lesioned (asterisk) optic nerve. **(b),** high power magnification of insert in (a) shows that the intensity of TN-R staining in the lesioned nerve (asterisk) is comparable to, if not higher than, in the unlesioned nerve. **(c),** 3 wks after the optic nerve crush, TN-R staining was still observed in the lesioned optic nerve (asterisk). **(d),** high power magnification of insert in (c) shows that the intensity of TN-R staining in the lesioned nerve (asterisk) was slightly weaker than in the unlesioned nerve. **(e),** 6 wks after the optic nerve crush, detectable levels of TN-R staining are still observed in the lesioned optic nerve (asterisk). **(f),** high power magnification of insert in (e) shows that the intensity of TN-R staining in the lesioned nerve (asterisk) was comparable to, if not slighter weaker than, in the unlesioned nerve. Scale bar in (a), (c), and (e) = 100 μm, Scale bar in (b), (d) and (f) = 100 μm

3.3.4 Expression of TN-R ligands and ECM interaction partners in the optic nerve

3.3.4.1. TN-R and F3

The unlesioned nerves at all time points displayed a typical F3 staining pattern, whereby individual RGC axons could be visualized within axon fascicles (Figure 17a). One week after the optic nerve crush, only a few F3-labeled fibers were seen in the optic nerve immediately adjacent to the retina (Figure 17d). These few fibers probably correspond to new and/or regenerating RGC axons. Elsewhere throughout the lesioned nerve, F3 staining was not observed (not shown). Six weeks after the optic nerve crush, F3-labeled fibers were observed in regions of the optic nerve below the lesion site, at the chiasm end (Figure 17g). In most instances the F3-labeled fibers were closely aligned with glial cells, indicated by their proximity to DAPI-labeled nuclei (Figure 16i), as has previously been reported (Haenisch et

al., 2005). The presumptive F3-expressing glial cells were located in TN-R-postive regions of the nerve (Figure 17h).

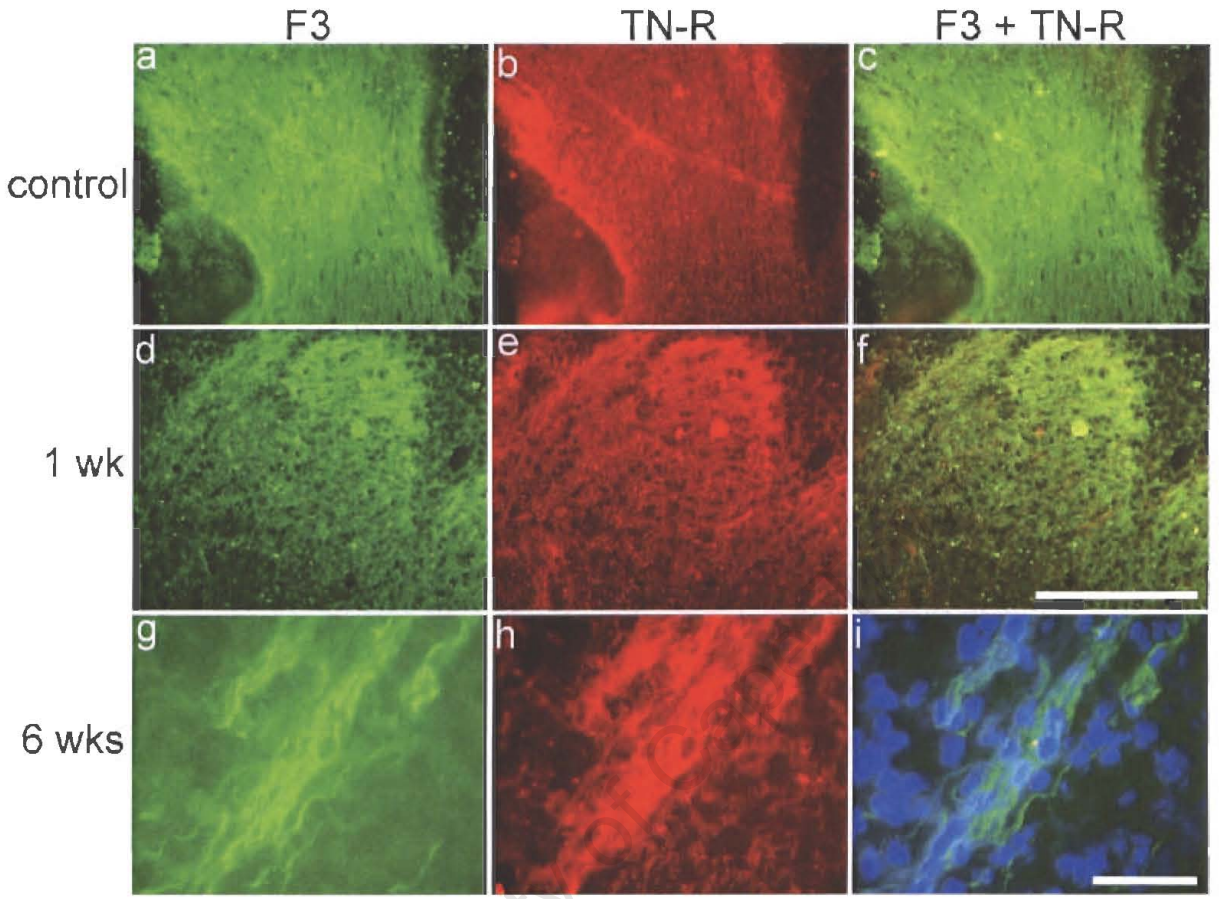

Figure 17. Expression of F3 and TN-R in the unlesioned and regenerating optic nerve. **(a),** rabbit anti-F3 sera (41.6) stains individual retinal ganglion (RGC) axons seen here in the region of the optic chiasm in the unlesioned (control) nerve. **(b),** the corresponding TN-R image shows typical punctuate staining of TN-R within fascicles of nerve fibers. **(c),** merged image of (a) and (c) shows that F3-labeled RGC axons extend through the TN-R-stained extracellular matrix within fascicles. **(d),** 1 week (wk) after the optic nerve crush, F3-labeled RGC axons are seen above the lesion site, directly adjacent to the retina, probably corresponding to new fibers that have just exited the retina. **(e),** the corresponding TN-R image shows that the intensity of TN-R immunoreactivity has not decreased after the injury compared to the control nerve in (b). **(f),** merged image of (d) and (e) shows substantial colocalization between F3-labeled RGC axons and the TN-R-stained optic nerve, directly adjacent to the retina. **(g),** 6 wks after the crush injury, F3 (41.6) sera stained cellular profiles in the optic chiasm end of the nerve. **(h),** the corresponding TN-R image shows that these profiles are also stained with TN-R antibodies. **(i),** merged image of (g) and the corresponding DAPI image (not shown), shows that the F3-labeled profiles are closely associated with nuclei, suggesting that they may correspond to glial processes. Scale bar in (a), (b), (c), (d) and (f) = 100 μm, Scale bar in (g), (h), and (i) = 50 μm

3.3.4.2. TN-R and CSPG

CSPG immunoreactivity in the optic nerve was extremely weak compared to in the retina (not shown). This low level of CSPG immunoreactivity may be a reflection of the actual levels of CSPGs in the unlesioned and regenerating goldfish optic nerve.

3.3.4.3. TN-R and laminin

In the unlesioned nerve, laminin staining clearly delineated the connective tissue components of the fascicles (Figure 18b) and TN-R staining was observed within the borders of these fascicles (Figure 18c). Partial colocalization between TN-R and laminin was seen at the fasicular boundaries (Figure 18d, arrow heads). One week after the optic nerve crush, a similar intensity of laminin staining was still be observed above and below the lesion site but had become somewhat disorganized in the region of the lesion site itself (Figure 18e). The change in the resulting colour of the superimposed green (laminin) and red (TN-R) images from yellow at the fascicle borders prior to the lesion to green one week after the lesion suggests that an increase in laminin levels or a decrease in TN-R occurs after the optic nerve crush (Figure 18h, arrow heads). By 3 weeks after the injury, slighty increased levels of laminin were observed, at least in regions of the optic nerve near the chiasm (Figure 18i and figure 18j). Again, TN-R staining was observed within the laminin boundaries (Figure 18k, arrow heads) and the change in the resulting colour of the superimposed green (laminin) and red (TN-R) images from green at the fascicle borders at 1 week post lesion to yellow 3 weeks after the lesion suggests that there is a further increase in laminin levels concomitant with increased TN-R levels at the fasicular boundaries (Figure 18l, arrow heads).

3.3.4.4. TN-R and fibronectin

In the unlesioned nerve, fibronectin staining was associated with fibroblasts that constitute the connective tissue layers (Figure 19a). One week after the optic nerve crush, fibronectin staining increased in the region of the lesion site (not shown), probably due to the presence of invading fibroblasts (Hirsch et al., 1995). At this timepoint there was partial colocalization of TN-R and fibronectin in the region of the optic nerve adjacent to the retina (not shown). The most intense fibronectin staining was observed 3 weeks after the injury (Figure 19d). Individual fibronectin-stained processes were observed at the lesion site (Figure 19d, arrow heads) where there was little to no colocalization with TN-R (Figure 19f). By 6 weeks post-injury, intensely labeled fibronectin-positive processes were observed in regions of the optic nerve adjacent to the chiasm (Figure 19g, arrow heads) where they colocalized with TN-R

staining in fascicles (Figure 19h, arrow heads). There was however also some spatial differences as fibronectin-positive fibers were seen growing in TN-R-negative pathways (Figure 19h, arrow heads).

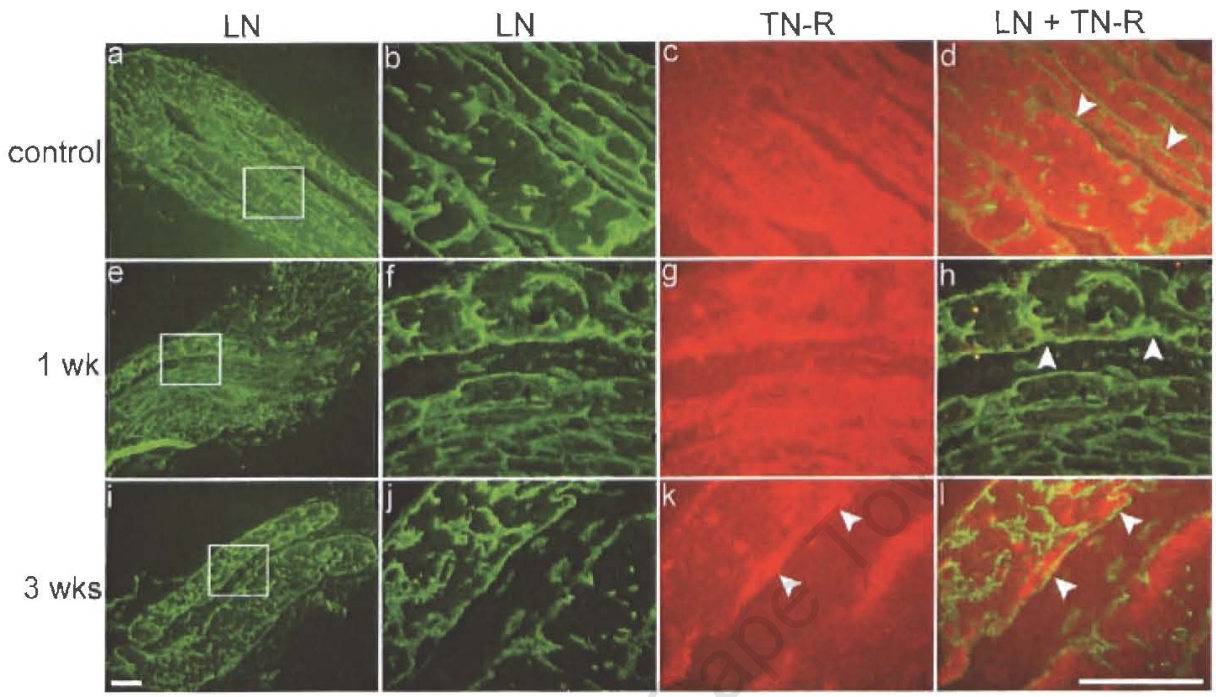

Figure 18. Expression of laminin and TN-R in the unlesioned and regenerating optic nerve. (a), rabbit polyclonal anti-laminin (LN) antibodies strongly stain the unlesioned (control) nerve at a low magnification. **(b),** high power magnification of insert in (a) shows that LN is associated with the connective tissue components of the fascicles. **(c),** the corresponding TN-R staining shows that TN-R is located within the connective tissue boundaries. **(d),** merged image of (b) and (c) shows partial colocalization of LN and TN-R at the borders of fascicles (arrow heads). **(e),** LN immunoreactivity remained intense in the lesioned nerve 1 week (wk) after the crush injury. **(f),** high power magnification of insert in (e) shows that there is a slight increase in the intensity of the laminin staining compared to control levels in (b). **(g),** the corresponding TN-R image shows intensity levels comparable to the control nerve levels in (c). **(h),** merged image of (f) and (g) confirms the slight increase in the intensity of the laminin compared to unlesioned levels, as evidenced by the greener coloured colocalization pattern with TN-R staining at the borders of fasicles (arrow heads). **(i),** after 3 wks, LN immunoreactivity remains intense in the lesioned nerve. **(j),** high power magnification of insert in (i) shows that there is a further slight increase in LN staining intensity in the lesioned nerve compared to at 1 wk in (f). **(k),** the corresponding TN-R image shows that TN-R staining is highest at the borders of fascicles (arrow heads). **(l),** merged image of (j) and (k) shows partial colocalized staining of LN and TN-R at the borders of the fascicles that is more intense compared to control levels in (d). Scale bars in (a), (e) and (i) = 100 μm, Scale bar in (b), (c), (d), (f), (g), (h), (j), (k), and (l) = 100 μm

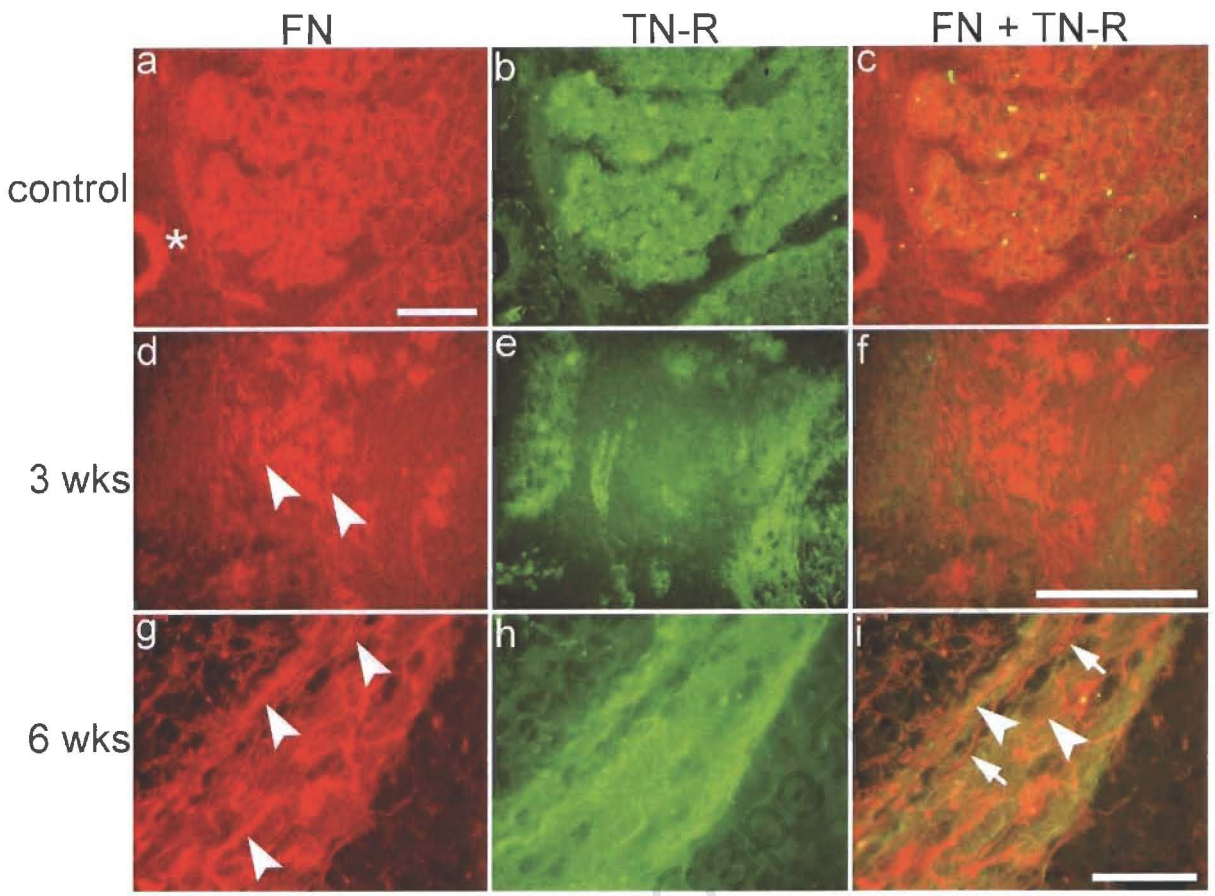

Figure 19. Expression of fibronectin and TN-R in the unlesioned and regenerating optic nerve. (a), rabbit polyclonal anti-fibronectin (FN) antibodies stain the connective tissue components of the fasicles and also stain blood vessels (asterisk) in the unlesioned (control) optic nerve. **(b),** the corresponding TN-R staining shows that in comparison, mouse monoclonal anti-TN-R antibodies stain the neural components of the nerve. **(c),** merged image of (a) and (b) shows partial colocalization of FN and TN-R at the borders of fascicles. **(d),** by 3 weeks (wks), an increase in FN-labeled fibers (arrow heads) is seen at the lesion site. **(e),** the corresponding TN-R staining in the lesion site is diffuse. **(f),** merged image of (d) and (e) shows that there is only partial colocalization of FN and TN-R expression in the lesion site. **(g),** after 6 wks, FN-labeled fibers, most likely fibroblasts, are observed below the lesion site, on the chiasm side. **(h),** the corresponding TN-R staining shows the characteristic punctuate staining of the nodes of Ranvier. **(i),** merged image of (g) and (h) shows significant colocalization of FN-labeled fibers within TN-R-positive regions (arrow heads), as well as as some FN-labeled fibers within TN-R-negative regions (arrows). Scale bar in (a), (b), (c), (d), (e), and (f) = 100 μm, Scale bar in (g), (h), and (i) = 100 μm

3.3.5 Expression of TN-R and its interaction partners in the optic tectum

During development, as well as during regeneration, axons from RGCs form topographical projections within the optic tectum, a visual brain center known as the superior colliculus in mammals. The optic tectum is located in paired lobes in the mid-region of the brain (Figure 1), and like the retina, it consists of neurons arranged in several layers, or concentric laminae.

The outermost layer is the pia mater (PM), followed by the stratum marginale (SM), stratum opticum (SO), stratum fibrosum et griseum superficale (SFGS), stratum album centrale (SAC), stratum griseum periventriculare (SGP), and the stratum fibrosum periventriculare (PV) (Yamagata and Sanes, 1995). Once growing axons reach the optic tectum in the SO, they terminate withinin the retinorecipient laminae, where they arborize and form synapses (Pesheva et al., 1995).

At each designated time point, the right optic tectum, where RGCs from the unlesioned optic nerve terminate, was observed as having a normal appearance and staining pattern. The nuclei were arranged in an orderly fashion corresponding to the respective annular rings in the tectum (Figure 20a). MBP staining was observed in the rostral SO, where the incoming RGCs axons are still myelinated (Figure 20c and Figure 21b), and in the SAC (Figure 20c and Figure 21b). No E587-positive RGC axons were seen in the tectum but this is to be expected as the new axons are located on the periphery of the tectum and are therefore unlikely to be seen in such a horizontal section (not shown). TN-R staining in the unlesioned optic tectum was intense in the SO (Figure 20e and Figure 21a) where it colocalized significantly with MBP staining (Figure 21c). TN-R staining was also visualised in the deeper tectal layers (Figure 20e and Figure 21a).

One week after the right optic nerve crush, staining in the left optic tectum, where RGCs from the lesioned right optic nerve terminate, although not dissimilar to the right optic tectum at a gross anatomy level, was decidedly different at a microscopic level. The nuclear staining pattern was more erratic (Figure 20b), MBP immunoreactivity in the rostral SO was diminished (Figure 20d and figure 21c) and no E587-positive fibers were observed (not shown). TN-R immunoreactivity was less in the SO but maintained in the deeper tectal layers (Figure 20e and Figure 21d).

The ECM proteins fibronectin and laminin showed both overlapping and distinct staining patterns in the unlesion optic tectum. Intense fibronectin immunoreactivity was seen predominantly in the glia limitans, a structure formed by astrocytes when they interface with meningeal cells, as well as surrounding blood vessels within all the tectal layers (Figure 22a). Intense laminin reactivity was also seen in the glia limitans and surrounding blood vessels within all the tectal layers (Figure 22b). In addition, laminin staining was also seen in the ECM of the tectum (Figure 22b) and 3 weeks after the optic nerve crush there was an increase in the intensity of the ECM-associated laminin immunoreactivity, particularly in the SO, where newly growing and regenerating RGC axons enter the tectum (Figure 22c). The

increase in laminin staining intensity along the route of incoming RGC axons may suggest that laminin plays a role in establishing a growth-supportive pathway in the SO for the RGC axons entering the optic tectum.

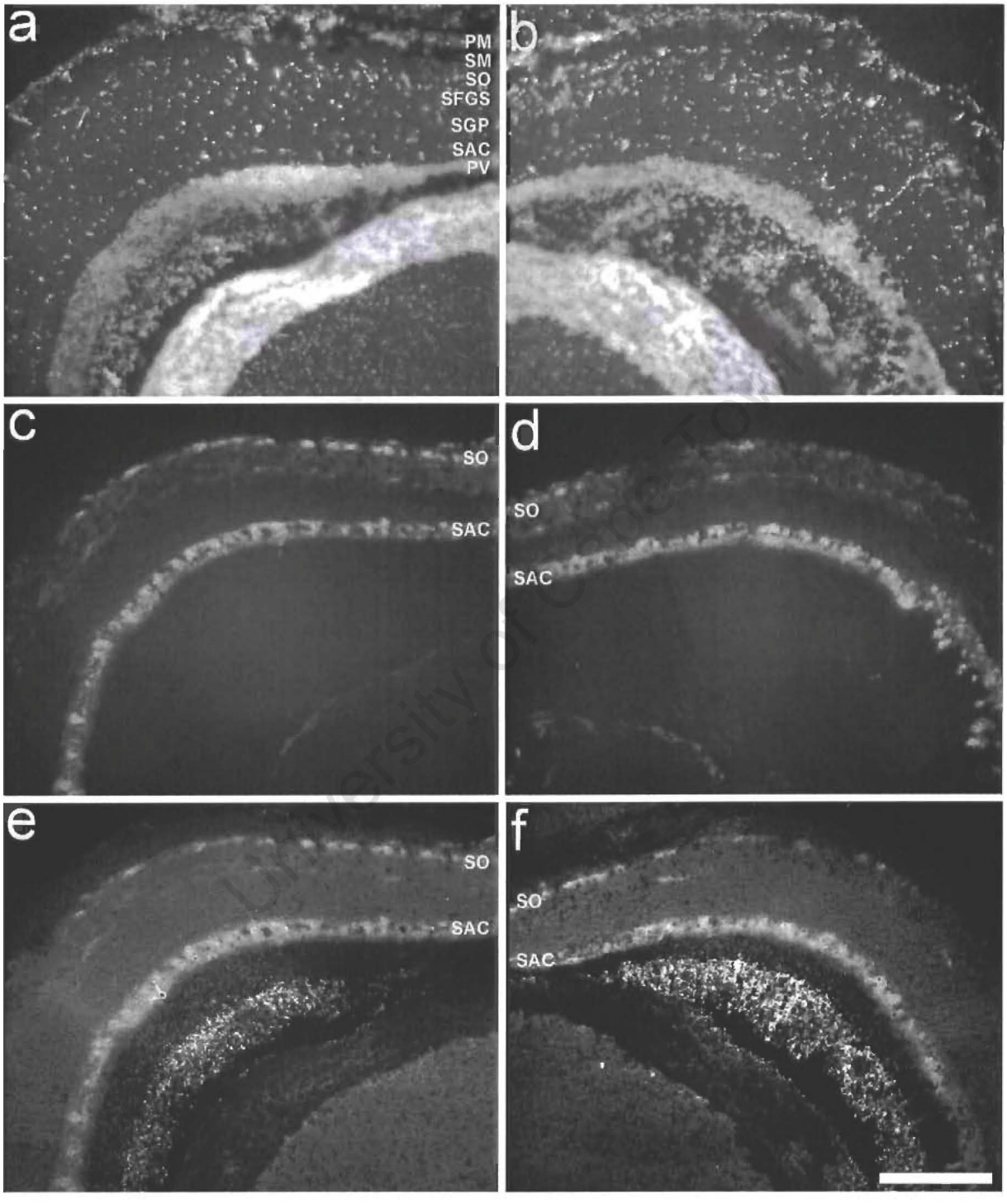

Figure 20. Characterization of the adult goldfish optic tectum before and after an optic nerve crush, rostral view. (a), DAPI stains the orderly arranged nuclei in concentric laminae in the tectum on the same side as the crushed nerve (unlesioned optic tectum). **(b),** 1 week after the optic nerve crush, DAPI staining in the tectum on the the opposite side as the crushed nerve (regenerating tectum) looks somewhat disorganized. **(c),** in

the unlesioned tectum, rat monoclonal anti-MBP antibodies stain the myelinated axons in the stratum functionale (SO), which become unmyelinated as they travel in a more caudal direction, as well as myelinated tracts in the deeper stratum album centrale (SAC). **(d),** 1 week after the optic nerve crush, MBP staining is diffuse in the SO but retained in the SAC. **(e),** in the unlesioned tectum, rabbit polyclonal anti-TN-R antibodies label the myelinated axons in the rostral SO, as well as myelinated tracts in the deeper SAC. **(f),** 1 week after the optic nerve crush, TN-R staining is also diffuse in the SO but retained in the SAC. Pia mater (PM), stratum marginale (SM), stratum fibrosum et griseum superficale (SFGS), stratum griseum periventriculare (SGP), and stratum griseum periventriculare (PV). Scale bar = 100 μm

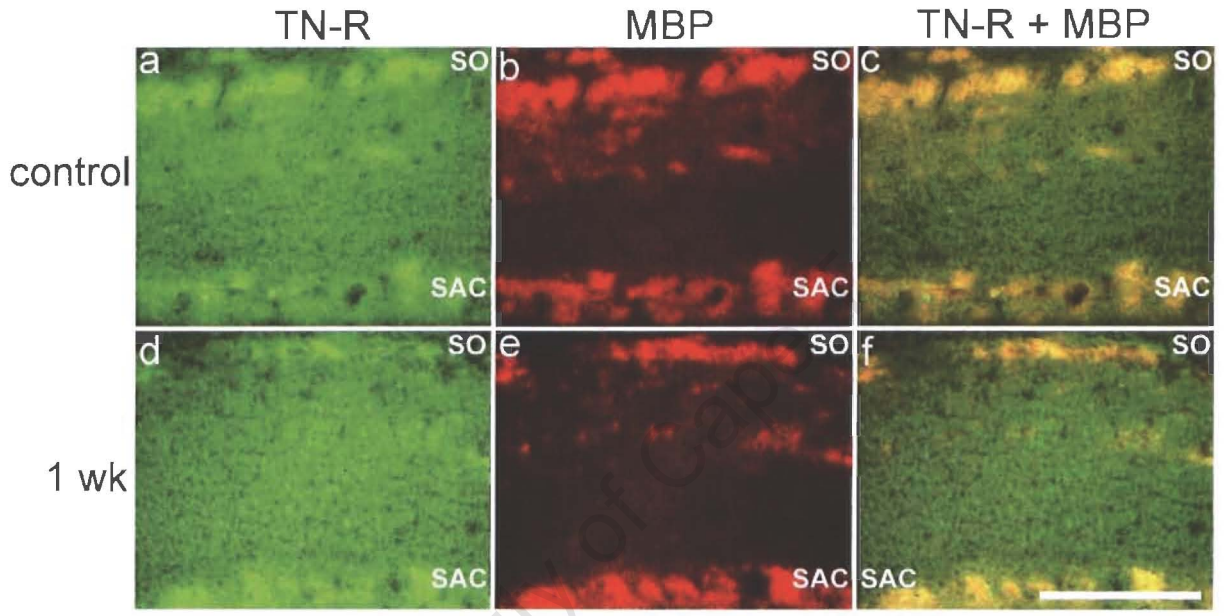

Figure 21. Expression of TN-R and MBP in the optic tectum before and after an optic nerve crush, rostral view. (a), in the unlesioned (control) optic tectum, rabbit polyclonal anti-TN-R antibodies stain the stratum opticum (SO), the most superficial retinorecepient layer, as well as along the entire length of the deeper stratum album centrale (SAC). **(b),** rat monoclonal anti-MBP antibodies also stain the SO in the control optic tectum as well as the myelinated tracts of the SAC. **(c),** merged image of (a) and (b) shows that there is substantial colocalization of TN-R and MBP in the SO and SAC of the unlesioned tectum. **(d),** 1 week (wk) after the optic nerve crush the intensity of TN-R staining in the SO is weaker compared to in (a). TN-R labeling in the SAC remained similar to in the control tectum in (a). **(e),** 1 wk after the optic nerve crush MBP staining intensity was reduced in the SO compared to in the control tectum in (b). MBP labeling in the SAC remained similar to in the control tectum in (b). **(f),** merged image of (d) and (e) shows that, while the deeper tectal layers continue to express TN-R and MBP, these oligodendroctye-associated proteins are both downregulated in a temporally and spatially similar manner in the SO. Scale bar = 100 μm

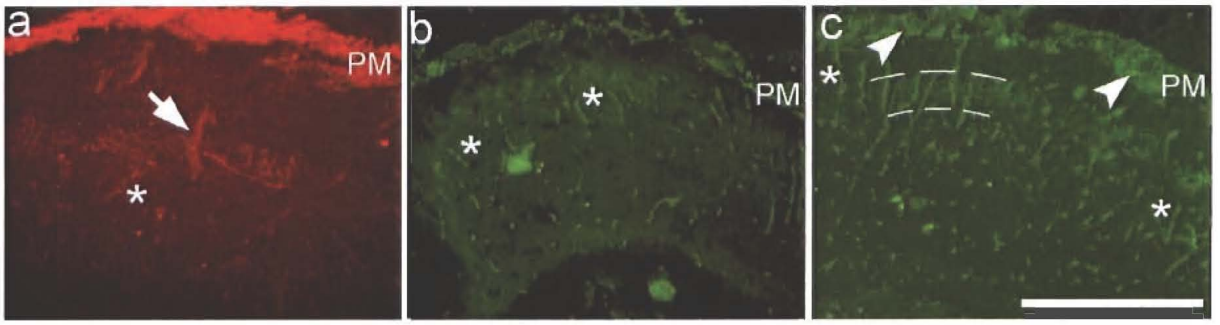

Figure 22. Expression of fibronectin and laminin in the optic tectum before and after an optic nerve crush. (a), rabbit polyclonal anti-fibronectin (FN) antibodies intensely stain the glia limitans, a structure where cells of the CNS border the pia mater (PM) in the unlesioned optic tectum. FN immunoreactivity was also associated with blood vessels (asterisk) and other cellular profiles in the mid-tectal layers (arrow head). **(b),** rabbit polyclonal anti-laminin (LN) antibodies also stained the glia limitans, although more weakly compared to fibronectin in (a), and LN immunoreactivity is also closely associated with blood vessels (asterisk). **(c),** 1 week after the optic nerve crush there was an increase in the intensity of the laminin staining. Individual fibers could be seen in the glia limitans (arrow heads), and there was an increase the non-basal lamina pathway of the stratum opticum (curved dashed lines). Scale bar = 100 μm

3.4 Regenerating goldfish optic nerve sections which express TN-R are permissive for the outgrowth of mammalian CNS neurites

The immunocytochemical results showed that the expression of TN-R persists in the optic nerve 3 weeks after an optic nerve lesion. As TN-R is considered to be an axon growth-inhibiting protein in mammals (Pesheva et al., 1993; Taylor et al., 1993), this raised the question of whether and how the substrate properties of the goldfish optic nerve were affected by the presence of this protein. In order to compare the substrate properties of the unlesioned versus regenerating goldfish CNS for axon outgrowth from mammalian neurons, it was analyzed whether neurite outgrowth from these cells was enhanced or inhibited on cryosections of 3 weeks post-injury goldfish optic nerve. Cryosectioning of the nerve ensured that the integrity of the endogenous proteins expressed in the tissue, such as TN-R, was preserved (Geisert et al., 1998). The adjacent uninjured left optic nerve served as an internal control.

PC12 cells are a single clonal line from a transplantable rat adrenal pheochromocytoma (Green and Tischler, 1976). These cells develop a neuronal phenotype in the presence of

nerve growth factor (NGF), and are well established models for the study of neurite outgrowth (Green and Tischler, 1976). Frozen stocks of PC12 cells were thawed and grown in NGF-supplemented media for 5-7 days until their morphology resembled that of mature neurons, after which they were seeded at a density of 10×10^5 onto cryosections of goldfish optic nerve. Neurite outgrowth from differentiated PC12 cells on the frozen sections of goldfish optic nerve differed depending on whether they were seeded close to a section of unlesioned or regenerating goldfish optic nerve. PC12 cells that were plated in the vicinity of the unlesioned nerve, which expressed comparatively low levels of fish TN-R, began to grow towards the section of nerve (Figure 23a). The cells and/or their neurites failed, however, to contact the substrate of unlesioned nerve: before actually reaching the tissue, the cells came to an abrupt halt, as though they had come up against a boundary/barrier that could not be crossed (Figure 23a, arrow heads). Individual PC12 cells which were seeded directly onto the unlesioned nerve failed to extend their processes on this substrate (not shown). In contrast, PC12 cells which were plated in the vicinity of the regenerating nerve, which expressed comparatively high levels of fish TN-R, grew freely across the optic nerve and formed extensive processes (Figure 23b). The presence of possible inhibitory elements in the unlesioned goldfish optic nerve may account for the failure of neurite outgrowth from the mammalian neurons on this tissue. The absence of inhibitory elements in the regenerating goldfish optic nerve however, does not explain why neurite outgrowth was promoted on this portion of nerve, as TN-R, a known axon growth-inhibiting protein was present in higher levels than in the unlesioned nerve. This result suggests that the levels of TN-R expression in the regenerating goldfish optic nerve do not act to prevent neurite outgrowth; indicating that fish TN-R, unlike its mammalian homologue, may not exert growth-inhibiting effects on axons or neurites.

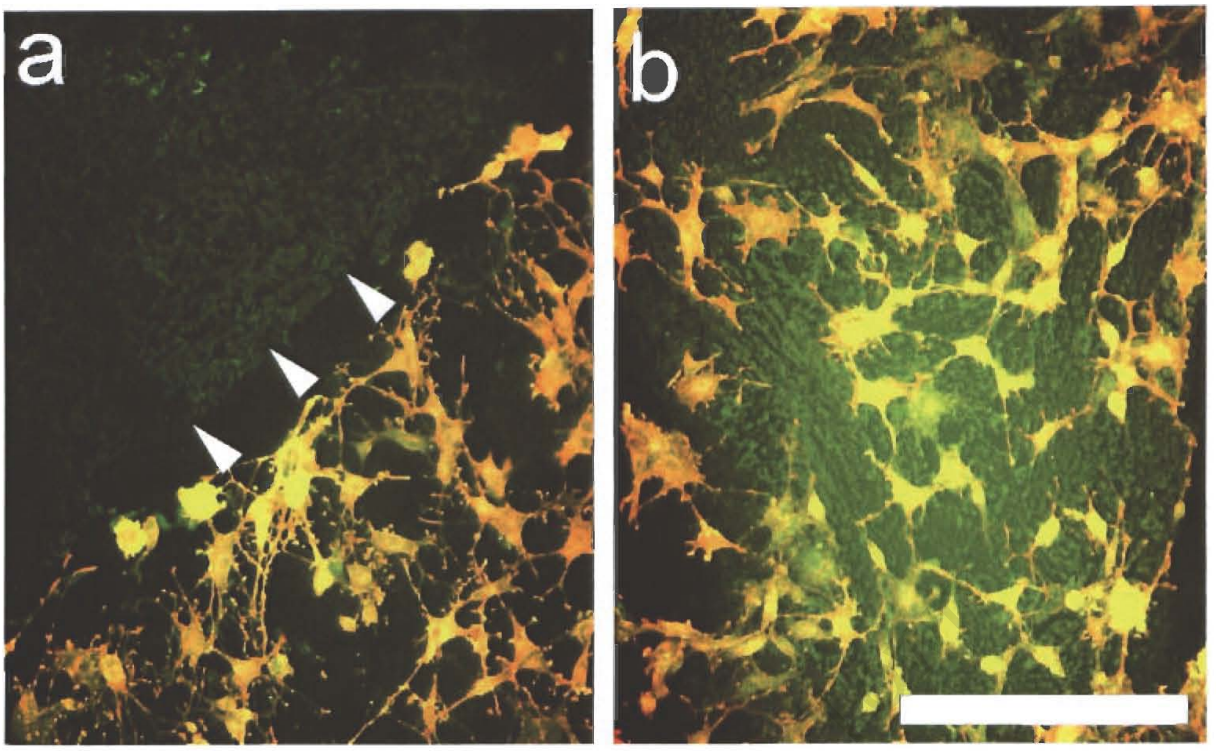

Figure 23. PC12 cells avoid growing on a section of unlesioned goldfish optic nerve but grow freely on a section of regenerating goldfish optic nerve. (a), PC12 cells labeled with mouse anti-Thy 1 (seen in yellow) fail to grow on a section of unlesioned goldfish optic nerve labeled with rabbit anti-TN-R (seen in green). A short distance separates the cells from the nerve (arrow heads). **(b),** PC12 cells labeled with mouse anti-Thy 1 (seen in yellow) grow extensively on a section of regenerating goldfish optic nerve labeled with rabbit anti-TN-R (seen in green). The change in growth substrate properties after injury in the 3 week-injury goldfish optic nerve occurs concomitantly with an increase in TN-R immunoreactivity (compare the staining intensity of TN-R in (a) and (b)). Scale bar = 100 μm

3.5 Homogenous fish TN-R is an inhibitory substrate for goldfish RGCs *in vitro*

The finding that the regenerating goldfish optic nerve, which in certain regions expressed TN-R at levels higher compared to the control nerve, was a growth-supportive substrate for mammalian neurons, pointed to the possibility that this putative axon growth-inhibiting protein was in fact not functioning as a neurite growth inhibitor in the fish CNS. In order to determine the effect of fish TN-R on goldfish CNS axon outgrowth, neurite outgrowth from microexplants of goldfish retina on substrates of fish TN-R was studied. This was done using two types of substrates, namely a uniform substrate of fish TN-R or patterned substrates, creating boundaries of fish TN-R on the coverslips. Moreover, the effect of fish TN-R on goldfish RGC outgrowth was compared to the effect of mammalian TN-R, and combinations

of TN-R with the ECM protein laminin, a known neurite growth-promoting substrate and interaction partner of TN-R, were analyzed for their effects on neurite outgrowth.

3.5.1 A uniform substrate of homogenous TN-R inhibited the neurite outgrowth from goldfish RGCs

Microexplants of goldfish retina were plated onto coverslips that had been coated with homogenous substrates of (i) laminin, (ii) fish TN-R, (iii) mouse TN-R, or (iv) human TN-R, and mixed substrates of (i) laminin and fish TN-R, (ii) laminin and mouse TN-R, or (iii) laminin and human TN-R. A mixed substrate constituted a combination of the two proteins, and was achieved by mixing the test substrates together before coating the coverslips with the proteins. On the control laminin-coated coverslips (Figure 24a), neurite outgrowth was extensive and multiple neurites grew out from most of the explants over considerable distances. In contrast, neurite outgrowth was inhibited on both fish and mouse TN-R-coated coverslips (Figure 24b and figure 24d, respectively). Only a single neurite was ever observed attempting to sprout from explants growing on fish TN-R (Figure 24b, arrow heads), while on mouse TN-R, none of the explants grew any neurites. Neurite outgrowth from goldfish retinal explants on human TN-R was also inhibited to the same extent as on fish and mouse TN-R (not shown). Goldfish RGC neurite outgrowth on both fish and mouse TN-R dramatically improved when the coverslips were coated with a combination of fish or mouse TN-R and laminin (Figure 24c and 24e, respectively). The extensive growth of neurites from explants on these mixed substrates closely resembled that seen on the laminin-coated substrates. Neurite outgrowth, however, remained inhibited on coverslips that had been coated with a combination of human TN-R and laminin (not shown). These observations demonstrated that although fish TN-R inhibits neurite outgrowth of goldfish RGCs when offered as a homogenous substrate, when fish TN-R is combined with laminin, an adhesive ECM protein, the inhibition was overcome and neurite outgrowth was enhanced. Extrapolated to the situation *in vivo*, these *in vitro* experiments suggest that the inhibitory effects of fish TN-R are overcome by the presence of adhesive proteins, such as laminin and fibronectin, which are expressed in the nervous system. In addition, this finding also showed that despite goldfish CNS axons being able to grow on a substrate of rodent optic nerve expressing mammalian TN-R (Bastmeyer et al., 1993), they are inhibited by mammalian (mouse and human) TN-R when it is offered as a homogenous substrate. It seems therefore that in the context of interactions with other substrate molecules, the axons do not display such a high degree of sensitivity to TN-R. Indeed, when mammalian TN-R is combined with adhesive

laminin, RGC neurites grow out of the goldfish retinal explants. Furthermore, the continued inhibition of goldfish RGC neurites on human TN-R, even in combination with laminin, may indicate that human TN-R may be a more potent inhibitor for these cells than fish or mouse TN-R.

3.5.2 A sharp border substrate of fish TN-R did not inhibit neurite outgrowth from goldfish RGCs

To distinguish between the possibility that TN-R inhibits axonal growth directly or merely prevents the axons from growing out of the explants, and to find out if RGC axons of adult goldfish are sensitive to TN-R boundaries, goldfish RGC neurites were allowed to exit a strip of retina and grow onto patterned coverslips that had been coated with alternating lanes of poly-L-lysine (PLL), a polyaminoacid that that facilitates neuron-substrate adhesion (Letourneau, 1975), and fish or mouse TN-R.

Goldfish RGC neurites from retinal strips were able to freely cross a substrate border of fish TN-R (Figure 25a). The pattern of outgrowth showed no aversion for the fish TN-R-coated lanes or preference for the PLL-coated lanes as they grew seemingly randomly across both stripes (Figure 25a). Thus, a substrate border of fish TN-R does not repel adult goldfish RGC axons *in vitro*, and fish TN-R appears no worse as a substrate than PLL. The observed lack of goldfish RGC outgrowth from microexplants on a uniform substrate of fish TN-R alone may therefore not reflect a direct inhibition by fish TN-R but rather a lack of positive or outgrowth-promoting substrate properties, suggesting that fish TN-R may act as neither an inhibitory or repellent protein *in vivo*. However, in comparison, goldfish RGC outgrowth on mouse TN-R-coated lanes was restricted (Figure 25b). Goldfish RGC neurites avoided growing on the mouse TN-R-coated lanes and were channelled onto the PLL-coated lanes. Mouse TN-R is therefore avoided as a growth substrate and a substrate border of mouse TN-R therefore does repel adult goldfish RGC axons *in vitro*. The inhibition of fish RGC outgrowth in response to a defined substrate border of mouse TN-R has been previously observed (Becker et al., 2004). The inhibition of goldfish RGC outgrowth from microexplants on uniform homogenous substrates of mouse TN-R alone could therefore reflect a prevention of outgrowth from the explants due to direct inhibition of neurite growth, as well as lack of outgrowth-promoting substrate properties. The observed channelling/repelling effect of the mammalian TN-R suggest that mammalian TN-R may have a more potent inhibitory effect on goldfish CNS axons than fish TN-R.

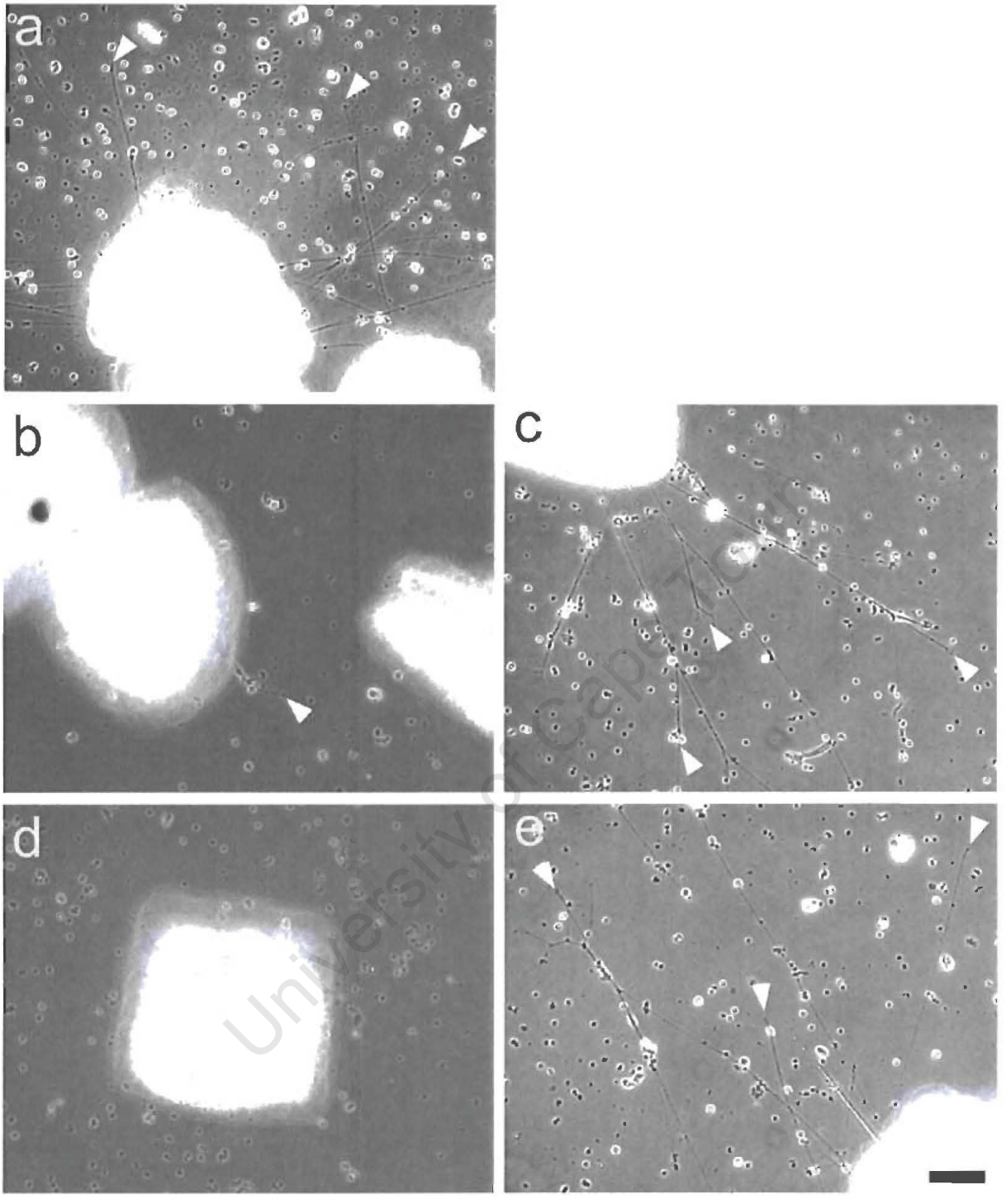

Figure 24. Neurite outgrowth from goldfish RGC microexplants is inhibited on homogenous substrates of both fish and mammalian TN-R. (a), outgrowth of goldfish RGC neurites on laminin as a sole substrate is extensive. **(b),** outgrowth of goldfish RGC neurites on fish TN-R as a sole substrate is minimal. **(c),** outgrowth of goldfish RGC neurites is improved on a mixed substrate of laminin and fish TN-R. **(d),** no outgrowth of goldfish RGC neurites is observed on mouse TN-R as a sole substrate. (e), outgrowth of goldfish RGC neurites improved on a mixed substrate of lamnin and mouse TN-R. Arrow heads denote ends of growing neurites. Scale bar = 100 μm

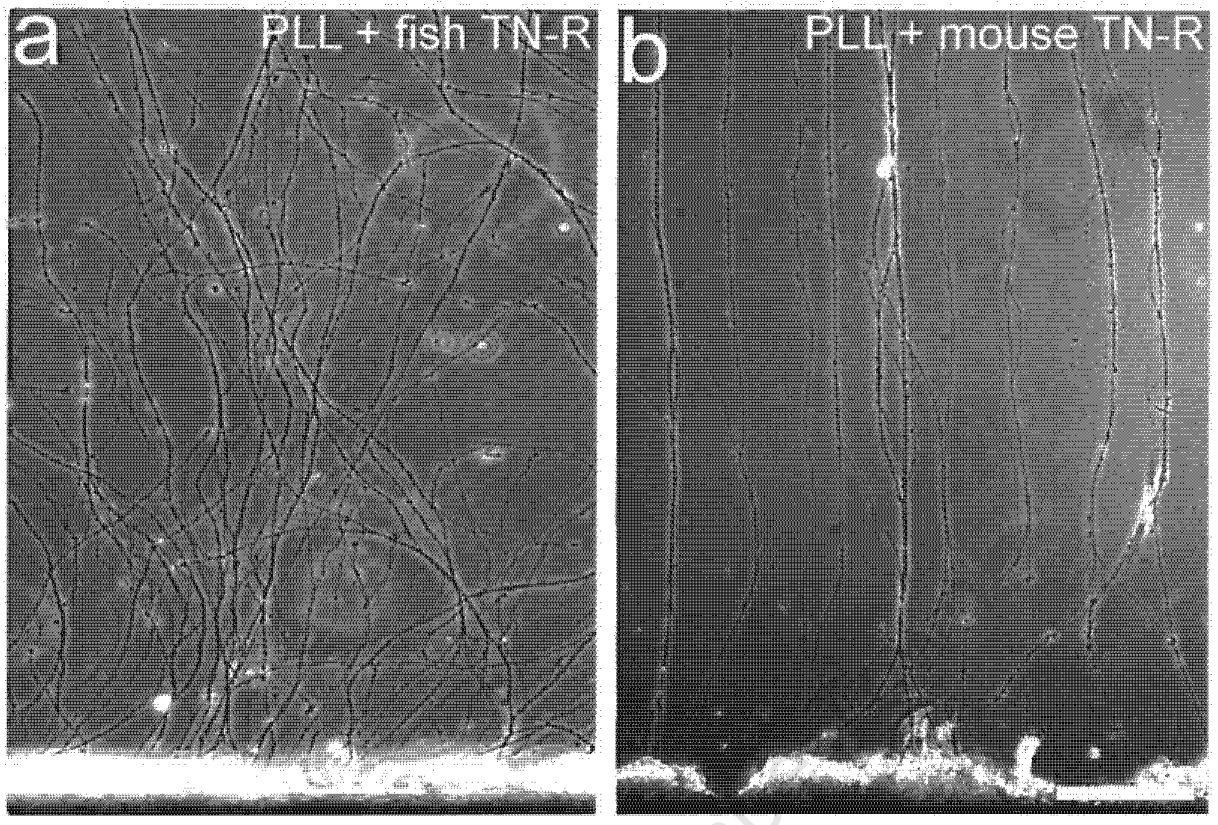

Figure 25. Goldfish retinal ganglion cell neurite outgrowth is restricted by a sharp substrate border of mouse TN-R but not fish TN-R. (a), goldfish retinal ganglion cells (RGCs) are not restricted by fish TN-R and grow freely across stripes of poly-L-lysine (PLL) and fish TN-R. **(b),** goldfish RGCs are repelled by a border of mouse TN-R and only grow along stripes of PLL. Scale bar = 100 μm

3.6 The OP13 cell line is a heterogeneous population of cells which express glial cell markers and receptors to TN-R and Nogo-A

Having examined the effect of TN-R on axon growth, the next part of this study addressed the influence of this ECM molecule on glial cell adhesion. In light of its mRNA expression, the OP13 cell line was used as a novel olfactory ensheathing glia cell line to test the influence of TN-R on glial cell adhesion. Before this could be done, the cell line needed to be characterized. The OP13 cell line was generated using the temperature sensitive simian virus 40 (SV40). SV40 is an oncogenic deoxyribonucleic acid virus belonging to the papovavirus group and encodes two proteins, the large (T) and small (t) tumor antigens. The T antigen has been shown to immortalise primary cells in culture by binding to, and thus inactivating a set of cell cycle proteins, the retinoblastoma family of growth suppressors (review by Hand, 1981) when grown at 33°C in media containing 10% fetal calf serum (FCS), the temperature sensitive nature of the virus allowed the cells to proliferate but when they were transferred to

39°C in media containing 1% FCS, they differentiated. The differentiation of the OP13 cells was determined by changes in their cellular morphology.

3.6.1 OP13 cells are morphologically and molecularly heterogeneous

At both culturing temperatures, the morphology of the cells was very heterogeneous. At 33°C, two distinct cell shapes were observed: flattened and spindle-shaped (Figure 26a and figure 26b, respectively). At 39°C, some of the cells took on a branched appearance, similar to that of oligodendrocytes (Figure 26c), while others were more spindle-shaped (Figre 26d). These differences in morphology were not only observed within the same culture flasks but also between different cultures. In order to determine whether the OP13 cell line represented a true OEG cell line, immunocytochemistry was performed using antibodies against known olfactory ensheathing glia (OEG) markers. As it currently stands, there is no single marker that can identify an OEG cell, and so a panel of antibodies against documented antigens was used. These antibodies included mouse anti-O4 supernatant (against a sulfatid), mouse anti-$p75^{NTFR}$ (against a low affinity neurotrophic factor receptor), mouse anti-Po (against peripheral myelin) and mouse anti-GFAP (against glial fibrillary acidic protein). The OP13 cells were immunonegative for O4, $p75^{NTFR}$ and Po (not shown). The absence of staining for $p75^{NTFR}$ was unexpected as PCR results from the group who generated the cell line showed that the cells express the $p75^{NTFR}$ mRNA (Illing et al., 2002). Even though it is possible that, despite detectable mRNA levels, the protein is not expressed, the specificity of the antibody came into question. Schwann cells, which are known to express $p75^{NTFR}$, only stained the spindle-shaped cells very faintly (not shown). The OP13 cells were, however immunopositive for GFAP, identifying them as a cell line of glial cell origin (Figure 27a). The staining pattern of GFAP was intracellular, as expected, but differences were observed between the two cell shape types. In the flattened cells, the staining was distinctly perinuclear (Figure 27a, asterisk) and in the elongated, spindle-shaped cells, the staining was more cytoplasmic (Figure 27a, arrow heads). The differential staining pattern may suggest that these two populations of cells reflect two functionally distinct cell types, of which the spindle-shaped cells are more likely to represent OEG, due to their elongated morphology and more typical cytoplasmic staining pattern.

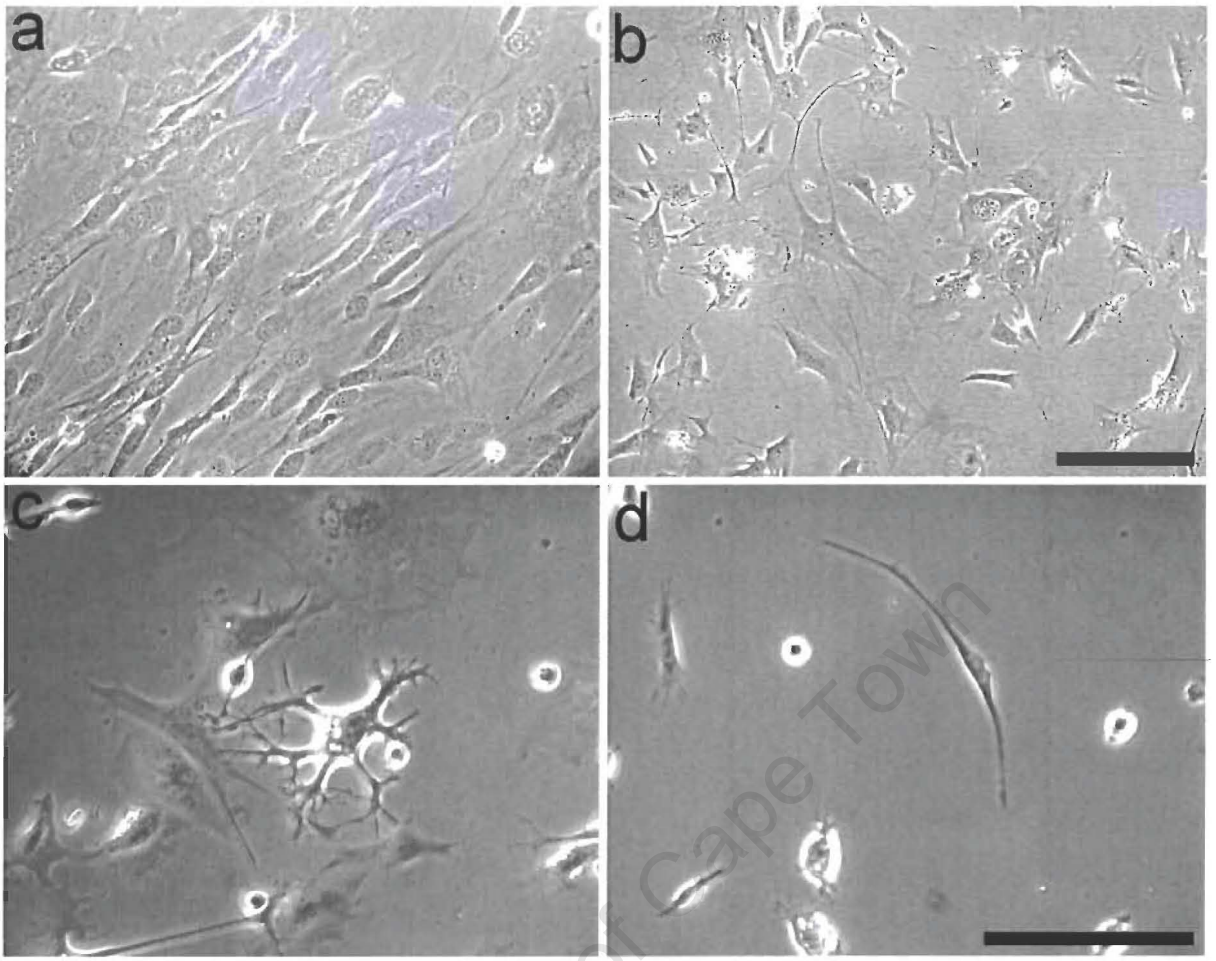

Figure 26. Phase contrast images of the OP13 cells depict a morphologically heterogenous population of cells. (a), OP13 cells grown in proliferation medium at 33°C are elongated in morphology. **(b),** OP13 cells grown in proliferation medium at 33°C also display a flattened out morphology. **(c),** some OP13 cells grown in differentiation medium at 39°C become branched. **(d),** some OP13 cells grown in differentiation medium at 39°C become spindle-shaped. Scale bar in (a) and (b) = 100 μm, Scale bar in (c) and (d) = 160 μm

3.6.2 OP13 cells express F3 and NgR

The migratory potential of OEG after transplantation into an experimental spinal cord injury site has been disputed. It has recently been shown that these cells do not migrate to any great extent away from their implantation site (Ruitenberg et al., 2002; Li et al., 2003; Boyd et al., 2004), suggesting that they may be inhibited by molecules present at the lesion site. In order to determine whether these glial cells would be able to respond to TN-R if it were to be offered as a substrate, immunocytochemistry was performed using antibodies against the receptor for TN-R, namely F3. As the spinal cord injury site is likely to contain more than one inhibitory protein, the cells were also stained with polyclonal rabbit anti-NgR, the receptor for another axon growth inhibitor, namely Nogo-A. OP13 cells were

immunopositive for both F3 (Figure 27b) and NgR (Figure 27c). As was the case with the GFAP result, the staining of F3 and NgR in the flattened cells was perinuclear, while in the spindle-shaped cells, the pattern was more cytoplasmic, particularly in the Nogo-A positive elongated cells (Figure 27c, arrowhead). Although it may seem unreasonable to suggest that an interaction between the OP13 cells and TN-R or Nogo-A would be possible in light of the fact that the receptors to these proteins are not expressed on the surface of the cells, the phenomenon of failure to translocate surface receptors to the outer aspect of the plasma membrane by cell lines *in vitro* is well known.

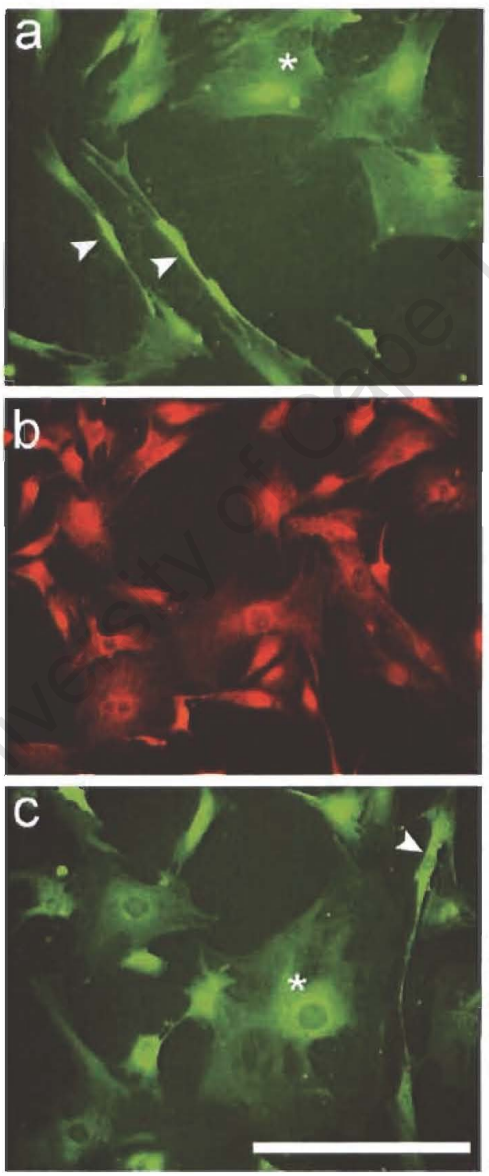

Figure 27. OP13 cells express glial cell markers and the receptors to TN-R and Nogo-A. (a), polyclonal rabbit anti-GFAP antibodies label both flattened (asterisk) and elongated (arrow heads) cells. **(b),** polyclonal rabbit anti-F3 (24III) sera stains both flattened and elongated cells. **(c),** polyclonal rabbit anti-NgR antibody labels flattened (asterisk) and spindle-shaped (arrow head) cells. Scale bar = 100 μm.

3.7 Mammalian TN-R is anti-adhesive for a novel OEG cell line

When cells in culture encounter an appropriate substrate, they form adhesive contacts on that substrate. In order to determine whether mammalian TN-R is an adhesive or anti-adhesive substrate for OEG, a promising candidate for cell transplantation at the site of spinal cord injury (SCI), a short-term cell adhesion assay was performed using OP13 cells, a potentially novel OEG cell line. Imuunocytochemistry results had shown that the cell line was of glial origin and that it expressed F3, the receptor for TN-R. An equal number of cells were plated onto coverslips that had been coated with either (i) laminin as a sole substrate, (ii) TN-R as a sole substrate, or (iii) a mixture of laminin and TN-R. As the cells also expressed NgR, the receptor for Nogo-A, the adhesive properties of TN-R for the attachment of OP13 cells were also compared with those of Nogo-P4, an inhibitory peptide representing Nogo-A. An equal number of OP13 cells were plated onto coverslips that had been coated with Nogo-P4 as a sole substrate, or a mixture of laminin and Nogo-P4. The cell adhesion cultures were photographed after 1, 6, 12 and 24 hrs, and the numbers of adherent cells were counted manually. Cells that were rounded up were not included in the count. The MetCalc ® version 4.16f statistical programme was used to analyze the data. In order to confront the OEG cell line with a sharp substrate boundary of TN-R, these cells were also plated onto coverslips that had been coated with alternating lanes of PLL and TN-R or Nogo-P4. To ensure that the test proteins that were used were functional, rat neonate dorsal root ganglia (DRG), which are sensitive to TN-R and Nogo-A, were also plated on these substrates.

3.7.1 The test proteins TN-R and Nogo-P4 inhibited the adhesion of rat neonate DRGs

In order to verify that the test proteins that were used were functional inhibitors, neonate rat DRGs, whose response to these substrates has been well documented (Caroni and Schwab, 1988a. b; Taylor et al., 1993; Spillman et al., 1998; Chen et al., 2000; GrandPré et al., 2000; Prinjha et al., 2000), were plated onto TN-R- and Nogo-P4-coated coverslips. After 24 hrs, phase contrast pictures were taken to observe whether the DRG neurite growth had been inhibited or promoted on these protein substrates. On laminin-coated coverslips, single DRG cells were seen to extend branched processes over the coverslip (Figure 28c, arrow heads). When the DRG suspensions were plated onto TN-R or Nogo-P4-coated coverslips however, not a single neurite could be observed growing on the coverslips (Figure 28f and figure 29f, respectively). It was only under conditions where laminin was combined with TN-R or Nogo-4 that neurite outgrowth occurred (Figure 28i and figure 29i, respectvely). The observed

DRG neurite inhibition on TN-R and Nogo-P4 alone proved that the test proteins were functionally inhibitory peptides, and therefore that the adhesion of the OP13 cells on TN-R, and particularly on Nogo-P4 was not as a result of the test proteins not being functionally active. It must be mentioned though that Nogo-A has been shown to override the positive effect of laminin, and there is therefore still a possibility that the Nogo-P4 peptide is not as inhibitory as the complete Nogo-A protein.

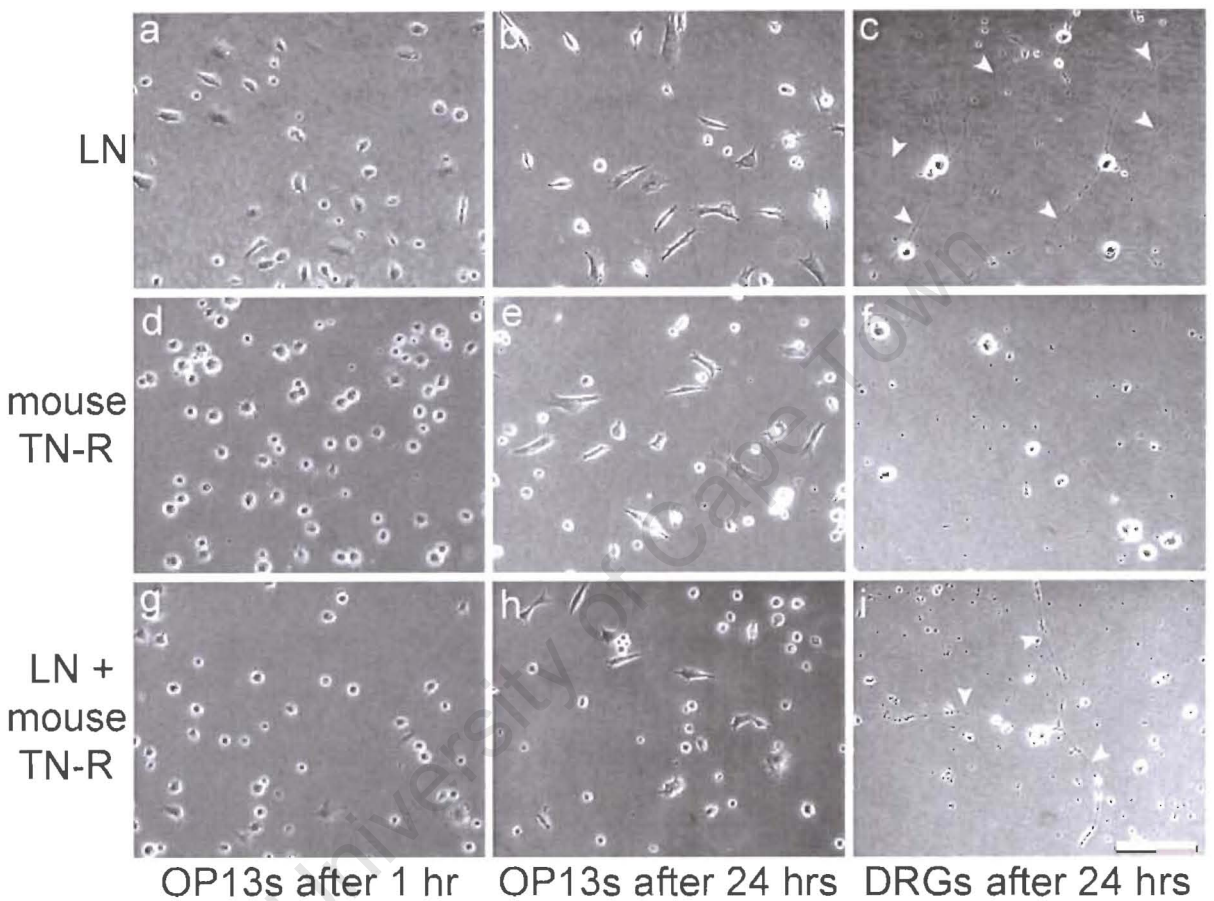

Figure 28. TN-R is an anti-adhesive substrate for OP13 cells in a short-term cell adhesion assay. (a), after 1 hr, the majority of the OP13 cells in view began adhering to the laminin (LN)-coated coverslip. **(b),** after 24 hrs, the majority of the OP13 cells in view had adhered to and adopted either a flattened out or spindle-shape morphology on the LN-coated coverslip. **(c),** dorsal root ganglia (DRG) adhered to a LN-coated coverslip and extended numerous neurites (arrow heads) after 24 hrs. **(d),** the majority of the OP13 cells in view remained rounded up on the mouse TN-R-coated coverslip after 1 hr. **(e),** Non-adherent, rounded up OP13 cells are still observed on the mouse TN-R-coated coverslips after 24 hrs. **(f),** No DRG neurite outgrowth was observed on mouse TN-R-coated coverslips after 24 hrs. **(g),** after 1 hr, the majority of the OP13 cells in view remained rounded up on coverslips that had been coated with a mixture of LN and mouse TN-R. **(h),** Non-adherent, OP13 cells are still observed on the LN and mouse TN-R-coated coverslips after 24 hrs. **(i),** DRG adhered to coverslips coated with a mixture of LN and mouse TN-R and extended numerous neurites after 24 hrs (arrow heads). Scale bar = 100 μm.

3.7.2 A uniform substrate of TN-R is anti-adhesive for OP13 cells compared to laminin and Nogo-P4

Statistical analysis using the Student-Newman-Keuls tests for all pairwise comparisons showed that there was by in large a normal distribution of the data. In instances where the data was not normally distributed, data sets were tested using the Kraskal-Wallis test, subsequently followed by the unpaired Wilkoxon test (p value > 0.05).

After 1 hr, phase contrast micrographs showed that cells plated onto laminin-coated coverslips had adhered to the substrate and become flattened out (Figure 28a), while many of those seeded onto TN-R had not adhered and still remained rounded up (Figure 28d). Statistically, the mean number of cells that had adhered to laminin as a sole substrate was greater than the mean number of cells that had adhered to TN-R as a sole substrate, although the difference was not significant (Figure 30). Fewer cells remained rounded up at this time point however, when TN-R was offered as a substrate together with laminin (Figure 28g). Despite the mean number of cells that had adhered to a mixture of laminin and TN-R being greater than on TN-R alone (Figure 29), the difference was not significant (Appendix III). Surprisingly, cells plated onto Nogo-P4-coated coverslips adhered to this substrate. After 1 hr, many of the cells seeded onto Nogo-P4 had adhered to the coverslip and had begun flattening out (Figure 29d), much like those plated onto the laminin-coated coverslips (Figure 29a). However, when Nogo-P4 was offered as a substrate together with laminin, fewer cells adhered to the mixed substrate and more cells remained rounded up (Figure 29g). Statistically, there was a highly significant difference between the number of cells adhering to Nogo-P4 compared to all the other substrates (p value < 0.001), even compared to laminin alone (Appendix III). The finding that, at this time point, Nogo-P4 was significantly more adhesive for the OP13 cells compared to TN-R, let alone laminin, was unexpected (Appendix III).

When the cell adhesion cultures were photographed 6 hrs later, cells with a rounded up appearance ie non-adherent cells, were still visible but more of the OP13 cells had adhered to the TN-R-coated coverslips and had begun displaying the characteristic morphologies as previously described, namely flattened and spindle-shaped (not shown). Significantly more cells adhered to the laminin substrate than to the TN-R alone substrate and the adhesive effects of laminin, when combined with TN-R, were sufficient to significantly increase the number of adherent cells compared to those on TN-R alone (Appendix III). Although after 6 hrs, a substrate of laminin alone and a substrate of Nogo-P4 alone were comparatively

adhesive, there was once again a statistically significant difference found between the numbers of OP13 cells which adhered to Nogo-P4 alone compared to TN-R alone, laminin alone or laminin and TN-R (Appendix III). In the case of both TN-R and Nogo-P4, the combining of the test protein together with adhesive laminin failed to significantly increase the number of adherent cells above those on the test proteins alone (Appenxix III). After 12 hrs, the morphology of the OP13 cells remained relatively unchanged compared to after 6 hrs (not shown). The mean number of cells that adhered to the TN-R-coated coverslips reached their maximum at this time point, after which the numbers of adherent cells began to decrease (Figure 29). There was no significant difference between adhesions on laminin alone compared to TN-R alone, and a mixture of laminin and TN-R continued to fail in improving the adhesive properties of TN-R alone (Appendix III). As seen at both earlier time points, there was a highly significant difference between the number of cells adhering to Nogo-P4 compared to all the other substrates (p value < 0.001), even compared to laminin alone (Appendix III).

At the end of the short-term OP13 cell adhesion assay, 24 hrs after seeding, a number of non-adherent cells were still seen in cultures grown on TN-R alone and laminin and TN-R (Figure 27c and figure 27h, respectively). The cells which had attached to the coverslips maintained their distinct morphologies and in some cases become more elongated. The lowest mean number of cells had adhered to a substrate combination of TN-R and laminin, followed closely by TN-R alone (Figure 29). There were significantly more OP13 cells that had adhered to laminin alone compared to TN-R alone and a mixture of TN-R and laminin (Appendix III). This result suggests that, compared to laminin, TN-R is an anti-adhesive substrate for this mammalian glial cell line when offered as a sole substrate. In addition, a combination of laminin with TN-R fails to significantly increase the number of cells that attach compared to TN-R alone (Appendix III), suggesting that laminin may interfere with TN-R-mediated adherence or vice versa. The most intriguing result from the cell adhesion assay is the observed adherence of the OP13 cells on a sole substrate of Nogo-P4. At all time points measured, a statistically significant more number of OP13 cells adhered to a substrate of Nogo-P4 compared to laminin alone, TN-R alone, laminin and TN-R, and laminin and Nogo-P4 (p value < 0.001) (Appendix III). This was a surprising finding as Nogo-P4 is a peptide sequence for Nogo-A, the most potent axon and/or neurite growth inhibitor reported to date. This is the first reported case of any cell type preferring a substrate of Nogo-A compared to another substrate. As was the case with TN-R and laminin, a combination of

laminin with Nogo-P4 did not significantly increase the number of cells that attach compared to Nogo-P4 alone (Appendix III). This was also a surprising observation as one might expect that the adhesive effects of both Nogo-P4 and laminin would be additive and therefore that even more cells would adhere to a combination of these substrates than to either of them alone. This lack of synergistic effect may indicate some sort of laminin interference with Nogo-P4-mediated adherence, as the presence of laminin has been shown to alter the attractive properties of other proteins, such as netrin, which becomes repulsive substrate in combination with laminin in mammals (Hopker et al., 1999).

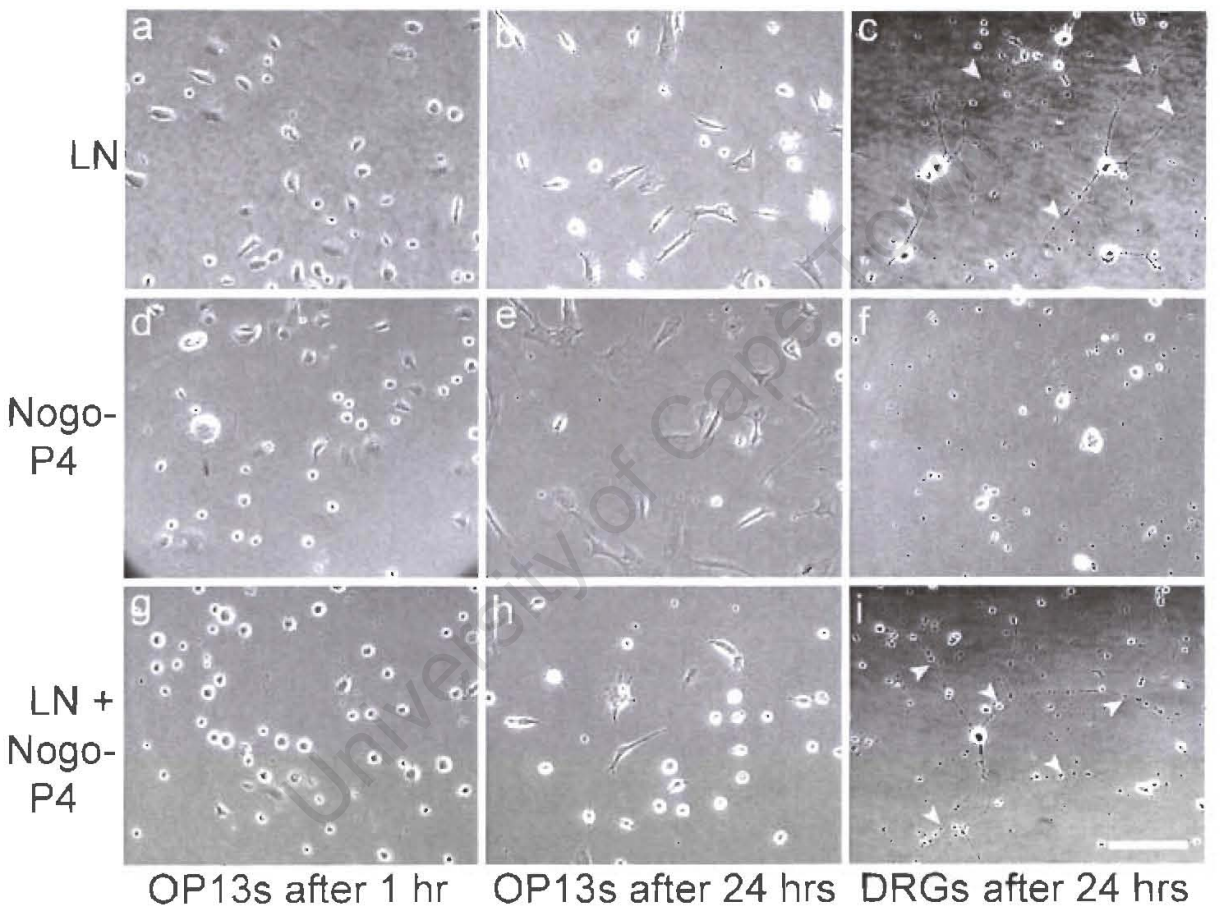

Figure 29. Nogo-P4 is an adhesive substrate for OP13 cells in a short-term cell adhesion assay. (a), after 1 hr, the majority of the OP13 cells in view adhered to a laminin (LN)-coated coverslip. **(b),** after 24 hrs, the majority of the OP13 cells in view had adhered to and adopted either a flattened out or spindle-shape morphology on the LN-coated coverslip. **(c),** dorsal root ganaglia (DRG) adhered to a LN-coated coverslip and extended numerous neurites (arrow heads) after 24 hrs. **(d),** the majority of the OP13 cells in view began adhering to the Nogo-P4-coated coverslip after 1 hr, although some non-adherent cells were visible. **(e),** the majority of the OP13 cells in view had adhered to and adopted either a flattened out or spindle-shape morphology on the Nogo-P4-coated coverslip after 24 hrs, and their morphologies were more elaborate than those on LN-coated coverslips at the same time point in (b). **(f),** No DRG neurite was observed on Nogo-P4-coated coverslips after 24 hrs. **(g),** after 1 hr, the majority of the OP13 cells in view remained rounded up on

coverslips that had been coated with a mixture of LN and Nogo-P4. **(h)**, after 24 hrs, fewer OP13 cells adhered to a coverslip coated with a mixture of LN and Nogo-P4 than on LN alone in (b). **(i)**, after 24 hrs DRG adhered to coverslips coated with a mixture of LN and mouse TN-R and extended numerous neurites (arrow heads). Scale bar = 100 µm.

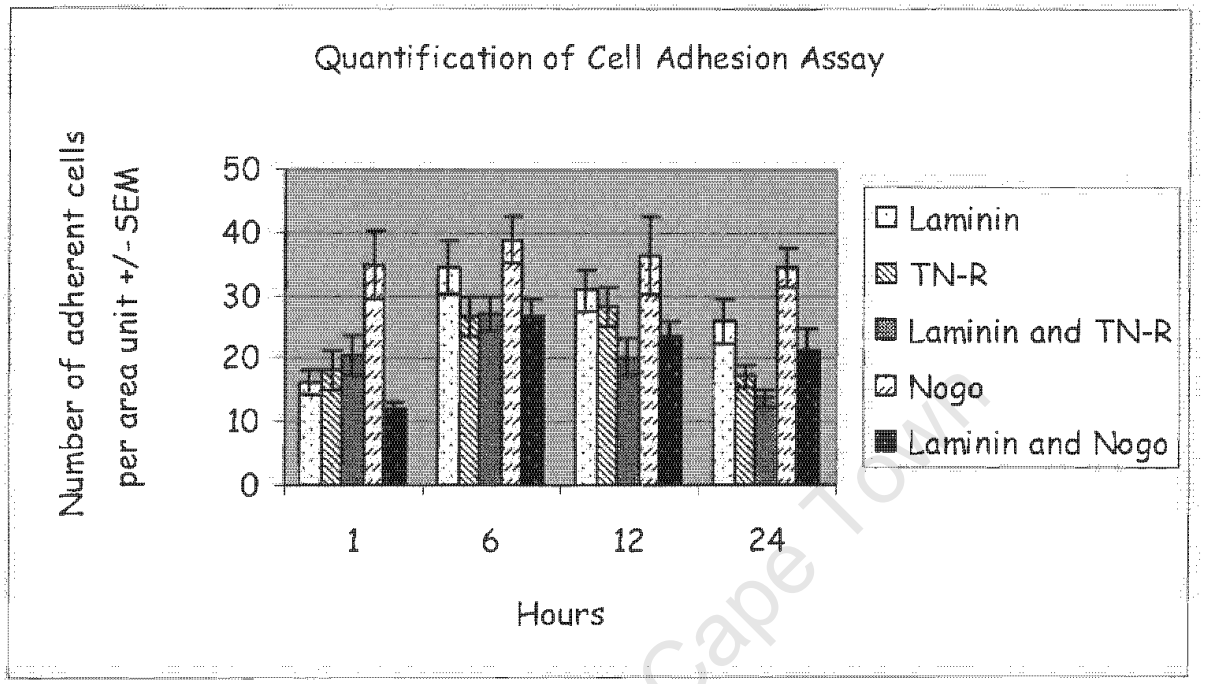

Figure 30. Quantitative analysis of the short-term OP13 cell adhesion assay showed that TN-R is anti-adhesive for the adhesion of OP13 cells and that Nogo is an adhesive substrate. After 1 hr, similar mean numbers of cells had attached to a substrate of laminin, TN-R, laminin and TN-R, and laminin and Nogo-P4 (Nogo) but many more cells had adhered to a substrate of Nogo. The adherence of OP13 cells on TN-R reached a peak after 12 hrs, where after it declined to even lower levels after 24 hrs than at 1 hr, even when offered in combination with laminin. A relatively large mean number of cells adhered to a substrate of Nogo, at all time points, even compared to laminin. The combination of laminin and TN-R, and laminin and Nogo, failed to increase the mean number of adherent cells compared to on TN-R alone or Nogo alone, respectively.

3.7.3 A sharp boundary of TN-R repells OP13 cells

In order to confront the OP13 cells with an abrupt substrate border of TN-R, as opposed to a uniform substrate of TN-R, a short-term cell adhesion assay was performed using a patterned substrate of TN-R. Differentiated OP13 cells were plated onto coverslips that had been coated with alternating lanes of PLL and TN-R. After 24 hrs, the cultures were fixed and stained with rabbit anti-TN-R antibodies to visualise the stripes of TN-R. Unfortunately, the OP13 cells washed off the coverslips during processing and so it was not possible to merge the images of the OP13 stained cells and the TN-R stripes. In order to then visualise the orientation the OP13 cells on such a substrate, phase contrast images where taken before

processing (Figure 31a) which could then be "superimposed" onto the stripe image (Figure 31b). On the TN-R stripe-coated coverslips, the OP13 cells adopted a particular orientation: they grew in relatively straight rows that corresponded to the PLL stripes. The OP13s also made a substrate choice by adhering to PLL-coated zig-zag lanes and avoiding the TN-R-coated zig-zag lanes (Figure 31c). This repellent or substrate choice effect of a sharp border of mammalian TN-R suggests that if these cells were to be implanted at a site where TN-R is present in the form of a boundary, then the cells would be inhibited from migrating away from the site of injection, as is seen *in vivo* (Pesheva et al., 1991, 1993; Taylor et al., 1993).

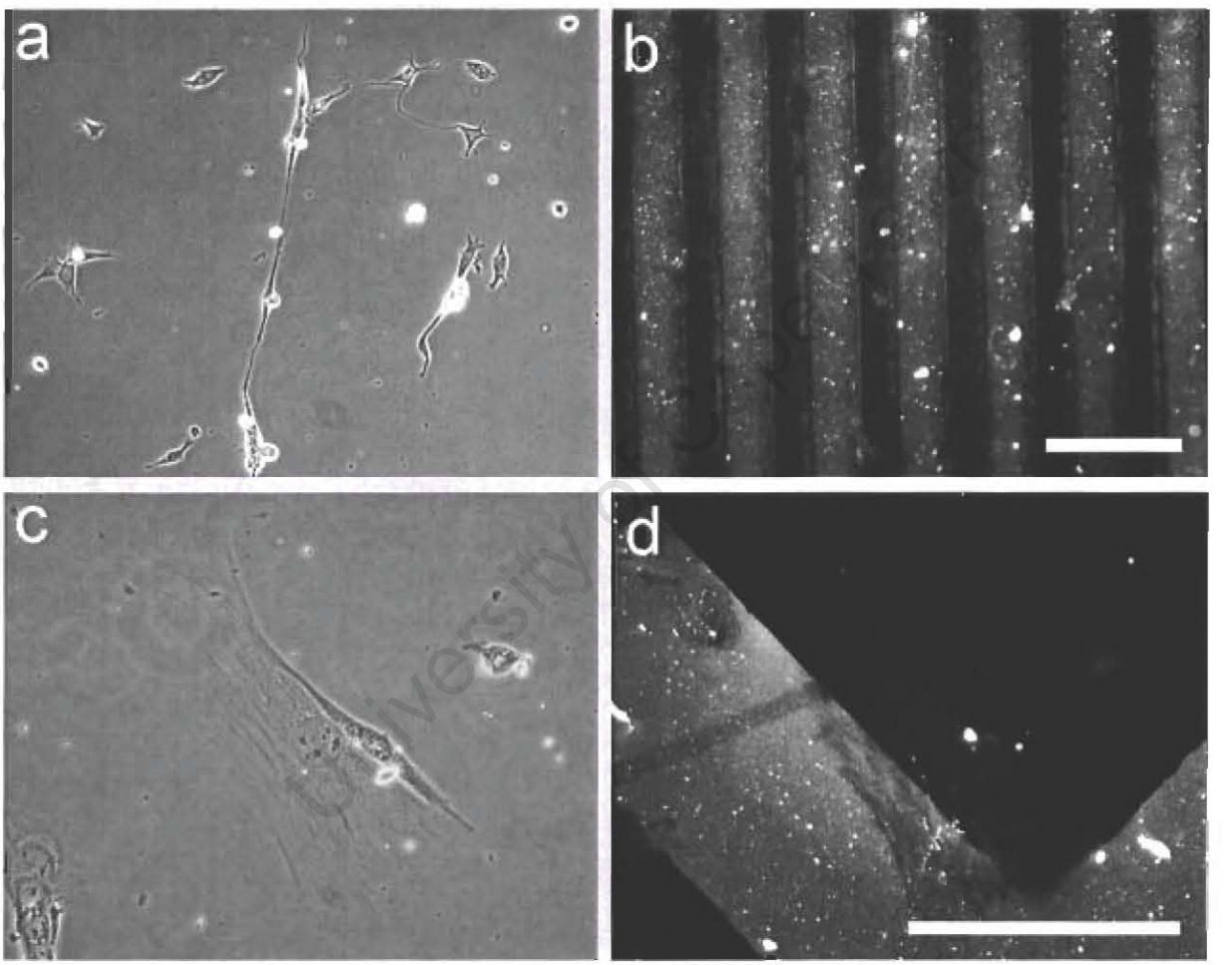

Figure 31. OP13 cells avoid a sharp border substrate of mouse TN-R. (a), phase-contrast image of OP13 cells growing on a straight stripe pattern of purified mammalian TN-R shows that the OP13 cells avoid the sharp border of TN-R. **(b),** rabbit polyclonal anti-TN-R antibodies stain a straight stripe pattern of purified mammalian TN-R. **(c),** phase-contrast image of OP13 cells growing on a zig-zag stripe pattern of purified mammalian TN-R shows that the OP13 cells avoid the sharp border of TN-R. **(d),** rabbit polyclonal anti-TN-R antibodies stain a zig-zag stripe pattern of purified mammalian TN-R. Scale bar = 100 μm

3.7.4 A patterned substrate of laminin and Nogo-P4 is adhesive Schwann cells

The observed adherence of the OP13 cells on a uniform substrate of Nogo-A raised the question of whether Nogo-A is an adhesive substrate for other glial cells that are also promising candidates of cell transplant mediated repair, namely Schwann cells. In order to further test the substrate properties of Nogo-A, a short-term cell adhesion stripe assay was therefore performed using Schwann cells. Schwann cells were grown on either (i) a uniform substrate of homogenous laminin, (ii) a uniform substrate of homogenous Nogo-P4, or on (iii) a patterned substrate of laminin and Nogo-P4 stripes alternating with laminin only stripes. Similarly to what was observed in the OP13 cell adhesion assay, the attachment of Schwann cells was not inhibited on the Nogo-P4 substrate and adhered to both laminin- and Nogo-A-coated coverslips (Figure 32a and figure 32b, respectively). The cells plated on the Nogo-P4 substrate displayed a similar resemblance to those plated onto the laminin substrate, indicating that, like laminin, Nogo-P4 was an adhesive substrate for Schwann cells. In comparison, when the cells were grown on a patterned coverslip where they were given a substrate choice, the Schwann cells adopted a very specific preference: they grew in very straight rows along what could only have been the combined laminin and Nogo-P4 stripes. The width of the stripes was 30μm, the exact distance at which each Schwann cell lined-up. The cells therefore chose to adhere to a substrate of laminin and Nogo-P4 instead of a substrate of laminin alone. The result from the uniform substrate assay suggests that laminin-secreting Schwann cells *in vivo* may not be inhibited by the presence of Nogo-A, and this might have implications for the response of Schwann cells implanted at a SCI site. In addition, the result from the patterned stripe assay suggests that laminin-secreting Schwann cells *in vivo* may be channeled by a sharp boundary of Nogo-A. This response could indicate a possible role for Nogo-A in the development of myelination in the PNS, when Nogo-A-expressing sensory neurons become myelinated by laminin-secreting Schwann cells.

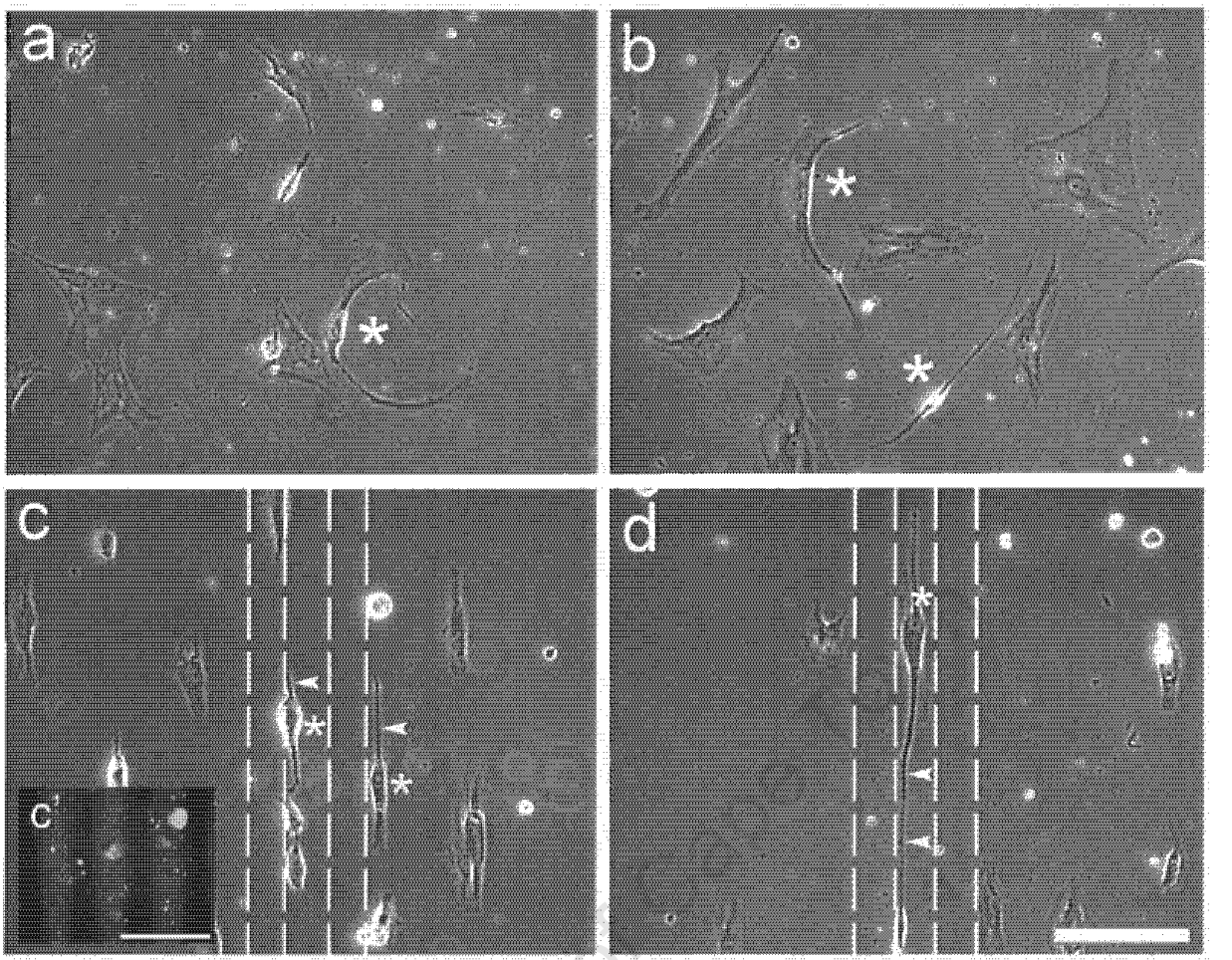

Figure 32. Nogo-P4 is an adhesive substrate for Schwann cells in a short-term cell adhesion stripe assay. **(a),** Schwann cells (asterisk) adopt a typical spindle-shaped pattern on a homogenous substrate of laminin compared to the surrounding flattened-out fibroblasts that are normally present in a primary culture from peripheral nerve explants. (b), Schwann cells (asterisk) also adopt their typical spindle-shaped morphology on a homogenous substrate of Nogo-P4. **(c),** Schwann cells (asterisk) elongate their axons (arrow heads) along a sharp substrate border of laminin and Nogo-P4 (dashed lines). **(c')**, immunohistochemical staining of Nogo-P4 stripes with rabbit polyclonal anti-Nogo-A antibody. **(d),** another image of a Schwann cell (asterisk) with a very long neurite (arrow heads) that aligns with the border of laminin and Nogo-P4 stripes. Scale bar = 100 µm

Chapter 4: Discussion

The purpose of this study was firstly to analyze the expression pattern of fish tenascin-R (TN-R) in the retinotectal pathway of the adult goldfish and its modifications after an optic nerve crush. It was demonstrated, for the first time, that fish TN-R is expressed in the retina, optic nerve and the optic tectum of the unlesioned goldfish and that during optic nerve regeneration, TN-R expression remains relatively constant in the optic nerve. Secondly, in order to understand why the presence of this putative axon-growth-inhibiting protein does not prevent the growth of retinal ganglion cells (RGCs) in the retinotectal pathway, the *in vitro* substrate properties of fish TN-R were analyzed. RGC outgrowth assays demonstrated that a homogenous substrate of fish TN-R is in fact inhibitory for neurite outgrowth. Despite the inhibitory effect of fish TN-R, the growth and regeneration of RGC axons along TN-R-containing pathways can be explained by the concomitant and colocalized expression of growth-supportive and growth-promoting laminin.

4.1 The expression pattern of fish TN-R in the adult goldfish brain mimics that seen in the adult mammalian brain

TN-R immunoreactivity in the adult goldfish brain was mainly localized to myelinated regions in the olfactory bulb, mid-brain, hind-brain, and spinal cord. This expression pattern is very similar to what has been reported for TN-R mRNA in the mammalian brain, where it is localized in the cerebellum, hippocampus and olfactory bulb (Fuss et al., 1993). The expression of TN-R by fish brain oligodendrocytes (Pesheva et al., 2006) in myelinated tracts in these regions may indicate a functional role for TN-R in myelination, as has been suggested in mammals (Fuss et al., 1993). TN-R has in fact been shown to act as an autocrine factor for the timed differentiation of oligodendrocytes (Pesheva et al., 1997) but this has yet to be demonstrated in fish oligodendrocytes.

4.2 The expression pattern of fish TN-R in several locations along the optic pathway does not indicate an inhibitory role in the growth of new or regenerating retinal ganglion cell axons

4.2.1 The expression of TN-R, its ligands and its interaction partners in the retina

The retina is a site of neurogenesis in the adult goldfish. New retinal ganglion cells (RGCs) are continuously added to the periphery of the retina and their axons grow through the optic fiber layer (OFL) to the center of the retina, where they exit through the optic nerve head into the optic nerve. The expression of TN-R, its ligands and its interaction partners in the retina may therefore be relevant to the growth of new and regenerating RGC axons.

4.2.1.1 TN-R expression

In the retina on the side of the unlesioned optic nerve at all time intervals, intense TN-R immunoreactivity was observed in fascicles of RGC axons in the OFL. Newly growing RGCs express the E587 antigen, a member of the L1 family of cell adhesion molecules (CAMs) which mediates selective fasciculation of the newest axons with young axons, and therefore the creation of the age-related order in the fish retina (Vielmetter et al., 1991; Bastmeyer et al., 1995). In this study, E587-postive RGC axons were seen growing in areas of the OFL which were both immunopositive and immunonegative for TN-R, indicating that the growth of new axons as they navigate themselves out of the retina is not inhibited by the presence of TN-R along their route. The expression pattern of TN-R in the retina is similar to what has been observed in mammals, where there is weak staining in the OFL (Bartsch et al., 1993) but contrasts to what has been observed in the zebrafish, a closely related species. In zebrafish, TN-R borders the pathway of RGC axons in the retina, where it is proposed to act as a repellent guidance molecule as newly growing RGC axons were only seen to grow in TN-R immunonegative regions (Becker et al., 2004). The difference in the spatial pattern of TN-R expression in goldfish compared to zebrafish indicates that the expression of this protein within the classes of lower vertebrates is not uniform. This suggest that TN-R may have a different function in the goldfish compared to the zebrafish, or that its function may not directly impact on regenation in the retina. The presence of TN-R in the OFL of the goldfish retina raises at least two questions: firstly, which cells are responsible for expressing TN-R within intraretinal fascicles of RGC axons in the OFL; and secondly, why the growth

of young RGC axons is uninhibited by the presence of this putative axon growth-inhibiting protein in the OFL.

It has previously been shown that, like in their mammalian counterparts, fish TN-R is expressed by fish oligodendrocytes (Pesheva et al., 2006). During development of the mammalian visual system, oligodendrocytes only migrate as far as a certain point in the optic nerve and do not reach the optic nerve head to enter the retina (Bartsch et al., 1989, 1994). This migratory pattern is due to the expression of guidance molecules in gradients: a high concentration of netrin at the optic chiasm repels the young oligodendrocytes towards the retina but a high concentration of semaphorin 3-A at the optic nerve head inhibits them from migrating further into the retina (Spassky et al., 2002). The absence of oligodendocytes in the mammalian retina therefore excludes the possibility that the TN-R in the OFL is oligodendrocyte-associated. In fish however, oligodendrocytes migrate along the entire length of the optic nerve, as evidenced by the expression of oligodendrocyte-derived TN-R, and into the retina. The intense TN-R staining in the goldfish OFL may therefore represent unmyelinated oligodendrocytes surrounding the axons of RGCs. In zebrafish, it has been argued that the TN-R immunoreactivity in the OFL is not glial cell associated but rather neuronal, as no TN-R mRNA labeling was found in the OFL, only at the outer margin of the inner nuclear layer (INL) (Becker et al., 2004). It seems unlikely; however, that ECM-deposited TN-R could make its way through the INL and inner plexiform layer (IPL), to the OFL, where it is so discretely localized. *In situ* hybridization would need to be performed in order to clarify which cells in the retina are responsible for the TN-R expression. Regardless of the source of TN-R in the OFL, the growth of new RGC axons in the OFL does not seem to be deterred by its presence. E587-positive fibers not only grew in TN-R-positive regions of the OFL but also exited the retina through the TN-R-positive optic nerve head. In complete contrast to in zebrafish, where TN-R has been suggested to act as repellent guidance molecule (Becker et al., 2004), goldfish TN-R may not have an inhibitory role in the growth of new or regenerating RGC axons. The outgrowth of RGC neurites on a homogenous substrate of fish TN-R was however inhibited, except in the presence of laminin. As there was a significant colocalization of TN-R and laminin, as well as TN-R and fibronectin, in the OFL, the presence of these growth-promoting proteins in the OFL may mediate or allow axon outgrowth in the presence of TN-R.

The OFL was not the only area in the retina where TN-R immunoreactivity was observed. Remote from the OFL, the synapse-rich outer plexiform layer (OPL), where the

photoreceptors, bipolar and horizontal cells make synaptic connections with each other, was also conspicuously labeled for TN-R protein. A similar expression pattern has been shown in mammals, where TN-R staining is most intense in the OPL, and weaker in the outer part of the INL and the IPL (Bartsch et al., 1993; Becker et al., 2000a). Prominent TN-R immunoreactivity in the OPL has also been observed in other lower vertebrates, such as the salamander and the zebrafish (Becker et al., 1999, 2003). As it has been suggested that the TN-R mRNA located at the outer margin of the INL of the zebrafish retina most likely corresponds to horizontal cells (Bartsch et al., 1993; Becker et al., 2003), and that the synthesis of TN-R in these cells could lead to its deposition in the adjacent OPL (Becker et al., 2003), it is possible that interneurons in the goldfish INL are also the source of TN-R in the goldfish OPL.

The retina on the side of the lesioned optic nerve was easily identifiable by the increase in E587-labeled RGC axons in the OFL. It is well established that after an optic nerve lesion all RGC axons reexpress the E587 antigen (Vielmetter et al., 1991; Giordano et al., 1997; Schmidt et al., 1998). Many of the RGCs upregulated the antigen as early as 1 week after the lesion, and most continued to express it 6 weeks later. This timecourse of E587 antigen expression was very similar to what has previously been reported (Ankerhold et al., 1998; Ankerhold and Stuermer, 1999; Lang et al., 2001). The pattern of TN-R expression in the retina following an optic nerve crush was also regulated. The intensity of TN-R staining in the OFL remained high after 1 week, when the regenerating RGCs would have been expected to have exited the retina. The regrowing RGC axons therefore initially grow through TN-R-positive regions of the OPL as they make their way out of the retina, and even once they have exited, TN-R could still affect their growth process by signalling through receptors on the axon shaft. Even though by 3 weeks post-injury there was a decrease in TN-R immunoreactivity that was still observed at 6 weeks, this timepoint correlates to when these axons would be expected to have already reached the optic chiasm and so there is therefore no correlation between decreased levels of TN-R in the retina and the success of RGC axon regeneration. Considering that there was a concomitant increase in the staining intensity of both laminin and fibronectin in response to the nerve crush, these upregulated levels of growth-supportive and growth-promoting proteins may mediate or allow regenerating RGC axons to grow in the presence of TN-R during the early stages of regeneration (1 to 3 weeks post-injury) when the RGC growth cones contact TN-R in the OFL, as well as during later

stages of regeneration (3 to 6 weeks post-injury) when TN-R, despite being down regulated, could still effect their outgrowth by binding to its receptors on the RGC axon shaft.

The ability of the RGC axons to grow in the TN-R-positive OPL could of course be a reflection of the neuron intrinsic properties of this particular population of cells as not all fish CNS neurons are capable of axon regeneration. Although fish optic nerve axons and ascending spinal axons are able to regenerate after injury, certain descending spinal axons, for example the Mauthner cell (M cell) axon, regrow poorly (see review by Zottoli et al., 1994; Becker et al., 1997): only 35% of lesioned M cells show some regenerative response after a lesion (Bhatt et al., 2004). Recently, several studies on the role of cyclic adenosine monophosphate (cAMP) in regeneration have suggested that this single molecule may act as a critical switch in determining whether severed axons can regenerate and restore function. Administration of a cAMP analogue into the somata of lesioned zebrafish M cells enables M cell axons to regenerate across the lesion site and restore function. In addition, M-cells that had spontaneously regrown after the lesion but in an aberrant fashion, with its axon making a U-turn at the lesion site to grow back towards the head, unexpectedly produced a branch from the aberrant axon that crossed the lesion site and extended appropriately into the caudal spinal cord when the synthetic cAMP was administered (Bhatt et al., 2004). This cAMP-induced switching in turning direction of growth cones has been shown in Xenopus spinal neurons, where growth cone responses to guidance cues can be converted by altering the levels of cAMP (Ming et al., 1997; Song et al., 1997, 1998). Goldfish RGCs may constitute a unique population of cells that secrete factors, perhaps axogenesis factor-1, -2 and/or -3, which stimulate cAMP, and therefore axon regeneration. In mammals, it has been suggested that the precipitous decrease in endogenous cAMP levels after birth may explain why only embryonic CNS neurons, which have elevated endogenous cAMP levels, have the capacity to regenerate during prenatal and postnatal development (Cai et al., 2001).

In contrast to the decrease in TN-R staining in the OFL 3 weeks after the optic nerve crush, the intensity of TN-R staining in the OPL increased during the time course of axon regeneration. The accompanying increase and decrease in TN-R staining in the OPL and OFL, respectively, supports the idea that the source of TN-R in the OPL may be neural (Becker et al., 2003); while in the OFL it may in fact be glial-associated.

4.2.1.2 TN-R and F3 expression

In the retina on the side of the unlesioned optic nerve at all time intervals, F3-labeled fibers in the OFL were weakly stained. The maximum number of F3-positive fibers was observed 3 weeks after the optic nerve crush, whereafter there was a marked decrease. This timecourse of F3 expression is similar to what has previously been reported in goldfish, where 2 weeks after an optic nerve transection, F3 mRNA was significantly upregulated in all RGCs and its expression level remained high for at least 6 weeks (Haenisch et al., 2005). In this study, F3-positive fibers were observed not only in the OFL but also in other retinal layers, particularly the inner plexiform layer (IPL), where bipolar, amacrine, and RGCs make synaptic connections with each other. As to which cells these F3-postive fibers belong to has been alluded to in a recent paper. Stuermer's group have shown that F3 mRNA expression in the adult goldfish retina is not restricted to the youngest RGCs at the periphery but distributed over the entire retina, indicating, firstly, that F3 is expressed by neurons other than RGCs, and secondly, that F3 may be required for both early and late processes during RGC development (Haenisch et al., 2005). The labeling of F3 on RGCs in the unlesioned retina suggests that it is not the absence of TN-R receptor expression that allows for the apparent non-sensitivity of goldfish RGC axons to TN-R. In addition, the upregulation of F3 during the early stages of regeneration indicates that the downregulation of F3 is also not the reason for the apparent non-sensitivity of goldfish RGC axons to TN-R. Indeed, the coincident expression of oligodendrocyte-expressed TN-R and its neuronal receptor F3 in the OFL suggests that this ligand-receptor pair may mediate a functional interaction between oligodendrocytes and the RGC axons in this region. The initial increase in F3 levels in the OFL may increase the interaction between TN-R-expressing oligodendrocytes and the F3-expressing RGC axons they surround.

In mammals it has been shown *in vitro* that the interaction between TN-R and F3 enhances F3-mediated neurite extension (Nörenberg et al., 1995), and that soluble TN-R increases the number of tectal cells with neurites on immobilized F3 (Zacharias et al., 1999). The interaction of TN-R with F3 *in vivo* in the goldfish retina may therefore have a regulatory influence on axon extension. Schachner's group have, however, shown that F3 mediates the repulsion of cerebellar neurons on a uniform as well as substrate borders of TN-R (Xiao et al., 1996). These seemingly contradictory effects of TN-R-F3 interactions on neurite outgrowth clearly demonstrate the dual nature of TN-R, which in this case, is dependent upon the cell type involved and the TN-R functional domain F3 binds to (see review by

Brümmendorf and Rathjen, 1996). In the case where the combined action of TN-R and F3 regulates axon extension of tectal cells, the immunoglobulin (Ig) domains of F3 bind to the fibronectin type III (FN III)-like domains 2-3 within TN-R (Nörenberg et al., 1995); while in the case where the combined action of TN-R and F3 regulates neurite repulsion of cerebellar cells, the Ig domains of F3 bind to the inhibitory epidermal growth factor (EGF)-like repeats within TN-R (Xiao et al., 1996). It may be that F3-expressing goldfish RGCs, like mammalian tectal cells, are one of the cell types that respond positively to TN-R, such that their axon outgrowth in the retina within TN-R-positive regions is promoted by binding to the FN III-like domains within TN-R.

It has been suggested that the interaction between F3 and TN-R expressed in the other retinal layers mediates the establishment of an intricate synaptic network in the IPL and OPL (Rathjen et al., 1991; Bartsch et al., 1993; Völkmer et al., 1998). TN-R colocalizes with neurofascin, another of its L1-like subgroup of the Ig super family interaction partners (Völkmer et al., 1998), which is expressed in the IPL and OPL of the chick retina (Rathjen et al., 1991). It is here that TN-R may reduce the interaction between neurofascin and another L1-like protein, neuronal NgCAM-related cell adhesion molecule (NrCAM), on the neurites of the interneurons in the plexiform layers of the retina by sterically blocking the NrCAM binding region within neurofascin while still allowing binding of F3 to neurofascin (Völkmer et al., 1998). As the combined action of neurofascin and NrCAM promotes axon outgrowth from tectal cells (Völkmer et al., 1996; Rathjen et al., 1987) the reduction of this interaction by TN-R and the subsequent shift in receptor usage from NrCAM to F3 (Völkmer et al., 1998) may allow for the refinement of synaptic connections between the multitudes of cellular processes within these plexiform layers. Although the expression of neurofascin and NrCAM in the goldfish retina are yet to be analyzed, a similar functional interaction between TN-R and F3 in the goldfish OPL may also exist.

The idea that TN-R in the OFL may not be inhibitory for RGC growth while possibly refining synaptic connections in the OPL, could be explained firstly by the different cell types involved, and secondly by the expression of different TN-R receptors and/or ligands. In the first instance, the RGCs may constitute a population of cells that are intrinsically able to grow in the presence of TN-R while the bipolar, amacrine and horizontal cells may be inherently incapable. In the second instance, the simultaneous expression of laminin and fibronectin in the OFL may permit the growth of RGCs in the TN-R positive OFL, and the gradual decline in the F3 receptor expression in the later stages of regeneration may also reduce the

sensitivity of the RGCs to TN-R that could still bind to receptors on the RGC shaft. The increase in TN-R immunoreactivity in the OPL, where laminin and fibronectin are not expressed, may allow TN-R to exert some type of inhibitory/pruning effect, as seen in the RGC outgrowth assays, on neurite outgrowth in the OPL.

4.2.1.3 TN-R and CSPG expression

The colocalized expression of TN-R and chondroitin sulphate proteoglycans (CSPGs) in the OFL in both the unlesioned retina and during time points in the regeneration process when newly growing axons travel along the OFL, was an unexpected finding because in zebrafish there are only very low levels of CSPG immunoreactivity (Becker and Becker, 2002). The staining pattern also contrasts to what has been reported in mammals, where the expression of CSPGs in axon-free regions of the developing nervous system, and in the inhibitory glial scar that forms after CNS injuries, suggests that CSPGs play a significant role in facilitating axon-guidance during development and in blocking successful regeneration (Snow et al., 1990; Snow and Letourneau, 1992; Snow et al., 2001). The expression of CSPGs in the OFL of the goldfish retina, a region populated with RGCs and their axons, was therefore surprising. The fact that the growth of newly growing and regenerating RGC axons is not hindered by the co-expression of both these putative axon growth-inhibiting proteins may be due to the concomitant expression of laminin and fibronectin, both axon growth-supporting proteins, in the OFL and/or the neuron intrinsic properties of the RGCs.

Although laminin and fibronectin are not highly expressed constituents of the mammalian CNS extracellular matrix (ECM), *in vitro* experiments have shown that growth cones grow onto a substrate consisting of a low laminin/high-CSPG ratio (Snow and Letourneau, 1992). It is therefore plausible that in the goldfish OFL the high levels of laminin override the otherwise inhibitory effects of the CSPGs, and that the levels of laminin are sufficient to overcome the increased inhibitory effect of CSPGs that occurs after an optic nerve crush. In certain instances, mammalian neurites sometimes paradoxically traverse regions expressing relatively high levels of CSPGs, where they become fasciculated (Snow et al., 2003). The level of CSPG expression in the goldfish OFL might therefore also be at a concentration that supports the growth and fasciculation of newly growing and regenerating RGC axons.

4.2.1.4 TN-R and laminin expression

In the retina on the side of the unlesioned optic nerve at all time intervals, intense laminin immunoreactivity was observed in the OFL. The laminin antibody stained distinct, thin

processes in the OPL and these profiles could belong to a number of different cell types. Firstly they could be blood vessel associated, as laminin is expressed in the basal lamina of endothelial cells lining blood vessels near the OFL (Essner and Lin, 1988; Mandarino et al., 1993). Secondly, these processes could belong to astrocytes, which are closely associated with blood vessels in the OFL (Jiang et al., 1994; MacLaren, 1996) and are known to express laminin (Liesi et al., 1984). A third possibility is that the laminin-labeled processes belong to oligodendrocytes. Goldfish oligodendrocytes are considered to be analogous to Schwann cells (review by Stuermer et al., 1992). As Schwann cells produce laminin (Cornbrooks et al., 1984), it is possible that TN-R-expressing oligodendrocytes in the retina express laminin, and that is therefore why there is such substantial colocalization of their staining patterns in the OFL.

Goldfish oligodendrocytes in the optic nerve that become injured after a nerve crush are known to dedifferentiate into an immature phenotype that is analogous to a Schwann cell (Ankerhold et al., 1998; Ankerhold and Stuermer, 1999). It is possible that oligodendrocytes in the retina also respond to the nerve crush by dedifferentiating into Schwann cell-like type cells that upregulate and secrete laminin and other ECM constituents. The potent axon growth and guidance capacity of laminin is well established and there is considerable evidence to support the critical role laminin plays during peripheral nervous system (PNS) regeneration (reviews by Martini, 1994, McKerracher et al., 1996, Fu and Gordon, 1997, Grimpe and Silver, 2002). The presence of laminin in the OFL of the retina on the side of the unlesioned nerve may therefore permit the growth of newly growing RGC axons despite the presence of TN-R and CSPGs; and during optic nerve regeneration, the persistant upregulated levels of laminin may contribute to the success of RGC axon regrowth within regions of axon growth-inhibiting protein expression.

4.2.1.5 TN-R and fibronectin expression

In the retina on the side of the unlesioned optic nerve at all time intervals, only low levels of fibronectin immunoreactivity was observed in the OFL. Three weeks after the optic nerve crush, there was however a substantial increase in fibronectin staining that colocalized with TN-R in the OPL. The fibronectin-labeled processes may be related to blood vessels but could also belong to astrocytes which, in mammals, are known to express fibronectin (Liesi et al., 1984; Tom et al., 2004) and enter the retina where they are closely associated with blood vessels in the OFL (Jiang et al., 1994; MacLaren, 1996). Mammalian TN-R has been shown

to inhibit fibronectin-mediated cell adhesion and neurite outgrowth (Pesheva et al., 1994). This inhibition is via steric hinderance and/or adverse conformational changes within the functional domains of fibronectin, as well as through interference with the functioning of integrins, the receptors for fibronectin (Pesheva et al., 1994; Probstmeier et al., 1999, 2000a). Fish TN-R has, however, been recently reported to bind to fibronectin without inhibiting fibronectin-mediated cell adhesion and neurite outgrowth (Pesheva et al., 2006). These differences in mammalian versus fish TN-R may be explained by the absence of chondroitin sulphate (CS) glycosaminoglycans (GAGs) on fish TN-R proteins (Pesheva et al., 2006), which are expressed on mammalian TN-R proteins, where they have been shown to be involved in TN-R-mediated inhibition of adhesion and outgrowth on fibronectin (Probstmeier et al., 2000a).

4.2.2 The expression of TN-R, its ligands and its interaction partners in the optic nerve

The optic nerve contains fascicles of mature RGC axons as well as new RGC axons en route to the optic tectum, which grow within a discrete region along the periphery of the nerve. After an optic nerve crush, injured axons regrow across the lesion site and through the nerve. The expression of TN-R, its ligands and its interaction partners in the optic nerve may therefore be relevant to the growth and guidance of new and regenerating RGC axons in this region.

4.2.2.1 TN-R expression

In the unlesioned optic nerve at all time intervals, weak TN-R immunoreactivity was observed. TN-R was equally distributed along the entire length of the nerve to within the neural tissue of the axon fascicles where it was punctuate in appearance. Considering that fish oligodendrocytes are located throughout the optic nerve, and that fish TN-R is expressed by oligodendrocytes *in vitro*, it is likely that the goldfish optic nerve oligodendrocytes express TN-R on their cell surface and/or deposit TN-R into their surrounding ECM. This staining pattern is similar to what has been observed in mammals, where there is a homogenous, weak staining of TN-R in the optic nerve (Bartsch et al., 1993; Wintergerst et al., 1993). Spots of increased TN-R immunoreactivity in the mammalian optic nerve correspond to an accumulation of the protein at the nodes of Ranvier (Bartsch et al., 1993; Wintergerst et al., 1993). The punctate TN-R staining observed in the goldfish optic nerve may therefore also correspond to the nodes of Ranvier, where TN-R is thought to bind to the β2 subunit of the sodium channel (Srinivasan et al., 1998; Xiao et al., 1999). The staining of TN-R in the

goldfish optic nerve is however different to that in mammals as mammalian TN-R is restricted to the myelinated chiasm-near end (Bartsch et al., 1989; 1994). In the salamander, TN-R expression is also equally distributed only at the chiasm-near end, an area corresponding to the furthest point of oligodendrocyte migration during development (Becker at al., 1999). The expression of guidance molecules in discrete gradients has been proposed to direct the migration of oligodendrocytes in the mammalian optic nerve (review by Tsai and Miller, 2002). It is therefore possible that the expression of guidance molecules in such gradients does not exist in the goldfish optic nerve or that the migration of goldfish oligodendrocytes is not inhibited by these gradients. In comparison to the zebrafish optic nerve, where newly added optic axons grow in a TN-R immunonegative pathway which is bordered by TN-R immunoreactivity (Becker et al., 2004), no such borders were observed in the goldfish optic nerve and E587-positive axons were seen growing in both TN-R-immunopostive and TN-R-immunonegative pathways.

The downregulation of myelin basic protein (MBP) staining throughout the injured nerve but particularly at the lesion site, does not necessarily reflect the death of oligodendrocytes as no signs of oligodendrocyte apoptosis have previously been reported (Ankerhold and Stuermer, 1999). Rather, the goldfish oligodendrocytes seem to respond to the optic nerve lesion by dedifferentiating into an immature phenotype that no longer expresses typical myelin markers (Ankerhold et al., 1998; Ankerhold and Stuermer, 1999). This type of oligodendrocyte response has also been documented in frogs (Lang and Stuermer, 1996). Although the dedifferentiated oligodendrocytes at the lesion site do not express MBP, they appear to continue to express TN-R in the goldfish optic nerve directly adjacent to the lesion site, at the retina-near end and the chiasm-near end, 1 week after the crush injury. It is only in the region of the lesion site itself that a downregulation of TN-R staining was observed. It is the oligodendrocytes in this injured region that are likely to respond by dedifferentiating the most, and therefore downregulating their repertoire of more advanced differentiation markers. At this time point, newly growing and regenerating RGC axons have begun crossing the lesion site. These axons therefore may not be exposed to high levels of TN-R as they regrow across the lesion site in the goldfish nerve. This, however, does not mean that the successful regeneration of these axons correlates with a general downregulation of fish TN-R, as oligodendrocytes in the retina-near nerve and in the chiasm-near nerve continue to express fish TN-R. These are regions where the axons have just grown through, where their growth is

uninhibited, and where they are going to grow through, where their growth is also uninhibited.

Although no quantitative measurements were taken, both the unlesioned and 1 week post-lesioned nerves were photographed with the same exposure time, and so a comparison between the TN-R staining intensity in each nerve could be made. It was clear that the lesioned nerve continued to express TN-R at levels comparable, or even slightly higher than the unlesioned nerve. By 3 weeks, when the RGC axons would have been expected to have already crossed the lesion site and the optic chiasm, there seems to be a slight decrease in TN-R immunoreactivity at the optic chiasm of the lesioned nerve compared to the unlesioned control. TN-R intensity levels do, however, become comparable again by 6 weeks. During this time period the expression of fish TN-R mimics the temporal expression of mammalian TN-R during development where mammalian TN-R expression precedes, and then stimulates, myelination.

Considering that the upregulation of mammalian TN-R in the rat CNS has been proposed to contribute to the poor axon regeneration in the mammalian CNS (Deckner et al., 2000; Probstmeier et al., 2000b); and that in the lower vertebrate salamander, the downregulation of TN-R after an optic nerve crush has been suggested to contribute to successful regeneration in these animals (Becker et al., 1999), it is interesting that the goldfish RGC axons are not inhibited by the continued expression of fish TN-R. Even though there is a down regulation of the protein at the lesion site, the RGC axons still need to grow along the entire length of the nerve, including areas where TN-R is still expressed, and possibly even upregulated. This may have suggested that, unlike its mammalian homologue, fish TN-R is not an axon growth-inhibiting protein. The results of the RGC outgrowth assays clearly demonstrated though that, when offered as a homogenous substrate, fish TN-R exerts an inhibitory effect on RGC neurite extention. There may however, still be functional difference that exist between fish TN-R and mammalian TN-R due to the fact that (i) TN-R might be present in lower amounts in fish than in mammals (Wanner et al., 1995) such that it does not exert a sufficiently inhibitory effect, (ii) posttranscriptional or posttranslational changes might have removed or modified the cell binding domains that are responsible for axon growth inhibition in mammalian TN-R, (iii) the neuronal receptor(s) or signalling pathways mediating axon growth inhibition may be absent or modified, or (iv) there are diffences in second messenger activation after receptor binding (reviews by He and Koprivica, 2004, Sandvig et al., 2004; Pesheva et al., 2006).

It is indeed the case that the relative amount of fish TN-R protein in the brain tissue of teleost fishes is considerably lower than in higher vertebrates (Pesheva et al., 2006) but as the tissue sample did not include the optic nerve, it can not be said for certain that there is also less TN-R in the fish optic nerve compared to mammals. Alternative splicing and glycosylation of the fish TN-R protein may account for the fact that TN-R monoclonal antibodies identified protein bands of 220 kDa and 170 kDa (Pesheva et al., 2006), these dimers being larger than the 160 kDa and 180 kDa proteins found in mammals. Possible glycoconjugates on the fish TN-R protein may therefore alter the function of the protein in these animals. The absence of a neuronal receptor for TN-R, namely F3, in the goldfish CNS can not account for the behaviour of the regenerating axons in the presence of TN-R as F3 is indeed expressed on the RGC axons but whether or not the inevitable ligand binding is likely to result in a similar intracellular response as elicited by mammalian neurons is unknown.

4.2.2.2 TN-R and F3 expression

In the unlesioned optic nerve at all time periods, anti-sera against F3 stained the surface of the RGC axons. After the optic nerve crush however, this typical staining pattern was not seen and only restored 6 weeks later. This time course of F3 expression is very similar to what has previously been reported. Haenisch et al., (2005) have recently shown that F3 mRNA is detected in the intact optic nerve but consistently downregulated 2 weeks after optic nerve transaction, after which mRNA expression levels begin to increase and reach initial levels after 6 weeks. As goldfish oligodendrocytes express F3 mRNA in culture, the authors suggest that the early downregulation in the optic nerve after transaction may be caused by the dedifferentiation of oligodendrocytes, which occurs after injury (Ankerhold et al., 1998). F3 mRNA may therefore only be expressed by differentiated oligodendrocytes and its re-expression at later stages may indicate axon-oligodendrocyte interactions that result in remyelination of regenerating axons (Haenisch et al., 2005). In fact, F3 has been described to interact with Notch expressed on oligodendrocytes and to stimulate the signalling pathway mediating oligodendrocyte maturation (Hu et al., 2003). As TN-R is known to be an autocrine factor for oligodendrocyte differentiation in mammals (Pesheva et al., 1997), perhaps F3, which associates with microdomains in oligodendrocytes (Krämer et al., 1999), and TN-R co-exist in rafts through which they signal maturation. In this study, the expression of F3 by what are likely to be oligodendrocytes 6 weeks after the optic nerve crush may support this hypothesis.

The punctate staining of TN-R observed in sections of control optic nerve may be representative of lipid raft staining (Kappler et al., 2002) at the nodes of Ranvier (Bartsch et al., 1993). As F3 is also a raft-associated protein, it is likely that the binding of TN-R to glycosyl-phosphatidylinositol (GPI)-linked F3 results in the translocation of F3 into rafts where it can bind a co-receptor and initiate intraneural signalling (Krämer et al., 1999). The upregulation of TN-R during regeneration may help maintain or enhance neuroglia signalling by retaining physical contact between the axon and the oligodendrocyte so that the OL receives the necessary signalling to redifferentiate into its mature myelinating phenotype (Krämer et al., 1999). The interaction between TN-R and F3 may also enhance F3-mediated neurite extension (Nörenberg et al., 1995).

4.2.2.3 TN-R and CSPG expression

In the unlesioned and lesioned optic nerve at all time periods, antibodies against CSPGs only weakly stained the optic nerve. A previous study showed that CSPG immunoreactivity is seen in the glia limitans, suggesting that these proteoglycans are expressed by non-neuronal components surrounding the axon fascicles (Battisti et al., 1992). Between 1 and 3 weeks post-lesion, increased CSPG expression was observed around the crush site, where the staining pattern was associated with regenerating axons (Battisti et al., 1992). The weak CSPG immunoreactivity observed in both the unlesioned and regenerating optic nerve in this study may be due to the use of different antibodies. It is possible that the epitope recognized by the CS-56 antibody is not present in all CS-expressing structures (Becker and Becker, 2002). When the same antibody was used to analyze the expression of CSPGs in closely related zebrafish, CSPG immunoreactivity was also not detectable in the unlesioned or regenerating optic nerve (Becker and Becker, 2002). In zebrafish, the CS-56 antibody did however intensely label nonretinorecipient pretectal brain nuclei, supporting the idea that in goldfish, despite low immunoreactivity in the optic nerve, the antibody specifically recognised CS epitopes expressed by cells in the retina.

4.2.2.4 TN-R and laminin expression

In the unlesioned goldfish optic nerve, laminin is readily visualized in the nerve where it is expressed in the connective tissue components of the fascicles (Hopkins et al., 1985; Liesi et al., 1985; Carbonetto and Cochard, 1987). The colocalization of TN-R and laminin at the edges of fascicles, where TAG-1-labeled RGC axons grow, may create a growth zone along which the newly growing RGC axons preferentially extend. This is supported by the results

from the RGC outgrowth assays where RGC neurites only extended from retinal explants when they were plated on a combined substrate of TN-R and laminin, as opposed to TN-R alone.

Laminin is upregulated after an optic nerve injury (Hopkins et al., 1985; Ford-Holevinski et al., 1986; Battisti et al., 1992) and in addition, the RGCs and the optic nerve glial cells are primed to respond to these increased levels of laminin by upregulating laminin-binding antigens (Smalheiser et al., 1992). The effects of increased laminin combined with TN-R at the fascicular borders during the time course of axon regeneration may significantly contribute to the success of axon regeration in these animals by creating growth-supportive guide-posts along the length of the optic nerve.

It has been proposed that the differences in the expression of and responsiveness to laminin may in part account for the different *in vivo* regenerative capacities of mammals and lower vertebrates (Lieisi, 1985; Ford-Holevinski et al., 1986; Carbonetto and Cochard, 1987). With the exception of blood vessels and the connective tissue nerve sheath, the mammalian optic nerve is devoid of laminin and there is no increase in laminin expression after a rat optic nerve crush (Ford-Holevinski et al., 1986; Carbonetto et al., 1987). Moreover, mature mammalian RGCs also lose their responsiveness to laminin (Cohen et al., 1986). This probably explains why, despite the presence of laminin, the outgrowth of embryonic and adult RGC axons from mouse retinal explants is still significantly reduced on a homogenous substrate of TN-R (Becker et al., 2000a).

4.2.2.5 TN-R and fibronectin expression

In the unlesioned goldfish optic nerve, in comparison to laminin, only weak fibronectin immunoreactivity was observed. Fibronectin was equally distributed along the entire length of the optic nerve where it was associated with the connective tissue sheaths and within the interfasciclular spaces. This staining pattern is similar to what has been observed in mammals, where there is a homogenous, weak staining of fibronectin in the optic nerve (Carbonetto et al., 1987).

Even though no glial scar as such forms at the optic nerve lesion site (Hirsch et al., 1995), fibroblasts from the connective tissue sheaths and/or the interfascicular spaces, migrate into the lesion, where they are thought to provide support for the rapidly regenerating retinal growth cones (Strobel and Stuermer, 1994; Hirsch et al., 1995). The increased number of nuclei at the lesion site throughout the time course of this study was therefore attributed to

infiltrating fibroblasts, which subsequently increased fibronectin staining at the lesion site. Such an increase in intense fibronectin immunoreactivity at the injury site has also previously been reported between 2 and 30 days after an optic nerve transection (Hirsch et al., 1995). The fibronectin staining however becomes restricted to the interfascicular spaces after the glial limitans has been restored around the regenerated fascicles (Hirsch et al., 1995). In addition, goldfish RGCs grow extensively on fibroblasts cultures that have been derived from regenerating optic nerves, implying that they are a growth-supportive substrate (Hirsch et al., 1995). The sustained presence of fibronectin at the crush site during the course of RGC regeneration may therefore provide physical and perhaps molecular support for axon growth (Hirsch et al., 1995).

In addition to fibroblasts, fibronectin may be produced by astrocytes in the neural tissue portions of the optic nerve. The expression of fibronectin, together with various other growth-promoting molecules, has been suggested to allow astrocytes to promote axonal outgrowth during development (Liesi et al., 1986; Matthiessen et al., 1989; Pasinetti et al., 1993), and astrocyte-associated fibronectin in adult mammalian white matter tracts has been shown to be critical for axonal regeneration, where it stimulates regeneration along the astrocyte surface (Tom et al., 2004). Despite the minimal colocalization between TN-R and fibronectin observed at the lesion site, the presence of TN-R should not affect the growth-supportive properties of the fibroblasts as fish TN-R does not interfere with fibronectin-mediated cell adhesion and neurite outgrowth (Pesheva et al., 2006).

4.2.3 The expression of TN-R, its ligands and its interaction partners in the optic tectum

The adult goldfish optic tectum is a functionally coupled bilateral structure with a laminar organization that receives RGC projections from the contralateral retina in a specific topographical order (Attadi and Sperry, 1963; Jacobson and Gaze, 1965). While the retinal layers increase in thickness, so the optic tectal layers enlarge as new RGC's are added (Meyer, 1978). After an optic nerve injury, the near-normal retinotopic projections are reestablished during a rostro-caudal sequence of innervations (Easter et al., 1981). The expression of TN-R in the optic tectum may therefore be relevant for restoring the topography of new and regenerating RGC axons within their target-specific laminae.

The first regenerating RGC axons arrive in the rostral tectum between 10-12 days after the optic nerve crush and reestablish synaptic connections with tectal neurons soon thereafter (Stuermer and Easter, 1984). The majority of the fibers however only begin occupying the

tectum at around 4 weeks after the lesion and it still takes a further several weeks before the near-normal topographical order is reestablished (Schmidt et al., 1988).

In the unlesioned adult goldfish optic tectum, myelin-associated TN-R expression was observed in fascicles in the superficial retino-receipient layers as well as in the deeper tectal layers. As newly growing RGC axons enter the tectum within the surface fascicles, the presence of this putative axon growth-inhibitor in this region therefore does not seem to negatively effect the growth of these axons. The observed downregulation of myelin-associated TN-R expression in the stratum opticum 1 week after the nerve crush is consistant with the injury response of oligodendrocytes. It is not only the oligodendrocytes in the optic nerve that respond to a lesion by dedifferentiating into an immature phenotype that no longer expreses mature myelin markers but also those that myelinate the RGC axons as they enter the rostral tectum. The subsequent downregulation of both MBP and TN-R expression was therefore to be expected.

The expression of TN-R in the optic tectum of other lower vertebrates has been previously analyzed but contrasts significantly with the pattern described in this study. In the adult zebrafish tectum, TN-R borders the pathway of optic axons; while in the adult salamander tectum, TN-R is detected in the deep tectal efferent layers but not in the optic fiber recipient layers (Becker et al., 1999; Becker et al.; 2004). Again, these differences indicate that the expression of TN-R within the classes of lower vertebrates is not uniform, and therefore that generalizations regarding function based on protein expression should be cautioned against.

In mammals, the developmental expression of TN-R in the superior colliculus has been analyzed in embryonic mice, where TN-R immunoreactivity is the most intense in the deep tectal layers as opposed to the more superficial retino-recipient layers (Becker et al., 2000a). Developing RGCs therefore do not come into direct contact with TN-R as they make their final terminal arborizations but rather course through TN-R-negative tectal layers. The developmental expression of TN-R in higher vertebrates may be important in signaling the establishment and refinement of neuronal connections as it is the only ECM glycoprotein able to increase the percentage of chick tectal neurons with actin-rich microprocesses and side branches along the shafts of neurites, as well as increase the size of growth cones *in vitro* (Zacharias et al., 2002). The authors showed that F3 on the neuronal surface acts as the cellular receptor, or is part of a receptor complex, that mediates these TN-R-dependent morphological changes (Zacharias et al., 2002). The attachment and neurite outgrowth from tectal cells has subsequently been shown to results from the interactions between TN-R and

certain lecticans: TN-R cooperates with the lectins brevican and neurocan by forming a bridge between the lectican substrate and F3 (Zacharias et al., 2006). The colocalized staining of TN-R and F3 in the SFGS and SGC layers of the embryonic chick optic tectum suggested that TN-R and F3 may interact with each other in these layers to stimulate the differentiation of tectal interneurons by inducing the formation of microprocesses and side branches (Zacharias et al., 2002). Whether this is the case *in vivo* is unknown but the expression of certain other lecticans in the tectum, which, unlike brevican and neurocan, compete with TN-R for binding to F3 *in vitro* (Zacharias et al., 2006), will first need to be assessed.

The function of TN-R in the adult mammalian superior colliculus has also begun to be elucidated by the generation of TN-R knock-out mice. During postnatal development, TN-R immunoreactivity is detected within perineuronal nets associated with large motor neurons (Bruckner et al., 2006). The immunocytochemical staining of TN-R within perineuronal nets surrounding the axon initial segment, a region largely devoid of synapses, supports the hypothesis that the ECM of perineuronal nets, and therefore TN-R, plays a role in regulating synaptic plasticity by providing a continuous micromilieu for different subcellular domains that integrate and generate electrical activity in neurons (Bruckner et al., 2006). The perineuronal nets in homozygous TN-R deficient mice display a granular component within their lattice-like structure at early stages of development (Haunso et al., 2000). The absence of TN-R disturbs the molecular scaffolding of ECM components of perineuronal nets as CSPGs complexed with hyaluronan aggregate abnormally, and the authors suggest that this abnormal aggregation may interfere with the development of the specific microenvironment of the ensheathed neurons (Haunso et al., 2000). The absence of TN-R may therefore permanently change the functional properties of net-associated neurons, which has indeed been demonstrated in TN-R deficient mice that subsequently exhibit reduced long-term potentiation (Saghatelyan et al., 2001).

As in the retina and optic nerve, the increase in laminin expression in the optic tectum may also play a key role in the success of RCG axon regeneration. The increased expression of laminin in the SO may act as a guide-post that sharpens the regenerating retinotectal projections as they arrive in the optic tectum (Kuhn et al., 1995; Schmidt and Schachner, 1998).

4.3 The substrate properties of goldfish CNS tissue are altered during the process of regenerating

For many decades, the success of goldfish RGC regeneration was believed to be attributable to the more favourable substrate properties of the goldfish optic nerve microenvironment. Fish oligodendrocytes were originally thought to be supportive of axonal growth as axons from goldfish and rat retinal explants grew relatively well on immature oligodendrocytes isolated from normal or lesioned goldfish optic nerves (Bastmeyer et al., 1991, 1993). This led researchers to conclude that fish oligodendrocytes and CNS myelin were devoid of neurite growth inhibitors (Bastmeyer et al., 1991, 1993; Wanner et al., 1995).

The methods used to assess the substrate properties of the fish CNS were, however, limited to the influence of oligodendrocytes and CNS myelin, and failed to take into account the complex composition of the CNS microenvironment and the properties of mature fish oligodendrocytes. So-called "cryoassays" have since been used to assess the permissivity of the fish optic nerve for neurite outgrowth (Carbonetto et al., 1987; Sivron et al., 1994). This culture system uses sections of neural tissue, in this case goldfish optic nerve, as a substrate for mammalian neurons and allows nerve fiber growth on the tissues to be directly visualized at the light microscope level (Carbonetto et al., 1987). Such cryoassays preserve most of the relevant tissue composition in a functionally active state in a frozen section, and are therefore likely to reflect the substrate properties of the entire CNS microenvironment more accurately than those assays that only make use of isolated tissue fractions such as myelin. Several important findings have been made using this type of assay: (i) cryosections of goldfish optic nerve are non-permissive substrates for the growth of neonate rat DRGs (Carbonetto and Cochard, 1987), and (ii) cryosections of rat and goldfish optic nerve are permissive substrates for the growth of goldfish RGCs (Lang, unpublished data). From these observations, it then became clear that: firstly, the fish CNS, like the mammalian CNS, was an inhibitory substrate for the growth of mammalian neurons and, secondly, that fish CNS neurons responded differently to a substrate of mammalian and fish CNS compared to mammalian neurons. In the first instance, the observation that the goldfish optic nerve inhibits the growth of mammalian neurons, suggested that the fish CNS, like the mammalian CNS, did indeed possess an inhibitory component. In the second instance, the observation that the goldfish RGC axons grew across both the fish and mammalian optic nerve cryosections suggested that fish CNS neurons were less sensitive to the inhibitory component of the fish CNS, and less

sensitive to the inhibitors of axon outgrowth in the mammalian CNS (Lang, unpublished data), possibly due to differential receptor expression and second messenger activation.

Using a well characterized mammalian neural cell line in a coculture cryoassay, it was shown that the substrate properties of the fish CNS improve after CNS injury, despite the presence of TN-R, a putative axon growth inhibitory protein. In much the same manner as neonate DRGs, PC12 cells avoided growing on a section of uninjured adult goldfish optic nerve but grew extensively on a section of regenerating goldfish optic nerve. The section of regenerating goldfish optic nerve expressed upregulated levels of TN-R. This increased expression of TN-R was confirmed by the earlier immunocytochemistry results where increased TN-R immunoreactivity was detected above and below the lesion site 1 week post-injury. This observation raised the following question: why is PC12 cell neurite outgrowth inhibited on the unlesioned control section of goldfish optic nerve but promoted on a regenerating section of a region of goldfish optic nerve expressing upregulated levels of TN-R? This is an interesting question as TN-R is a known inhibitor of mammalian neurons, and so it may be expected that neurite outgrowth from PC12 cells on a substrate of TN-R-expressing optic nerve would be inhibited and not promoted. The observed difference between neurite outgrowth on the unlesioned versus regenerating goldfish optic nerve does not appear to be due to a diffusible agent(s) released from the tissue (Schwab and Thoenen, 1985) as both sections of nerve were present in each culture dish. It has been suggested that this type of local effect requires direct contact between the neurons and the nerve (Carbonetto et al., 1987), and so the difference in neurite outgrowth may reflect a greater adhesion of the cells to the regenerating nerve than to the unlesioned nerve, as has been shown by the expression of several CAMs. Such a change in growth permissiveness after injury has also been observed in another culture system: the mammalian sciatic nerve, which is a peripheral nerve capable of regeneration (review by Kiernan, 1979), is only permissive for neurite outgrowth of adult DRGs after axonal injury (Bedi et al., 1992).

In the goldfish model of regeneration, it has been proposed that the altered structure and function of the goldfish oligodendrocytes accounts for the growth-promoting substrate properties of the regenerating goldfish optic nerve. Oligodendrocytes in the fish optic nerve respond to injury much like the PNS Schwann cells in that they dedifferentiate from cells which express myelin molecules to apparently axon growth-promoting glial cells which ultimately remyelinate the regenerated axons (Wolburg et al., 1981; Stuermer and Easter, 1984). After an optic nerve crush, goldfish oligodendrocytes show no sign of apoptosis

(Ankerhold and Stuermer, 1999) and secrete trophic molecules, such as axogenesis factor -1, -2 and -3 (Schwalb et al., 1995, 1996), which stimulate axon outgrowth via a common purine sensitive pathway (Petrausch et al., 2000a) to bring about these molecular changes. When isolated from normal or lesioned optic nerves, goldfish oligodendrocytes in culture synthesize the CAMS E587 antigen and NCAM (Bastmeyer et al., 1994) which help guide the regenerating axons to their target in the optic tectum. Goldfish oligodendrocytes also produce the E587 antigen *in vivo* in a spatiotemporal correlation with retinal axon regeneration (Ankerhold et al., 1998). The fore mentioned beneficial properties of goldfish oligodendrocytes all contribute towards a growth-supportive extrinsic environment in which the goldfish RGCs can grow and regrow. This growth-supportive extrinsic environment, particularly the presence of CAMS, may also account for the behaviour of the PC12 cells on this substrate. The upregulated levels of TN-R do not seem effect the growth of PC12 cells, and this may reflect the possibility that the potential inhibition caused by the protein is outweighed by the upregulation of other growth-promoting molecules in the extrinsic environment.

The observation that the unlesioned goldfish optic nerve is a permissive substrate for the outgrowth of goldfish RGC neurites has also previously been shown (Lang, unpublished data) but conflicts with the findings of an earlier study in which the unlesioned goldfish optic nerve was shown to be non-permissive to the growth of goldfish RGC neurites (Sivron et al., 1994). This discrepancy can be explained by the fact that the unlesioned section of goldfish optic nerve was pre-incubated with O4 supernatant, which may have blocked the adhesive contacts between the goldfish RGCs and the sections of goldfish optic nerve (Wanner et al., 1995). The observation that the goldfish optic nerve becomes a permissive substrate after an optic nerve injury has also previously been shown by Sivron et al. (1994) but this group attributed the growth-supportive substrate properties of the regenerating optic nerve to the elimination or neutralisation of axon growth inhibitors, a scenario that does not correlate with the immunocytochemistry findings of this study where the persistant expression of at least one putative axon growth-inhibiting protein, namely TN-R, was demonstrated. The growth-supportive extrinsic environment created by the dedifferentiated oligodendrocytes after injury may account for the behaviour of the goldfish RGCs on this substrate of regenerating CNS tissue but this does not fully explain the regenerative ability of fish CNS axons as the goldfish RGC neurites also grew equally well on the unlesioned optic nerve, in which oligodendrocytes retain their mature morphology and expression profile. Not only do the

goldfish RGC neurites grow on the unlesioned goldfish optic nerve but they also grow on sections of lesioned rat optic nerve (Lang, unpublished data), which are known to be inhibitory for rat DRG neurites (Carbonetto and Cochard, 1987; Carbonetto et al., 1987). This suggests that it is not only the growth-supportive microenvironment that allows goldfish RGCs to regenerate but that the neuron-intrinsic properties of fish CNS neurons allow them to grow on what would be an inhibitory substrate for mammalian neurons. It should also be taken into consideration that these fish RGCs are already conditioned by axotomy before they are exposed to the substrates of intact fish or rat optic nerve sections. This is therefore an artificial situation where the axons would have upregulated their growth machinery, which might allow them to override potential inhibitors.

During the process of axon regeneration, goldfish RGCs undergo dramatic structural and molecular changes (Petrausch et al., 2000a). Several matrix and adhesion molecules in the optic nerve, which are required for growth and guidance, are upregulated during axonal regeneration and are transported to the new axon segments at a much faster rate than in the unlesioned optic axon segments (Petrausch et al., 2000a). These growth-related molecules include growth-associated phosphoprotein with molecular mass of 43 kDa (GAP-43) (Benowitz et al., 1983), axogenesis factor-1, -2 and 3 (Schwalb et al., 1995), the E587 antigen (Vielmetter et al., 1991), reggie-1 and -2 (Lang et al., 1998), netrin-1 (Petrausch et al., 2000b), and neural (N)CAM (Bastmeyer et al., 1990). In addition, functional upregulation of protein kinase C, which is associated with synaptic plasticity in many projections, occurs in the optic nerve after an optic nerve crush, providing a possible mechanism whereby the regenerating retinotectal projections are refined (Schmidt, 1998). On the other hand, axotomized mammalian RGCs not programmed to re-start the process of axonal elongation that they displayed in earlier developmental stages (review by Chierzi and Fawcett, 2001).

The presence of TN-R does not seem to affect the growth of goldfish RGC neurites, and this may reflect the possibility that the inhibition afforded by the protein is cancelled out by the upregulation of other growth-promoting molecules in the extrinsic environment such as laminin and fibronectin and/or that the neuron-intrinsic properties of goldfish RGCs cause them to be less sensitive to axon growth-inhibiting proteins.

4.4 Fish TN-R may not inhibit goldfish RGCs axon growth *in vivo*

The results of the ICC experiments and PC12 cell cryoassay showed that the outgrowth of neither fish nor mammalian neurons is inhibited by the presence of TN-R in the fish CNS

microenvironment. This indicated that fish TN-R may not possess the same growth-inhibiting properties as its mammalian homologue. Microexplants of goldfish retina grown on a uniform substrate of fish TN-R as a sole substrate, however, showed that, like mammalian TN-R, fish TN-R did not support neurite outgrowth. This could be attributed to (i) an inhibitory action on goldfish CNS neurons or (ii) a simple lack of outgrowth-promoting properties of this homogenous substrate. As is the case with mammalian TN-R, this inhibition may be mediated by TN-R's receptor, F3 (Pesheva et al., 1993), which was shown here to be expressed on the goldfish RGC axons. This *in vitro* neurite outgrowth assay condition does not, however, reflect the true *in vivo* situation: ECM proteins, such as TN-R, do not exist "alone" but in combination with many other ECM proteins. One such protein, laminin, is a growth-promoting substrate for CNS neurons that supports both the attachment and subsequent nerve fiber growth of CNS axons (Ford-Holevinski et al., 1986; Carbonetto and Cochard, 1987; Smalheiser et al., 1994). When laminin and TN-R were mixed and offered as a uniform substrate, the fish CNS neurites grew extensively over the coverslip. The combined effect of growth-promoting laminin and growth-inhibiting ECM proteins is likely to also override the inhibitory effect of axon growth-inhibitors *in vivo*. In fact, it has been reported that the addition of laminin to purified mammalian CNS myelin, can override the neurite growth inhibitory activity in CNS myelin (David et al., 1995). As growth-promoting ECM proteins such as laminin and fibronectin are expressed in overlapping regions of TN-R expression and become elevated in the fish optic nerve after injury (Ford-Holevinski et al., 1986; Hopkins et al., 1985; Battisti et al., 1992), it is likely that the regeneration of injured adult goldfish RGCs *in vivo* is not inhibited by TN-R expressed along the retinotectal pathway because the axons also contact areas of laminin-expression, which nullify the inhibitory effects of fish TN-R. As the NCAM F3 that is expressed along the goldfish RGC axons binds to both TN-R and laminin (Zisch et al., 1992), competitive binding may play a role here. The elevated levels of laminin may out-compete the persistant levels of TN-R for binding to F3, thereby preventing a direct interaction between the axons and the inhibitory protein.

Interestingly, the goldfish RGCs respond differently than mammalian neurons to mammalian TN-R. Mammalian TN-R has been shown to be a repulsive substrate for mammalian CNS neurons, even when offered in a mixture with adhesive substrates such as laminin (Pesheva et al., 1989, 1991). The goldfish RGCs, however, are not inhibited on a combined substrate of mammalian TN-R and laminin, but extend their neurites on the substrate, just as they do on

sections of mammalian optic nerve. This observation provides further credence to the notion that fish CNS neurons are more intrinsically capable of regeneration than their mammalian counterparts. The effect of mammalian TN-R on neural cell adhesion and neurite outgrowth in other lower vertebrates has also been assessed. Becker et al. (1999) showed that adult salamander RGC axons are not able to grow from retinal explants on a substrate of mammalian TN-R, even in the presence of laminin, indicating that salamander RGC axons are inhibited by mammalian TN-R. The differential effects of mammalian TN-R on goldfish and salamander RGCs suggests that even though lower vertebrates are generally able to regenerate their CNS, inter-species differences in neuron intrinsic properties are likely to exist.

The *in vitro* effect of fish TN-R on goldfish RGC outgrowth was also assessed by offering the neurites a sharp substrate border of fish TN-R. The arrangement of narrow alternating stripes of fish TN-R and poly-L-lysine (PLL) forced the growing axons to choose between these two substrates of unequal growth-supporting activities (Vielmetter et al., 1990). Surprisingly, despite goldfish RGC neurite outgrowth on a homogenous uniform substrate of fish TN-R being inhibited, an abrupt boundary of fish TN-R had no negative effect on outgrowth from retinal stripes. The growing axons showed no preference for the growth-supporting PLL stripes but grew on both fish TN-R and PLL stripes. These findings contrast with was has previously been reported in earlier lower vertebrate studies. Becker et al. (1999) showed that adult salamander RGC axons are not able to cross a sharp substrate border of TN-R in the presence of laminin, indicating that TN-R inhibits the regrowth of salamander RGC axons. Likewise, Becker et al. (2004) showed that a substrate border of tenascin-R repels growing adult zebrafish optic axons *in vitro*. Both these studies however, used mouse TN-R to test the response of zebrafish axons, which may not reflect a response that the axons would have elicited on salamander or zebrafish TN-R, respectively.

Although the exact mechanism underlying the differential outgrowth of neurites on uniform versus boundaries is yet completely understood, it can be asserted that neither fish nor mammalian TN-R as a homogeneous substrate support neurite growth but only mammalian TN-R actually repels axons at boundaries. In the case of a uniform, homogenous substrate, the inhibitory effect of fish TN-R may be explained by the fact that the entire surface of the growth cone is exposed to the fish TN-R, which binds to F3 expressed on the circumference of the growth cone or axon shaft, which activates the Src kinases (Zisch et al., 1995), which leads to growth cone collapse through cytoskeletal changes. In the case of a sharp boundary

substrate, the lack of inhibitory effect of fish TN-R may be explained by the fact only a certain area of the growth cone is exposed to the fish TN-R, and so perhaps fewer receptors bind to it and hence its inhibitory effect is diminished.

It has been suggested that guidance molecules can be expressed at discrete borders or in gradients during development to provide migrating cells with directional cues (review by Sanes, 1998). Glial boundaries are wide-spread during mammalian CNS development and it has been suggested that they serve to separate different fiber tracts and thereby preserve the laterality of the CNS (review by Steindler, 1993). Once synaptic connections have been made, these glial boundaries disappear (review by Steindler, 1993) but become upregulated following CNS trauma, and form a glial scar at the lesion site. In so doing, the mammalian glial cells seal off the wound and reduce the chances of inappropriate connections being formed (review by Steindler, 1993), yet at the same time also inhibit the regeneration of damaged axons at the injury site. Becker et al. (2003) have reported that in the developing zebrafish, TN-R immunoreactivity is not detectable in the optic nerve, optic tract, or tectal optic neuropil but immediately borders the optic tract caudally. When morpholinos were injected into fertilized zebrafish eggs, the expression of TN-R in zebrafish larvae *in vivo* was reduced, and led to the straying of axons from the optic tract (Becker et al., 2003). This strongly suggested that TN-R was a repellent guidance molecule for optic axons during zebrafish development (Becker et al., 2003). In the adult zebrafish, TN-R borders the pathway of optic axons in the retina and brain, with little change after an optic nerve lesion, again suggesting a role for TN-R as a repellent guidance molecule for continuously added optic axons, as well as for optic axons that regrow after an optic nerve crush in adult zebrafish (Becker et al., 2004). In the adult goldfish, however, we did not find that TN-R was expressed in discrete borders but that new and regenerating goldfish RGC axons grew through both TN-R-positive and TN-R-negative regions on their way to their target in the optic tectum. Functional differences in proteins therefore exist even within closely related species and this highlights the risk in making generalizations regarding such findings.

Interestingly, goldfish RGC outgrowth was inhibited on both a uniform homogenous substrate of mammalian TN-R and a sharp substrate border of mammalian TN-R. In the stripe assay, the goldfish RGC neurites were confronted with the option on growing on either the mammalian TN-R stripes and/or the adhesive PLL stripes. By choosing to avoid the stripes of mammalian TN-R and instead grow on the stripes of PLL, the goldfish CNS neurons displayed an increased sensitivity to boundaries of mammalian TN-R compared to boundaries

of fish TN-R. The inhibitory effect of a sharp boundary of mammalian TN-R has previously been demonstrated by mammalian neurons (Pesheva et al., 1991, 1993; Taylor et al., 1993). Earlier studies in other lower vertebrates showed that adult salamander RGC axons are not able to cross a sharp substrate border of mammalian TN-R, indicating that edges of TN-R inhibit the regrowth of salamander RGC axons (Becker et al., 1999). Likewise, Becker et al. (2004) showed that a substrate border of mammalian TN-R repels growing adult zebrafish optic axons *in vitro*. The repulsive effect of mammalian TN-R on the goldfish RGCs, as well as on salamander and zebrafish RGCs (Becker et al., 1999; 2004) may suggest that mammalian TN-R is a more potent inhibitor than fish TN-R when offered as a sharp substrate border.

4.5 The OP13 cell line may represent a potentially novel OEG cell line

The *in vitro* characterization of primary OEG has to date been difficult due to their mixed molecular and morphological phenotypes. OEG are considered an intermediate glial cell type mainly because of their parallel expression of astrocyte and Schwann cell-specific markers (review by Wewetzer et al., 2002). OEG express astrocyte-specific GFAP (Barber and Lindsay, 1982) and Schwann cell-specific markers like $p75^{NTFR}$, polysialic acid NCAM (PSA-NCAM), O4 and Po (review by Wewetzer et al., 2002). In addition, OEG display different morphological phenotypes in cultures. Franceschini and Barnett (1996) reclassified OEG into two cell types based on morphology and antigenic phenotype: (1) spindle-shaped low affinity $p75^{NTFR}$-positive cells (Schwann cell-like "S" type), and (2) flattened PSA-NCAM-positive cells (astrocyte "A" type). As yet, no specific antibody has been raised against OEG and attempts to undertake a systematic differential analysis of gene expression has so far also been unsuccessful. In order to verify whether or not the OP13 clone was indeed a true OEG cell line, their morphological and antigenic profiles were characterized.

The morphological phenotype of the OP13 cells was extremely heterogeneous. Cultures grown at the growth permissive temperature of 33°C and the differentiating temperature of 39°C contained both spindle-shaped and flattened cells, as has been reported in primary cultures (Franceschini and Barnett, 1996). The majority of the cells were flat in shape and this may be as a result of successive passaging as cultured OEG begin to lose their glial phenotype characteristics and take on the appearance of undifferentiated fibroblasts (Sonigra et al., 1999). The elongated cells were of the minority. These two morphologically distinct cell populations displayed differential staining patterns when labeled with the panel of known

OEG markers. The cells were immunopositive for the glial cell-specific marker GFAP (Ramon-Cueto and Nieto Sampedro, 1992; Chuah and Au, 1993; Doucette and Devon, 1995). Schwann cells, astrocytes and OEG are all positive for GFAP. Astrocytes and OEG are the only glial cells in the adult olfactory nerve fiber layer and olfactory bulb but during development, only one type of glial cell is found in this layer, namely OEG (Doucette, 1993). Taking into account that the OP13 cell line was generated from the embryonic olfactory placode, this excludes the possibility that these cells are Schwann cells or astrocytes because neither cell type are present in this tissue. The expression of $p75^{NTFR}$ is a commonly accepted indication of OEG lineage but studies from embryonically derived OEG have not been conclusive. The observation that the cells failed to stain for $p75^{NTFR}$ was unexpected as PCR results had shown that these cells express the $p75^{NTFR}$ mRNA (Illing et al., 2002). It may just have been that the cells do not express $p75^{NTFR}$ at a protein level in cell culture. For example, Kafitz and Greer (1999) and Lipson et al. (2003) showed that embryonic OEG express $p75^{NTFR}$ mRNA but Hisaoka et al. (2004) showed that they were immnuonegative for $p75^{NTFR}$. The lack of $p75^{NTFR}$ staining may also reflect the poor quality of the antibody. In fact, Schwann cells, which are known to strongly express $p75^{NTFR}$, only stained the spindle-shaped cells very faintly (not shown). Expression analysis with a greater number of antibodies will be more informative.

The only conclusion that can be drawn is that the OP13 cell line is a glial cell line, and that due to their GFAP staining and tissue origin, are likely to represent a clonal population of OEG. GFAP staining in the flattened cells, which were in the majority, was perinuclear. This close proximity to the nucleus may suggest that the protein is associated with the Golgi apparatus, perhaps being temporarily stored in vesicles. GFAP staining in the spindle-shaped cells was, however, cytoplasmic. This intracellular staining pattern of the fibrils is more typical of a GFAP-positive cell. The flattened and spindle-shaped cells are therefore not only morphologically distinct but also molecularly distinct populations of cells. Whether these two groups of cells are reminiscent of the different classes of OEG *in vivo* is not known. Considering that OEG ensheath portions of the olfactory axons within both the PNS and CNS portions of the olfactory nerve (Doucette, 1993; Raisman, 1985), perhaps the OEG from these separate regions of the nervous system are different, although cultures of primary OEGs are heterogeneous irrespective of whether they were obtained from the olfactory epithelium (PNS tissue) or olfactory bulb (CNS tissue).

Further antigenic characterization of the OP13 cell line involved determining their receptor expression. As one of the aims of the study was to analyze the adhesive properties of mammalian TN-R on these cells, the next logical step was to show whether or not the OP13 cells would be able to respond to a substrate of TN-R through its receptor, F3. In addition to F3 expression, Nogo-A receptor (NgR) expression was also analyzed as Nogo-A is another axon growth-inhibiting protein present at CNS injury sites (Hunt et al., 2003). Similarly to what was seen with the GFAP staining, a differential staining pattern for both F3 and NgR was observed in the morphologically distinct cell types. F3 and NgR staining in the flattened cells was perinuclear, while in the spindle-shaped cells it was cytoplasmic. Although many receptors are intracellular, most are expressed on the surface of the cell where they can come into direct contact with their ligand. Both F3 and NgR are found on the cell surface where they attach to the cell membrane by a GPI anchor (F3: Brümmendorf et al., 1989; NgR: Fournier et al., 2001). The expression of F3 is not limited to only neurons, where it associates with the non-caveolar raft proteins reggie-1 and reggie-2 (Lang et al., 1998; Stuermer et al., 2001) but is also expressed by oligodendrocytes, where it associates with microdomains (Krämer et al., 1999). If F3 is expressed by at least one glial cell type, namely oligodendrocytes, it is then reasonable to assume that other glial cells, such as OEG, may also express this cell adhesion molecule. OEG have indeed previously been reported to express a number of cell adhesion molecules, including PSA-NCAM (Chuah and Au, 1993; Kafitz and Greer, 1997). The expression of NgR by OEG has, up until now, not yet been reported. A recent study by Richard and colleagues (2005) has, however, shown that embryonic olfactory neurons express Nogo-A, raising the possibility that its receptor, NgR, may be expressed by other cells in the olfactory system with which the olfactory neurons interact, namely OEG.

4.6 Mammalian TN-R is anti-adhesive for glial cells that may be transplanted at the site of SCI injury

TN-R has a differential effect on the adhesion of cells in the CNS. TN-R purified from higher vertebrates (chick to human) brain tissue is anti-adhesive for CNS neurons (Pesheva et al., 1989, 2006). In comparison, it is an adhesive substrate for the macroglial oligodendrocytes (Pesheva et al., 1997) and supports the attachment of astrocytes in the presence of laminin (Pesheva et al., 1989) but is anti-adhesive for microglia (Angelov et al., 1998). Here it was shown that TN-R is also anti-adhesive for a potential OEG cell line, representative of peripheral glia. The adhesive effects of TN-R, which becomes upregulated in mammalian

models of CNS injury, may be important in the context of cell transplant-mediated CNS repair. The ability of candidate cells, such as OEG, to migrate after repair is important for both SCI and neurodegenerative diseases, such as multiple sclerosis, where multiple sites of demyelination persist. Before a cell can migrate through the 3-D microenvironment of the CNS, it first needs to be able to attach itself to the substrate with which it is in direct contact with. It has been demonstrated that OEG remain quite localized to their implantation site (Ruitenberg et al., 2002; Li et al., 2003; Boyd et al., 2004). As the mammalian injury site is known to contain axon growth-inhibiting proteins, this raises the question of whether the migratory potential of these cells may be limited by the presence of such inhibitory proteins, for example, TN-R.

The results from the cell adhesion assay had shown that, after 24 hrs, a uniform substrate of homogenous TN-R alone was anti-adhesive for OP13 cells compared to a uniform substrate of homogenous laminin alone ($p < 0.05$). The neuronal receptor mediating the antiadhesive effects of rodent TN-R has been identified as the GPI-anchored F3 (Pesheva et al., 1993) and the application of anti-F3 antibodies completely abolishes axon growth inhibition by human TN-R (Pesheva et al., 2006). Despite OEG being non-neuronal cells, immunocytochemistry results showed that the OP13 cells expressed F3. It is therefore possible that TN-R interferes with the attachment of these cells also via a F3-mediated mechanism. In spite of the intracellular expression of F3 by the OP13 cells *in vitro*, the cells were none the less responsive to the substrate, indicating that a direct interaction had occurred. It is possible that F3 only becomes translocated to the OP13 cell membrane once the cells have come into contact with the TN-R substrate and become actively involved in the process of cell adhesion. Indeed, the translocation of F3 to the axonal surface has already been shown to be dependendent on the activity of the neuron (Pierre et al., 2001). It is also conceivable that the mechanism whereby this anti-adhesive interaction is mediated is different from that described for neurons. Astrocytes do not adhere to or spread out on a substrate of TN-R, and yet these cells do not express the TN-R receptor F3 (Pesheva et al., 1989). The poor attachment of OP13 cells on a uniform substrate of homogenous TN-R may therefore be mediated by a F3-independent mechanism. Irrespective of which receptor/ligand mediates the anti-adhesive effect of TN-R, this finding suggests that, if this potential OEG cell line were to be implanted at a SCI site, the cells would not be likely to adhere to and then migrate away from the lesion site. It may, however, not be necessary in some cases for OEG to migrate long distances as

the diffusible trophic factors and CAMs that they secrete into their immediate CNS microenvironment could be sufficient to promote axon growth in that area.

During the mid-way stages of the cell adhesion assay (6 and 12 hrs) there was a statistically significant difference between the numbers of cells adhering to a uniform substrate of homogenous laminin alone compared to a uniform substrate of laminin mixed with TN-R. At the first and final stages (1 and 24 hrs, respectively), although the mean number of cells also differed, it was not statistically significant. As laminin is an adhesive substrate, the fact that it did not increase the number of OP13 cells when offered in combination with TN-R, compared to TN-R alone, was unexpected, and suggests that TN-R may interfere with laminin-mediated cellular adhesion. When TN-R is offered as a substrate with laminin to CNS neurons, the cells detach (Pesheva et al., 1989), whereas TN-R does not affect the behaviour of DRG and neuroblastoma cells on laminin substrates (Pesheva et al., 2006). In glial cells, the effects of laminin and TN-R have also been dichotomous. TN-R can only support the stable adhesion of astrocytes in the presence of laminin (Pesheva et al., 1998). TN-R is also an anti-adhesive substrate for microglia, and this inhibitory effect is even more potent than for astrocytes because, as is the case with the OP13 cells, combining laminin with TN-R does not improve the adherence of microglia to TN-R substrates (Angelov et al., 1998).

The dual nature of TN-R as both an adhesive and anti-adhesive protein, depending on, amongst other things, the cell type, is therefore quite evident. The inhibitory effect of TN-R on microglia has been localized to a distinct domain of the glycoprotein: the EGF-like repeats inhibit the adhesion and migration of microglia (Liao et al., 2005). Although microglia are generally considered to be aggressive cells that are capable of inducing neuronal damage via their secretary products, they are, none the less bifunctional cells which may also exert beneficial effects on neuronal survival via the secretion of trophic factors (Angelov et al., 1998). It is therefore not surprising that, in contrast to the EGFL repeats, the FN III 6-8 repeats of TN-R actually promote the adhesion and migration of microglia (Liao et al., 2005). These observations suggest that distinct TN-R domains may modulate the adhesion and migration of microglia by binding to different receptors on the microglia cell surface (Liao et al., 2005). The anti-adhesive effects of TN-R on the OP13 cells may therefore reflect a binding of OP13-expressed F3 to the EGFL repeats of TN-R. As to why the addition of laminin attenuates the adhesion of OP13 cells on TN-R remains unclear. Considering that laminin is an ECM interaction partner for TN-R, perhaps by being mixed together before coating the coverslips allows the laminin to bind to a region of the TN-R protein, other than

the EGFL repeats, leaving the EGFL repeats free to bind to OP13-expressed F3, or another OP13 receptor or ligand, that then mediates the anti-adhesive effect of TN-R on these cells. It is well documented that TN-R interferes with another of its ECM interaction partners, namely fibronectin. TN-R has been shown to inhibit fibronectin-mediated neural cell adhesion and axon growth by interacting directly with fibronectin and by interfering with integrin function (Pesheva et al., 1994; Probstmeier et al., 1999, 2000a). If TN-R is capable of preventing fibronectin-mediated adhesion of neurons, which do not adhere to TN-R, then it is possible that TN-R interferes with laminin-mediated adhesion of OP13 cells, which also do not adhere to TN-R. As OEG have been shown to express laminin (Ramón-Cueto and Nieto Sampedro, 1992; Crandall et al., 2000), this may have negative implications for their transplantation in SCI. Perhaps the limited migration of OEG from their injection site in animal models of SCI not only reflects inhibition caused by the presence of upregulated axon growth-inhibiting proteins such as TN-R but that their adherence and subsequent migration may also be further attenuated by the endogenous ECM proteins expressed by the OEG themselves.

4.7 Nogo-P4 is adhesive for glial cells that may be transplanted at the site of SCI injury

Interestingly, a statistically significant greater number of OP13 cells adhered to a substrate of Nogo-P4 compared to TN-R at each time point ($p < 0.001$). This was an intriguing finding as Nogo-P4 is a peptide sequence for Nogo-A, one of the most potent inhibitors synthesized by oligodendrocytes. This may be the first described case of any cell type preferring a substrate of Nogo-A compared to another substrate. Nogo-A, its receptor, and the downstream signalling cascades it activates have been one of the main targets in SCI models in recent years. The neutralization of Nogo-A (Caroni and Schwab 1988b; Schnell and Schwab, 1990; Bregman et al., 1995; Brosamle et al., 2000; Chen et al., 2000; Merkler et al., 2001; Raineteau et al., 2001), its receptor (Fournier et al., 2002; Liu et al., 2002; Lee et al., 2004), or components of its downstream signaling cascades (Lehmann et al., 1999; Fournier et al., 2003) promotes axon regeneration *in vitro* and *in vivo*, as well as functional motor recovery. However, the generation of the much anticipated transgenic nogo-A/p75^{NTFR} knock-out mice yielded conflicting results: axon regeneration was only slightly improved (Nogo-A: Simonen et al., 2003, p75^{NTFR}: Wang et al., 2002b) or not at all (Nogo-A: Kim et al., 2003; Zheng et al., 2003, p75^{NTFR}: Song et al., 2004). The basis of these discrepancies is not resolved but may reflect the possibility that the Nogo-A protein does not represent the original IN-250

inhibitory component as there is a difference between the molecular weight of the rat and bovine protein which has yet to be fully explained.

At least two possible mechanism exist that may explain the observed adhesion of OP13 cells on Nogo-P4. Traditionally, the accepted high-affinity neuronal receptor for Nogo-A is NgR. Despite OEG being non-neuronal cells, immunocytochemistry results showed that the OP13 cells expressed NgR. It is therefore possible that the cells adhere to the Nogo-P4 substrate via this GPI-anchored receptor. Recently, however, it has been shown that Chinese hamster ovary (CHO) cells that have been co-transfected with a Caspr-F3 complex bind to substrates coated with Nogo-66 (Nie et al., 2003), the extracellular domain of Nogo-A which is molecularly equivalent to Nogo-P4. *In vivo*, membrane bound F3 exists as a complex with another adhesion protein, Caspr, at CNS paranodes (Girault and Peles, 2002) and it has been suggested that Nogo-A from the oligodendrocyte membrane interacts with this complex at the paranodes during the early stages of myelination (Nie et al., 2003). As immunocytochemistry results had shown that the OP13 cells express F3, this suggests that an NgR-independent mechanism mediating OP13 adhesion to Nogo-P4 may exist. It was subsequently shown though that when the CHO cells were transfected with F3 alone or when F3 was removed from the cells by digesting the GPI-anchor, binding to Nogo-66 no longer occured (Nie et al., 2003). The possibility that the OP13 cells express Caspr can, however, not be excluded. In addition, other binding partners for Nogo-A have also been identified, for example, $p75^{NTFR}$, Lingo, Bcl-2, MBP and α-Tubulin (review by Teng et al., 2004). Further immunocytochemistry experiments using antibodies against Caspr and the other known Nogo-A ligands will need to be performed in order to demonstrate that OP13 attachment on a substrate of Nogo-P4 is mediated by ligands and/or receptors other than NgR.

The clustering of Nogo-A at paranodes, which coincides with the developmental period of myelination, has led researchers to believe that paranodal Nogo-A may participate in this process and may interact with a molecule other than NgR, which is only diffusely expressed along axons, to perform a function distinct from inhibition of axonal sprouting (Nie et al., 2003). The neuronal expression of Nogo-A in the central and peripheral nervous systems during development suggests that Nogo-A may indeed have such an additional role. In the early chick embryo, Nogo-A expression is observed in the axons and in striated muscle (O'Neill et al., 2004). Interestingly, the expression of Nogo-A in pre-E13 chick spinal cord, when chick embryos still maintain their potential to regenerate their spinal cord, is insufficient to inhibit axon regeneration (O'Neill et al., 2004). In fetal mice, Nogo-A is

diffusely expressed in the brain, brainstem, trigeminal ganglion, spinal cord, and DRGs at all stages (Josephson et al., 2002). In the fetal and developing nervous system of rats and humans, the expression of nogo mRNA is widespread, and includes the spinal cord, DRG, autonomic ganglia, trigeminal ganglion, trigeminal pontine nucleus, and in developing muscle tissue (Josephson et al., 2001).

There is a growing body of evidence to suggest that Nogo-A plays an important role in neurite outgrowth, particularly in the developing rat olfactory system. Differentiating olfactory neurons in the olfactory epithelium and olfactory bulb strongly express both Nogo-A mRNA during embryonic and postnatal development (Richard et al., 2005). Nogo-A protein is distributed along the entire length of the axon as it extends towards the olfactory bulb and accumulates in the growth cone of the axon and at axonal branching points (Richard et al., 2005). This aggregation of Nogo-A in the growth cone is similar in appearance to that of microtubule-associated proteins, indicating that Nogo-A may be involved in the processes of axonal growth and dendritic modeling through the regulation of microtubule dynamics (Richardson et al., 2005).

4.8 A possible physiological role for Nogo-A during myelination in the PNS

In trying to understand the adhesive effects of Nogo-P4 on the OP13 cells, a similar short-term cell adhesion assay was performed using another glial cell type, namely Schwann cells. In the regenerating peripheral nervous system (PNS), the myelinating Schwann cells support the regrowth of damaged axons in the PNS and are therefore also an attractive candidate for cell transplantation in SCIs (reviews by Bunge 1994; Jones et al., 2001; Pearse and Bunge, 2006). Schwann cell adhesion on a number of different substrates was compared. Schwann cells were plated onto coverslips that had been coated with either a uniform substrate of homogenous laminin or Nogo-P4, or on a patterned substrate of alternating laminin and laminin and Nogo-P4. As was observed in the OP13 cell adhesion assays, the Schwann cells displayed no aversion to the Nogo-P4 substrate. Schwann cells seeded onto either laminin as a sole substrate or Nogo-P4 as a sole substrate adhered equally well and did not adopt any particular orientation. When the Schwann cells were plated onto a patterned substrate, however, they acquired a very striking orientation. The cells grew in evenly spaced rows, the distance between which correlated with the width of the laminin and Nogo-P4- coated stripes. The combination of laminin and Nogo-P4 was therefore more adhesive for the Schwann cells than laminin or Nogo-P4 alone and provided a directional clue whereby the cell processes

elongated along the border of the stripe. The response of the Schwann cells to either a uniform or patterned substrate of Nogo-P4 suggests that, if these cells were to be implanted at a SCI site, their adhesion and subsequent migration are not likely to be negatively effected by the presence of Nogo-A at the lesion site. This was, however, only a preliminary finding and the experiment would need to be repeated in order to verify this observation.

The result of the Schwann cell stripe assay does not only have implications for the function of Nogo-A under pathological conditions but may also allude to a possible role for Nogo-A during normal development. The expression of Nogo-A in the PNS is developmentally regulated: before the onset of myelination, Nogo-A is expressed by sensory neurons in fetal mice DRG, and becomes downregulated in the adult mouse (Josephson et al., 2002). In comparison, Nogo-A is not detectable in peripheral nerve Schwann cells (Pot et al., 2002), the resident myelinating glial cells in the PNS. Developing sensory neurons first grow their axons to their targets before the Schwann cells migrate outwards and myelinate their respective axon portions. This is a complex, yet precise and efficient process, and the molecular cues governing the exact migration of the Schwan cells to their particular positions are not yet fully understood. It is an attractive idea to consider the possibility that Nogo-A, expressed by the developing PNS neurons as they migrate towards or once they have reached their target, in some way mediates the interaction of the laminin-secreting Schwann cells with the axons during the early stages of myelination.

Chapter 5: Conclusion

There is considerable variability in the regenerative capabilities of different central nervous system (CNS) axons, both between different species and within the same species. Mammalian adult CNS axons do not regenerate after injury but neonatal axons do, and in lower vertebrates, such as fish, frogs and reptiles (Lang et al., 1998, 2002) some neurons are able to regrow well while others are not. In trying to understand the role played by tenascin-R (TN-R) in the regeneration process of retinal ganglion cell (RGC) axons in the visual system of the adult goldfish, a model for successful CNS repair, this study set out to analyze the expression pattern and substrate properties of this extracellular matrix protein.

Fish TN-R expression is associated with myelinated tracts in the goldfish brain as well in perineuronal nets surrounding motor neuron cell bodies in the spinal cord. In the goldfish retina, fish TN-R is expressed in the optic fiber layer, where the axons of new and regenerating RGCs grow, and continues to be expressed during the early stages of regeneration when the RGC axons are growing out of the retina. These unexpected findings contrast with what has been reported in both mammals as well as in other lower vertebrates, where TN-R is thought to act as a repellent guidance cue. Instead, fish TN-R expression in the goldfish colocalizes with the growth-supportive extracellular matrix (ECM) proteins laminin and fibronectin, suggesting that fish TN-R may not be involved with the inhibition of axon outgrowth in the goldfish retina. In addition, as TN-R has been suggested to play a role in neuronal protection against activated microglia after mammalian peripheral nerve injury, its persistent expression after an optic nerve crush may serve a similar function by protecting the goldfish RGCs against perineuronal net destruction caused by the increased number of microglia in the crushed nerve that may invade the retina. In future studies, different microglial markers could be used to elucidate the relationship between goldfish RGCs and goldfish microglia after an optic nerve crush.

TN-R is homogenously expressed throughout the length of the optic nerve where, as in mammals, its staining pattern has a punctuate appearance, indicative of the nodes of Ranvier, where TN-R localizes and immobilizes the β-subunit of the Na^+ channel, such that normal saltatory conduction of impulses can occur. The presence of TN-R within optic nerve fascicles also does not seem to exert an inhibitory effect on axon outgrowth as newly added RGC axons grow in a TN-R immunopositive pathway. TAG-1 labeled RGC axons were seen growing along the borders of fascicles where TN-R and laminin colocalize, suggesting that

their combined properties serve as a preferential growth zone. Moreover, other than in the lesion site, the intensity of TN-R immunoreactivity remains relatively constant during the course of axon regeneration, and again colocalizes with laminin at the borders of the connective tissue fascicles. Whereas the persistent expression of TN-R in the injured mammalian optic nerve and the downregulation of TN-R in the salamander are believed to contribute to the failure and success, respectively, of axon regeneration in these animals, the continued expression of TN-R in the goldfish optic nerve may contribute to the rapid remyelination that restores the functioning of the RGCs so soon after injury.

In the goldfish optic tectum, TN-R expression is localized to the stratum opticum (SO) the primary retinorecipient tectal layer where incoming RGCs travel before arborizing and finally synapsing with tectal neurons in the deeper tectal layers, as well as in the deeper stratum album centrale (SAC). The concomitant expression of laminin in the SO, which becomes upregulated here after an optic nerve crush, further suggests that the expression of TN-R within this pathway does not inhibit the growth of goldfish RGCs, but may act in concert with laminin to guide the regenerating axons. Again, this expression pattern contrasts with what has been observed in the embryonic mammalian superior colliculus, where TN-R is restricted to the deep layers, and in the zebrafish, where TN-R borders the optic pathway in unlesioned animals and during axon regrowth.

The immunohistochemical results, together with the observation that sections of regenerating goldfish optic nerve, which express TN-R, is a growth-supportive substrate for a neuronal cell line, therefore seemed to indicate that, unlike in mammals and other lower vertebrates, the function of TN-R in the goldfish retinotectal system was not an inhibitory one. Subsequent in *vitro* outgrowth assays however showed that isolated fish TN-R, like mammalian TN-R, exerts an inhibitory effect on the outgrowth of RGC neurites when it is offered as a homogenous substrate. It is only when fish TN-R is combined with laminin that it can support neurite outgrowth. The colocalized expression of TN-R and laminin throughout the entire retinotectal pathway, may explain why goldfish RGC axons are able to regenerate through the injured optic nerve in the presence of high levels of axon growth-inhibiting TN-R. In the mammalian CNS, only low levels of laminin are present and mammalian CNS neurons lose their responsiveness to laminin as they age.

Multiple factors however must underlie the success of axon regeneration in the adult goldfish and the neural intrinsic properties of the RGCs should therefore also be taken into account. Fish RGC axons and ascending spinal axons are able to regenerate after injury but certain

descending spinal axons regrow poorly. Cyclic adenosine monophosphate (cAMP) may act as a critical switch in determining whether severed axons can regenerate and may therefore be one of the determinating factors in the success of goldfish RGC axon regeneration. The administration of cAMP is likely to become an integral part in reparative treatments as animal models using combination therapies of cellular transplants and cAMP have proven successful.

Interestingly, although RGC axons were inhibited on both a homogenous substrate of fish and mammalian TN-R, these axons responded differently to fish TN-R compared to mammalian TN-R when the proteins were offered as a sharp border substrate. Whereas the RGC neurites only grew on poly-L-lysine (PLL), being channelled onto the PLL stripes by the repellent mammalian TN-R, the RGC neurites grew across both the PLL and fish TN-R stripes. The mechanisms underlying the differential outgrowth of neurites on homogenous versus defined substrate boundaries is not yet completely understood but it can be said that a homogenous substrate of fish TN-R does not support neurite outgrowth while a sharp substrate border of mammalian TN-R repells RGC neurites.

The inhibitory effect of mammalian TN-R is not only relevant to axon regeneration but also to the migration of glial cells, which may have implications for therapies involving implantation of such cells into a CNS injury site. *In vitro* cell adhesion assays using homogenous mammalian TN-R was anti-adhesive for a novel olfactory ensheathing glia (OEG) cell line, and the attachment of these cells to the TN-R did not significantly improve even in the presence of laminin. However, when the adhesion of the OEG cell line on a substrate of TN-R was compared to adhesion on a substrate of Nogo-P4, the peptide sequence for a region of the myelin-associated axon outgrowth inhibitor Nogo-A, there was a surprising statistically significant difference. More cells adhered to a substrate of Nogo-P4 compared to all other test substrates, even compared to laminin. This unexpected result prompted further cell adhesion assays, this time using Schwann cells, another promising cell type for transplant mediated repair of the CNS. Schwann cells were observed growing preferentially along borders of Nogo-P4 and laminin, suggesting a potential functional interaction of the substrate properties of these proteins. The expression of Nogo-A by neurons in the developing peripheral nervous system may therefore provide a directional cue for the migration of laminin-secreting Schwann cells which then come and myelinate the axons of these cells.

In conclusion then, while fish TN-R is non-supportive of axon growth as a sole substrate, similar to its mammalian counterpart, the inhibitory effects of fish TN-R on the outgrowth of RGC's along the goldfish retinotectal system are likely to be overcome by the concomitant expression of growth-supportive laminin, and possibly other neurite outgrowth-promoting proteins. These findings, however, do not exclude a potential role of fish TN-R in axon growth and guidance. In addition, TN-R may also subserve other functions, such as neuroprotection and neuronal plasticity, as supported by the finding that TN-R in fish is organized in perineuronal nets. On the other hand, the inhibitory effects of mammalian TN-R, in the absence of laminin expression levels comparable to those in the fish CNS, may prove to be a potentially limiting factor for the integration and migration of glial cells implanted into the CNS to promote repair.

It is evident from both this and other studies, that future treatment stategies for spinal cord injuries will need to target both the intrinsic capabilities of the implanted cells and modulation of the extrinsic CNS microenvironment they will be transplanted into. The continued study of both of these models of CNS repair will hopefully contribute towards a breakthrough in the field of axon regeneration, which will ultimately provide hope to patients with paralysis.

Appendix I: Cell culture media and other solutions

1 Leibowzitz L-15 medium with L-glutamine

1. Dissolve 14.54 g (Highveld Biological) in 900 ml ddH_20

2. Adjust pH to pH 7.4

3. Adjust ddH_20 to 1L

4. Filter sterilize through 0.22µ Millipore filter

5. Aliquot into two 500 ml sterile blue-lipped glass bottles

6. Store at 4°C

2 Ham's F12 medium with L-glutamine

1. Dissolve 10.63 g (Highveld Biological) and 1.18 g $NaHCO_3$ (Associated Chemical Enterprises) in 900 ml ddH_20

2. Adjust pH to pH 7.4

3. Adjust ddH_20 to 1L

4. Filter sterilize through 0.22 µ Milipore filter

5. Aliquot into two 500 ml sterile blue-lipped glass bottles

6. Store at 4°C

3 Dulbecco's modifies Eagle's MEM (DMEM) with glucose, pyruvate and L-glutamine

1. Dissolve 13.53 g (Highveld Biological) and 3.7 g NaHCO3 (Associated Chemical Enterprises) in 900 ml ddH_20

2. Adjust pH to pH 7.4

3. Adjust ddH_20 to 1L

4. Filter sterilize through 0.22 µ Milipore filter

5. Aliquot into two 500 ml sterile blue-lipped glass bottles

6. Store at 4°C

4 Heat inactivation of fetal calf serum (FCS)

1. Thaw FCS at 4°C

2. Heat at 56°C for 20 min. Swirl bottle occasionally to avoid layer of jelly forming at the bottom

3. Cool to RT

4. Store at -20°C

5 L-glutamine

L-glutamine was prepared in the following manner and supplemented to the media every three weeks:

1. Dissolve 2.92 g l-glutamine (200mM; GIBCO) in 100 ml ddH_20

2. Filter sterilize through 0.22 µ Millipore filter

3. Aliquot into 2 ml eppendorphs

4. Store at -20°C

5. Dilute 1:100 for final concentration of 2 mM

6 Nerve growth factor

1. Reconstitute 100 µg of nerve growth factor (NGF, Sigma) in 1 ml tissue culture media containing 1% FCS.

2. Aliquot into sterile 1 ml eppendorphs

3. Store at -20°C

4. Dilute 1:100 for a final concentration of 0.1 ng/ml

7 Forskolin

1. Reconstitute forskolin (Sigma) in 1 ml in dimethyl sulphoxide (DMSO; AnalR®, South Africa)

2. Store at 4°C

3. Dilute 1:1000 for use in neuronal cultures

8 Insulin-Transferrin-Selenium A Supplement

Dilute 1:100 of stock (Gibco) for use in adherent cultures

9 Antibiotics

9.1 Penicillin/Streptomycin

1. Dissolve 60 g penicillin (Sigma) and 10 g streptomycin (Sigma) in 1L dd$H_2$0

2. Filter sterilize through 0.22 µ filter

3. Aliquot into sterile 20 ml McCartnet bottles

4. Store at -20°C

5. Dilute 1:100 for a final concentration of 100 µg/ml for routine use

9.2 Gentamycin sulfate

1. Use 1.25 µl/ml of 40 mg/ml stock for a final concentration of 50 µg/ml for maintenance

2. Use 5 µl/ml of 40 mg/ml stock for a final concentration of 200 µg/ml for treatment

9.3 Fungizone (Sigma)

1. Dilute 1: 1000 of 250 µg/ml stock for a final concentration of 0.25 µg/ml for maintenance

2. Dilute 1: 100 of 250 µg/ml stock for a final concentration of 2.5 µg/ml for treatment

10 Complete media

10.1 Goldfish glial cell medium

Leibovitz L-15 (L-15, 0.693 g/50 ml, Highveld Biological) ┐
Ham's F12 media (0.563 g/50 ml, Highveld Biological) ┘ 1:1

10% fetal calf serum (FCS, Highveld Biological)

4% methyl cellulose (Sigma)

2 mg/ml $NaHCO_3$ (Merk)

fungizone (0.25 µg/ml, Sigma)

gentamicin sulphate (50 µg/ml, Sigma)

10.2 Goldfish RGC medium

1. Cells were incubated in an Auto Flow CO_2 water-jacketed incubator (Nu Aire Inc., Florida, USA) at 28°C in a humid atmosphere containing 2% CO_2 in the air

2. The culture medium was a 1:1 mixture of Leibowitz L15 and Ham's F12 supplemented with 15 % FCS, 1% NGF, fungizone and gentamycin

10.3 PC12 medium

DMEM stock

10% FCS and

1% penicillin /streptomycin (Sigma).

10.4 Rat neonate DRG medium

DMEM stock

15% FCS and

1% penicillin /streptomycin (Sigma).

11 Other solutions

11.1 Phosphate buffered saline (0.15M) pH 7.4

NaCl (0.14M, Saarchem)	8.00 g
Na_2HPO_4 anhydrous (8.8M, Saarchem)	1.26 g
KCl (2.7M, AnalaR)	0.02 g
KH_2PO_4 (1.47 M AnalaR)	0.02 g

1. Dissolve in 800 ml dH2O

2. pH to 7.4

3. Made up to 1L

4. Autoclave in 500 ml bottles for tissue culture usage

11.2 Bovine serum albumin

Dissolve 1 g of bovine serum albumin fraction V (Roche) in 100 ml PBS for use as a blocking agent

11.3 Ethyl 3-aminobenzoate methanesulfonate salt (MS222)

1. Dissolve 250 mg in 500 ml tap water for a final concentration of 0.05 % when anesthetising goldfish prior to an optic nerve crush

2. Dissolve in 500 mg in 500 ml tap water for a final concentration of 0.1 % when terminally anesthetising a goldfish prior to an optic nerve crush

11.4 Trypsin/EDTA

1. Dissolve 0.05 g trypsin (Sigma) in 100 ml PBS

2. Add 0.02 g ethylenedioaminetetra-axteic acid (EDTA, Sigma)

3. Filter sterilize through 0.22 µ filter into steril 10 ml McCartney bottles

4. Store at –20°C

11.5 Mowiol (mounting medium)

1. Add 75 g Mowiol 4-88 (polyvinylalcohol, Hoechst AG) to 300 ml PBS and stir for 16 hrs at RT

2. Add 150 ml glycerol (Associated Chemical Enterprises (PTY) LTD) and stir for 16 hrs at RT

3. Centrifuge for 15 min at 4000 rpm in 50 ml falcon tubes

4. Adjust pH to pH 8-8.5

5. Aliquot and store at –20°C

6. Add a pinch of n-Propylgallate (anti-fade, Sigma) to the mowiol the day before using the mowiol to reduce immunofluorescence fading. Once added, incubate the mounting medium at 37°C overnight to dissolve and briefly vortex before use so as not to aspirate any insoluble granules

Appendix II: Protocols and procedures

1 Aptese-coated glass objective slides

1. Wash slides (Labstar1000, Lasec) in 2% Deconex (Borer Chemie, Switzerland) in tap water for 10 min
2. Rinse slides in running tap water for 3 min
3. Rinse in acetone (Associated Chemical Enterprises, South Africa) for 1 min
4. Immerse slides in 2% 3-aminopropyltriethoxy-silane (APTS, Sigma) in acetone (Associated Chemical Enterprises (PTY) LTD) for 5 min under the fume hood
5. Wash in ddH_20 for 2 min
6. Dry at 42°C overnight

2 Substrates for goldfish RGC and PC12 neurite outgrowth assays

1. Boil 12 mm glass coverslips (Marienfeld, Germany) in nitric acid for 30 min
2. Wash coverslips 10 x 15 min in ddH_2O
3. Coat coverslips with PPL (0.01% in sterile ddH_2O) for 30 min at 37°C.
4. Wash coverslips 3 x ddH_2O
5. For goldfish RGC neurite outgrowth assays, coat coverslips with purified tenascin-R protein (TN-R) (20 µg/ml) onto the PLL layer for 30 min at 37°C
6. Carefully aspirate the tenacin-R and immediately wash 1 x PBS
7. Coat the coverslips with laminin (5 or 10 µg/ml) for 30 min at 37°C
8. Block the surface with 1% BSA in PBS (heat-inactivated) for 60 min at 37°C
9. Wash 3 x PBS and keep in PBS until use later that day

* in some instances, TN-R and laminin were also pre-mixed before coating

3 Substates for goldfish RGC, OP13 cell and Schwann cell stripe assays

1. In the fume hood, boil 24 x 24 mm square glass coverslips (Marienfeld, Germany) in nitric acid for 30 min
2. Wash silicon matrixes and coverslips 10 x 15 min in ddH_2O separately
3. Autoclave silicon matrixes and coverslips separately

4. Place matrixes in a sterile petri dish and dry overnight in a 38°C oven and air dry coverslips in the hood

5. Coat coverslips with PLL for 30 min at 37°C, wash 3 x sterile ddH_2O and air dry

6. Place PLL-coated surface of coverslip down onto the grid surface of matrix

7. Mark the corners of the grid with a permanent marker for orientation

8. Using a HAMILTON syringe (HAMILTON Bonaduz AG, Switzerland), inject 10µl of protein or peptide into the matrix channel, ensuring that all the grid stripes are filled

9. Place in a covered sterile petri dish and allow to stand for 1hr in the hood

10. Gently remove coverslip off matrix and rinse in PBS/medium

11. The coverslip is now ready to be used that day

* in some instances, TN-R and laminin were also pre-mixed before coating

4 Culturing of PC12 cells on frozen sections of goldfish optic nerve

1. Resuscitate liquid nitrogen frozen stocks by thawing them in the palm of the hand before transferring to a 10 ml falcon tube with pre-warmed DMEM-medium containing 10% FCS. This dilutes the dimethyl-sulphoxide (DMSO), which is harmful to cells at RT

2. Spin cells in a centrifuge (Hettich, Mikro 20) set at 2000 rpm for 3 min

3. Aspirate off supernatant fluid and resuspend pellet of cells in pre-warmed complete PC12 medium

4. Seed into 94/16 mm petri dishes (Greiner Bio-One, Germany) and incubate cells in a Sanyo incubator (Nu Aire Inc., USA) at 37°C in a humid atmosphere containing 5% CO_2 in the air. The medium was changed every 2-3 days as required.

5. After 5-7 days *in vitro*, or once the cells were confluent, the medium was changed to differentiating PC12 medium and the cells took on a mature neuronal phenotype

6. The cells were then dislodged by briefly incubating them with 0.05% trypsin containing 0.02% EDTA at RT for a few minutes until the cells looked refractile (rounded up). The trypsin was then deactivated by adding a few ml of DMEM media containing FCS

7. The cells were then transferred to a 10ml falcon tube containing DMEM media containing FCS and spun at 1000 for 3 min

8. The pellet was resuspended and a cell count was performed using a Coulter Counter

9. The cells were then plated at a low density (1 x 10^5 cells per 94/16 mm dish) onto the coverslip covered with sections of goldfish optic nerve. An uncoated coverspip was then placed on top and separated from the underlying by steel spacers.

10. Incubate cells in Sanyo incubator (Nu Aire Inc) at 37°C in a humid atmosphere containing 5% CO_2 in the air.

5 Culturing of the OP13 cell line

The OP13 cells were thawed down by Faeiza Davids, a technical officer in Professor Illing's laboratory, and passaged four times before being transported under sterile conditions to Dr Lang's laboratory.

6 Cell morphology

Morphological changes in the OP13 and Schwann cells were observed and recorded with the aid of a Zeiss Aviovert 200 Microscope with digital camera attachment.

7 Cell counting

The numbers of adherent OP13 cells that attached to each substrate were counted manually. The diameter of the petri dish in which the cells were growing was used as a line guide along which each adherent cell was counted. Cells which remained rounded up were not included in each count.

Appendix III: Raw data corresponding to OP13 cell adhesion assay and statistical analysis

1 OP13 cell adhesion counts

EXPERIMENT NUMBER	TIME		SUBSTRATE				
			Laminin	TN-R	Laminin/TN-R	Nogo-P4	Laminin/Nogo-P4
Experiment 1	1 hr	dish 1	28	21	14	68	12
		dish 2	5	3	6	61	11
		dish 3	8	4	5	77	5
		dish 4	10	0	10	37	9
		dish 5	23	20	10	32	15
		dish 6	18	1	32	33	11
		dish 7	8	6	42	33	18
		dish 8	28	0	8	87	2
		MEAN	16	6.875	15.875	53.5	10.375
Experiment 2		dish 1	21	12	37	29	10
		dish 2	13	24	32	26	13
		dish 3	11	39	24	26	9
		dish 4	26	14	17	21	14
		MEAN	17.75	22.25	27.5	25.5	11.5
Experiment 3		dish 1	21	23	20	25	8
		dish 2	15	23	5	36	18
		dish 3	8	29	32	25	17
		dish 4	16	27	15	17	12
		MEAN	15	25.5	18	25.75	13.75
		STD DEV	7.635171	12.07132	12.31107	21.35406	4.442222
Experiment 1	6 hrs	dish 1	21	16	14	72	30
		dish 2	28	13	27	35	45
		dish 3	85	17	18	54	38
		dish 4	37	4	30	28	15
		dish 5	28	18	17	42	16
		dish 6	52	26	22	54	8
		dish 7	45	6	53	28	26
		dish 8	32	0	21	67	36
		MEAN	41	14.28571	25.25	47.5	26.75
Experiment 2		dish 1	44	28	35	50	23
		dish 2	37	34	35	31	27
		dish 3	52	28	12	42	32
		dish 4	35	39	17	33	35
		MEAN	42	32.25	24.75	39	29.25
Experiment 3		dish 1	14	33	30	38	34
		dish 2	20	31	21	36	24
		dish 3	17	32	32	24	22
		dish 4	30	37	41	21	23

		MEAN	20.25	33.25	31	29.75	25.75
		STD DEV	17.44885	12.28481	10.99072	14.87489	9.542012
Experiment 1	12 hrs	dish 1	41	6	13	107	14
		dish 2	16	14	7	44	32
		dish 3	26	17	16	52	39
		dish 4	25	5	13	36	16
		dish 5	30	19	21	41	9
		dish 6	22	27	38	26	10
		dish 7	40	12	51	29	17
		dish 8	20	12	21	95	33
		MEAN	27.5	14	22.5	53.75	21.25
Experiment 2		dish 1	55	36	18	38	24
		dish 2	43	41	24	36	25
		dish 3	46	31	11	21	29
		dish 4	42	41	7	32	24
		MEAN	46.5	37.25	15	31.75	25.5
Experiment 3		dish 1	16	37	14	24	17
		dish 2	17	35	22	25	27
		dish 3	9	25	32	27	33
		dish 4	32	36	24	20	19
		MEAN	18.5	33.25	23	24	24
		STD DEV	13.68454	12.53196	11.63615	25.1561	8.861903
Experiment 1	24 hrs	dish 1	60	6	17	60	9
		dish 2	19	11	9	43	19
		dish 3	14	5	12	52	23
		dish 4	17	17	6	32	50
		dish 5	9	20	12	37	45
		dish 6	9	23	20	21	49
		dish 7	10	16	11	24	43
		dish 8	18	5	12	58	18
		MEAN	19.5	12.875	12.375	40.875	32
Experiment 2		dish 1	38	16	17	35	15
		dish 2	28	19	10	31	24
		dish 3	29	6	9	24	18
		dish 4	44	16	5	40	12
		MEAN	34.75	14.25	10.25	32.5	17.25
Experiment 3		dish 1	30	23	24	38	14
		dish 2	18	25	23	34	15
		dish 3	20	26	14	21	19
		dish 4	27	25	15	26	12
		MEAN	23.75	24.75	19	29.75	15
		STD DEV	13.86542	7.538512	5.561774	12.30176	14.14435

2 One-way analysis of variance (ANOVA)

ANOVA analysis was performed using the MetCalc ® version 4.16f where:

Factor code (FC) 1 = 1hr, FC2 = 4 hrs, FC3 = 12hrs and FC4 = 24 hrs

Furthermore for each time sequence:

1 = LN, 2 = TN-R, 3 = LN and TN-R, 4 = Nogo-P4 and 5 = LN and Nogo-P4

ONE-WAY ANALYSIS OF VARIANCE

DATA: COUNTS

FACTOR CODES: FC1 = 1 HOUR

Source of variation	Sum of squares	D.F.	Mean square
Between groups (influence factor)	8755.5143	4	2188.8786
Within groups (other fluctuations)	10993.9286	65	169.1374
Total	19749.4429	69	

F-ratio: 12.941

Significance level: P = 0.000

Student-Newman-Keuls test for all pairwise comparisons

Factor	n	mean	Different (P<0.05) from factor nr
(1) 1	14	16.7857	(4)
(2) 2	14	13.5714	(4)
(3) 3	14	18.7143	(4)
(4) 4	14	42.2143	(1)(2)(3)(5)
(5) 5	14	11.0714	(4)

ONE-WAY ANALYSIS OF VARIANCE

DATA: COUNTS

FACTOR CODES: FC2 = 4 HOURS

Source of variation	Sum of squares	D.F.	Mean square
Between groups (influence factor)	4915.6286	4	1228.9071
Within groups (other fluctuations)	11450.1429	65	176.1560
Total	16365.7714	69	

F-ratio: 6.976

Significance level: P = 0.000

Student-Newman-Keuls test for all pairwise comparisons

Factor	n	mean	Different (P<0.05) from factor nr
(1) 1	14	37.8571	(2)(3)(5)
(2) 2	14	20.9286	(1)(4)
(3) 3	14	25.1429	(1)(4)
(4) 4	14	43.5714	(2)(3)(5)
(5) 5	14	27.7857	(1)(4)

ONE-WAY ANALYSIS OF VARIANCE

DATA: COUNTS

FACTOR CODES: FC3 = 12 HOURS

Source of variation	Sum of squares	D.F.	Mean square
Between groups (influence factor)	5049.8571	4	1262.4643
Within groups (other fluctuations)	16092.7143	65	247.5802
Total	21142.5714	69	

F-ratio: 5.099

Significance level: P = 0.001

Student-Newman-Keuls test for all pairwise comparisons

Factor	n	mean	Different (P<0.05) from factor nr
(1) 1	14	31.3571	(4)
(2) 2	14	23.7857	(4)
(3) 3	14	19.7143	(4)
(4) 4	14	43.2857	(1)(2)(3)(5)
(5) 5	14	22.5714	(4)

ONE-WAY ANALYSIS OF VARIANCE

DATA: COUNTS

FACTOR CODES: FC4 = 24HOURS

Source of variation	Sum of squares	D.F.	Mean square
Between groups (influence factor)	5393.6286	4	1348.4071
Within groups (other fluctuations)	8681.6429	65	133.5637
Total	14075.2714	69	

F-ratio: 10.096

Significance level: P = 0.000

Student-Newman-Keuls test for all pairwise comparisons

Factor	n	mean	Different (P<0.05) from factor nr
(1) 1	14	24.5000	(2)(3)(4)
(2) 2	14	14.8571	(1)(4)
(3) 3	14	13.3571	(1)(4)(5)
(4) 4	14	37.7857	(1)(2)(3)(5)
(5) 5	14	25.2857	(3)(4)

3 Corresponding Box and Whisker plots

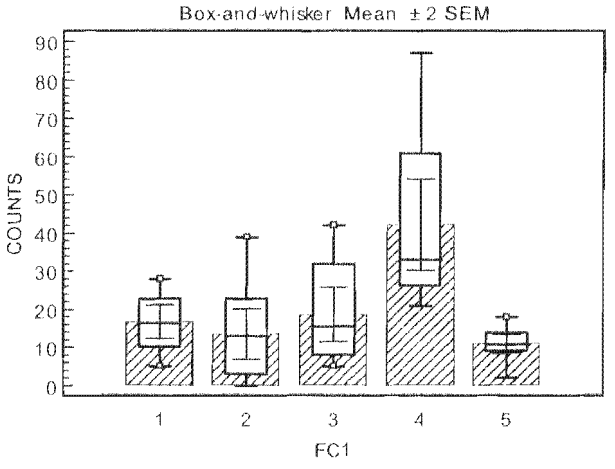

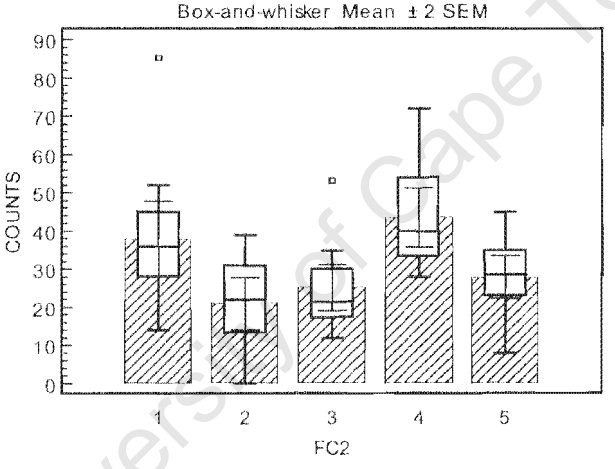

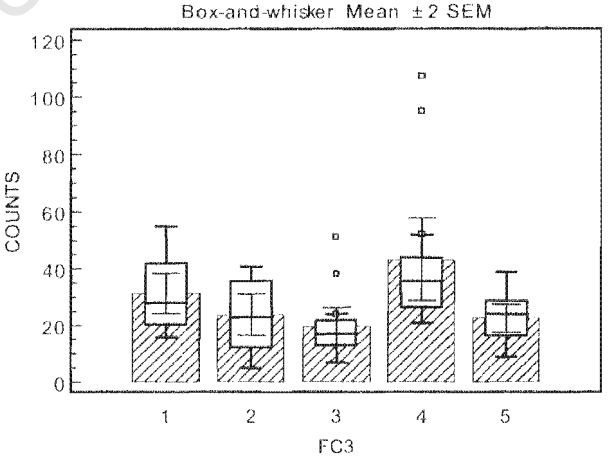

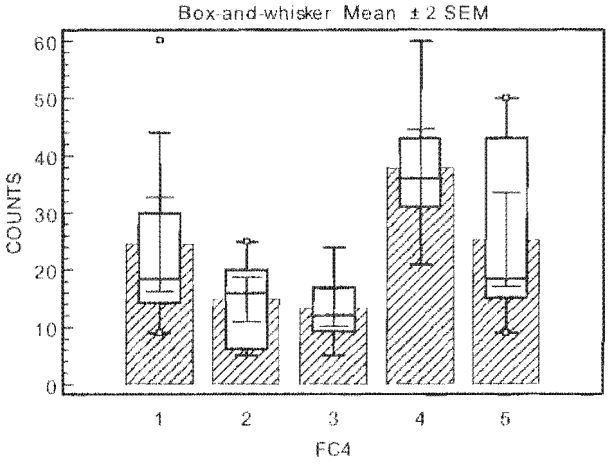

References

Ahmed Z, Suggate EL, Brown ER, Dent RG, Armstrong SJ, Barrett LB, Berry M and Logan A (2006). Schwann cell-derived factor-induced modulation of the NgR/p75NTR/EGFR axis disinhibits axon growth through CNS myelin *in vivo* and *in vitro*. Brain 129:1517-1533.

Alvarez-Buylla A and Garcia-Verdugo JM (2002). Neurogenesis in adult subventricular zone. J Neurosci 22:629-634.

Angelov DN, Walther M, Streppel M, Guntinas-Lichius O, Neiss WF, Probstmeier R and Pesheva P (1998). Tenascin-R is antiadhesive for activated microglia that induce downregulation of the protein after peripheral nerve injury: a new role in neuronal protection. J Neurosci 18:6218-6229.

Ankerhold R, Leppert CA, Bastmeyer M and Stuermer CAO (1998). E587 antigen is upregulated by goldfish oligodendrocytes after optic nerve lesion and supports retinal axon regeneration. Glia 23:257-270.

Ankerhold R and Stuermer CAO (1999). Fate of oligodendrocytes during retinal axon degeneration and regeneration in the goldfish visual pathway. J Neurobiol 41:572-584.

Asher RA, Morgenstern DA, Shearer MC, Adcock KH, Pesheva P and Fawcett JW (2002). Versican is upregulated in CNS injury and is a product of oligodendrocyte lineage cells. J Neurosci 22:2225-2236.

Aspberg A, Binkert C and Ruoslahti E (1995). The versican C-type lectin domain recognies the adhesion protein tenascin-R. Proc Natl Acad Sci USA 92:10590-10594.

Attardi DG and Sperry RW (1963). Preferential selection of central pathways by regenerating optic fibers. Exp Neurol 7:46-64.

Bandtlow CE, Heumann R, Schwab ME and Thoenen H (1987). Cellular localization of nerve growth factor synthesis by *in situ* hybridization. EMBO J 6:891-899.

Bandtlow CE and Schwab ME (2000). NI-35/250/nogo-a: a neurite growth inhibitor restricting structural plasticity and regeneration of nerve fibers in the adult vertebrate CNS. Glia 29:175-181.

Bahr M and Bonhoeffer F (1994). Perspectives on axonal regeneration in the mammalian CNS. Trends Neurosci 17:473-479.

Barber PC and Lindsay RM (1982). Schwann cells of the olfactory nerves contain glial fibrillary acidic protein and resemble astrocytes. Neurosci 7:3077-3090.

Barnett SC, Alexander CL, Iwashita Y, Gilson JM, Crowther J, Clark L, Dunn LT, apanastassiou V, Kennedy PG and Franklin RJ (2000). Identification of a human olfactory ensheathing cell that can effect transplant-mediated remyelination of demyelinated CNS axons. Brain123 :1581-1588.

Barnett SC and Riddell JS (2004). Olfactory ensheathing cells (OECs) and the treatment of CNS injury: advantages and possible caveats. J Anat 204:57-67.

Bartsch U, Kirchhoff F and Schachner M (1989). Immunohistochemical localization of the adhesion molecules L1, N-CAM, and MAG in the developing and adult optic nerve. J Comp Neurol 284:451-462.

Bartsch U, Pesheva P, Raff M and Schachner M (1993). Expression of Janusin (J1-160/180) in the retina and optic nerve of the developing adult mouse. Glia 9:57-69.

Bartsch U, Faissner A, Trotter J, Dörries U, Bartsch S, Mohajeri H and Schachner M (1994). Tenascin demarcates the boundary between the myelinated and nonmyelinated part of retinal ganglion cell axons in the developing and adult mouse. J Neurosci 14:4756-4768.

Bastmeyer M, Schlosshauer B and Stuermer CAO (1990). The spatiotemporal distribution of N-CAM in the retinotectal pathwat of the adult goldfish detected by monoclonal antibody D3. Dev 108:299-311.

Bastmeyer M, Beckman M, Schwab ME and Stuermer CAO (1991). Growth of regenerating goldfish axons is inhibited by rat oligodendrocytes and CNS myelin but not by goldfish optic nerve tract oligodendrocyte-like cells and fish CNS myelin. J Neurosci 11:626-640.

Bastmeyer M, Bahr M and Stuermer CAO (1993). Fish optic nerve oligodendrocytes support axonal regeneration of fish and mammalian retinal ganglion cells. Glia 29:330-346.

Bastmeyer M, Jeserich G and Stuermer CAO 1994). Similarities and differences between fish oligodendrocytes and Schwann cells *in vitro*. Glia 11:300-314.

Bastmeyer M, Ott H, Leppert CA and Stuermer CAO (1995). Fish E587 glycoprotein, a member of the L1 family of cell adhesion molecules, participates in axonal fasciculation and the age related order of ganglion cell axons in the goldfish retina. J Cell Bio 130:969-976.

Battisti WP, Shinar Y, Schwartz M, Levitt P and Murry M (1992). Temporal and spatial patterns of laminin, chondroitinsulfate proteoglycan and HNK-1 immunoreactivity during regeneration in the goldfish. J Neurocytol 21:557-573.

Baumann N and Pham-Dinh D (2001). Biology of oligodendrocyte and myelin in the mammalian central nervous system. Physiol Rev 81:871-927.

Becker T, Wullimann MF, Becker CG, Bernhardt RR and Schachner M (1997). Axonal regrowth after spinal cord transection in adult zebrafish. J Comp Neurol 377:577-595.

Becker CG, Becker T, Meyer RL and Schachner M (1999). Tenascin-R inhibits the growth of optic fibers *in vitro* but is rapidly eliminated during nerve regeneration in the salamander *Pleurodeles waltl*. J Neurosci 19:813-827.

Becker T, Anlinker B, Becker CG, Taylor J, Schachner M, Meyer RL and Bartsch U (2000a). Tenascin-R inhibits regrowth of optic fibers *in vitro* and persists in the optic nerve of mice after injury. Glia 29:330-346.

Becker CG, Meyer RL and Becker T (2000b). Gradients of ephrin-A2 and ephrin-A5b mRNA during retinotopic regeneration of the optic projection in adult zebrafish. J Comp Neurol 427:469-483.

Becker CG and Becker T (2002). Repellent guidance of regenerating optic axons by chondroitin sulphate glycosaminoglycans in zebrafish. J Neurosci 22:842-853.

Becker CG, Schweitzer J, Feldner J, Becker T and Schachner M (2003). Tenascin-R as a repellent guidance molecule for developing optic axons in zebrafish. J Neurosci 23:6232-6237.

Becker CG, Schweitzer J, Feldner J, Schachner M and Becker T (2004). Tenascin-R as a repellent guidance molecule for newly growing and regenerating optic axons in adult zebrafish. Mol Cell Neurosci 26:376-389.

Becker T, Lieberoth BC, Becker CG and Schachner M (2005). Differences in the regenerative response of neuronal cell populations and indications for plasticity in intraspinal neurons after spinal cord transaction in adult zebrafish. Mol Cell Neurosci 30:265-278.

Bedi KS, Winter J, Berry M and Cohen J (1992). Adult rat dorsal root ganglion neurons extend neurites on predegenerated but not on normal peripheral nerves *in vitro*. Eur J Neurosci 4:193-200.

Benowitz LI, Shashoua VE and Yoon MG (1981). Specific changes in rapidly transported proteins during regeneration of the goldfish optic nerve. J Neurosci 1:300-307.

Benowitz LI and Lewis ER (1983). Increased transport of 44,000- to 49,000-dalton acidic proteins during regeneration of the goldfish optic nerve: a two dimensional gel analysis. J Neurosci 3:2153-2163.

Berglund EO, Murai KK, Fredette B, Sekerhova G, Maturano B, Weber L, Mugnaini E and Ranscht B (1999). Ataxia and abnormal cerebellar microorganization in mice with ablated contactin gene expression. Neuron 24:739-750.

Bernhardt RR (1999). Cellular and molecular bases of axonal regeneration in the fish central nervous system. Exp Neurol 157:223-240.

Bernstein JJ (1964). Relation of spinal cord regeneration to age in adult goldfish. Exp Neurol 9:161-174

Bernstein JJ and Gelderd JB (1970). Regeneration of the long spinal tracts in goldfish. Brain Res 20:33-38.

Bhatt DH, Otto SJ, Depoister B and Fetcho (2004). Cyclic AMP-induced repair of zebrafish spinal circuits. Science 305:254-258.

Bovolenta P and Fernaud-Espinosa I (2000). Nervous system proteoglycans as modulators of neurite outgrowth. Prog Neurobiol 61:113-132.

Boyd JG, Lee J, Skihar V, Doucette R and Kawaja MD (2004). LacZ-expressing olfactory ensheathing cells do not associate with myelinated axons after implantation into the compressed spinal cord. Proc Natl Acad Sci U S A 101:2162-2166.

Bregman BS, Kunkel-Bagden E, Schnell L, Dai HN, Gao D and Schwab ME (1995). Recovery from spinal cord injury mediated by antibodies to neurite growth inhibitors. Nature 378:498-501.

Brenneke F, Schachner M, Elger CE and Lie AA (2004). Up-regulation of the extracellular matrix glycoprotein tenascin-R during axonal reorganization and astroglyosis in the adult rat hippocampus. Epil Res 58:133-143.

Brosamle C, Huber AB, Fiedler M, Skerra A and Schwab ME (2000). Regeneration of lesioned corticospinal tract fibers in the adult rat induced by a recombinant, humanized IN-1 antibody fragment. J Neurosci 20:8061-8068.

Bruckner G, Szeoke S, Pavlica S, Grosche J and Kacza J (2006). Axon initial segment ensheathed by extracellular matrix in perineuronal nets. Neuroscience 138:365-375.

Brümmendorf T, Wolff JM, Frank R and Rathjen FG (1989). Neural cell recognition molecule F11: homology with fibronectin type III and immunoglobulin type C domains. Neuron 2:1351-1361.

Brümmendorf T and Rathjen FG (1993). Axonal glycoproteins with immunoglobulin-and fibronectin type III-related domains in vertebrates: structural features, binding activities, and signal transduction. J Neurochem 61:1207-1219.

Brümmendorf T and Rathjen FG (1996). Structure/function relationships of axon-associated adhesion receptors of the immunoglobulin superfamily. Curr Opin Neurobiol 6:584-593.

Buffo A, Zagrebelsky M, Huber AB, Skerra A, Schwab ME, Strata P and Rossi F (2000). Application of neutralizing antibodies against NI-35/250 myelin-associated neurite growth inhibitory proteins to the adult rat cerebellum induces sprouting of uninjured purkinje cell axons. J Neurosci 20:2275-2286.

Bunge MB (1994). Transplantation of purified populations of Schwann cells into lesioned adult rat spinal cord. J Neurol 242(1 Suppl 1):S36-39.

Cai D, Qui J, Cao Z, McAtee M, Bregman BS and Filbin MT (2001). Neuronal cyclic AMP controls the developmental loss in ability of axons to regenerate. J Neurosci 21:4731-4739.

Carbonetto S and Cochard P (1987). *In vitro* studies on the control of nerve fiber growth by the extracellular matrix of the nervous system. J Physiol 82:258-270.

Carbonetto S, Evans D and Cochard P (1987). Nerve fiber growth in culture on tissue substrata from central and peripheral nervous systems. J Neurosci 7:610-620.

Caroni P and Schwab ME (1988a). Two membrane protein fractions from rat central myelin with inhibitory properties for neurite outgrowth and fibroblast spreading. J Cell Biol 106:1281-1288.

Caroni P and Schwab ME (1988b). Antibody against myelin-associated inhibitor of neurite growth neutralizes nonpermissive substrate properties of CNS white matter. Neuron 1:85-96.

Carr VM and Farbman AI (1992). Ablation of the olfactory bulb up-regulates the rate of neurogenesis and induces precocious cell death in olfactory epithelium. Exp Neurol 115:55-59.

Catterall WA (1981). Localization of sodium channels in cultured neural cells. J Neurosci 1:777-783.

Celio MR and Blumcke I (1994). Perineuronal nets - a specialized form of extracellular matrix in the adult nervous system. Brain Res Brain Res Rev 19:128-45.

Celio MR, Spreafico R, De Biasi S and Vitellaro-Zuccarello L (1998). Perineuronal nets: past and present. Trends Neurosci 21:510-515.

Chen DF, Jhaveri S and Schneider GE (1995). Intrinsic changes in developing retinal neurons result in regenerative failure of their axons. Proc Natl Acad Sci USA 92:7287-7291.

Chen MS, Huber AB, van der Haar ME, Frank M, Schnell L, Spillman AA, Christ F and Schwab ME (2000). Nogo-A is a myelin-associated neurite outgrowth inhibitor and an antigen for monoclonal antibody IN-1. Nature 403:434-439.

Chierzi S and Fawcett JW (2001). Regeneration in the mammalian optic nerve. Restor Neurol Neurosci 19:109-118.

Chiquet M and Fambrough DM (1984). Chick myotendinous antigen. I. A monoclonal antibody as a marker for tendon and muscle morphogenesis. J Cell Biol 98:1926-1936.

Chong MS, Woolf CJ, Turmaine M, Emson PC and Anderson PN (1996). Intrinsic versus extrinsic factors in determining the regeneration of the central processes of rat dorsal root ganglion neurons: the influence of a peripheral nerve graft. J Comp Neurol 370:97-104.

Chuah MI and Au C (1993). Cultures of ensheathing cells from neonatal olfactory bulbs. Brain Res 601:213-220.

Cohen J, Burne JF, Winter J and Bartlett P (1986). Retinal ganglion cells lose response to laminin with maturation. Nature 6:465-467.

Cornbrooks CJ, Carey DJ, McDonald JA, Timpl R and Bunge RP (1983). *In vivo* and *in vitro* observation on laminin production by Schwann cells. Proc Natl Acad Sci USA 80:3850-3854.

Crandall JE, Dibble C, Butler D, Pays L, Ahmad N, Kostek C, Puschel AW and Schwarting GA (2000). Patterning of olfactory sensory connections is mediated by extracellular matrix proteins in the nerve layer of the olfactory bulb. J Neurobiol 45:195-206.

David S and Aguayo AJ (1981). Axonal elongation into peripheral nervous system "bridges" after central nervous system injury in rats. Science 214:913-933.

David S, Braun PE, Jackson DL, Kottis V and McKerracher L (1995). Laminin overrides the inhibitory effects of peripheral nervous system and central nervous system myelin-derived inhibitors of neurite growth. J Neurosci Res 42:594-602.

Deckner M, Lindholm T, Cullheim S and Risling M (2000). Differential expression of tenascin-C, tenascin-R, tenascin/J1, and tenascin-X in spinal cord scar tissue and in the olfactory system. Exp Neurol 166:350-362.

Domeniconi M, Cao Z, Spencer T, Sivasankaran R, Wang K, Nikulina E, Kimura N, Cai H, Deng K, Gao Y, He Z and Filbin M (2002). Myelin-associated glycoprotein interacts with the Nogo66 receptor to inhibit neurite outgrowth. Neuron 35:283-290.

Doucette JR, Kiernan JA and Flumerfelt BA (1983). The re-innervation of olfactory glomeruli following transection of primary olfactory axons in the central or peripheral nervous system. J Anat 137:1-19.

Doucette JR (1984). The glial cells in the nerve fiber layer of the rat olfactory bulb. The Anat Rec 210:385-391.

Doucette R (1990). Glial influences on axonal growth in the primary olfactory system. Glia 3:433-449.

Doucette JR (1991). PNS-CNS transition zone of the first cranial nerve. J Comp Neurol. 312:451-466.

Doucette JR (1993). Glial progenitor cells of the nerve fiber layer of the olfactory bulb: effect of astrocyte growth media. J Neurosci Res 35:274-287.

Doucette JR and Devon R (1995). Elevated intracellular levels of cAMP induce olfactory ensheathing cells to express GAL-C and GFAP but not MBP. Glia 13:130-140.

Dowding AJ, Maggs A and Scholes J (1991). Diversity amongst the microglia in growing and regenerating fish CNS: immunohistochemical characterization using FL.1, an anti macrophage monoclonal antibody. Glia 4:345-364.

Easter SS, Rusoff AC and Kish PE (1981). The growth and organisation of the optic nerve and tract in juveline and adult goldfish. J Neurosci 1:793-811.

Easter SS and Stuermer CAO (1984). An evaluation of the hypothesis of shifting terminals in goldfish optic tectum. J Neurosci 4:1052-1063.

Essner E and Lin WL (1998). Immunocytochemical localization of laminin, type IV collagen and fibronectin in rat retinal vessels. Exp Eye Res 47:317-327.

Faissner A, Kruse J, Chiquet-Ehrismann R and Mackie E (1988). The high-molecular-weight J1 glycoproteins are immunochemically related to tenascin. Differentiation 37:104-114.

Faissner A and Steindler D (1995). Boundaries and inhibitory molecules in developing neural tissues. Glia 13:233-254.

Fawcett JW (1992). Intrinsic neuronal determinants of regeneration. Trends Neurosci 15:5-8.

Fawcett JW and Asher RA (1999). The glial scar and central nervous system repair. Brain Res Bull 49:377-391.

Feron F, Perry C, McGrath JJ and Mackay-Sim A (1998). New techniques for biopsy and culture of human olfactory epithelial neurons. Arch Otolaryngol Head Neck Surg 124(8):861-6.

Ford-Holevinski TS, Hopkins JM, McCoy JP and Agranoff BW (1986). Laminin supports neurite outgrowth from explants of axotomized adult rat retinal neurons. Brain Res 393:121-126.

Fournier AE, GrandPré T and Strittmatter SM (2001). Identification of a receptor mediating Nogo-66 inhibition of axonal regeneration. Nature 409:341-346.

Fournier AE, Gould GC, Liu BP and Strittmatter SM (2002). Truncated soluble Nogo receptor binds Nogo-66 and blocks inhibition of axon growth by myelin. J Neurosci 22:8876-8883.

Fournier AE, Takizawa BT and Strittmatter SM (2003). Rho kinase inhibition enhances axonal regeneration in the injured CNS. J Neurosci 23:1416-1423.

Franceschini IA and Barnett SC (1996). Low-affinity NGF-receptor and E-N-CAM expression define two types of olfactory nerve ensheathing cells that share a common lineage. Dev Biol 173:327-343.

Franklin RJ, Gilson JM, Franceschini IA and Barnett SC (1996). Schwann-cell like myelination following transplantation of an olfactory bulb-ensheathing cell line into areas of demyelination in the adult CNS. Glia 17:217-224.

Fu SY and Gordon T (1997). The cellular and molecular basis of peripheral nerve regeneration. Mol Neurobiol 14:67-116.

Fuss B, Wintergerst ES, Bartsch U and Schachner M (1993). Molecular characterization of the neural recognition molecule J1-160/180: a modular structure similar to tenascin. J Cell Biol 120:1237-1249.

Gard AL and Pfeiffer SE (1989). Oligodendrocyte progenitors isolated directly from developing telencephalon at a specific phenotypic stage: myelinogenic potential in a defined environment. Dev 106:119-132.

Geisert EE Jr, Seo H, Sullivan CD, Yang LJ and Grefe A (1998). A novel approach to identify proteins associated with inhibitors of neurite outgrowth. J Neurosci Res Meth 79:21-29.

Gennarini G, Cibelli G, Rougon G, Mattei M and Goridis C (1989). The mouse neuronal cell surface protein F3: a phosphatidylinositol-anchored member of the immunoglobulin superfamily related to chicken contactin. Cell Biol 109:775-788.

Giaume C and McCarthy KD (1996). Control of gap-junctional communication in astrocytic networks. Trends Neurosci 19:319-325.

Gimnopoulos D, Becker CG, Ostendorff HP, Bach I, Schachner M and Becker T (2002). Expression of the zebrafish recognition molecule F3/F11/contactin in a subset of differentiating neurons is regulated by cofactors associated with LIM domains. Mech of Dev 119S:S135-S141.

Giordano S, Laessing U, Ankerhold R, Lottspeich F and Stuermer CAO (1997). Molecular characterization of the E587 antigen: an axonal recognition molecule expressed in the goldfish central nervous system. J Comp Neurol 377:286-297.

Girault JA and Peles E (2002). Development of nodes of Ranvier. Curr Opin Neurobiol 12:476-485.

Goldberg JL and Barres BA (2000). The relationship between neuronal survival and regeneration. Annu Rev Neurosci 23:576-612.

Goldberg JL, Klassen MP, Hua Y and Barres BA (2002). Amacrine-signaled loss of intrinsic axon growth ability by retinal ganglion cells. Science 296:1860-1864.

Gordon-Weeks PR, Giffin N, Weekes CS and Barben C (1989). Transient expression of laminin immunoreactivity in the developing rat hippocampus. J Neurocytol 18:451-463.

Gordon-Weeks PR, Golding JP, Clarke JD and Tonge D (1992). A study of the expression of laminin in the spinal cord of the frog during development and regeneration. Exp Physiol 77:681-692.

GrandPré T, Nakamura F, Vartanian T and Strittmatter SM (2000). Identification of the Nogo inhibitor of axon regeneration as a Reticulon protein. Nature 403:439-444.

Graziadei PPC and Monti-Graziadei GA (1979). Neurogenesis and neuron regeneration in the olfactory system of mammals. I. Morpholoical aspects of differentiation and structural organization of the olfactory sensory neurons. J Neurocytol 8:1-18.

Graziadei PPC and Monti-Graziadei GA (1980). Neurogenesis and neuron regeneration in the olfactory system of mammals. III. Deafferation and reinnervation of the olfactory bulb following transaction of the fila olfactoria in rat. J Neurocytol 9:145-162.

Green LA and Tischler AS (1976). Establishment of a noradrenergic clonal line of rat adrenal pheochromocytoma cells which respond to nerve growth factor. Proc Natl Acad Sci USA 73:2424-2428.

Grimpe B and Silver J (2002). The extracellular matrix in axon regeneration. Prog Brain Res 137:333-349.

Grumet M, Hoffman S, Crossin KL and Edelman GM (1985). Cytotactin, an extracellular matrix protein of neural and non-neural tissues that mediates glia-neuron interaction. Proc Natl Acad Sci U S A 82:8075-8079.

Gutowski NJ, Newcombe J and Cuzner ML (1999). Tenascin-R and C in multiple sclerosis lesions: relevance to extracellular matrix remodelling. Neuropathol Appl Neurobiol 25:207-14.

Haenisch C, Diekmann H, Klinger M, Gennarini G, Kuwada JY and Stuermer CAO (2005). The neuronal growth and regeneration associated Cntn1 (F3/F11/Contactin) gene is duplicated in fish: expression during development and retinal axon regeneration. Mol Cell Neurosci 28:361-374.

Hagihara K, Miura R, Kosaki R, Berglund E, Ranscht B and Yamaguchi Y (1999). Immunihistochemical evidence for the brevican-tenascin-R interaction: colocalization in perineuronal nets suggests a physiological role for the interaction in the adult brain. J Comp Neurol 410:256-264.

Hand R (1981). Functions of T antigens of SV40 and polyomavirus. Biochim Biophys Acta. 651:1-24.

Haunso A, Ibrahim M, Bartsch U, Letiembre M, Celio MR and Menoud P (2000). Morphology of perineuronal nets in tenascin-R and parvalbumin single and double knockout mice. Brain Res 864:142-145.

He Z and Koprivica V (2004). The Nogo signalling pathway for regeneration block. Annu Rev Neurosci 27:341-368.

Hirsch S, Cahill MA and Stuermer CAO (1995). Fibroblasts at the transaction site of the injured goldfish optic nerve and their potential role during retinal axon regeneration. J Comp Neurol 360:599-611.

Hisaoka T, Morikawa Y, Kitamura T and Senba E (2004). Expression of a member of tumor necrosis factor receptor superfamily, TROY, in the developing olfactory system. Glia 45:313-324.

Hopker VH, Shewan D, Tessier-Lavigne M, Poo M and Holt C (1999). Growth-cone attraction to netrin-1 is converted to repulsion by laminin-1. Nature 401:69-73.

Hopkins JM, Ford-Holevinski TS, McCoy JP and Agranoff BW (1985). Laminin and optic nerve regeneration in the goldfish. J Neurosci 5:3030-3038.

Hu QD, Ang BT, Karasak M, Hu WP, Cui XY, Duka T, Takeda Y, Chia W, Sankar N, Ng YK, Ling EA, Maciag T, Small D, Trifonova R, Kopan R, Okano H, Nakafuku M, Chiba S, Hirai H, Aster JC, Schachner M, Pallen CJ, Watanabe K and Xiao ZC (2003). F3/contactin acts as a functional ligand for Notch during oligodendrocyte maturation. Cell 115:163-175.

Hunt D, Coffin RS, Prinjha RK, Campbell G and Anderson PN (2003). Nogo-A expression in the intact and injured nervous system. Mol Cell Neurosci 24:1083-1102.

Illing N, Boolay S, Siwoski JS, Casper D, Lucero MT and Roskams AJ (2002). Conditionally immortalized clonal cell lines from the mouse olfactory placode differentiate into olfactory receptor neurons. Mol Cell Neurosci 20:225-243.

Imaizumi T, Lankford KL, Waxman SG, Greer CA and Kocsis JD (1998). Transplanted olfactory ensheathing cells remyelinate and enhance axonal conduction in the demyelinated dorsal columns of the rat spinal cord. J Neurosci 18:6176-6185.

Isom LL, Ragsdale DS, De Jongh KS, Westenbroek RE, Reber BF, Scheuer T and Catterall WA (1995). Structure and function of the beta 2 subunit of brain sodium channels, a transmembrane glycoprotein with a CAM motif. Cell 83:433-442.

Jacobson M and Gaze RM (1965). Selection of appropriate tectal connections by regenerating optic nerve fibers in adult goldfish. Exp neurol 13:418-430.

Jessen KR (2004). Glial cells. Int J Biochem Cell Biol 36:1861-1867.

Jiang B, Liou GI, Behzadian MA and Caldwell RB (1994). Astrocytes modulate retinal vasculogenesis: effects on fibronectin expression. J Cell Sci 107:2499-2508.

Jones LL, Oudega M, Bunge MB and Tuszynski MH (2001). Neurotrophic factors, cellular bridges and gene therapy for spinal cord injury. J Physiol 15:83-89.

Josephson A, Trifunovski A, Widmer HR, Widenfalk J, Olson L and Spenger C (2002). Nogo-receptor gene activity: cellular localization and developmental regulation of mRNA in mice and humans. J Comp Neurol. 453:292-304.

Josephson A, Widenfalk J, Widmer HR, Olson L and Spenger C (2001). NOGO mRNA expression in adult and fetal human and rat nervous tissue and in weight drop injury. Exp Neurol 169:319-328.

Kafitz KW and Greer CA (1999). Olfactory ensheathing cells promote neurite extension from embryonic olfactory receptor cells *in vitro*. Glia 25:99-110.

Kappler J, Baader SL, Franken S, Pesheva P, Schilling K, Rauch U and Gielselmann V (2002). Tenascins are associated with lipid rafts isolated from mouse brain. Biochem and Biophys Res Comm 294:742-747.

Keyvan-Fouladi N, Raisman G and Li Y (2003). Functional repair of the corticospinal tract by delayed transplantation of olfactory ensheathing cells in adult rats. J Neurosci 23:9428-9434.

Kiernan JA (1979). Hypotheses concerned with axonal regeneration in the mammalian nervous system. Biol Rev Camb Philos Soc 54:155-197.

Kim JE, Li S, GrandPre T, Qiu D and Strittmatter SM (2003). Axon regeneration in young adult mice lacking Nogo-A/B. Neuron 38:187-199.

Koch M, Olson PF, Albus A, Jin W, Hunter DD, Brunken WJ, Burgeson RE and Champliaud MF (1999). Characterization and expression of the laminin γ3 chain: a novel, non-basement membrane-associated, laminin chain. J Cell Biol 145:605-618.

Kottis V, Thibault P, Mikol D, Xiao ZC, Zhang R, Dergham P and Braun PE (2002). Oligodendrocyte-myelin glycoprotein (OMgp) is an inhibitor of neurite outgrowth. J Neurochem 82:1566-1569.

Krämer E-M, Klein C, Koch T, Boytinck M and Trotter J (1999). Compartementation of Fyn Kinase with glycosylphoshatidylinositol-anchored molecules in oligodendrocytes facilitates kinase activation during myelination. J Biol Chem 274:29042-29049.

Kruse J, Keilhauer G, Faissner A, Timpl R and Schachner M (1985). The J1 glycoprotein - a novel nervous system cell adhesion molecule of the L2/HNK-1 family. Nature 316:146-148.

Kuhn TB, Schmidt MF and Kater SB (1995). Laminin and fibronectin guideposts signal sustained but opposite effects to passing growth cones. Neuron 14:275-285.

Lakatos A, Franklin RJ and Barnett SC (2000). Olfactory ensheathing cells and Schwann cells differ in their *in vitro* interactions with astrocytes. Glia 2:214-225.

Lakatos A, Barnett SC and Franklin RJ (2003). Olfactory ensheathing cells induce less host astrocyte response and chondroitin sulfate proteoglycan expression than Schwann cells following transplantation into adult CNS white matter. Exp Neurol 184:237-24.

Landreth GE and Agranoff BW (1976). Explant culture of adult goldfish retina: effect of prior optic nerve crush. Brain Res 118:299-303.

Lang DM and Stuermer CAO (1996). Adaptive plasticity of *Xenopus* glial cells *in vitro* and after CNS fiber tract lesions *in vivo*. Glia 18:92-106

Lang DM, Lommel S, Jung M, Ankerhold R, Petrausch B, Laessing U, Wiechers MF, Plattner H amd Stuermer CAO (1998). Identification of reggie-1 and reggie-2 as plasmamembrane-associated proteins which cocluster with activated GPI-anchored cell adhesion molecules in non-caveolar micropatches in neurons. J Neurobiol 37:502-523.

Lang DM, Warren Jr. JT, Klisa C, Stuermer CAO (2001). Topographic restriction of TAG-1 expression in the developing retinotectal pathway and target dependent reexpression during axon regeneration. Mol Cell Neurosci 17:398-414.

Laywell ED, Dorries U, Bartsch U, Faissner A, Schachner M and Steindler DA (1992). Enhanced expression of the developmentally regulated extracellular matrix molecule tenascin following adult brain injury. Proc Natl Acad Sci U S A 89:2634-2638.

Lazarov-Spiegler O, Solomon AS and Schwartz M (1998). Peripheral nerve-stimulated macrophages simulate a peripheral nerve-like regenerative response in rat transected optic nerve. Glia 24:329-337.

Leaver SG, Harvey AR and Plant GW (2006). Adult olfactory ensheathing glia promote the long-distance growth of adult retinal ganglion cell neurites *in vitro*. Glia 53:467-476.

Lee JK, Kim JE, Sivula M and Strittmatter SM (2004). Nogo receptor antagonism promotes stroke recovery by enhancing axonal plasticity. J Neurosci 24:6209-6217.

Lehmann M, Fournier A, Selles-Navarro I, Dergham P, Sebok A, Leclerc N, Tigyi G and McKerracher L (1999). Inactivation of Rho signalling pathway promotes CNS axon regeneration. J Neurosci 19:7537-7547.

Letourneau PC (1975). Cell to substratum adhesion and guidance of axonal elongation. Dev Biol 44:92-101.

Li Y, Field PM and Raisman G (1997). Repair of adult rat corticospinal tract by transplants of olfactory ensheathing cells. Science 227:2000-2002.

Li Y, Field PM and Raisman G (1998). Regeneration of adult rat corticospinal axons induced by transplanted olfactory ensheathing cells. J Neurosci 18(24): 10514-10524.

Li Y, Sauve Y, Lund RD and Raisman G (2003). Transplanted olfactory ensheathing cells promote regeneration of cut adult rat optic nerve axons. J Neurosci 23:7783-7788.

Liao H, Bu WY, Wang TH, Ahmed S and Xiao ZC (2005). Tenascin-R plays a role in neuroprotection via its distinct domains that coordinate to modulate the microglia function. J Biol Chem 280:8316-8323.

Liesi P, Kaakkola S, Dahl D and Vaheri A (1984). Laminin is induced in astrocytes of adult brain by injury. EMBO J 3:683-686.

Liesi P (1985). Laminin-immunoreactive glia distinguish regenerative adult CNS systems from nonregenerative ones. EMBO J 4:2505-2511.

Liesi P, Kirkwood T and Vaheri A (1986). Fibronectin is expressed by astrocytes cultured from embryonic and early postnatal rat brain. Exp Cell Res 163:175-251.

Lindholm T, Cullheim S, Carlstedt T and Risling M (2001). Expression of tenascin-R and J1 mRNA in motor neurons after a traumatic lesion in the spinal cord. Neuroreport 12:3513-3517.

Lipson AC, Widenfalk J, Lindqvist E, Ebendal T and Olson L (2003). Neurotrophic properties of olfactory ensheathing glia. Exp Neurol 180:167-171.

Liu BP, Fournier A, GrandPre T and Strittmatter SM (2002). Myelin-associated glycoprotein as a functional ligand for the Nogo-66 receptor. Science 297:1190-1193.

MacLaren RE (1996). Development and role of retinal glia in regeneration of ganglion cells following retinal injury. Br J Ophthalmol 80:458-464.

Maggs A and Scholes J (1990). Reticular astrocytes in the fish optic nerve: macroglia with epithelial characteristics form an axially repeated lacework pattern, to which nodes of Ranvier are apposed. J Neurosci 10:1600-1614.

Mandarino LJ, Sundarraj N, Finlayson J and Hassell HR (1993). Regulation of fibronectin and laminin synthesis by retinal capillary endothelial cells and pericytes *in vitro*. Exp Eye Res 57:609-621.

Marin-Padilla M and Amieva MR (1989). Early neurogenesis of the mouse olfactory nerve: Golgi and electron microscopic studies. J Comp Neurol 288:339-352.

Martini R (1994). Expression and functional roles of neural cell adhesion surface molecules and extracellular matrix components during development and regeneration of peripheral nerves. J Neurocytol 23:1-28.

Matthiessen HP, Schmalenbach C and Müller HW (1998). Astroglia-released growth-inducing activity for embryonic hippocampal neurons is associated with laminin bound in a sulfated complex and free fibronectin. Glia 2:177-188.

McKerracher L, David S, Jackson DL, Kottis V, Dunn RJ and Braunn PE (1994). Identification of myelin-associated glycoprotein as a major myelin-derived inhibitor of neurite outgrowth. Neuron 13:805-811.

McKerracher L, Chamoux M and Arregui CO (1996). Role of laminin and integrin interactions in growth cone guidance. Mol Neurobiol 12:95-116.

Merkler D, Metz GA, Raineteau O, Dietz V, Schwab ME and Fouad K (2001). Locomotor recovery in spinal cord-injured rats treated with an antibody neutralizing the myelin-associated neurite growth inhibitor Nogo-A. J Neurosci 21:3665-3673.

Meyer RL (1978). Evidence from thymidine labeling for continuing growth of retina and tectum in juveline goldfish. Exp Neurol 59:99-111.

Meyer RL, Sakurai K and Schauwecker E (1985). Topography of regenerating optic fibers in goldfish traced with wheat germ injectories into retina: evidence of discontinuous microtopography in the retinotectal projection. J Comp Neurol 239:27-43.

Milev P, Chiba A, Haring M, Rauvala H, Schachner M, Ranscht BKMR and Margolis RU (1998). High affinity binding and overlapping localization of neurocan and phosphacan/protein tyrosine phosphatase-zeta/beta with tenascin-R, amphotectrin, and the heparin-binding growth-associated molecule. J Biol Chem 273: 6998-7005.

Miller RH (1996). Oligodendrocyte origins. Trends Neurosci 19:92-96.

Ming GL, Song HJ, Berninger B, Holt CE, Tessier-Lavigne M and Poo MM (1997). cAMP-dependent growth cone guidance by netrin-1. Neuron 19:1225-1235.

Moreno-Flores MT, Bradbury EJ, Martin-Bermejo MJ, Agudo M, Lim F, Pastrana E, Avila J, Diaz-Nido J, McMahon SB and Wandosell F (2006). A clonal cell line from immortalized olfactory ensheathing glia promotes functional recovery in the injured spinal cord. Mol Ther 13:598-608.

Morganti MC, Taylor J, Pesheva P and Schachner M (1990). Oligodendrocyte-derived JI-160/180 extracellular matrix glycoproteins are adhesive or repulsive depending on the partner cell type and time of interaction. Exp Neurol 109:98-110.

Mukhopadhyay G, Doherty P, Walsh FS, Crocker PR and Filbin MT (1994). A novel role for myelin-associated glycoprotein as an inhibitor of axonal regeneration. Neuron 13:757-767.

Murray M (1982). A quantitative study of regenerative sprouting by optic axons in goldfish. J Comp Neurol 209:352-362.

Nagata S, Fujita N, Takeuchi K and Watanabe K (1996). cDNA cloning and expression of the *Xenopus* homologue of the neural adhesion molecule, contactin (F3/F11). Zoolog Sci 13:813-20

Navarro X, Valero A, Gudino G, Fores J, Rodriguez FJ, Verdu E, Pascual R, Cuadras J and Nieto-Sampedro M (1999). Ensheathing glia transplants promote dorsal root regeneration and spinal reflex restitution after multiple lumbar rhizotomy. Ann Neurol 45:207-215.

Nie D-Y, Zhou Z-H, Ang B-T, Teng FYH, Xu G, Xiang T, Wang C-y, Zeng L, Yasuo T, Xu T-L, Ng Y-K, Faivre-Sarrailh C, Popko B, Watanabe K, Pallen CJ, Tang BL and Xiao Z-C (2003). Nogo-A at CNS paranodes is a ligand of Caspr: possible regulation of K+ channel localizatio. EMBO J 22:5666-5678.

Nörenberg U, Hubert M, Brümmendorf T, Tarnok A and Rathjen FG (1995). Characterization of functional domains of tenascin-R (restrictin) polypeptide – cell attachment site, binding with F11, and enhancement of F11-mediated neurite outgrowth by tenascin-R. J Cell Biol 130:473-484.

O'Neill P, Whalley K and Ferretti P (2004). Nogo and Nogo-66 receptor in human and chick: implications for development and regeneration. Dev Dyn 231:109-121.

Pasinetti GM, Nichols NR, Tocco G, Morgan T, Laping N and Finch CE (1993). Transforming growth factor beta 1 and fibronectin messenger RNA in rat brain: responses to injury and cell-type localization. Neurosci 54:893-907.

Pearse DD and Bunge MB (2006). Designing cell- and gene-based regeneration strategies to repair the injured spinal cord. J Neurotrauma 23:438-452.

Perez-Bouza A, Wigley CB, Nacimiento W, Noth J and Brook GA (1998). Spontaneous orientation of transplanted olfactory glia influences axonal regeneration. Neuroreport 9:2971-2975.

Pesheva P, Spiess E and Schachner M (1989). J1-160 and J1-180 are oligodendrocyte-secreted substrates for cell adhesion. J Cell Biol 109:1765-1778.

Pesheva P, Probstmeier R, Spiess E and Schachner M (1991). Divalent cations modulate the inhibitory substrate properties of murine glia-derived J1-160 and J1-180 extracellular matrix glycoproteins for neuronal adhesion. Eur J Neurosci 3:356-365.

Pesheva P, Gennarinin G, Goridis C and Schachner M (1993). The F3/11 cell adhesion molecule mediates the repulsion of neurons by the extracellular matrix glycoprotein J1-160/180. Neuron 10:69-82.

Pesheva P, Probstmeier R, Skubitz AP, McCarthy JB, Furcht LT and Schachner M (1994). Tenascin-R (J1-160/180) inhibits fibronectin-mediated cell adhesion: functional relatedness to tenascin-C. J Cell Sci 107:2323-2333.

Pesheva P, Gloor S, Schachner M and Probstmeier R (1997). Tenascin-R is an intrinsic autocrine factor for oligodendrocyte differenciation and promotes cell adhesion by a sulfatide-mediated mechanism. J Neurosci 17:4642-4651.

Pesheva P and Probstmeier R (2000a). The yin and yang of tenascin-R in CNS development and pathology Prog Neurobiol 61:465-493.

Pesheva P and Probstmeier R (2000b). Association of tenascin-R with murine brain myelin membranes: involvement of divalent cations. Neurosci Lett 283:165-168.

Pesheva P, Probstmeier R, Lang DM, McBride R, Hsu NJ, Gennarini G, Spiess E and Peshev Z (2006). Early coevolution of adhesive but not antiadhesive tenascin-R ligand-receptor pairs in vertebrates: a phylogenetic study. Mol Cell Neurosci 32:366-386.

Petrausch B, Jung M, Leppert CA and Stuermer CAO (2000a). Lesion-induced regulation of netrin receptors and modification of netrin-1 expression in the retina of fish and grafted rats. Mol Cell Neurosci 16:350-364.

Petrausch B, Tabibiazar R, Roser T, Jing Y, Goldman D, Stuermer CAO, Irwin N and Benowitz LI (2000b). A purine-sensitive pathway regulates multiple genes involved in axon regeneration in goldfish retinal ganglion cells. J Neurosci 20:8031-8041.

Pierre K, Dupouy B, Allard M, Poulain A and Theodosis DT (2001). Mobilization of the cell adhesion glycoprotein F3/contactin to axonal surfaces is activity dependent. Eur J Neurosci 14:645-656.

Pot C, Simonen M, Weinmann O, Schnell L, Christ F, Stoeckle S, Berger P, Rulicke T, Suter U and Schwab ME (2002). Nogo-A expressed in Schwann cells impairs axonal regeneration after peripheral nerve injury. J Cell Biol 159:29-35.

Prinjha R, Moore SE, Vinson M, Blake S, Morrow R, Christie G, Michalovich D, Simmons DL and Walsh FS (2000). Inhibitor of neurite outgrowth in humans. Nature 403:383-384.

Probstmeier R, Michels M, Franz T, Chan BMC and Pesheva P (1999). Tenascin-R interferes with integrin-dependent oligodendrocyte precursor cell adhesion by a ganglioside-mediated signalling mechanism. Eur J Neurosci 11:2474-2488.

Probstmeier R, Braunewell K-H and Pesheva P (2000a). Involvement of chondroitin sulfates on brain-derived tenascin-R in carbohydrate-dependent interactions with fibronectin and tenascin-C. Brain Res 863:42-51.

Probstmeier R, Stichel CC, Muller HW, Asou H and Pesheva P (2000b). Chondroitin sulfates expressed on oligodendrocyte-derived tenascin-R are involved in neural cell recognition. Functional implications during CNS development and regeneration. J Neurosci Res 60:21-36.

Probstmeier R, Nellen J, Gloor S, Wernig A and Pesheva P (2001). Tenascin-R is expressed by Schwann cells in the peripheral nervous system. J Neurosci Res 64:70-78.

Properzi F, Carulli D, Asher RA, Muir E, Camargo LM, van Kuppevelt TH, ten Dam GB, Furukawa Y, Mikami T, Sugahara K, Toida T, Geller HM and Fawcett JW (2005). Chondroitin 6-sulfate synthesis is upregulated in injured CNS, induced by injury-related cytokines and enhanced in axon-growth inhibitory glia. Eur J Neurosci 21:378-390.

Rabacchi SA, Bonfanti L, Liu X-H and Maffei L (1994). Apoptotic cell death induced by optic nerve lesion in the neonatal rat. J Neurosci 14:5292-5301.

Raff M, Whitmore AV and Finn JT (2002). Axonal self-destruction and neurodegeneration. Science 296:868-871.

Raineteau O, Fouad K, Noth P, Thallmair M and Schwab ME (2001). Functional switch between motor tracts in the presence of the mAb IN-1 in the adult rat. Proc Natl Acad Sci U S A 98:6929-6934.

Raisman G (1985). Specialized neuroglial arrangement may explain the capacity of vomernasal axons to reinnervate central neurons. Neurosci 14:237-254.

Ramón-Cueto A, Plant GW, Avila and Bunge MB (1998). Long-distance axonal regeneration in the transected adult rat spinal cord is promoted by olfactory ensheathing glia transplants. J Neurosci 18:3803-3815.

Ramón-Cueto A and Nieto-Sampedro M (1992). Glial cells from adult rat olfactory bulb: immunocytochemical properties of pure cultures of ensheathing cells. Neurosci 47:213-220.

Ramón-Cueto A and Nieto-Sampedro M (1994). Regeneration into the spinal cord of transected dorsal root axons is promoted by ensheathing glia transplants. Exp Neurol 127:232-244.

Ramón-Cueto A, Cordero MI, Santos-Benito FF and Avila J (2000). Functional recovery of paraplegic rats and motor axon regeneration in their spinal cords by olfactory ensheathing glia. Neuron 25:425-435.

Rathjen FG and Schachner (1984). Immunocytochemical and biochemical characterization of a new neuronal cell surface component (L1 antigen) which is involved in cell adhesion. EMBO J 3:1-10.

Rathjen FG, Wolff JM, Frank R, Bonhoeffer F and Rutishauser U (1987). Membrane glycoproteins involved in neurite fasciculation. J Cell Biol 104:343-353.

Rathjen FG, Wolf JM and Chiquet-Ehrismann R (1991). Restrictin: a chick neural extracellular matrix protein involved in cell attachment co-purifies with the cell recognition molecule F11. Dev 113:151-164.

Richard M, Giannetti N, Saucier D, Sacquet J, Jordan F and Pellier-Monnin V (2005). Neuronal expression of Nogo-A mRNA and protein during neurite outgrowth in the developing rat olfactory system. Eur J Neurosci 22:2145-2158.

Ritchie JM and Rogart RB (1977). Density of sodium channels in mammalian myelinated nerve fibers and nature of the axonal membrane under the myelin sheath. Proc Natl Acad Sci U S A 74:211-215.

Rodger J, Bartlett CA, Beazley LD and Dunlop SA (2000). Transient up-regulation of the rostrocaudal gradient of ephrin A2 in the tectum coincides with reestablishment of orderly projections during optic nerve regeneration in goldfish. Exp Neurol 166:196-200.

Ruitenberg MJ, Plant GW, Christensen CL, Blits B, Niclou SP, Harvey AR, Boer GJ and Verhaagen J (2002). Viral vector-mediated gene expression in olfactory ensheathing glia implants in the lesioned rat spinal cord. Gene Ther 9:135-146.

Saghatelyan AK, Dityatev A, Schmidt S, Schuster T, Bartsch U and Schachner M (2001). Reduced perisomatic inhibition, increased excitatory transmission, and impaired long-term potentiation in mice deficient for the extracellular matrix glycoprotein tenascin-R. Mol Cell Neurosci 17:226-240.

Saghatelyan A, de Chevigny A, Schachner M and Lledo PM (2004). Tenascin-R radiates activity dependent recruitment of neuroblasts in the adult mouse forebrain. Nat Neurosci 7:347-356.

Sanes JR (1989). Extracellular matrix molecules that influence neural development. Ann Rev Neurosci 12:491-516.

Sandvig A, Berry M, Barrett LB, Butt A and Logan A (2004). Myelin-, reactive glia-, and scar-derived CNS axon growth inhibitors: expression, receptor signalling, and correlation with axon regeneration. Glia 46:225-251.

Schmidt JT, Turcotte JC, Buzzard M and Tieman DG (1988). Staining of regenerated optic arbors in goldfish tectum: progressive changes in immature arbors and a comparison of mature regenerated arbors with normal arbors. J Comp Neurol 269:565-591.

Schmidt JT and Schachner M (1998). Role for cell adhesion and glycosyl (HNK-1 and oligomannoside) recognition in the sharpening of the regenerating retinotectal projection in goldfish. J Neurobiol 37:659-671.

Schnell L and Schwab ME (1990). Axonal regeneration in the rat spinal cord produced by an antibody against myelin-associated neurite growth inhibitors. Nature 343:269-272.

Schüppel K, Brauer K, Hartig W, Grosche J, Earley B, Leonard BE and Bruckner G (2002). Perineuronal nets of extracellular matrix around hippocampal interneurons resist destruction by activated microglia in trimethyltin-treated rats. Brain Res 958:448-453.

Schwab ME and Thoenen H (1985). Dissociated neurons regenerate into sciatic but not optic nerve explants in culture irrespective of neurotrophic factors. J Neurosci 5:2415-2423.

Schwab ME and Caroni P (1988a). Oligodendrocytes and CNS myelin are nonpermissive substrates for neurite outgrowth and fibroblast spreading *in vitro*. J Neurosci 8:2381-2393.

Schwab ME and Schnell L (1998). Region-specific appearance of myelin constituents in the developing rat spinal cord. J Neurocytol 18:161-169.

Schwalb JM, Boulis NM, Gu MF, Winickoff J, Jackson PS, Irwin N and Benowitz LI (1995). Two factors secreted by the goldfish optic nerve induce retinal ganglion cells to regenerate axons in culture. J Neurosci 15:5541-5525.

Schwalb JM, Gu MF, Stuermer C, Bastmeyer M, Hu GF, Boulis N, Irwin N and Benowitz LI (1996). Optic nerve glia secretes a low-molecular-weight factor that stimulates retinal ganglion cells to regenerate axons in goldfish. Neurosci 72:901-910.

Schwob JE (2002). Neural regeneration and the Peripheral Olfactory System. The Anatomical Record 269:33-49.

Sharma SC, Jadhao AG and Prasada Rao PD (1993). Regeneration of supraspinal projection neurons in the adult goldfish. Brain Res 620:221-228.

Shearer MC and Fawcett JW (2001). The astrocyte/meningeal cell interface - a barrier to successful nerve regeneration? Cell Tissue Res 305:267-273.

Simonen M, Pedersen V, Weinmann O, Schnell L, Buss A, Ledermann B, Christ F, Sansig G, van der Putten H and Schwab ME (2003). Systemic deletion of the myelin-associated outgrowth inhibitor Nogo-A improves regenerative and plastic responses after spinal cord injury. Neuron 38:201-211.

Sivron T, Schwab ME and Schwartz M (1994). Presence of growth inhibitors in fish optic nerve myelin: postinjury changes. J Comp Neurol 343:237-246.

Sivron T and Schwartz M (1995). Glial cell types, lineages, and responses to injury in rat and fish: implications for regeneration. Glia 13:157-165.

Smale KA, Doucette R and Kawaja MD (1996). Implantation of olfactory enshaething cells in the adult rat brain following fimbria-fornix transection. Exp Neurol 137:225-233.

Smalheiser NR, Collins BJ and Sharma SC (1992). Characterization of novel set of membrane antigens associated with axonal growth III: Expression in the regenerating goldfish optic nerve and tectum. Brain Res Dev Brain Res 69:277-282.

Snow D and Letourneau PC (1992). Neurite outgrowth on a step gradient of chondroitin sulphate proteoglycan (CS-PG). J Neurobiol 23:322-336.

Snow D, Steindler DA and Silver J (1990). Molecular and cellular characterization of the glial roof plate of the spinal cord and optic tectum: a possible role for a proteoglycan in the development of an axon barrier. Dev Biol 138:359-376.

Snow D, Mullins N and Hynds DL (2001). Nervous system-derived chondroitin sulphate proteoglycans regulate growth cone morphology and inhibit neurite outgrowth: a light, epifluorescence, and electron microscopy study. Microsc Res Tech 54:273-286.

Snow D, Smith JR, Cunningham AT, McFarlin J and Goshorn EC (2003). Neurite elongation on chondroitin sulphate proteoglycans is characterized by axonal fasciculation. Exp Neurol 182:310-321.

Sonigra RJ, Brighton PC, Jacoby J, Hall S and Wigley CB (1999). Adult rat olfactory nerve ensheathing cells are effective promoters of adult central nervous system neurite outgrowth in co-culture. Glia 25:256-269.

Song HL, Ming GL and Poo MM (1997). cAMP-induced switching in turning direction of nerve growth cones. Nature 388:275-279.

Song H, Ming G, He Z, Lehmann M, McKerracher L, Tessier-Lavigne M and Poo MM (1998). Conversion of neuronal growth cone responses from repulsion to attraction by cyclic nucleotides. Science 281:1515-1518.

Song XY, Zhong JH, Wang X and Zhou XF (2004). Suppression of p75NTR does not promote regeneration of injured spinal cord in mice. J Neurosci 24:542-546.

Spassky N, de Castro F, Le Bras B, Heydon K, Queraud-LeSaux F, Bloch-Gallego E, Chedotal A, Zalc B and Thomas JL (2002). Directional guidance of oligodendroglial migration by class 3 semaphorins and netrin-1. J Neurosci 22:5992-6004.

Spillman AA, Bandtlow CE, Lottspeich F, Keller F and Schwab ME (1998). Identification and characterization of a bovine neurite growth inhibitor (bNI-220). J Biol Chem 273:19283-19293.

Srinivasan J, Schachner M and Catterall WA (1998). Interaction of voltage-gated sodium channels with the extracellular matrix molecules tenascin-C and tenascin-R. Proc Natl Acad Sci U S A 95:15753-15757.

Steindler DA (1993). Glial boundaries in the developing nervous system. Annu Rev Neurosci 16:445-470.

Stewart GR and Pearlman AL (1987). Fibronectin-like immunoreactivity in the developing cerebral cortex. J Neurosci 7:3325-3333.

Strobel G and Stuermer CAO (1994). Growth cones of regenerating retinal axons contact a variety of cellular profiles in the transacted goldfish optic nerve. J Comp Neurol 364:435-448.

Stuermer CAO and Easter SS Jr (1984). Rules of order in the retinotectal fascicles of goldfish. J Neurosci 4:1045-1051.

Stuermer CAO, Bastmeyer M, Bahr M, Strobel G and Paschke K (1992). Trying to understand axonal regeneration in the CNS of fish. J Neurobiol. 23:537-550.

Stuermer CA, Lang DM, Kirsch F, Wiechers M, Deininger SO and Plattner H (2001). Glycosylphosphatidyl inositol-anchored proteins and fyn kinase assemble in noncaveolar plasma membrane microdomains defined by reggie-1 and -2. Mol Biol Cell 12:3031-3045.

Sykova E (2004). Diffusion properties of the brain in health and disease. Neurochem Int 45:453-466.

Taylor J, Pesheva P and Schachner M (1993). Influence of janusin and tenascin on growth cone behaviour *in vitro*. J Neurosci Res 35:347-362.

Tarnowski BI, Spinale FG and Nicholson JH (1991). DAPI as a useful stain for nuclear quantification. Biotech Histochem 66:297-304.

Teng FY, Ling BM and Tang BL (2004). Inter- and intracellular interactions of Nogo: new findings and hypothesis. J Neurochem 89:801-806.

Timpl R, Rodde H, Robey PG, Rennard SI, Foidart J-M and Martin GR (1979). Laminin – a glycoprotein from basement membrane. J Biol Chem 254:9933-9937.

Tom VJ, Doller CM, Malouf A and Silver J (2004). Astrocyte-associated fibronectin is critical for axonal regeneration in adult white matter. J Neurosci 24:9282-9290.

Tsai HH and Miller RH (2002). Glial cell migration directed by axon guidance cues. Trends Neurosci 25:173-176.

Velasco A, Bragado MJ, Jimeno D, Caminos E, Lillo C, Aijón J and Lara JM (1995). Growing and regenerating axons in the visual system of teleosts are recognized with the antibody RT97. Brain Res 883:98-106.

Vielmetter J, Stolze B, Bonhoeffer F and Struermer CAO (1990). *In vitro* assay to test diferential substrate affinities of growing axons and migratory cells. Exp Brain Res 81:283-287.

Vielmetter J, Lottspeich F and Stuermer CAO (1991). The monoclonal antibody E587 recognizes growing (new and regenerating) retinal axons in the goldfish retinotectal pathway. J Neurosci 11:3581-3593.

Villegas-Perez MP, Vidal-Sanz M, Bray GM and Aguayo AJ (1988). Influences of peripheral nerve grafts on the survival and regrowth of axotomized retinal ganglion cells in adult rats. J Neurosci 8:265-280.

Völkmer H, Leuschner R, Zacharias U and Rathjen FG (1996). Neurofascin induces neurites by heterophilic interactions with axonal NrCAM while NrCAM requires F11 on the axonal surface to extend neurites. J Cell Biol 135:1059-1069.

Völkmer H, Zacharias U, Nörenberg U, and Rathjen FG (1998). Dissection of complex molecular interactions of neurofascin with axonin-1, F11, and tenascin-R, which promote attachment and neurite formation of tectal cells. J Cell Biol 142:1083-1093.

Wang KC, Koprivica V, Kim JA, Sivasankaran R, Guo Y, Neve RL and He Z (2002a). Oligodendrocyte-myelin glycoprotein is a Nogo receptor ligand that inhibits neurite outgrowth. Nature 417:941-944.

Wang KC, Kim JA, Sivasankaran R, Segal R and He Z (2002b). p57 interacts with the Nogo receptor as a co-receptor for Nogo, MAG and OMgp. Nature 420:74-78.

Wanner M, Lang DM, Brandtlow CE, Schwab ME, Bastmeyer M and Steurmer CAO (1995). Reevaluation of the growth-permissive substrate properties of goldfish optic nerve myelin and myelin proteins. J Neurosci 15:7500-7508.

Weber P, Bartsch U, Rasband MN, Czaniera R, Lang Y, Bluethmann H, Margolis RU, Levinson SR, Shrager P, Montag D and Schachner M (1999). Mice deficient for tenascin-R display alterations of the extracellular matrix and decreased axonal conduction velocities in the CNS. J Neurosci 19:4245-4262.

Wewetzer K, Verdu E, Angelov DN, Navarro X (2002). Olfactory ensheathing glia and Schwann cells: two of a kind? Cell Tissue Res 309:337-345.

Wintergerst ES, Fuss B and Bartsch U (1996). Localization of janusin mRNA in the central nervous system of the developing and adult mouse. Eur J Neurosci 5:299-309.

Wolburg H (1981). Myelination and remyelination in the regenerating visual system of the goldfish. Exp Brain Res 43:199-206.

Wollner DA and Catterall WA (1986). Localization of sodium channels in axon hillocks and initial segments of retinal ganglion cells. Proc Natl Acad Sci U S A 83:8424-8428.

Wu YJ, La Pierre DP, Wu J, Yee AJ and Yang BB (2005). The interaction of versican with its binding partners. Cell Res 15:483-494.

Xioa ZC, Taylor J, Montag D, Rougon G and Schachner M (1996). Distinct effects of recombinant tenascin-R domains in neural cell functions and identification of the domain interacting with the neurnal recognition molecule F3/11. Eur J Neurosci 8:766-782.

Xioa ZC, Bartsch U, Margolis RK, Rougon G, Montag D and Schachner M (1997). Isolation of tenascin-R binding protein from mouse brain membranes. A phosphacan-related chondroitin sulfate proteoglycan. J Biol Chem 272:32092-32101.

Xiao ZC, Revest JM, Laeng P, Rougon G, Schachner M and Montag D (1998). Defasiculation of neurites is mediated by tenascin-R and its neuronal receptor F3/11. J Neurosci Res 52:390-404.

Xiao ZC, Ragsdale DS, Malhotra JD, Mattei LN, Braun PE, Schachner M and Isom LL (1999). Tenascin-R is a functional modulator of sodium channel beta subunits. J Biol Chem 274:26511-26517.

Yamagata M and Sanes JR (1995). Lamina-specific cues guide outgrowth and arborization of retinal axons in the optic tectum. Dev 121:189-200.

Yang JT and Hynes RO (1996). Fibronectin receptor functions in embryonic cells deficient in alpha 5 beta 1 integrin can be replaced by alpha V integrins. Mol Biol Cell 7: 1737–1748.

Yang H, Xiao ZC, Becker B, Hillenbrand R, Rougon G and Schachner M (1999). Role for myelin-associated glycoprotein as a functional tenascin-R receptor. J Neurosci Res 55:687-701.

Zacharias U, Nörenberg U and Rathjen FG (1999). Functional interations of the immunoglobulin superfamily members F11 are differentially regulated by the extracellular matrix proteins tenascin-R and tenascin-C. J Biol Chem 274:24357-24365.

Zacharias U, Leuschner R, Nörenberg U and Rathjen FG (2002). Tenascin-R induces actin-rich microprocesses and branches along neurite shafts. Mol Cell Neurosci 21:626-633.

Zacharias U and Rauch U (2006). Competition and cooperation between tenascin-R, lecticans and contactin 1 regulate neurite growth and morphology. J Cell Sci 119:3456-3466.

Zhang Y, Tohyama K, Winterbottom JK, Haque NS, Schachner M, Lieberman AR and Anderson PN (2001). Correlation between putative inhibitory molecules at the dorsal root entry zone and failure of dorsal root axonal regeneration. Mol Cell Neurosci 3:444-459.

Zheng B, Ho C, Li S, Keirstead H, Steward O and Tessier-Levigne M (2003). Lack of enhaned spinal regeneration in Nogo-deficient mice. Neuron 38:213-224.

Zisch AH, D'Alessandri L, Amrein K, Ranscht B, Winterhalter KH and Vaughan L (1995). The glypiated neuronal cell adhesion molecule contactin/F11 complexes with src-family protein tyrosine kinase Fyn. Mol Cell Neurosci 6:263-279.

Zisch AH, D'Alessandri L, Ranscht B, Falchetto R, Winterhalter KH and Vaughan L (1992). Neuronal cell adhesion molecule Contactin/F11 binds to tenascin via its immunoglobulin-like domains. J Cell Biol 119:203-213.

Zottoli SJ, Bentley AP, Feiner DG, Hering JR, Prendergast BJ and Rieff HI (1994). Spinal cord regeneration in adult goldfish: implications for functional recovery in vertebrates. Prog Brain Res 103:219-228.